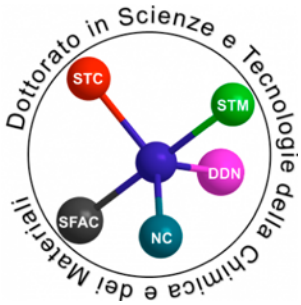

Università degli studi di Genova

Doctoral School in Sciences and Technologies of Chemistry and Materials

Ph.D. in Chemical Sciences and Technologies
XXXI cycle

Exploitation of Photochemistry and Visible Light Photoredox Catalysis towards novel transformations in Organic Synthesis: Multicomponent Reactions, synthesis of heterocycles and other applications

Ph.D. canidate: **Manuel Anselmo**

Advisor: **Prof. Andrea Basso**

INDEX

CHAPTER 1:
INTRODUCTION

In this chapter, the main topics relative to this thesis work are analyzed and discussed.

An hystorical and theoretical background on Photochemistry is given in **Paragraph 1.1**. A connection with Photocatalysis (**Paragraph 1.2**) is exploited to introduce the topic of Visible Light Photoredox Catalysis (**Paragraph 1.3**) as the main issue of the thesis. While the topic of visible light photoredox catalysis is central during the whole dissertation, some other issues play a secundary role and and their connection with the main topic is mainly analyzed. The chemistry of arendiazonium tetrafluoroborates, discussed in **Paragraph 1.4**, and the concept of multicomponent reaction, discussed in **Paragraph 1.5**, are key arguments to introduce **Chapters 2, 3 and 4**. In **Paragraph 1.6** instead, an introduction to hydrogen atom transfer reactions, which are of great relevance in **Chapter 4**, is given. The chemistry of acyl radicals, which introduces instead to **Chapter 5**, is discussed in **Paragraph 1.7**. In conclusion, the possibility to perform all these different types of chemistry under flow conditions is then discussed in **Paragraph 1.8**, introducing the reader to the topic of flow chemistry.

1.1 Photochemistry: hystory and theoretical background

Light is the basis for life on planet Earth. Since the dawn of time, mankind is aware of the vital importance of light, which was always at the centre of every culture. Nonetheless, the full understanding of its true nature didn't take place until recent times, with the progress of Science. Starting from Isaac Newton and Christiaan Huygens debate in the 17th century, up to the Noble Prize assigned to Albert Einstein in 1921, together with the concomitant advent of quantum mechanics, many theories were postulated, describing the physics of light[1.1].

Today, scientists are fully aware of the dualistic nature of light, behaving both as a wave and as a particle. But light was not studied only under a physical point of view. In fact, the chemists started using light for chemical reactions before the knowledge of its physical interaction with matter was disclosed to everyone's domain. Indeed, sunlight itself suggested to chemists to exploit photochemistry. Experimental evidence of sunlight induced changes in the general appearance of materials or their functionality were noticed: the bleaching effect, the preservation of oil paintings and the "chalking" of exterior paint, the deleterious effects on beer and the spoiling of gun cotton[1.2].

But it was only in 1834 that the era of Organic Photochemistry started to arise, when Hermann Trommsdorff observed the colour change of Santonin when exposed to visible light[1.3]. This substance, which was then employed as an anthelminthic drug, was the first example of a substrate for solid state photochemistry[1.4]. The transformation was observed not only in solution but also at

the solid state. In fact, when irradiated with visible light, a change in the crystalline structure of Santonin takes place, causing the crystals to burst[1.5]. Interestingly, research on the photochemistry of Santonin linked many personalities in Italy, like Fausto Sestini and Stanislao Cannizzaro, leading to the advent of Italian Photochemistry[1.6].

Figure 1.1.1: Italian Photochemists

from left to right: Stanslao Cannizaro (1826-1910), Fausto Sestini (1839-1904), Giacomo Ciamician (1857-1922)
from the book: 'Nascita della Fotochimica in Italia', Chimica e Cultura, Maurizio D'Auria

Stanislao Cannizzaro, which can be considered the father of Italian Photochemistry, concentrated his studies on the determination of the chemical structures of Santonin and Lumisantonin, its photorearrangement product, which were only elucidated by the combined work of Woodward-Yates and Barton some years later[1.7]. The key aspect of this transformation is that the true reactant is the electronically excited state and not the ground state of the molecule. This concept lays at the basis of photochemistry. An organic compound can in fact follow a reactivity path totally distinct from the thermal one once it is irradiated at the appropriate wavelenght. Selective excitation of an organic compound can lead to its electronically excited state and thus to a photochemical reaction, furnishing one or more photo-products.

The essential criteria for all photochemical reactions consists in the event of light absorption by a given molecule while the light radiation energy matches the energy difference of ground and excited states. According to the Frank-Condon principle, the atom coordinates do not change during light absorption and thus the excited state is never formed into an energy minimum. As a consequence, the excess energy of the excited state can promote a variety of events, as it can be seen in the Jablonski Diagram (Figure 1.1.2).

Figure 1.1.2: The Jablonski Diagram

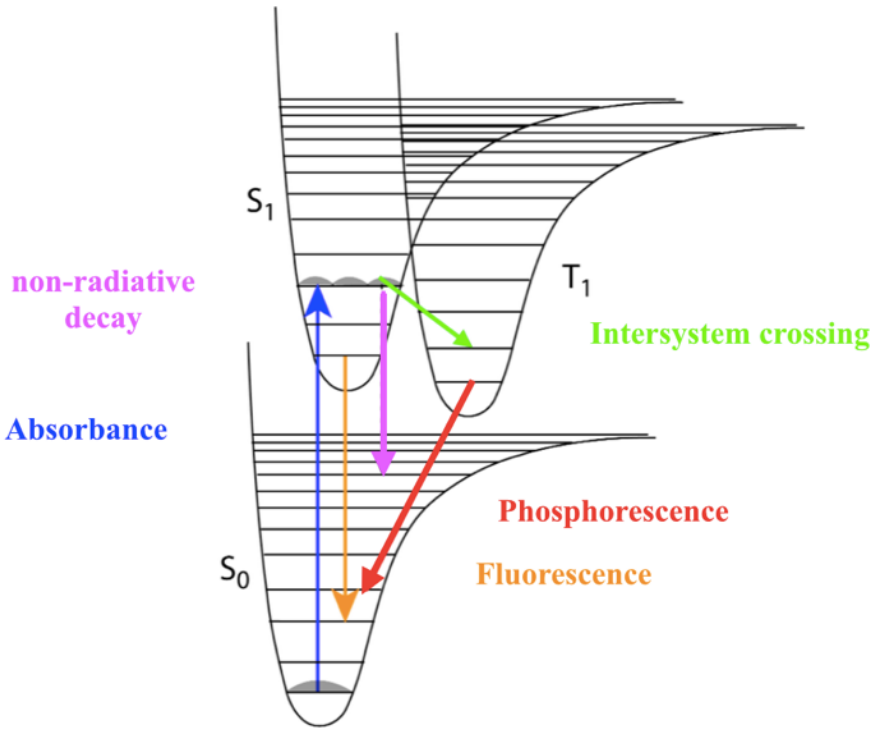

In particular, after excitation of a given molecule, the following events can take place: vibronic relaxation, intersystem crossing leading to spin inversion, emission of light (fluorescence, phosphorescence), excited state energy quenching via energy transfer to another molecule, thermal deactivation. When none of the previously mentioned events take place, a photochemical reaction may occur.

Due to the nature of a photochemical reaction, two main advantages over a thermal one can be outlined:

1) a photochemical reaction is independent from temperature;
2) the free energy change of a photochemical reaction can be either negative or positive.

The second point clearly underlines the possibility for an uphill process to take place, together with chemical reactions which are simmety-forbidden in the ground state. In addition to these advantageous conditions, it is worth-mentioning that photochemical substrate activation often occurs without additional reagents, which often diminishes the formation of byproducts. Due to this fact, photochemical reactions became particularly interesting in the context of green chemistry[1.8]. Some of these principles were foresaw by the Giacomo Ciamician already in 1912[1.9].

Sunlight, a cheap, abundant and renewable energy source can be exploited to carry out photochemical reactions. With this respect, inspiration can be taken from nature, which carries out a moltitude of photochemical reactions, like photosynhtesis, vitamin D biosynthesis, plankton bioluminescence and all the reactions at the basis of the cycle of vision in the eye[1.10]. Remarkably, numerous retinal molecules of 11-*cis*-retinal inside the reader's eye are undergoing ultrafast *cis-trans* photoisomerization while reading these lines, triggering a cascade of biochemical events leading to visual perception. On top of that, proof of photochemistry has been found also outside our planet: the photochemical synthesis of aminoacids was identified inside the interstellar multicomponent ice mixtures[1.11].

Since its discovery, photochemistry has been widely applied and investigated. Photocycloadditions, photoisomerizations and other photoreactions were exploited as powerful synthetic methods towards complex natural products synthesis[1.12]. Synthetic designs based on photochemical transformations have the potential to afford complex polycyclic carbon skeletons with impressive efficiency, which are of high value in total synthesis. A revolution in polymer synthesis has taken place thanks to the advent of photochemistry; the use of light to mediate controlled radical polymerization has emerged as a powerful strategy for rational polymer synthesis and advanced materials fabrication[1.13]. Also bio-materials were designed via photochemical transformations; recently, there have been increasing interest in using photochemical reactions in the fields of tissue engineering[1.14].

Nonetheless, despite the potential of photochemistry was well known and evident to the chemical research panorama, it is quite astonishing to find out that, despite all its attractive features, this field remained quite underdeveloped until recent times. The main reason of this fact lays in the relatively low number of visible light absorbing molecules in the panorama of substrates available for performing chemical reactions. The Grotthuss-Draper law states that 'Light must be absorbed by a compound in order for a photochemical reaction to take place'. With this respect, photochemistry can be applied only in the specific and particular case of light absorbing compounds. In addition, visible light absorption is remarkably more attractive with respect to UV absorption; the latter radiation is more energetic (thus less convenient) and as a consequence less selective. Moreover, UV irradiation of a chemical compound can lead to a variety of side events.

On the other hand, UV absorption capabilities are much more frequent in a molecule compared to visible light absorption, further tightening the field of interest of photochemistry. In addition, the molecular excited-state lifetimes of excited molecules are often quite short (milliseconds to nanoseconds time range) and reactions sometimes require a long time to reach completion. For these reasons, photochemistry remained a relatively underdeveloped area of synthetic organic chemistry for many years.

1.2 From Photochemistry to Photocatalysis

In some photochemical reactions, the reactant molecules do not absorb radiation and no chemical reaction occurs. However, if a suitable foreign substance, called sensitizer, which absorbs radiation, is added to the reactant, the reaction takes place. The sensitizer gets excited during absorption of radiation and transfers its energy to the reactants and initiates the reaction. Naturally, the energy of the excited state of the sensitizer must be higher than that of the excited state of the reactant. The basic requirement is that the energy of the donor should be around 5 kcal/mol higher than the energy required for the excitation of the acceptor molecule.

Photosensitization has become an established method for a number of reactions, such as those involving the generation of singlet oxygen; these reactions have wide applications, from polymer science to cancer therapy[1.15] and they will be further discussed in **Paragraph 1.8**.

Among many applications of photochemistry, energy-transfer mediated organometallic catalysis was investigated, for example exploiting the chemistry of electronically excited Nickel compounds[1.15]. Catalysis is indeed the true added value which allowed photochemistry to open access to huge advances in the panorama of chemical research. A photosensitizer can, as a matter of fact, be considered as a catalyst, because it answers the definition of a substance that allows or accelerates a chemical reaction while remaining unaltered at the end of the process. On the other hand, the action of the photosensitizer towards the chemical reaction is purely physical, via the absorption and the transfer of energy. When it comes to photosensitization, no change in chemical structure nor exchange of atoms or electrons takes place.

In general, photocatalysis refers to any reaction that requires the simultaneous presence of a catalyst and light. As it can be seen from Figure 1.2.1, a photocatalyst (C), differently from a thermal catalyst, is effective only in the excited state (C*) and activates the reagent (R), upon light absorption, through a chemical reaction (leading to product P).

Figure 1.2.1: reaction pathways

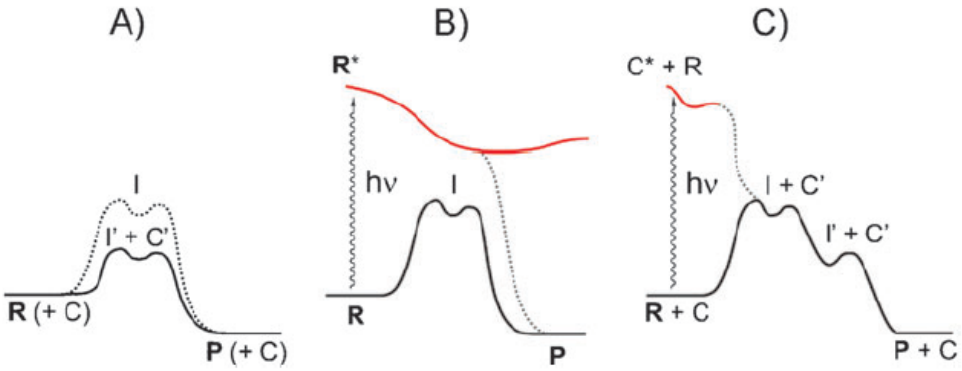

from left to right: A) thermal reaction, B) photochemical reaction, C) photocatalyzed reaction

A thermal reaction (pathway A, at the left of **Figure 1.2.1**) is catalyzed by the catalyst C via intermediate I'. A photochemical reaction (pathway B, in the centre of **Figure 1.2.1**) starts from the excited state surface (highlighted in red) of the excited reagent R*; such excitation follows the absorption of light by means of the reagent. In a photocatalyzed reaction (pathway C, at the right of **Figure 1.2.1**) the catalyst C is active only in the excited state (C*), following the absorption of light (by means of the catalyst). In the latter case, the chemical transformation of reagent R occurs entirely on the ground state surface. An intermediate I is formed (a radical or radical ion), which in principle can be formed also through a thermal process. The excited catalyst C* gives a catalyst derivative C' upon interaction with the reactant R. If either the species C' or I react independently, a photochemical reaction occurs. The mild conditions and the large chemical change caused are important features of a photocatalyzed reaction. These reactions would thus occur thermally only under harsh conditions.

The events described in the previous lines are summarized in the general photocatalytic cycle which is reported in Scheme 1.2.1.

Scheme 1.2.1: a general photocatalytic cycle

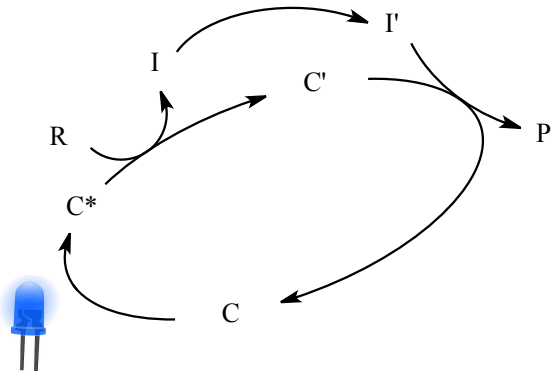

C: catalyst; C*: excited state catalyst, C': catalyst derivative, R: reagent; I: intermediate, P: product

Photocatalysis is probably the most powerful method to overcome the limitations of pure photochemistry and a valuable tool to break down the barrier erected by the lack of absorption typical of most organic molecules. Up to the beginning of the 20th century the term 'photocatalysis' was wrongly tagged to reactions accellerated by light but still following thermal pathways. Only at the beginning of 1970's, photcatalysis started to arise, promoted by the human need for renewable resources, such as the exploitation of solar energy for the generation of hydrogen from water splitting[1.17]. In addition, research on water purification via photocatalytic methods, thus avoiding or considerably reducing chemical pollution, also started to become deeply investigated[1.18]. Chemical synthesis was the last research field embracing the concept of photocatalysis; this explains why the major advances started only recently. Photocatalysis can either proceed in heterogeneous or homogeneous phase. In the first case, semiconductors are mostly employed as catalysts, capable to promote electron transfer events on their surface, while in the second case, the catalytic activity is generally imputed to small molecules[1.19].

In the panorama of photocatalysis, reactions involving photoinduced electron transfer (PET) rather than atom transfer from the catalyst, which absorbs in the visible range, are of particular importance. Absorption of visible light is highly convenient because this radiation is hardly absorbed in the media by any common compound other than the catalyst; in other words, the irradiation is selective for the catalyst. In addition, sunlight can be employed as a free and renewable light source to induce catalysis. This kind of photocatalysis is named visible light photoredox catalysis.

1.3 Visible Light Photoredox Catalysis

In the last two decades, a dramatic expansion in the research area of VLPC has taken place. In fact, since the beginning of the 21st century, the number of publications in this field witnessed an exponential growth, as it can be seen in **Figure 1.3.1**[1.20].

Figure 1.3.1: exponential growth in the number of publications in VLPC

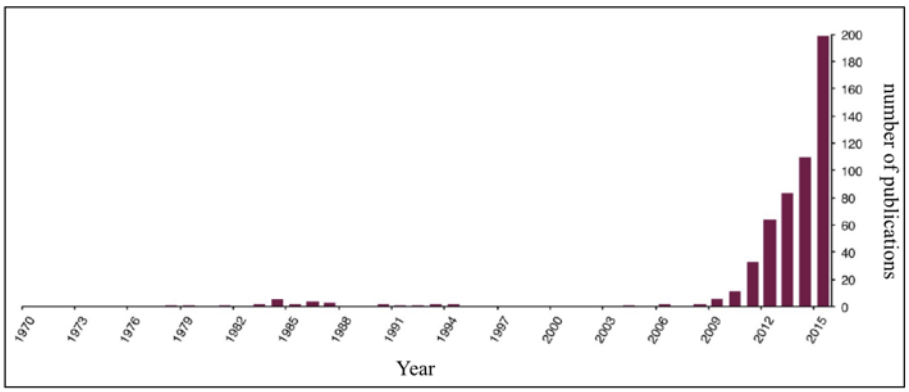

The key factor in the recent yet rapid growth of this activation platform consisted in the recognition that readily accessible metal polypyridyl complexes and organic dyes can facilitate the conversion of visible light into chemical energy under exceptionally mild conditions. As a consequence of the absorption of visible light, these substances provide facile access to open-shell reactive species, which most commonly consist of radical species. As a result, radical chemistry recently became much more accessible to researchers thanks to VLPC, and this powerful methodology offered a complementary approach to classic organic synthesis. Remarkably, VLPC potential sometimes greatly overcomes that of classic organic synthesis. The possibility to simultaneously access both strong oxidant and strong reducing reaction conditions at the same time is imputable exclusively to VLPC in the panorama of organic synthesis, thus providing access to previously inaccessible redox-neutral reaction platforms. In fact, this electronic duality contrasts directly with traditional redox reaction wherein the reaction medium can be either oxidative or reductive (but not both).

Coming to a mechanistic insight of VLPC, as it can be seen in **Scheme 1.3.1**, two main situations can occurr: the excited state of the photoredox catalyst can either give rise to an oxidative or to a reductive catalytic cycle[1.21].

Scheme 1.3.1: Oxidative and Reductive Quenching

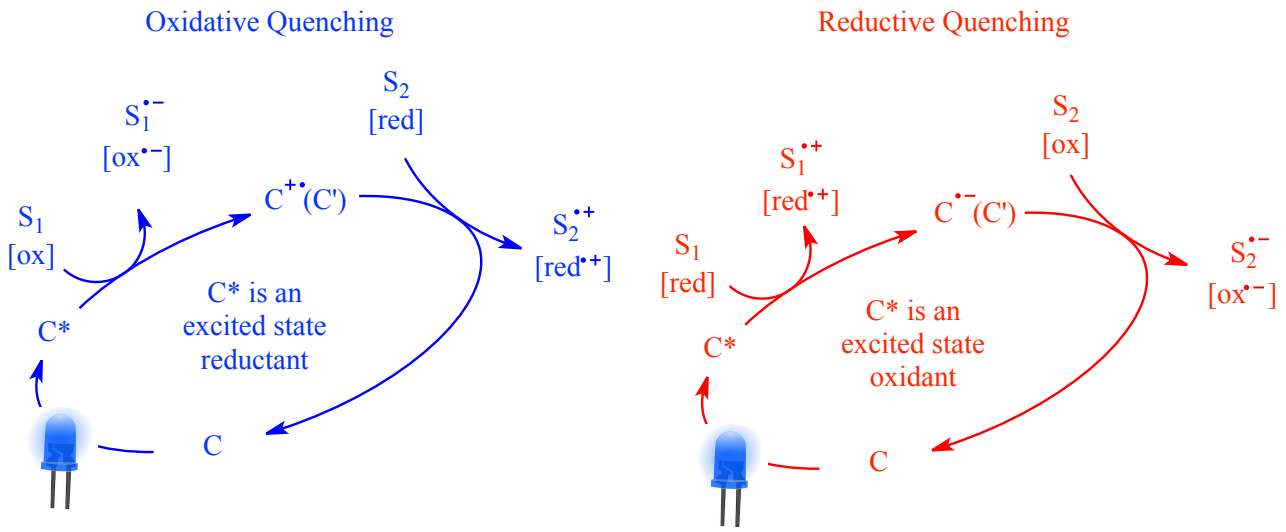

In the first case, the excited photoredox catalyst is quenched by donating an electron to a substrate or an oxidant followed by its regeneration by reduction in the catalyst turnover step (Oxidative Quenching, blue cycle in **Scheme 1.3.1**). In the second case, the catalyst is quenched by accepting an electron from the substrate or a reductant followed by regeneration by oxidation in the catalyst turnover step (Reductive Quenching, red cycle in **Scheme 1.3.1**).

In general, regardless of whether the substrate undergoes an electron transfer reaction in the PET step or in the turnover step, there are three possible redox outcomes for the substrate: net oxidative, net reductive, and redox-neutral (**Scheme 1.3.2**).

Scheme 1.3.2: possible redox outcomes in VLPC

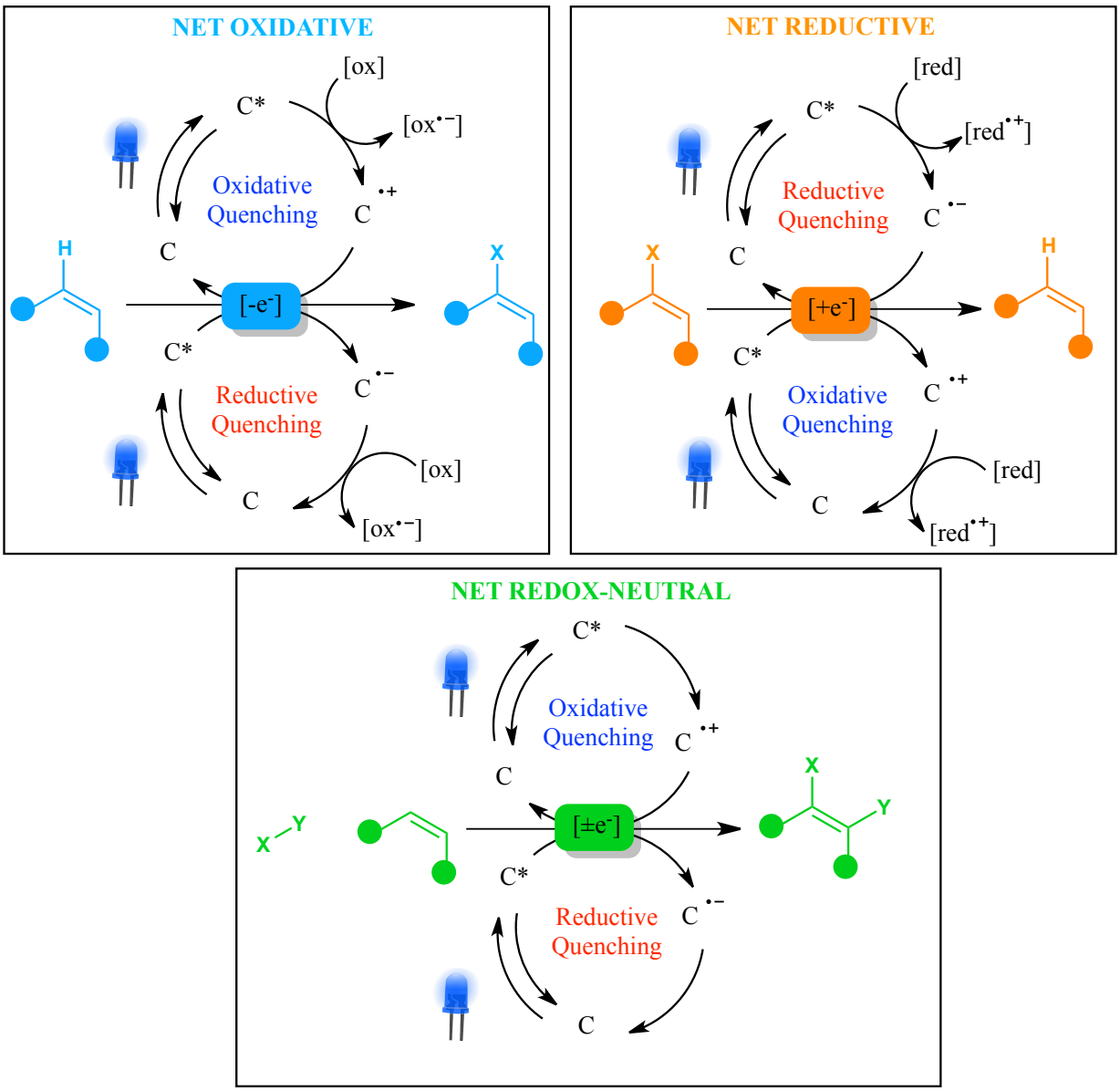

A net oxidative reaction (top-left in **Scheme 1.3.2**) requires an external oxidant, which can accept electrons in either the PET step or in the turnover step. In a similar manner, a net reductive reaction (top-right in **Scheme 1.3.2**) requires an external reductant, which can donate electrons in either the PET step or in the turnover step. Differently, redox-neutral processes (bottom-centre in **Scheme 1.3.2**) are more complex and often involve return electron transfer with the oxidized or reduced catalyst, sometimes mediated by a co-catalyst. Commonly, each photoredox catalyst is active towards both reduction and oxidation steps, even though the redox potential of each compound makes it more indicated towards one main transformation.

The most common photosensitizers known to organic chemists are purely organic molecules: Eosin Y, Rose Bengal and Methylene Blue are among the most used ones.

Scheme 1.3.3: common photosensitizers and visible light photoredox catalysts

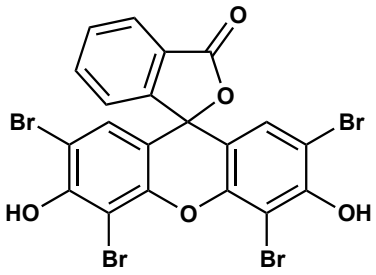

Eosin Y

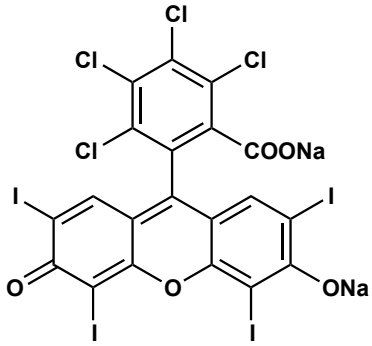

Rose Bengal

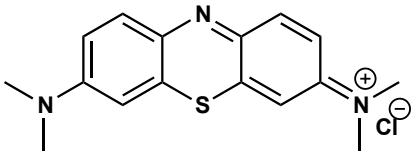

Methylene Blue

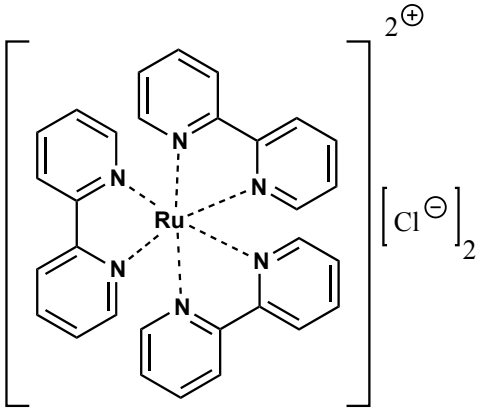

$Ru(bpy)_3Cl_2$

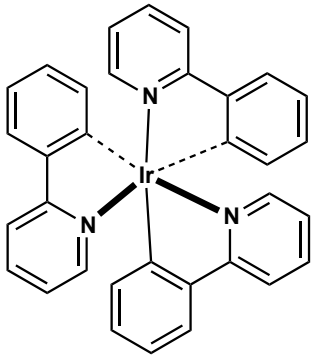

$Ir(ppy)_3$

These molecules can be also employed as photoredox catalysts, but organometallic complexes such as $Ru(bpy)_3Cl_2$ and $Ir(ppy)_3$ are by far superior to this extent. Both species absorb in the blue region of visible light (having an absorption maximum around 440 nm), where most organic molecules are unable to absorb, thus minimising potential deleterious side reactions and allowing the use of cheap, narrow-band emitting, low energy consuming light emitting diodes (LEDs).

In the case of Ruthenium and Iridium polypyridyl complexes, one electron from the metal center of the complex can be promoted to a ligand centered π^* orbital (metal to ligand charge transfer, MLCT). This transition results in a species in which the metal has effectively been oxidized, while the ligand framework has undergone a single-electron reduction. The initially occupied singlet MLCT state undergoes rapid ISC to give the lowest energy triplet MLCT state. As a result, a long-lived photoexcited species that can be either reduced or oxidized very easily compared to the ground state species is generated.

Figure 1.3.2: simplified molecular orbital depiction of $Ir(ppy)_3$ and $Ru(bpy)_3Cl_2$

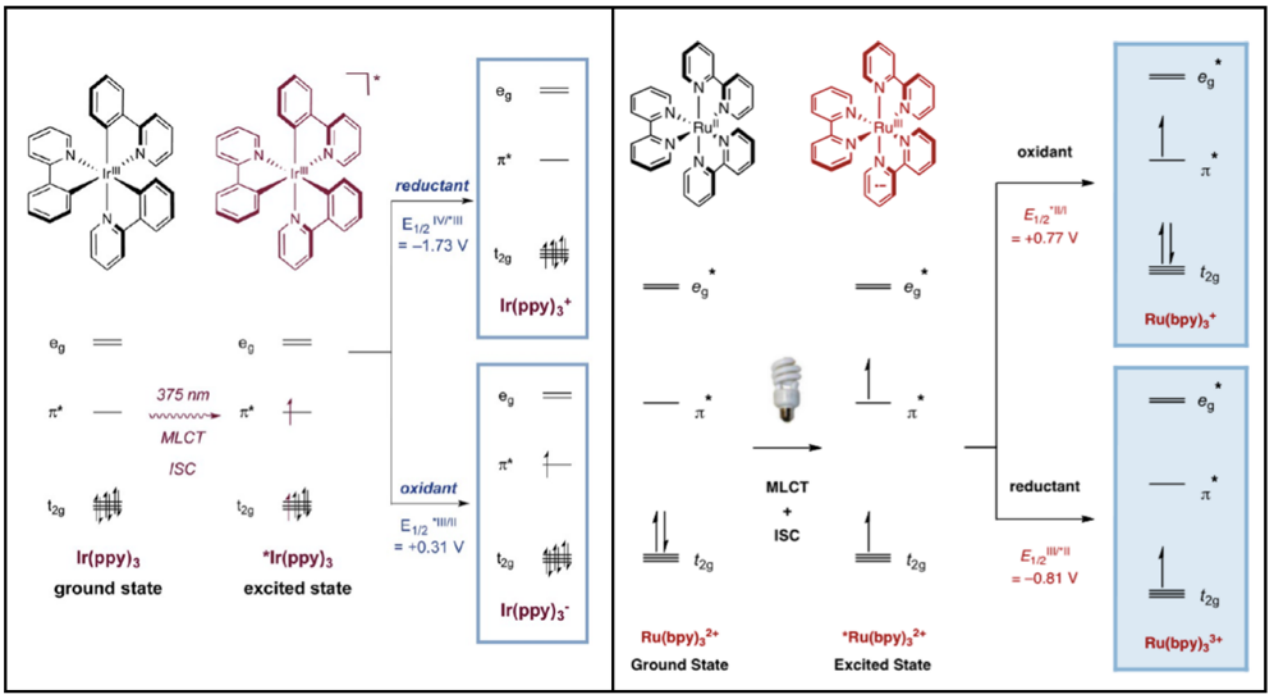

simplified molecular orbital depiction of the photochemistry of: on the left, $Ir(ppy)_3$[1.22]; on the right, $Ru(bpy)_3Cl_2$[1.23]

As a consequence of the previously discussed photochemically driven events, photoredox catalysts are able to convert visible light into significant levels of chemical energy. Remarkably, the triplet state of $Ir(ppy)_3$ is 56 kcal/mol above the ground state energy level. Adding even more interest to the exploitation of the aforementioned polypyridyl complexes, is the possibility to tune their redox potential by changing the functionalization of the ligands causing a modulation of their reductive/ oxidative power, making these compounds very versatile catalysts for synthesis.

Figure 1.3.3: tuning of the redox potential by ligand exchange

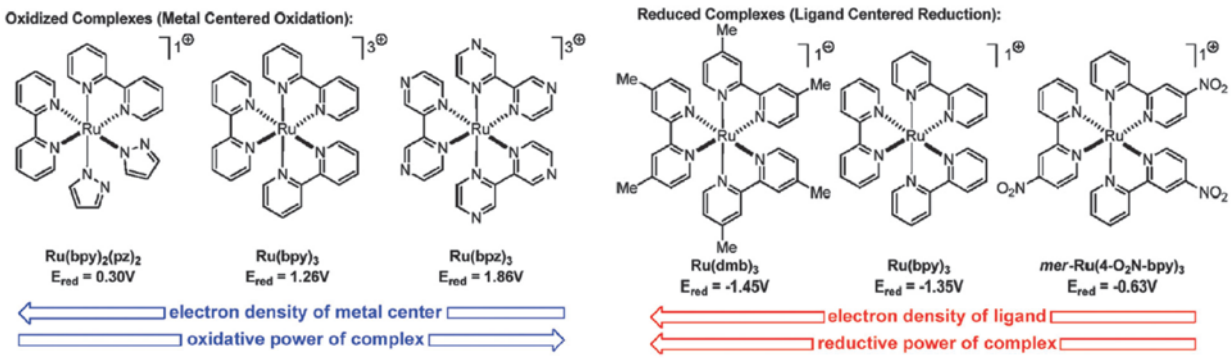

Over the last four decades, VLPC has found widespread application in the fields of water splitting[1.24], carbon dioxide reduction[1.25] and the development of novel solar cell materials[1.26].

Starting from the end of the 70's, a continuosly growing number of research groups started to dedicate their work to what at the time was a new emerging field, leading to an expansion which is still in progress nowadays (as it is demonstrated by **Figure 1.3.1**).

Among the very first applications of VLPC in organic synthesis, Kellog et al[1.27] reported, in 1978, the photomediated reduction of sulfonium ions to the corresponding alkanes and thioethers, employing $Ru(bpy)_3Cl_2$ as a catalyst. Subsequent reports by Fukuzumi[1.28] established that similar catalytic systems could facilitate the reduction of a wide range of organic substrates, including electron-deficient olefins and aromatic ketones, along with benzylic and phenacyl halides.

The first net-oxidative photoredox catalyzed reaction using arendiazonium salts as the terminal oxidant for the conversion of benzylic alchols to the corresponding aldehydes was reported by Cano-Yelo and Deronzier in 1984[1.29]. To the same authours is to be imputed the first redox neutral transformation in the field, when they disclosed the first photoredox catalyzed Pschorr reaction[1.30]. This pioneering work laid the foundations for a wide research area in VLPC, based on the chemistry of arendiazonium salts, which will be further discussed in **Paragraph 1.4**.

Despite the early demonstration of the potential of VLPC for synthetic applications, the area remained relatively underappreciated by the broader community untile the late 2000s. The last ten years in fact had witnessed the fluorishing of VLPC applications in organic synthesis. During this time, researchers developed new photoredox catalytic methods which often outmatched classical ones. Several new outstanding C-C bond forming methodolgies superior or complementarhy to those previously established have been disclosed. For example, Nishibayashi and co-workers utilized excited Ir^{III} catalysts for the visible-light-mediated, oxidative decarboxylation of arylacetic acids to give benzyl radicals, which can be trapped with electron-deficient olefins[1.31]. Such transformation didn't require stoichiometric Zn or Ni catalysts, which were previously employed for oxidative decarboxylation reactions[1.32]. Another example was reported by Molander et al, in which the photoredox/nickel-catalyzed cross-coupling reaction between primary alkyl organotrifluoroborates and aryl bromides was performed [1.33]. This method represents an attractive alternative to the Suzuki-Miyaura cross-coupling, offering advantageous mild reaction conditions and improved functional group tolerance [1.34].

As it is demonstrated by the previously mentioned work by Molander et al, dual catalysis[1.35] is often encountered in this field. For example, Glorius et al developed the three-component, dual gold/photoredox-catalyzed intermolecular oxyarylation of 1-Octene[1.36]. In this work, VLPC was used to establish new multicomponent methodologies. The topic of multicomponent reactions (MCRs) in organic synthesis will be discusses in detail in **Paragraph 1.5**. Dual catalysis was also exploited by MacMillan et al in the direct aldehyde C-H arylation and alkylation via the combination of Nickel catalysis, a hydrogen atom transfer (HAT) strategy and VLPC[1.37]. The topic of HAT will be further discussed in **Paragraph 1.6**.

The aforementioned work by MacMillan furnished a powerful methodology to access synthetically useful ketones. In order to do so, acyl radicals were generated from aldehydes via photoredox catalysis and thus they were coupled with halides by means of Nickel catalysis. The chemistry of acyl radicals will be further discussed in **Paragraph 1.6**.

Noteworthy, in the examples just presented, VLPC is often coupled with transition metal catalysis. The merger of photoredox and transition metal catalysis is often referred to as 'metallaphotoredox'; this approach has enabled the invention of a large and varied range of cross-coupling reactions[1.38]. Many metallaphotoredox applications have been adopted by the pharmaceutical industry[1.39]. The synergistic cooperativity of VLPC was not limited only to organo- and transition-metal catalysis but also to other domains such as biocatalysis or electrocatalysis[1.40]. The possibility to apply VLPC in combination with the technology of a solar cell was investigated by Choi et al, obtaining promising results towards biomass conversion[1.41]. On a similar conceptual level, Yun, Jeong and Park designed a novel light-driven platform for cofactor-free, whole-cell P450 photo-biocatalysis using Eosin Y as a photoredox catalyst [1.42], thus demonstrating the applicability of VLPC to bioorganic chemistry.

To sum-up, VLPC became a very well-established tool in organic synthesis, as it is demonstrated by the myriad of applications reported in the literature. This methodology is still young and we can only expect it to improve in the years to come. Natural product synthesis is also fully embracing VLPC to reach high levels of complexity with a lower number of simple passages, simpler with respect to the what was done in the past. The combination of this methodology with flow chemistry, as it will be discussed in **Paragraph 1.8**, opens the way to super-efficient transformations, which hopefully will become more and more important also on an industrial scale.

1.4 Visible Light Photoredox Catalyzed reactions of arendiazonium tetrafluoroborates

The reactions of arendiazonium salts are among the oldest which have been intensively studied by organic chemists. A number of transformations involving arendiazonium salts are known, among which there are: reactions with nucleophiles, heterolytic dediazotization reactions with electrophiles, formation of arynes by loss of nitrogen and photolytic dediazotizations[1.43]. Among these reactions, photolysis is a reaction of particular relevance. In fact, direct irradiation of arendiazonium salts leads to aryl cations [1.44]. Depending on both the substitution of the aromatic ring and the reaction conditions, either singlet or triplet aryl cations can be obtained. In the first case, solvolysis reactions can take place, leading for example to acetanilides when the reaction is conducted in acetonitrile media. In the second case, different nucleophilic trapping reactions can take place depending on the conditions.

Unlike all these situations, when VLPC conditions are applied to arendiazonium salts, these compounds behave as exceptional aryl radical precursors. Commonly, via a single elctron transfer (SET) event the excited state of the photoredox catalyst reduces the arendiazonium cation to an aryl radical, along with loss of nitrogen.

Remarkably, arendiazonium salts are probably the best source of aryl radicals known to organic chemists, followed by aryl halides, aryl triflates, diaryliodonium salts, aryltriazenes and arylhydrazines. The chemistry of aryl radicals is highly relevant in the panorama of organic synthesis[1.45], playing a fundamental role in Meerwein[1.46], Sandmeyer[1.47] and Gomberg-Bachmann[1.49] reactions. Aryl radicals are also employed by nature; the Gasteromycete *Stephanospora caroticolor* supposedly generates aryl radicals as a natural defensive mechanisms[1.50]. Among the previously mentioned transformations, Sandmeyer and Meerwein are probably the most useful reactions. These two transformations are intimately related; both involving an aryl radical coupling[1.51] with a radical trap. Sandmeyer reactions typically involve heteroatomic compounds such as halide anions, which are also trapped by the aliphatic radical intermediates generated by the coupling of aryl radicals with olefins in Meerwein reactions.

Scheme 1.4.1: Meerwein and Sandmeyer reactions

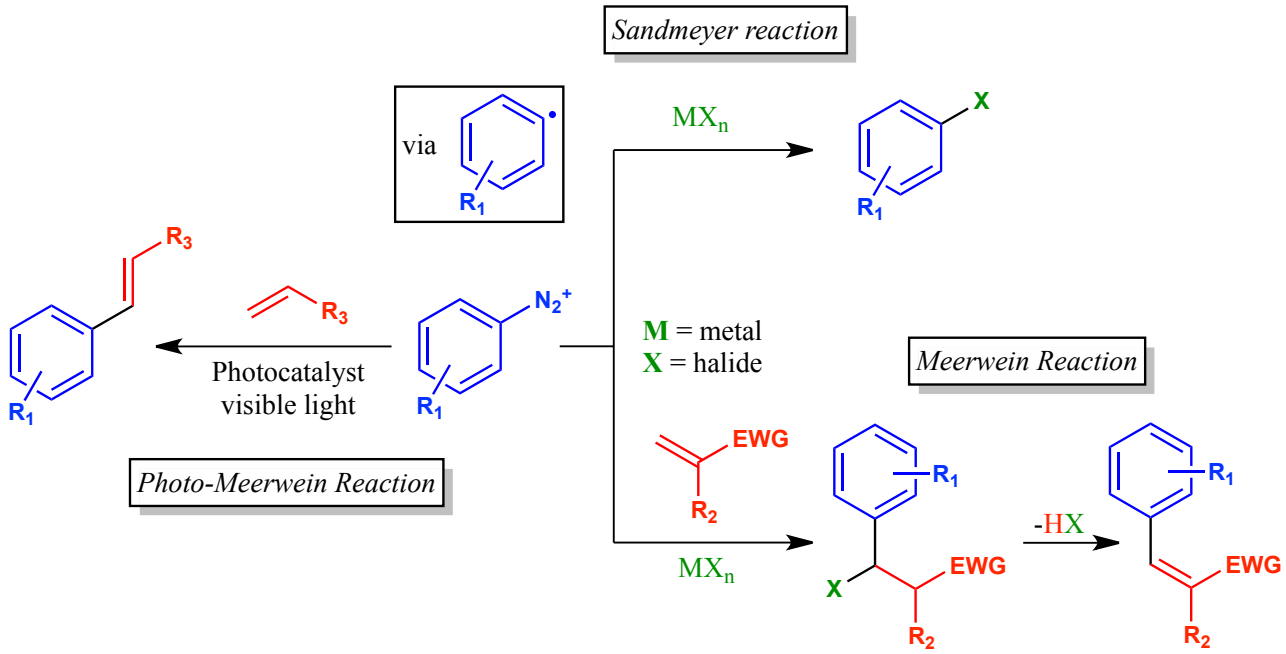

Sandmeyer reactions are often side-reactions the occurrence of which can be identified during Meerwein reaction procedures. Although Meerwein reactions were originally performed by means of copper(II) catalysis, it was demonstrated that VLPC can also promote them[1.52] with great results. When a photoredox catalyst is employed in Meerwein conditions, reduction of the arendiazonium cation generates the aryl radical, which then attacks the olefinic trap. The readily formed radical intermediate is oxidized to carbocation restoring back the photoredox catalyst to its

original form. At this point, nucleophilic attack to the carbocation furnishing a typical Meerwein product as well as deprotonation leading to a cross-coupled unsaturated compound complete the transformation[1.53].

Scheme 1.4.2: mechanistic pathways of the Meerwein reaction by means of VLPC

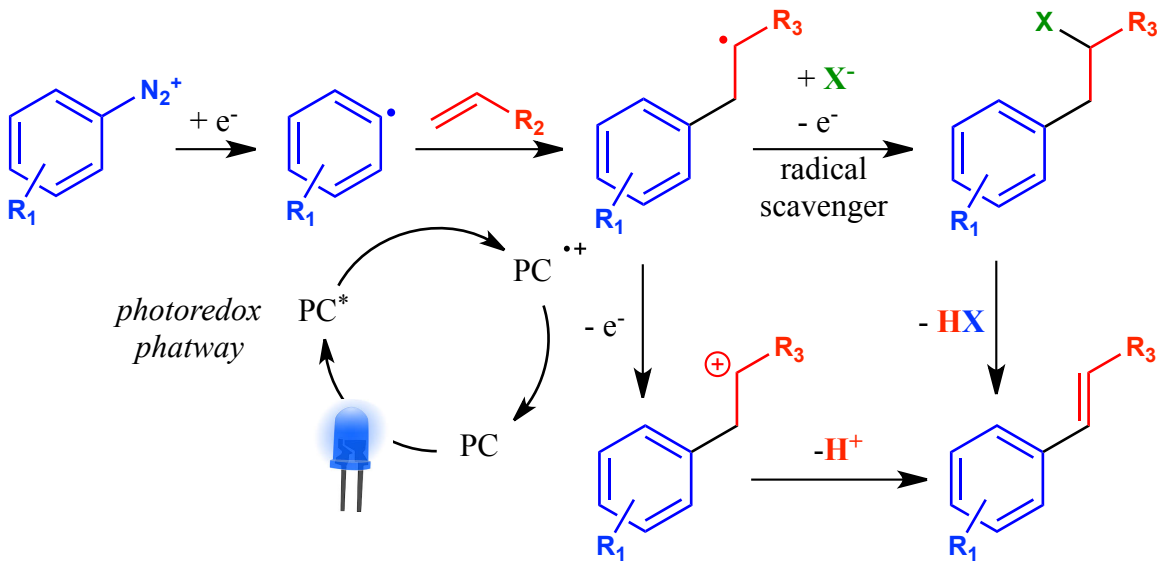

With respect to this chemisty, König et al disclosed the photoredox catalyzed Meerwein arylation of heteroarenes[1.54] furnishing a synthetic alternative to existing transition metal catalyzed cross-coupling reactions. A similar application from the same working group, involves the use of alkynes as radicals traps instead of aromatic compounds, followed by an intramolecular annulation reaction[1.55].

Scheme 1.4.3: Photo-Meerwein chemistry by König et al

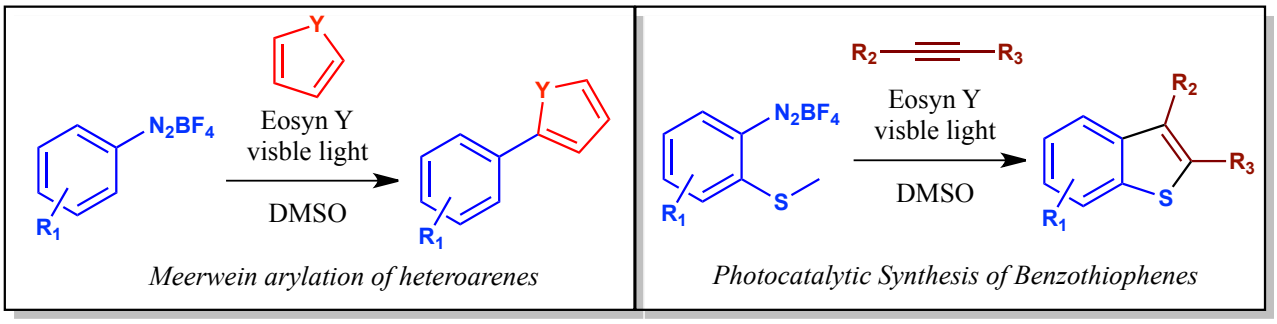

Benzothiophene derivatives became readily accessible in a single synthetic transformation via this methodology, opening the way to natural product synthesis.

Having developed considerable experience in this field, the group of Konig further elaborated their research by disclosing, in 2014, a photoredox catalyzed amino-arylation of alkenes[1.56]. This

methodology, consisting of a four component Meerwein transformation, was the inspiration for the doctorate work reported in this thesis and it will be further discussed at the beginning of **Chapter 2**.

1.5 Multicomponent Reactions

At present day, multicomponent reactions (MCRs) occupy a position of great relevance in the organic chemistry panorama. A MCR is defined as the condensation of three or more molecules, in a single synthetic step, to afford a product bearing the majority of the atoms contained in the starting materials. This approach allows to reach considerable levels of complexity starting from relatively simple molecules. In addition, contrary to traditional multistep procedures, time- and energy-consuming along with waste-producing purification steps can be avoided, establishing a considerable advantage with respect to classic organic synthesis.

Scheme 1.5.1: classic linear reaction sequence VS multicomponent approach

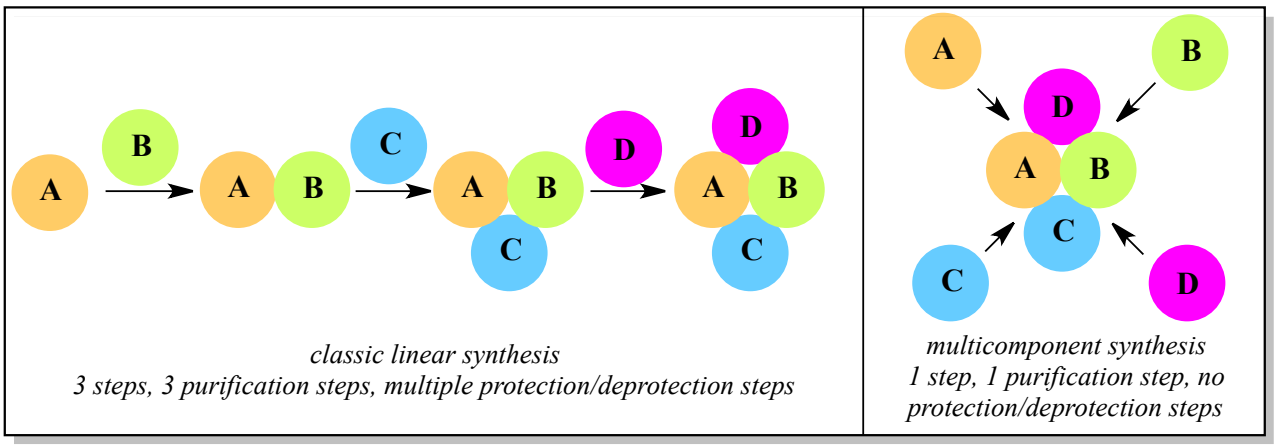

The multicomponent approach becomes particularly relevant with respect to the growing request for large libraries of complex molecules to be used for high throughput screening assays in the discovery process of new drugs carried on by pharmaceutical companies. Clearly, MCRs stand in the pathway leading to the 'ideal synthesis'[1.57], in which desired products are obtained in excellent overall yield, with few synthetic steps and according to an environmental compatibility.

Scheme 1.5.2: Ideal Synthesis

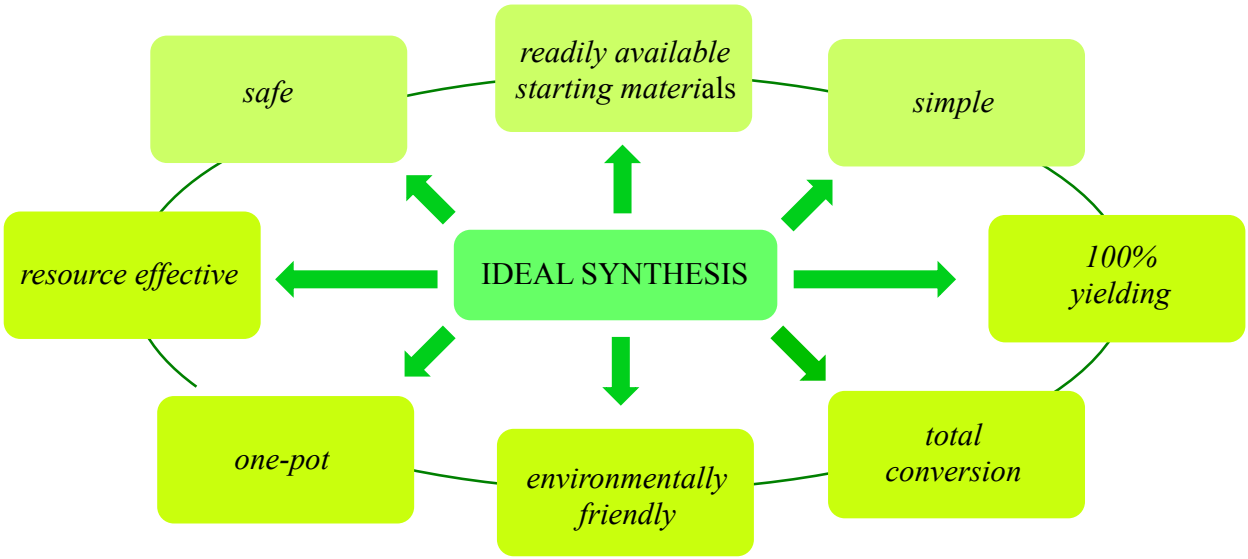

Even though the first MCRs date back to 1850 (Strecker synthesis[1.58]), it should be noted that early organic chemists did not immediately recognize their huge potential. Only about one century later, when Ivar Karl Ugi discovered the four component condensation bearing his name[1.59], the scientific community started to appreciate the potential of MCRs. In fact, it was soon understood by the chemical community that many enormous challenges could be faced using MCRs as powerful tools. For example, the diversity oriented synthesis (DOS) approach could greatly benefit from MCRs. In contrapposition to target oriented synthesis (TOS) and combinatiorial synthesis, DOS allows to explore a far greater chemical space, with the aim to achieve collection of compounds via step- and atom-economic procedures[1.60].

Figure 1.5.1: The DOS approach VS Combinatorial chemistry and the TOS approach

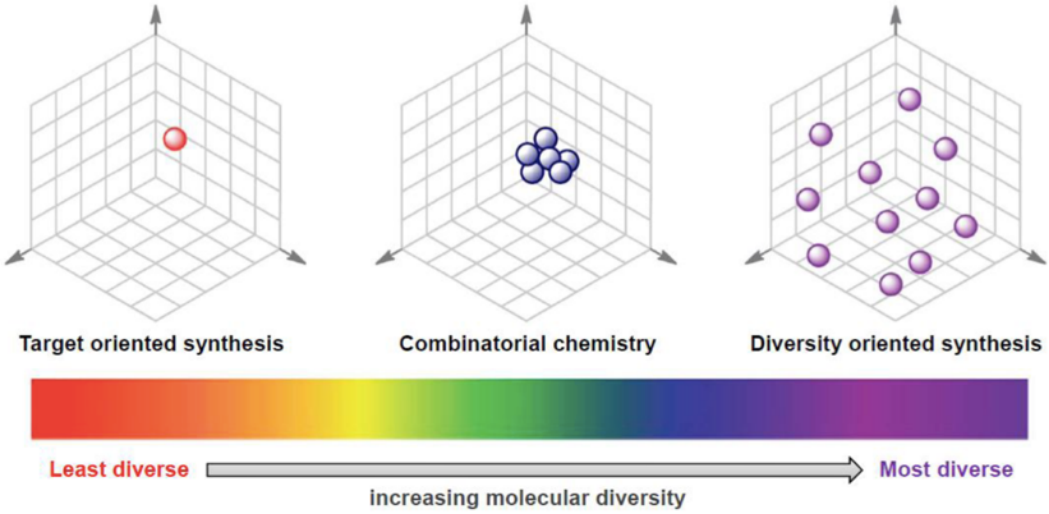

With this respect, MCRs can assume the charachteristics of multidiversity generating reactions (MDGR), whenever each component brings a diversity input in the final product. For example, the Ugi reaction commonly behaves as a MDGR while the Strecker reaction does not. Among the thousands of applications of MCRs, it is certainly worth mentioning the work by Orru et al[1.61] in which three MCRs are combined in an higher order reaction leading to a total eight-component reaction, thus assembling in the final product a remarkable amount of chemical complexity.

Scheme 1.5.3: 8CR by Orru et al (each colored fragment derives from one of eight substrates)

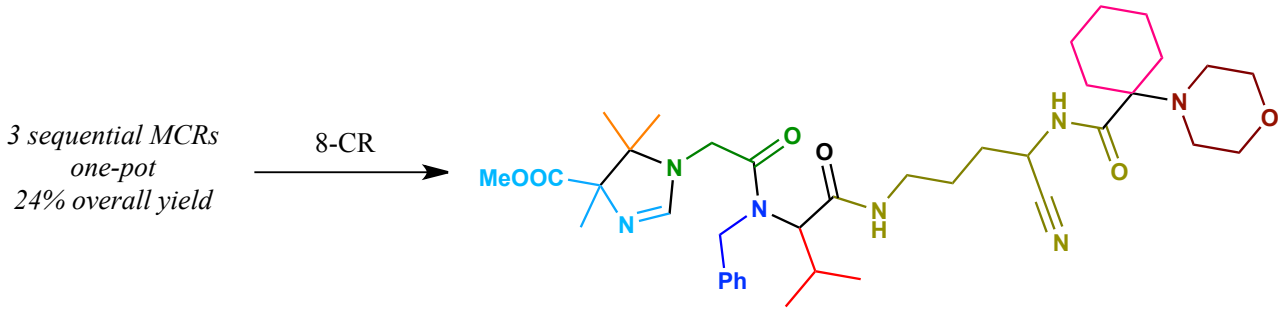

Despite the potential of this approach, MCRs are not all-mighty and thus they suffer from some limitations. Their tendecy to give side-reactions, along with limited scaffold diversity and poor stereocontrol sometimes narrow the application range of MCRs. In order to overcome such limitations, the synergistic application of catalysis could lead to clean desired reactions with higher levels of stereocontrol together with increased efficiencies. Multicomponent-multicatalytic reactions, often referred to as $(MC)^2R$, can merge the advantages of multicomponent chemistry with those of catalysis[1.62]. To some extent, these reactions try to mimic the efficiency of Nature, which applies enzymatic machinery to transform a series of starting materials into complex and intricate structures.

An example from Nature is given by the biosynthesis of terpenes, in particular that of pentalenolactone D[1.63]. In fact, inside the cell, two units of isopentenyl pyrophosphate and one of dimethylallylpyrophosphate are coupled, cyclized and oxidized via harmonic enzimatic steps to achieve with extreme efficiency and selectivity a formal multicomponent product.

Although most $(MC)^2R$ are developed with classic transition metal catalysis of Palladiun and Rhodium, some synergistic applications with Iridium photoredox catalysts have been disclosed[1.64]. For example, Glorius et al exploited dual photoredox and gold catalysis to perform intermolecular multicomponent oxyarylation of alkenes[1.65]. In their application, diaryliodonium salts are coupled with olefins with the insertion of methanol, acting both as the nucleophile and the solvent.

Scheme 1.5.4: Dual Gold-Photoredox catalytic reaction

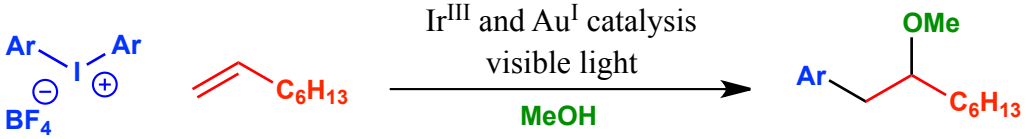

This reaction however does not belong to the class of MDGRs, because no diversity input in the final product is to be imputed to the utilization of MeOH. An application of VLPC to MDGRs is reported by Rueping et al with their work on oxidative three-component reactions for the direct synthesis of α-amino amides and imides from tertiary amines[1.66]. Despite these applications, the synergistic utilization of VLPC and multicomponent reactions is at present date still underdeveoped and thus will most certainly remain a hot research topic for several years to come. For this reason, my doctoral research work focused on this research field, as it will be discussed at the beginning of **Chapter 2**.

1.6 Hydrogen Atom Transfer reactions

Hydrogen atom transfer (HAT) is a chemical transformation consisting of the concerted movement of two elementary particles, a proton and an electron, between two substrates in a single kinetic step[1.67].

Scheme 1.6.1: HAT schematic reaction

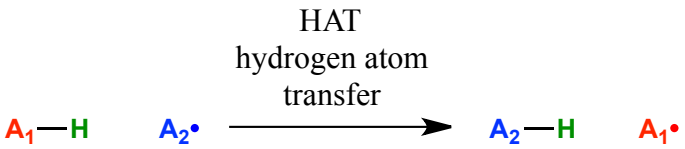

On a conceptual point of view, HAT may be viewed as a special case of concerted proton coupled electron transfer (PCET); the electron and proton are transferred between the same donor and acceptor, sharing the starting and final orbitals involved in their movement[1.68]. HAT reactions, which are attracting more and more interest in the field of organic synthesis, are also ubiquitous in Nature. These reactions are in fact known to play a role in atmospheric phenomena like the combustion of hydrocarbons and aerobic oxidations[1.69].

On a biological point of view, several metalloenzymes are known to operate through a series of reactions involving an HAT step; the role of such processes in the destructive effects of reactive oxygen species (ROS) in vivo and in the mechanism of action of antioxidants has been studied in depth [1.70].

In the field of organic synthesis instead, HAT reactions offer unique opportunities to directly functionalize C-H bonds, often with high degrees of selectivity. In simple terms, HAT reactions are a powerful tool in the subfield of organic synthesis known as C-H activation[1.71].

C(sp^3)-H activation refers to a type of reaction where a saturated carbon-hydrogen bond is cleaved and replaced with a carbon-X bond, where X is commonly carbon, nitrogen or oxygen. During the last decade, the C-H straigthforward activation approach has fluorished in the field of organic synthesis[1.72]. This method became particularly attractive to the eyes of organic chemists because it allows to gain rapid and efficient access to complex functionalized products, in an environmentally friendly approach, starting from simple and readily accessible hydrocarbons.

The most popular C–H activation reactions are catalyzed by transition metals. C–H bonds, which are traditionally considered unreactive, can be cleaved by coordination with the metal[1.73]. C-H activation provides the perfect opportunity for late-stage functionalization of complex molecules. Treating the C-H bond as a functional group is highly desirable in organic synthesis, allowing the preparation of target compounds in fewer steps with respect to classic methods, directly derivatizing close precursors of the desired compounds[1.74]. In addition, rapid access to a wide range of products can facilitate the preparation of large libraries of compounds to be tested by medicinal chemists[1.75]. Many examples of C–H functionalization approaches, leading to direct modification of lead structures and providing new analogs, without resorting to complicated *de-novo* synthesis, can be found in the literature[1.76]. Of particular relevance among the many examples of late stage diversification via C-H activation[1.77] were some applications in natural product synthesis[1.78], organic light emitting diode (OLED) technology materials[1.79] and metallorganic frameworks (MOFs) preparation[1.80].

With this respect, HAT reactions are becoming a major interpreter in the class of C-H activations. In fact, HAT reactions offer some advantages over other C-H activation methodologies, like those based on directing group strategies[1.81]. For example, with respect to “directed” functionalization procedures, HAT reactions occur without any need of a strong binding of the substrate to the catalyst. Since there is no need to insert a directing moiety in the scaffold of interest, a considerable amount of time and precious resources can be saved.

Alkane C−H bonds have long been recognized to be cleaved by hydrogen abstraction by a variety of radical species, such as halogen radicals, oxygen centered-radicals, and even carbon-centered radicals[1.82]. In principle, such free radical-mediated S_H2 (homolytic bimolecular substitution)-type hydrogen abstraction has excellent potential to contribute to site-selective C(sp3)−H functionalization, if powerful methodologies to control the site-selectivity are developed. Examples in the literature can be found in the C-H bromination of alkanes[1.83] and in the functionalization of saturated alchohols[1.84].

In recent years, photocatalytic radical approaches for C–H bond cleavage via HAT have attracted increasing attention as viable alternatives to thermal approaches, significantly contributing to the development of the field. With this respect, upon light absorption, a photocatalyst can promote this kind of transformation in two different ways: via a direct or indirect HAT process. In the first case, the excited state photocatalyst itself is responsible for hydrogen abstraction from a substrate. An example of this reactivity is reported by Ravelli, Fukuyama and Ryu with their work on the site-selective C–H functionalization by decatungstate anion photocatalysis[1.85]. With respect to indirect HAT processes, the photocatalyst is responsible for the generation of an hydrogen abstracting species. This chemical outcome can be achieved with three distinct modalities, as it can be seen in **Scheme 1.6.2**[1.86].

Scheme 1.6.2: different modalities of photocatalytic HAT processes

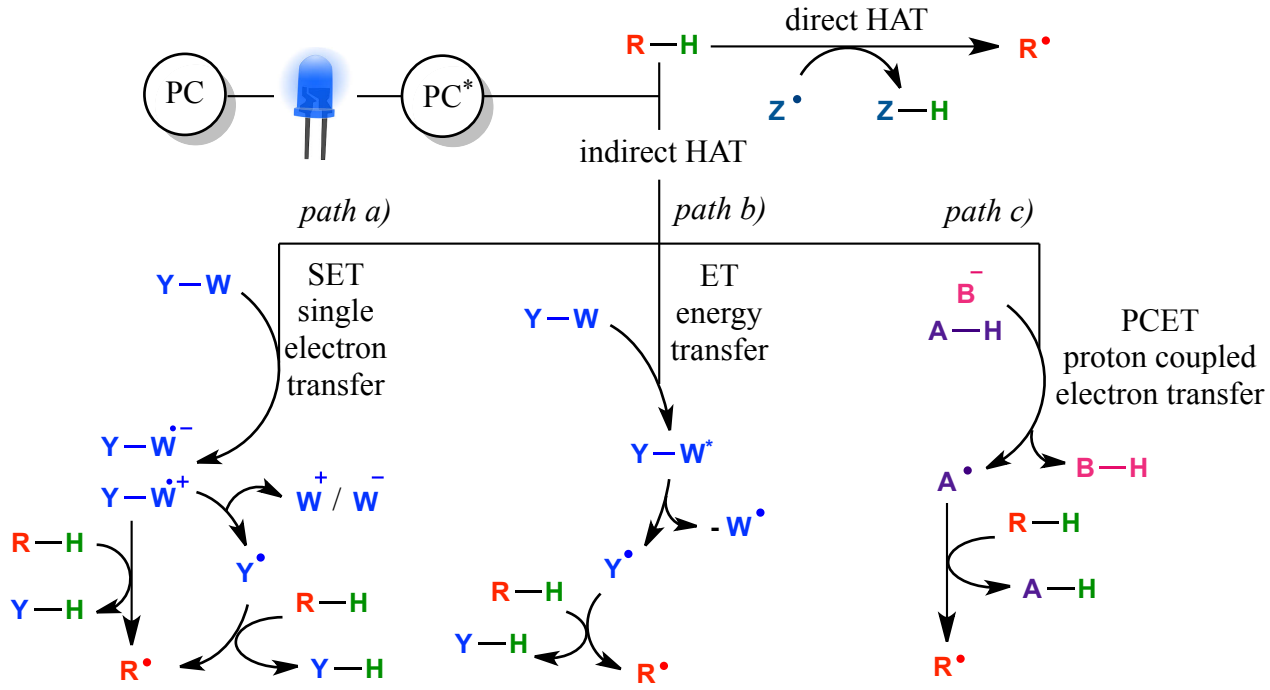

According to path *b)* (in the centre of **Scheme 1.6.2**), an energy transfer between the excited photocatalyst (PC*), thus acting as a photosensitizer, and a subtrate (YW), takes place. The latter, having reached the excited state (YW*), can undergo the homolytic cleavage of a labile bond, generating a thermal hydrogen abstractor (radical Y) prone to perform the desired HAT transformation. According to path *c)* instead (at the right of **Scheme 1.6.2**), the excited photocatalyst (PC*) can promote a PCET with an additive (AH), also involving a suitable base (B). As a consequence, a radical intermediate (radical A) is generated, capable of performing hydrogen abstraction. Finally, according to path *a)* (at the left of Scheme 1.6.2), the photocatalyst (PC), acting in this case as a photoredox catalyst, promotes a SET step resulting in the generation of a radical ion (YW as either a radical anion or a radical cation, depending on the redox outcome of the transformation). The newly formed radical ion intermediate YW might be directly engaged in

hydrogen abstraction or it can rather undergo the loss of a charged moiety (W^+/W^-), evolving in a new radical species (radical Y), which is ultimately responsible for the transformation.

As it was just discussed, VLPC can be conveniently exploited to promote HAT reactions. With this regard, an appropriate compound is needed to interact with the excited state photoredox catalyst in order to generate the HAT performing radical. An HAT reaction performed by such radical can be performed with two different strategies: regeneration of the starting compound (HAT catalyst) or consumption of the hydrogen abstracting species (HAT reactant). In the first case, the compound responsible of HAT upon interaction with the excited state photoredox catalyst can be used in substoichiometric amount, and it can thus be defined as a HAT catalyst. An example is reported by Macmillan, which employs quinuclidine as a HAT catalyst (shown on the left side of **Scheme 1.6.3**) [1.87].

Scheme 1.6.3: HAT catalyst VS HAT reagent approach

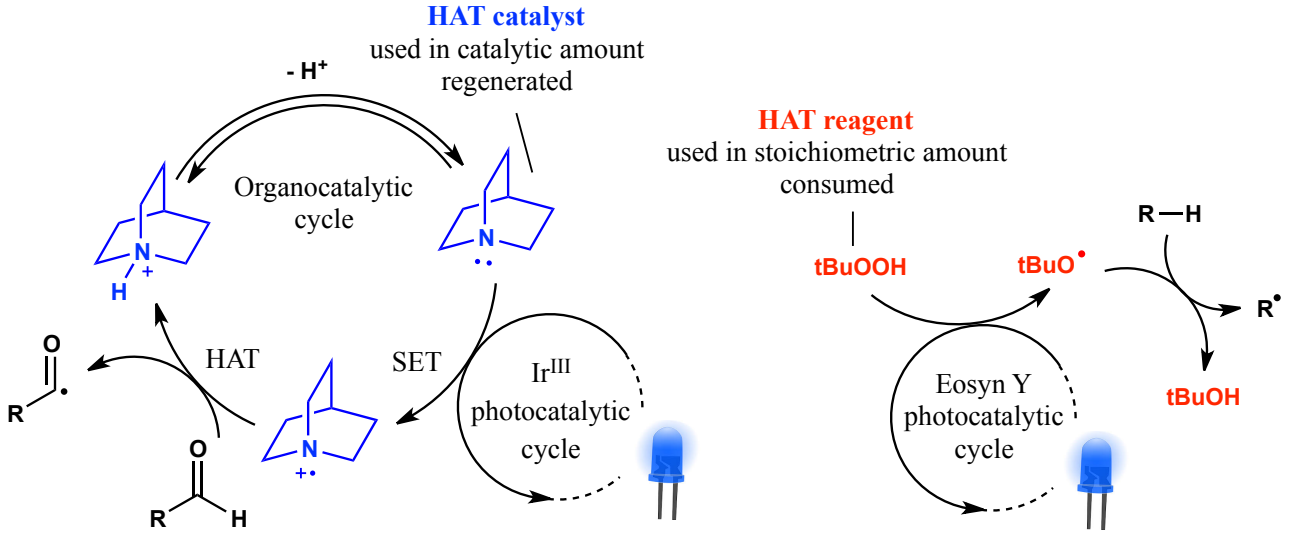

In the second case instead, reactants such as tert-butylhydroperoxide (shown on the right side of **Scheme 1.6.3**)[1.88] or CCl_4 generate a radical which can perform HAT only once, thus requiring their use in stoichiometric amount.

Several examples of mild C(sp^3)–H functionalization methods promoted by catalytic amounts of HAT components, such as thiols[1.89], quinuclidine[1.90][, benzoic acid[1.91] and N-hydroxy compounds[1.92], with cooperative use of photoredox catalysts, were recently reported. Noteworthy, the synthetic utility of these reactions is highly dependent on the strenght of the inherent bond dissociation energy (BDE). As a consequence, reaction control can be problematic when the HAT catalyst has too high BDE while limited applicability can be envisioned when BDE is too low. It is thus evident that, despite the large variety of powerful transformations disclosed with this approach, the general application of a similar methodology could be challenging. One possible solution to this

problem relies in the design of tunable HAT catalysts, as it was demonstrated by Kanai et al, who designed sulfonamides with easily adjustable BDEs via modification of their nitrogen and sulfur functionalization[1.93].

1.7 The chemistry of acyl radicals

Radical chemistry has always taken a backseat to ionic chemistry. This "discrimination" might be imputed to the historically accepted notion that radical species are chaotic, uncontrollable, and mysteriously baffling. Despite these misconceptions, a plethora of useful and elegant chemical transformations has been developed over the years using radical intermediates[1.94].

Among the milestones of radical chemistry, it is certainly worth mentioning Waters's work on the thiol-catalyzed aldehyde homolysis from 1952, an early methodology which provided efficient means of accessing acyl radicals[1.95]. Following, much interest has been directed towards acyl radical chemistry. In fact, the development of acyl radical based methodologies furnished a powerful tool for the construction of carbon-carbon bonds in modern synthetic organic chemistry[1.96]. In particular, acyl radicals are valuable intermediates for the preparation of ubiquitous functional groups in nature such as unsymmetrical ketones and amides. Moreover, the addition of acyl radicals to olefins is a key carbon-carbon bond forming step in the synthesis of natural products and other valuable heterocyclic compounds[1.97].

In view of the appealing features described above, many different methods have been developed for the generation and exploitation of acyl radicals. The reaction of selenoesters with stannyl and tris(trimethylsilyl)silyl radicals has been one of the most practical ways to generate these radical intermediates[1.98]. Other methods concerned the use of acyl hydrazines[1.99] or thiolesters [1.100].

Notably, a common difficulty involved with the chemistry of acyl radicals is their facility to undergo decarbonylation generating a new carbon centered radical and carbon monoxide. As a consequence, depending on the stability of the new radical species, certain kinds of acyl radicals can become difficult to manipulate. Nonetheless, several methodologies have been established to overcome this problem; for example Skrydstrup et al developed a reaction procedure based on samarium iodide to conveniently generate acyl radicals, avoid their decarbonylation, and couple them with olefins[1.101]. Moreover, acyl radicals decarbonylation reaction has even been reversed from problem to solution. In fact, several transition methal catalyzed methodologies to carbonylate carbon centered radicals to achieve acyl radicals have been established[1.102].

In any case, all things considered, not too many methods to generate and utilize acyl radicals have been disclosed; moreover, most of the mentioned methodologies take advantage of aggressive reactants. In fact, unordinary and rather complex reagents, together with relatively harsh conditions, often need to be employed. In the last three years (2015-2018), the synthetic organic chemistry

community have witnessed the number of publications involving acyl radical chemistry spreading like wildfire. The key factor which allowed the intensification in this particular research area has been the utilization of VLPC towards this aim. At the same time, in 2015, the groups of MacMillan and Fu opened the way to this new research field by disclosing the photoredox catalyzed decarboxylative arylation of a-oxo acids[1.103]. On a similar mindstream, synergistically employing VLPC and Nickel catalysis, the same group reported in 2017 another methodolgy to synthesize ketones starting from aldehydes [1.104]. Carboxylic acids also became useful substrates for this kind of reactivity; many research groups investigated the generation of acyl radicals via single electron reduction of transient mixed anhydride intermediates [1.105]. With this regard, it is mandatory to mention the work by Scheffold et al, who pioneered this kind of transformation already in 1983, using light in combination with Vitamin B12[1.106].

Noteworthy, in 2017, the group of Xu disclosed in two different papers the possibility to employ aroyl chlorides as starting materials for the generation of acyl radicals via VLPC[1.107]. This approach has been the inspiration of part of my doctoral work, which will be discussed in detail in **Chapter 5**.

In conclusion, among the very last innovations in this chemistry there are the possibilty to generate acyl radicals from terminal alkynes[1.108] and from the direct deoxygenation of carboxylic acids [1.109]. Everything leads to think that this research field will remain really hot for several years to come, especially keeping into account the lack of methodologies to access aliphatic acyl radicals with respect to aromatic ones. Also this aspect will be further discussed in **Chapter 5**.

1.8 Continuous Flow Photochemistry

This century has witnessed an overwhelming advancement in the understanding and synthesis of organic compounds. By contrast, laboratory technology has remained much the same; in common laboratories reactions are still labor-intensive and are performed in round-bottom flasks housing stirring bars and reflux condensers. This style of chemistry, performed inside a fixed volume reactor, is termed batch chemistry. A change is expected to take place in the years to come with respect to the way we perform chemicals reactions (**Figure 1.8.1**).

In fact, despite the batch approatch is often suitable for chemical transformations, increasing research has demonstrated that flow chemistry can highly surmount it by providing a wide range of benefits. Flow chemistry is defined as the process of performing chemical reactions inside a tube. According to the purpose of the experiment, the tubings can be selected from a wide variety of materials (glass, polymer, metal) and dimensions (from microliter to hectoliter scale). The reaction mixture flowing inside is either prepared in advance or directly within the tubings; different streams of reactant solutions can be merged by means of junctions.

Figure 1.8.1: Past, present and future of the way we perform chemical reactions

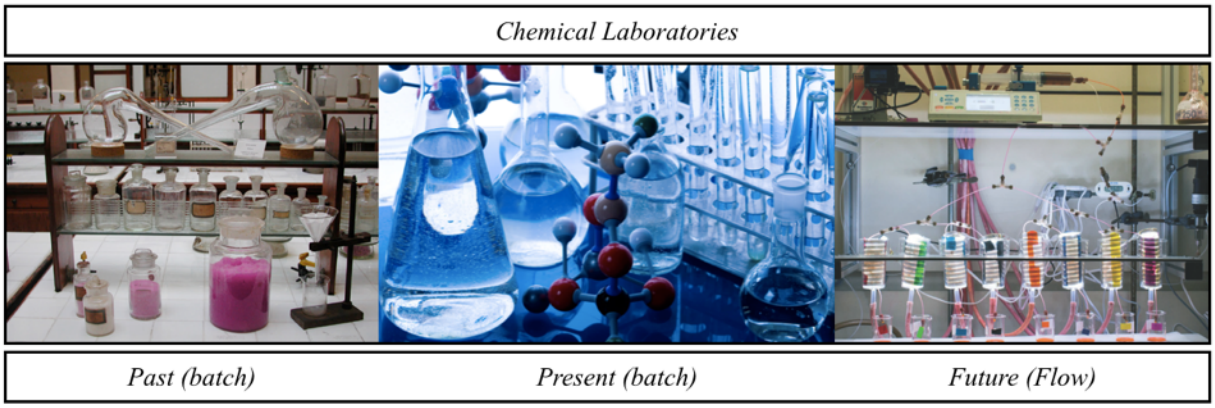

The continuous movement of the solution inside the device is provided by the action of a pump, which can be as simple as a laboratory syringe pump or as complex as an HPLC pump. Many more items can be includesd in the flow reactor path, like for example: valves, junctions, work-up or purification elements, checkpoints for integrated, real-time, on-line analysis and much more. At the end of the tube, the reaction solution containing the product is collected (Scheme 1.8.1).

Scheme 1.8.1: Flow VS batch approach

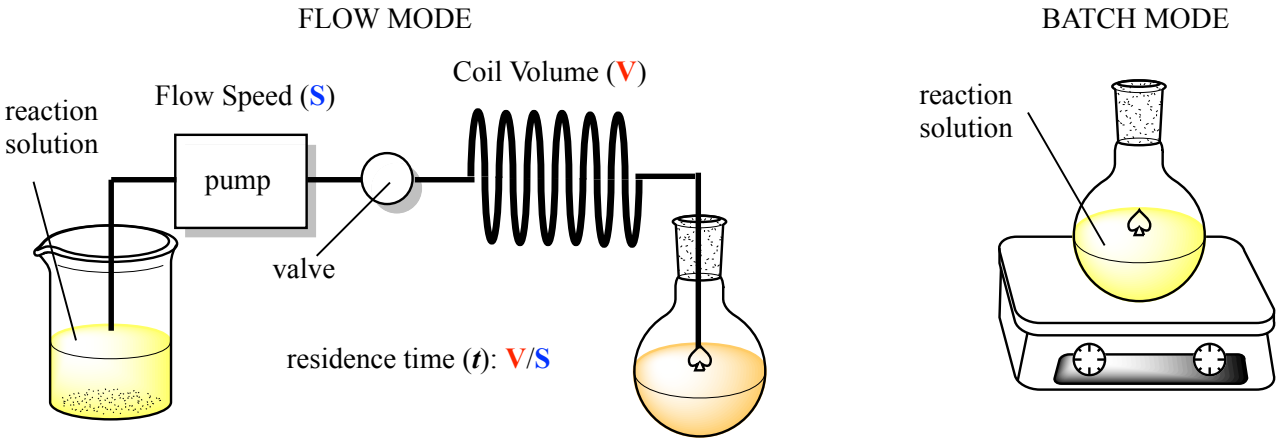

In batch chemistry the reaction time corresponds to the time the reaction is allowed to occur at the desired conditions. In flow chemistry, the reaction time is computed differently; the residence time is the parameter of interest in this case. The residence time (t) is defined as the ratio between the volume of the reactor (V) and the flow speed (S).

Multiple advantages are provided by the use of continuous flow chemistry. To begin with, translating reactions into continuous flow can provide levels of control and automation that are not possible in batch reactions. Interfacing flow systems with computer technology is no big deal nowadays, leading to the possibility to modify reaction parameters, such as the flow speed, without difficulty. Advancements of 'in-line' technology provided the opportunity to explore more complex,

multistep transformations. Due to these facts, reactions become highly repetable and easier to optimize. Compared to a batch reactor, the reaction efficiency of a flow process is improved along with heat to mass transfer, homogenity and mixing[1.110]. All these advantages sum-up and allow the waste production of a flow chemical device to be considerably reduced by performing continuous flow chemistry with respect to batch chemistry. Moreover, the utilization of hazardous compounds is rendered much safer by means of this technology. For example, generating toxic compounds in situ for immediate consumption in sequential reactions avoids stockpiling of risk-prone compounds [1.111]. A continuos flow production eliminates the risk of dealing with huge amounts of toxic compounds deriving from batch reactors which expose the plant personnel to hazardous working conditions. The same is true for potentially explosive compounds. In fact, the destructive potential of a batch reactor going out of control is order of magnitudes more serious than any event taking place in a confined, highly controlled, flow process, which can be managed with much more ease.

Despite the numerous benefits brought by flow chemistry, the main disadvantage connected with its application is related to the clogging of the tubings. In fact, heterogeneous solutions, along with reactions occurring with the precipitation of solids, are often problematic to deal with in flow. The reduced dimensions of the tubes, which can be as thin as few micrometers, make them prone to blockage. The cleaning procedure of such occluded tubes is often made difficult by the low surface of contact with a cleaning solution. As a consequence, the experiment should be planned keeping in mind this eventual difficulty.

The potential of organic synthesis in combination with flow technology is limitless. Examples in the literature demonstrate the successful use of flow chemistry towards applications in transition metal catalysis[1.112], multicomponent reactions[1.113], asymmetric organocatalysis[1.114], polymer chemistry[1.115], multistep natural product synthesis[1.116] and much more. Separation and recycling methods of transion metal catalysts can be conveniently set-up in flow to design synthetic routes in agreement with the principles of green chemistry[1.117]. Convenient use of flow set-ups has been involved with reactive, unstable intermediates and suppress otherwise unavoidable side-reactions[1.118]. Flow chemistry is playing an increasing role in the realization of synthetic routes for the preparations of drug candidates, API (active pharmaceutical ingredient) compounds[1.119].

Not only researchers are turning their attention towards the appealing features of flow chemistry, but also the world of industry. It is well known than any process improvement can be translated in huge monetary savings on industrial level, but this is particularly true for chemical industries, which commonly modify their plants not any sooner than every fifty years. For these reasons, flow chemistry, which was very much underestimated a couple of decades ago, is fastly catching on also on industrial level. Along all the benefits already discussed above, the easier scalability and optimization of flow reactions with respect to batch ones make them highly desirable for industrial production. R&D (research and development) departments in companies can save remarkable time and efforts by scaling-up flow processes with respect to batch ones. Looking towards flow

chemistry as a new process intensification method, examples in the application of flow conditions with microwave assited, high temperature and high pressure regime in industry are reported in the literature[1.120]. For these reasons, the production of prexasertib monolactate monohydrate, suitable for use in human clinical trials, was conveniently realized in flow conditions, according to CGMP (current good manufacturing practices)[1.121].

Among the many research fields exploiting flow chemistry, photochemistry and photocatalysis are certainly among the ones gaining the biggest benefit from it. In fact, the requirement of light-permeation, which is fundamental for the successful occurrence of a photochemical reaction, is very much satisfied in a flow reactor. Even more so, the thin diameter of the tubings employed in flow reactors allow for optimal light-permeation and thus optimal reaction efficiency. At the sime time, the undesired phenomenon of overirradiation, which can lead to undesired reactivity in batch mode, can be completely suppressed. In fact, in flow conditions, the molecules inside the solution are homogeneously absorbing the radiation with a minimized diffusion in comparison with batch conditions (**Scheme 1.8.2**).

Scheme 1.8.2: Batch VS flow approach in photochemistry

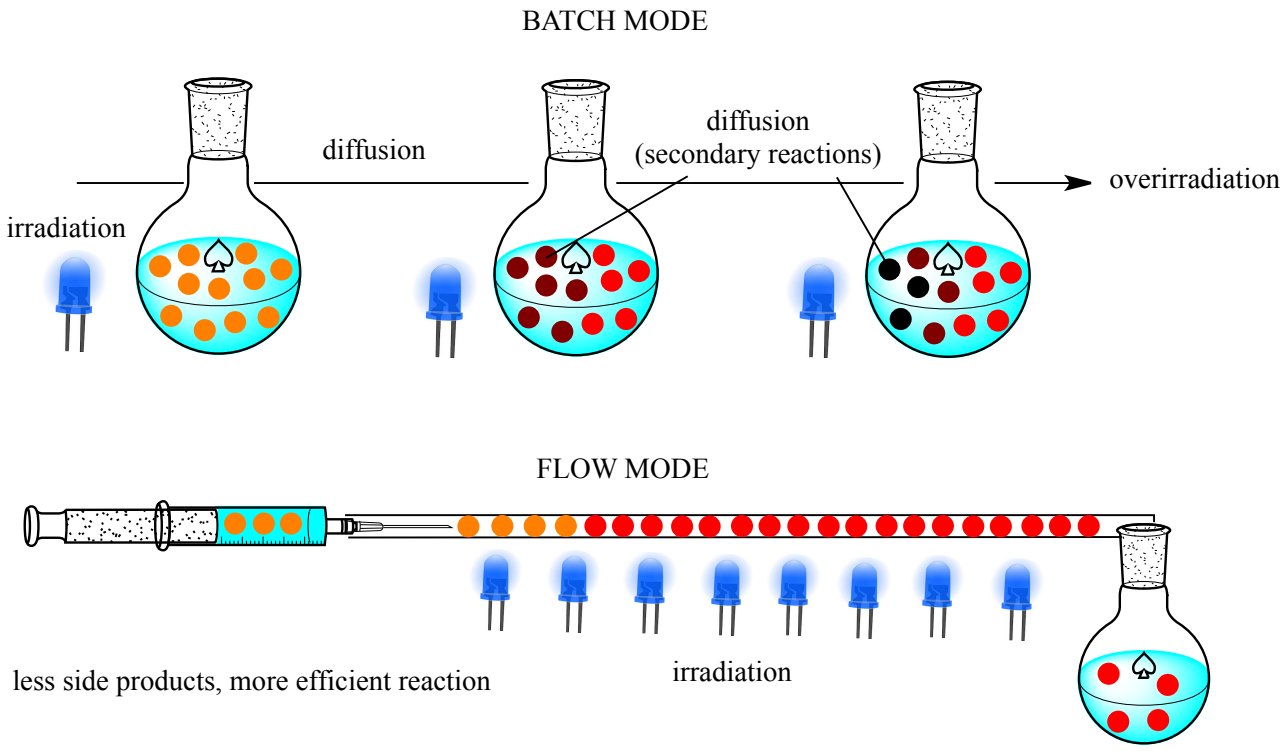

In comparison with batch conditions, the light radiation need to cross the solution for a shorter path lenght inside a flow reactor thus leading to a higher photon transport, as it is stated by the Lambert-Beer Law.

In relation to what has been previously discussed, the requirement for the application of flow photochemistry involves the use of materials transparent to the radiation generated by an efficient light source. Commonly, quartz, glass or polymers such as PTFE (Politetrafluoroethylene), FEP (Fluorinated Ethylene Propylene) and PMMA (Polimethylmethacrylate), are the standard constituting materials for UV-VIS transparent radiations. In particular, polymer based tubes are composed of cheap, easy to handle stable and flexible materials although they can suffer from swelling and they are often uncompatible with high temperatures. On the other hand, glass and quartz can resist to considerable heating but they constitute exclusively rigid tubings being at the same time more expensive than plastic materials. Light sources are highly available in the market for a wide range of application and prices. In the recent years, OLEDs are dominating the scene of light sources, possessing all the desirable benefits such as low prices, long lifetime, high efficiency, precise wavelenght emission and low energy consumption.

Nowadays, a high percentage of the publications in the topic of photocatalysis involve the utilization of flow chemistry. Many outstanding papers have been released to the chemical audience, sharing the advantageous application of flow chemistry. Nonetheless, it might be observed that, most of the times, the equipments employed by the authors differ quite a lot from one another. A general classification of the devices employed can be made on the basis of three parameters: internal or external irradiation, monophasic or multiphasic solution, homogeneous or heterogeneous catalysis. Harvesting the maximum amount of photons is certainly economically relevant; for this reason devices provided with internal irradiation, that is a light source irradiating from the insides of the instrument, are generally more efficient. The typical set-up for such a device is the so called 'immersion-well system' (**Figure 1.8.2**) represented by the Booker-Milburn apparatus [1.122].

Figure 1.8.2: Internal-irradiation continuous and semicontinuous flow assets

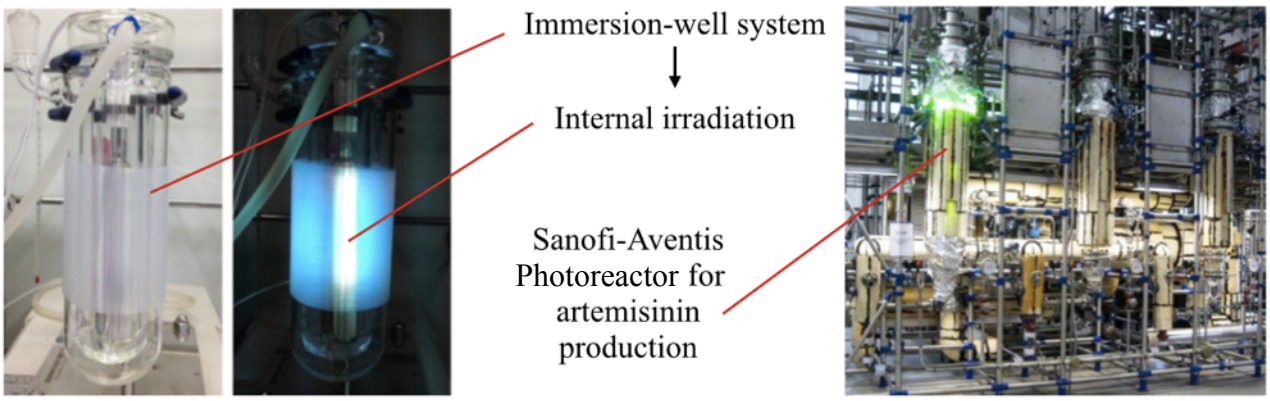

Sanofi Aventis employs an immersion-well reactor for the industrial production of artemisinin[1.123]. External irradiation devices are more easily built; any transparent coil can be irradiated by an external light source such as simple sunlight. The main disadvantage connected with external irradiation relies in the difficulty connected with directing the light towards the zone of interest. On the other hand, along with the benefits of devices easier to design, build and clean, the external irradiation allows for fancier applications. For example, Opatz et al designed a so called 'sunflow' reactor building a rotating device which could follow the orientation of the sun to better harvest sunlight[1.124]. Another very interesting work from Poliakoff et al describes the so called 'Photovap', which is a rotating semicontinuous flow device based on a modified rotary evaporator (Figure 1.8.3)[1.125].

Figure 1.8.3: Photovap rotating device by Poliakoff et al

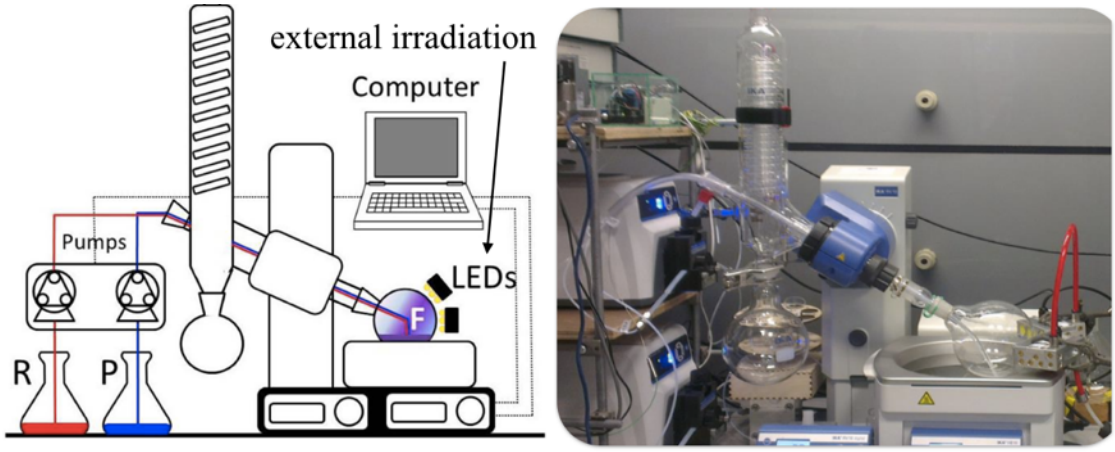

The smart idea of generating an efficiently irradiated thin film in flow was shared by other research groups, like the groups of Raston and Stubbs, who applied it to their microfluidic vortex device [1.126].

In contrast to classic single channel devices, employed for monophasic solution reactions, more complex reactors are designed for multiphasic gas-liquid solutions. The photochemistry of singlet oxygen, requiring the interaction of gas and liquid phase, is in fact widely explored in flow[1.127]. With this regard, the tube in tube reactor[1.128], based on a semipermeable separating membrane, along with the falling film reactor[1.129], are among the most commonly utilized devices.

Coming to original applications, inspired by the oxygen photochemistry taking place within the atmosphere, Vassilikogiannakis et al developed the 'NebPhotOx', a continuous flow system based on a pneumatic nebulizer[1.130].

A very high perentage of the publications in flow photochemistry deals with homogeneous catalysis; with VLPC applications being among the most important ones[1.131]. While being at the

moment underdeveloped, research on heterogeneous phase continuous flow photocatalysis will be certainly among the main research topics in the next years. A number of enabling technologies such as catalyst support, packed-bed reactors and structural packaging, in combination with the innovations in illumination technology, will certainly allow the research groups to unravel many new attractive discoveries in this field.

1.9 References

1.1
A. Einstein *Physikalische Zeitschrift* **1917**, 18, 121-128.

1.2
K. Glusac *Nature Chem.* **2016**, 8, 734–735.

1.3
H. Trommsdorff *Eur. J. Org. Chem.* **1834**, *11*, 2, 190-207.

1.4
A. Natarajan, C. K. Tsai, S. I. Khan, P. Mc Carren, K. N. Houk, M. A. Garcia-Garibay *J. Am. Chem. Soc.* **2007**, *129*, 32, 9846-9847.

1.5
Matsuura T.; Sata Y.; Katsuyuki O. *Tetrahedron Lett*. **1968**, *44*, 4627-4630.

1.6
A. Albini, M. fagnoni *Green Chem.*, **2004**, *6*, 1-6.

1.7
Barton D. H. R., Moss G. P.; Whittle J. A. *J. Chem. Soc. C* **1968**,0, 1813-1818.

1.8
S. L. Y. Tang; R. L. Smithb; M. Poliakoff *Green Chem.* **2005**, *7*, 761-762.

1.9
A. Albini; M. Fagnoni *Chem. Sus. Chem.* **2008**, *1*, 63–66.

1.10
(a) G. D. Zhu; W. H. Okamura *Chem.Rev.* **1995**, *95*, 1877-1952.
(b) N. A. Anderson; J. J. Shiang; R. J. Sension J. Phys. Chem. A **1999**, *103*, 10730–10736.
1.11

K. I. Öberg *Chem. Rev.* **2016**, *116*, 17, 9631-9663.

1.12
T. Bach; J. P. Hehn *Angew. Chem. Int. Ed.* **2011**, *50*, 1000-1045.

1.13
S. Chatani; C. J. Kloxinb; C. N. Bowman *Polym. Chem.* **2014**, *5*, 2187-2201.

1.14
B. P. Chan *Tissue Engineering: Part B* **2010**, 16, 5, 509-522.

1.15
M. C. DeRosa; R. J. Crutchley *Coord. Chem. Rev.* **2002**, 351-371.

1.16
E. R. Welin; C. Le; D. M. Arias-Rotondo; J. K. Mc Cusker; D. W. C. MacMillan *Science* **2017**, *355*, 6323, 380-385.

1.17
K. Maeda; K. Domen *J. Phys. Chem. Lett*. **2010**, *1*, 18, 2655-2661.

1.18
M. N. Chonga; B. Jin; C. W. K Chow; C. Saint *Water Res.* **2010**, 44, 2997-3027.

1.19
M. A. Fox; M. T. Dulay *Chem. Rev.* **1993**, *93*, 341-357.

1.20
M. H. Shaw; J. Twilton; D. W. C. MacMillan *J. Org. Chem.* **2016**, *81*, 6898−6926.

1.21
N. A. Romero; D. A. Nicewicz *Chem. Rev.* **2016**, *116*, 17, 10075–10166.

1.22
M. H. Shaw; J. Twilton; D. W. C. MacMillan *J. Org. Chem.* **2016**, *81*, 6898-6926.

1.23
C. K. Prier; D. A. Rankic; D. W. C. MacMillan *Chem. Rev.* **2013**, *113*, 5322-5363.

1.24

D. Zheng; X. N. Cao; X.Wang *Angew. Chem. Int. Ed.* **2016**, 55, 11512–11516.

1.25
Ueda Y.; Takeda H.; Yui T.; Koike K.; Goto Y.; Inagaki S.; Ishitani O. ChemSusChem **2015**, *8*, 439-442.

1.26
K. Kalyanasundaram; M. Gratzel *Coord. Chem. Rev.* **1998**, *177*, 347−414.

1.27
D. M. Hedstrand; W. H. Kruizinga; R. M. Kellogg *Tetrahedron Lett.* **1978**, *19*, 1255−1258.

1.28
K. Hironaka; S. Fukuzumi; T. Tanaka *J. Chem. Soc. Perkin Trans. 2* **1984**, 1705-1709.

1.29
H. Cano-Yelo; A. Deronzier *Tetrahedron Lett.* **1984**, *25*, 5517−5520.

1.30
H. Cano-Yelo; A. Deronzier *J. Chem. Soc. Perkin Trans. 2* **1984**, 1093-1098.
H. Cano-Yelo; A. Deronzier *J. Photochem.* **1987**, *37*, 315−321.

1.31
Y. Miyake; K. Nakajima; Y. Nishibayashi *Chem. Commun.* **2013**, 49, 7854-7856.

1.32
M. O. Konev, E. R. Jarvo *Angew. Chem. Int. Ed.* **2016**, 55, 11340-11342.

1.33
J. C. Tellis, D. N. Primer, G. A. Molander *Science* **2014**, 345, 433-436.

1.34
N. Miyaura, A. Suzuki *Chem. Rev.* **1995**, *95*, 2457-2483.

1.35
K. L. Skubi; T. R. Blum; T. P. Yoon *Chem. Rev.* **2016**, *116*, 17, 10035–10074.

1.36

M. N. Hopkinson; A. Tlahuext-Aca; F. Glorius *Acc. Chem. Res.* **2016**, *49*, 10, 2261–2272.

1.37

X. Zhang; D. W. C. MacMillan *J. Am. Chem. Soc*. **2017**, *139*, 11353−11356.

1.38

(a) D. Kalyani, K. B. McMurtrey; S. R. Neufeldt, M. S. Sanford *J. Am. Chem. Soc.* **2011**, 133, 18566-18569.
(b) X. Z. Shu; M. Zhang; Y. He; H. Frei; F. D. Toste *J. Am. Chem. Soc.* **2014**, 136, 5844-5847.

1.39

(a) E. B. Corcoran; M. T. Pirnot; S. Lin; S. D. Dreher; D. A. Di Rocco; I. W. Davies; S. L. Buchwald; D. W. C. MacMillan *Science* **2016**, *353*, 279-283.
(b) M. S. Oderinde; M. Frenette; D. W. Robbins; B. Aquila; J. W. Johannes *J. Am. Chem. Soc.* **2016**, *138*, 1760-1763.

1.40

X. Lang, J. Zhaob; X. Chen *Chem. Soc. Rev*. **2016**, 45, 3026–3038.

1.41

H. G. Cha; K. S. Choi *Nat. Chem.* **2015**, *7*, 328–333.

1.42

Park J. H., Lee S. H., Cha G. S., Choi D. S., Nam D. H., Lee J. H., Lee J. K., Yun C. H., Jeong K. J., Park C. B. *Angew. Chem. Int. Ed*., **2015**, *54*, 969–973.

1.43

Zollinger H. *Acc. Chem. Res.*, **1973**, *6*, 10, 335–341.

1.44

S. Milanesi, A. Albini, M. Fagnoni *J. Org. Chem.*, **2005**, *70*, 2, 603–610.

1.45

Pratsch G., Heinrich M.R. **2011** Modern Developments in Aryl Radical Chemistry. In: Heinrich M., Gansäuer A. (eds) Radicals in Synthesis III. Topics in Current Chemistry, vol 320. Springer, Berlin, Heidelberg.

1.46

Meerwein H.; Buchner E.; van Emster K. *J. Prakt. Chem*. **1939**, *152*, 237–266.

1.47

T. Sandmeyer *Berichte der deutschen chemischen Gesellschaft* **1884**, *17*, 3, 1633–1635.

1.48
R. Pschorr Ber. 1896, 29, 496-501.

1.49
M. Gomberg; W. E. Bachmann *J. Am. Chem. Soc.* **1924**, *42*, 10, 2339–2343.

1.50
M. Lang; P. Spiteller; V. Hellwig; W. Steglich *Angew. Chem. Int. Ed.* **2001**, *40*, 1704-1705.

1.51
M. R. Heinrich *Chem. Eur. J.* **2009**, *15*, 820 – 833.

1.52
D. P. Hari; T. Hering; B. König *Angew. Chem. Int. Ed.* **2014**, *53*, 725 –728.

1.53
D. P. Hari; B. König *Angew. Chem. Int. Ed.* **2013**, *52*, 4734 – 4743.

1.54
D. P. Hari; P. Schroll; B. König J. Am. Chem. Soc. **2012**, 134, 2958−2961

1.55
D. P. Hari; T. Hering; B. König *Org. Lett.* **2012**, *14*, 20, 5334-5337.

1.56
same reference as indicated in 1.52

1.57
P. A. Wender *Chem. Rev.* **1996,** *96*, 1-2.

1.58
Masakatsu Shibasaki, Motomu Kanai e Tsuyoshi Mita, The Catalytic Asymmetric Strecker Reaction in Organic Reactions, vol. 70, nº 1, **2008**

1.59
(a) Ugi I.; Meyr R.; Fetzer U.; Steinbrückner C. *Angew. Chem.* **1959**, *71*, 11, 386.
(b) Ugi I.; Steinbrückner C. *Angew. Chem.* **1960**, *72*, 7, 267–268.
(c) Ugi, I. *Angew. Chem. Int. Ed.* 1962, 1, 1, 8–21.

1.60
Burke M. D.; Schreiber S. L. *Angew. Chem., Int. Ed.* **2004**, *43*, 46-58.

1.61
Elders N.; van der Born D.; Hendricks L. J. D.; Timmer B. J. J., Krause A.; Janssen E.; de Kanter F. J. J.; Ruijter E.; Orru R. V. A. *Angew. Chem. Int. Ed.* **2009**, *48*, 5856-5859.

1.62
J. Tsoung, J. Panteleev, M. Tesch, M. Lautens *Org. Lett.* **2014**, *16*, 1, 110-113.

1.63
A. G. Francisco; J. Fañanás, F. Rodríguez *Eur. J. Inorg. Chem.* **2016**, *9*, 1306-1313.

1.64
same reference as indicated in 1.36

1.65
M. N. Hopkinson; M. Sahoo; F. Glorius *Adv. Synth. Catal.* **2014**, *356*, 2794–2800.

1.66
M. N. Hopkinson; B. Sahoo; F. Glorius *Org. Lett.* **2013**, *15*, 9, 2092-2095.

1.67
Hydrogen-Transfer Reactions Eds.: J. T. Hynes, J. P. Klinman, H. H. Limbach, R. L. Schowen, Wiley-VCH Verlag GmbH & Co., **2007**.

1.68
S. Hammes-Schiffer; A. A. Stuchebrukhov *Chem. Rev.* **2010**, *110*, 6939–6960.

1.69
same reference as indicated in 1.67

1.70
T. Groves in Cytochrome P450: Structure, Mechanism, and Biochemistry, 3rd ed., Ed.: P. R. Ortiz de Montellano, Kluwer Academic/Plenum Publishers, New York, **2005**.

1.71
R. Sarpong *Beilstein J. Org. Chem.* **2016**, *12*, 2315–2316.
1.72

J. J. Li, C-H Bond Activation in Organic Synthesis, CRC Press, **2017**.

1.73
K. Godula, D. Sames *Science* **2006**, *312*, 5770, 67-72.

1.74
J. F. Hartwig; M. A. Larsen; *ACS Cent. Sci.* **2016**, *2*, 281−292.

1.75
T. Cernak; K. D. Dykstra; S. Tyagarajan; P. Vachalb; S. W. Krskab *Chem. Soc. Rev*., **2016**, *45*, 546-576.

1.76
same reference as indicated in 1.75

1.77
J. Wencel-Delord; F. Glorius *Nat. Chem.* **2013**, *5*, 369–375.

1.78
K. Zhang, B. M. Shafer, M. D. Demars, H. A. Stern, R. Fasan *J. Am. Chem. Soc.* **2012**, *134*, 18695-18704.

1.79
K. Beydoun, M. Zaarour, J. A. G. Williams; H. Doucet; V. Guerchais *Chem. Commun.* **2012**, *48*, 1260-1262.

1.80
T. Dröge, A. Notzon, R. Fröhlich, F. Glorius *Chem. Eur. J.* **2011**, *17*, 11974–11977.

1.81
K. Qvortrup, D. A. Rankic, D. W. C. MacMillan *J. Am. Chem. Soc.* **2014**, *136*, 2, 626-629.

1.82
(a) Fokin A.; Schreiner P. R. *Chem. Rev.* **2002**, *102*, 1551-1594.
(b) Yi H.; Zhang G.; Wang H.; Huang Z.; Wang J.; Singh A. K.; Lei A. *Chem. Rev.* **2017**, *117*, 9016-9085.
(c) Matcha K.; Antonchick A. P. *Angew. Chem. Int. Ed.* **2013**, *52*, 2082-2086.
(d) Ji J.; Liu P.; Sun P. *Chem. Commun.* **2015**, *51*, 7546-7549.

1.83

(a) D. Wang; H. Jiang; X. Zong; Q. Xu; Y. Ma; G. Li; C. Li *Chem. Eur. J.* **2014**, *20*, 1275-1282.
(b) R. K. Quinn; Z. A. Könst; S. E. Michalak; Y. Schmidt; A. R. Szklarski; A. R. Flores; S. Nam; D. A. Horne; C. D. Vanderwal; E. J. Alexanian *J. Am. Chem. Soc.* **2016**, *138*, 696-702.

1.84
G. Majetich; K. Wheless *Tetrahedron* **1995**, 51, 7095-7129.

1.85
D. Ravelli; M.Fagnoni; T. Fukuyama; T. Nishikawa; I. Ryu *ACS Catal*. **2018**, *8*, 701–713.

1.86
L. Capaldo, D. Ravelli *Eur. J. Org. Chem.* **2017**, *15*, 2056–2071.

1.87
X. Zhang, D. W. C. MacMillan *J. Am. Chem. Soc.* **2017**, *139*, 11353−11356.

1.88
(a) D. Xia; Y. Li; T. Miao; P. Lia; L. Wang *Green. Chem.* **2017**, *19*, 1732–1739.
(b) M. H. Keylor, J. E. Park, C. J. Wallentin, C. R. J. Stephenson *Tetrahedron* **2014**, *70*, 4264-4269.

1.89
K. Qvortrup, D. A. Rankic, D. W. C. MacMillan *J. Am. Chem. Soc.*, **2014**, *136*, 626-629.

1.90
Jeffrey J. L., Terrett J. A., MacMillan D. W. C. *Science* **2015**, *346*, 1532-1536.

1.91
S. Mukherjee; B. Maji; A. Tlahuext-Aca; F. Glorius *J. Am. Chem. Soc.* **2016**, *138*, 16200-16203.

1.92
X. Liu; L. Lin; X. Ye; C. H. Tan, Z. Jiang *J. Org. Chem.* **2017**, 6, 422-425.

1.93
H. Tanaka, K. Sakai, A. Kawamura, K. Oisaki, M. Kanai *Chem. Commun.*, **2018**, *54*, 3215-3218.

1.94
(a) M. Yan; J. C. Lo; J. T. Edwards; P. S. Baran *J. Am. Chem. Soc.* **2016**, *138*, 12692-12714.
(b) Kochi J. K., Ed. Free Radicals, Vol. 1: Dynamics of Elementary Processes; Wiley-Interscience: New York, **1973**.
(c) Curran D. P. *Synthesis* **1988**, 6, 417-439.
(d) Jasperse C. P.; Curran D. P.; Fevig T. L. *Chem. Rev.* **1991**, *91*, 1237-1286

(e) Radicals in Organic Synthesis, 1st ed.; Eds.: Renaud P., Sibi M.; Wiley-VCH: Weinheim, **2001**.
(f) Togo H. Advanced Free Radical Reactions for OrganicSynthesis; Elsevier: Amsterdam, **2003**.
(g) Zard S. Z. Radical Reactions in Organic Synthesis; Oxford University Press: Oxford, **2003**.

1.95
E. F. P. Harris, W. A. Waters *Nature* **1952**, *170*, 212–213.

1.96
C. Chatgilialoglu *Chem. Rev.* **1999**, *99*, 1991-2069.

1.97
(a) L. Zhang; M. Koreeda *Org. Lett.* **2004**, *6*, 4, 537-540.
(b) M. L. Bennasar; T. Roca; F. Ferrando *Org. Lett.* **2004**, 6, 759-762.

1.98
I. Ryu; N. Sonoda *Chem. Rev.* **1996**, *96*, 177-194.

1.99
S. Bath, N. M. Laso, H. Lopez-Ruiz, B. Quiclet-Sirea, S. Z. Zard *Chem. Commun.* **2003**, 204-205.

1.100
L. Benati; G. Calestani; R. Leardini; M. Minozzi; D. Nanni; P. Spagnolo; S. Strazzari *Org. Lett.* **2003**, *5*, 1313-1316.

1.101
C. M. Jensen; K. B. Lindsay; R. H. Taaning; J. Karaffa; A. M. Hansen; T. Skrydstrup *J. Am. Chem. Soc.* **2005**, *127*, 6544-6545.

1.102
S. Sumino, A. Fusano, T. Fukuyama, I. Ryu *Acc. Chem. Res.* **2014**, *47*, 5, 1563-1574.

1.103
(a) L. Chu, J. M. Lipshultz, D. W. C. MacMillan *Angew. Chem. Int. Ed.* **2015**, *54*, 7929–7933.
(b) G. Z. Wang, R.Shang; W. M. Cheng, Y. Fu *Org. Lett*. **2015**, *17*, 4830-4833.

1.104
X. Zhang; D. W. C. MacMillan *J. Am. Chem. Soc.* **2017**, 139, 11353-11356.

1.105

(a) G. Bergonzini; C. Cassani; C.J. Wallentin *Angew. Chem. Int. Ed.*, **2015**, *54*, 14066-14069.
(b) S. Dong; G. Wu; X. Yuan; C. Zoua; J. Ye *Org. Chem. Front.*, **2017**, *4*, 2230-2234.
(c) C. L. Joe; A. G. Doyle *Angew. Chem. Int. Ed.* **2016**, 55, 4040-4043.
(d) J. Amani, G. A. Molander *Org. Lett.* **2017**, *19*, 3612−3615.

1.106
R. Scheffold; R. Orlinski *J. Am. Chem. Soc* **1983**, *105*, 7200-7202.

1.107
(a) C. G. Li, G. Q. Xu, P. X. Xu *Org. Lett.* **2017**, *19*, 512−515.
(b) M. Xu, J. Q. Chen, D. Liu, Y. Bao, Y. M. Lianga, P. F. Xu *Org. Chem. Front*. **2017**, *4*, 1331-1335.

1.108
M. Zhang, J. Xie, C. Zhu *Nature Comm.* **2018**, *9*, 1-10.

1.109
S. Sultan; M. A. Rizvi; J.Kumar; B. A. Shah *Chem. Eur. J.* **2018**, *24*, 10617-10620.

1.110
P. D. Morse, R. L. Beingessner, T. F. Jamison *Isr. J. Chem.* **2017,** *57*, 218-227.

1.111
(a) Gutmann B., Cantillo D., Kappe C. O. *Angew. Chem. Int. Ed.* **2015**, *54*, 6688-6728.
(b) M. Movsisyan, E. I. P. Delbeke, J. K. E. T. Berton, C. Battilocchio, S. V. Leyb, C. V. Stevens *Chem. Soc. Rev.* **2016**, *45*, 4892–4928.

1.112
J. Wegner, S. Ceylana, A. Kirschning *Chem. Commun.* **2011**, *47*, 4583–4592.

1.113
N. Pagano, A. Herath, N. D. P. Cosford *J. Flow Chem.* **2011**, *1*, 28–31.

1.114
I. Atodiresei, C. Vila, M. Rueping *ACS Catal.* **2015**, *5*, 3, 1972–1985.

1.115
C. H. Hornung; C. Guerrero-Sanchez; M. Brasholz; S. Saubern; J. Chiefari; G. Moad; E. Rizzardo; S. H. Thang *Org. Process Res. Dev.* **2011**, *15*, 593–601.
1.116

C. H. Hornung, C. Guerrero-Sanchez, M. Brasholz, S. Saubern, J. Chiefari, G. Moad, E. Rizzardo, S. H. Thang *Chem. Soc. Rev.* **2017**, *46*, 1250-1271.

1.117
I. Vural Gürsel, T. Noël, Q. Wanga, V. Hessel *Green Chem.* **2015**, *17*, 2012-2026.

1.118
H. Usutani; D. G. Cork *Org. Process Res. Dev.* **2018**, *22*, 6, 741-746.

1.119
D. L. Huges *Org. Process Res. Dev.* **2018**, 22, 1, 13-20.

1.120
R. Morschhäuser, M. Krull, C. Kayser, C.Boberski, R. Bierbaum; P. A. Püschner, T. N. Glasnov, C. O. Kappe *Green Process Synth* **2012**, *1*, 281–290.

1.121
K. P. Cole1, J. McClary Groh, M. D. Johnson, C. L. Burcham, B. M. Campbell, W.D. Diseroad, M. R. Heller, J. R. Howell, N. J. Kallman, T. M. Koenig, S. A. May, R. D. Miller, D.Mitchell, D. P. Myers, S. S. Myers, J. L. Phillips, C. S. Polster, T. D. White, J. Cashman, D. Hurley, R. Moylan, P. Sheehan, R. D. Spencer, K. Desmond, P. Desmond, O. Gowran *Science* **2017**, 356, 1144–1150.

1.122
Zhang Y., Blackman M. L., Leduc A. B., Jamison T. F. *Angew. Chem. Int. Ed.* **2013**, *52*, 4251-4255.

1.123
J.Turconi; F. Griolet; R. Guevel; G. Oddon; R. Villa; A. Geatti; M. Hvala; K. Rossen; R. Göller; A. Burgard *Org. Process Res. Dev.* **2014**, *18*, 3, 417-422.

1.124
A. M. Nauth; A. Lipp; B. Lipp; T. Opatz *Eur. J. Org. Chem.* **2017**, 15, 2099-2103.

1.125
C.A. Clark; D. S. Lee; S. J. Pickering; M. Poliakoff; M. W. George *Org. Process Res. Dev.* **2016**, *20*, 10, 1792-1798.

1.126
Lyzu Y., Xianjue C., A. K. Stubbs, L. C. Raston *Scientific Reports* 2013, 3, 2282, 1-6.

1.127

(a) P. R. Ogilby *Chem. Soc. Rev.* **2010**, *39*, 3181-3209.
(b) A. A. Ghogare; A. Greer *Chem. Rev.* **2016**, *116*, 17, 9994-10034.

1.128
L. Yang, K. F. Jensen *Org. Process Res. Dev.* **2013**, *17*, 6, 927-933.

1.129
K. Jähnisch, U. Dingerdissen *Chem. Eng. Technol.* **2005***,* 28, 4, 426 - 427.

1.130
G. I. Ioannou, T. Montagnon, D. Kalaitzakis, S. A. Pergantis, G.
Vassilikogiannakis *ChemPhotoChem* **2017**, *1*,173-177.

1.131
Z. J. Garlets, J. D. Nguyen, C. R. J. Stephenson *Isr. J. Chem.* **2014**, *54*, 351–360.47

CHAPTER 2:
PHOTOCATALYZED SYNTHESIS OF ISOCHROMANONES AND ISOBENZOFURANONES UNDER BATCH AND FLOW CONDITIONS

In this chapter, the first part of my doctoral research work will be discussed. With my first Ph.D. project, a synthetic methodology leading to three different heterocyclic scaffolds by means of VLPC was achieved. The herein reported research work resulted in a scientific publication[2.1].

2.1 Start of the doctoral research work and initial aims

My doctoral research work started in November 2015 in the BioOrganic chemistry group Genova (BOG group) which is seated in the Department of Chemistry and Industrial Chemistry (DCCI) belonging to the University of Genova, Italy. I was assigned to the supervision of Prof. Andrea Basso, whose main research interests are centered around the topics of Diversity Oriented Synthesis (DOS), MCRs and Photochemistry. Together with my supervisor, we decided to start investigating the research field of VLPC, attracted by the potential of this methodology, as demonstrated by the increasing number of publications related to it. Despite our research group had no previous experience in the field of VLPC, we started this new research line with enthusiasm, aiming to broaden the research interests of the group.

My doctoral project started with the aim to develop new MCRs by means of VLPC. To our eyes, it was in fact attractive to apply the experience of my research group in MCRs in the new light of VLPC. Inspiration was taken by the work of Prof. Bukhard König and his research group, which is very active on this research field as it was mentioned in **Chapter 1**. Shortly before the beginning of my doctoral activity, this research group disclosed a new MCR based on a Photoredox catalyzed Meerwein addition reaction[2.2]. With this intermolecural amino-arylation of alkenes methodology, a four components reaction involving an arendiazonium tetrafluoroborate ***2.1***, an alkene ***2.2***, a nitrile ***2.3*** and water was developed.

Scheme 2.1.1: Intermolecular amino-arylation of alkenes by König et al

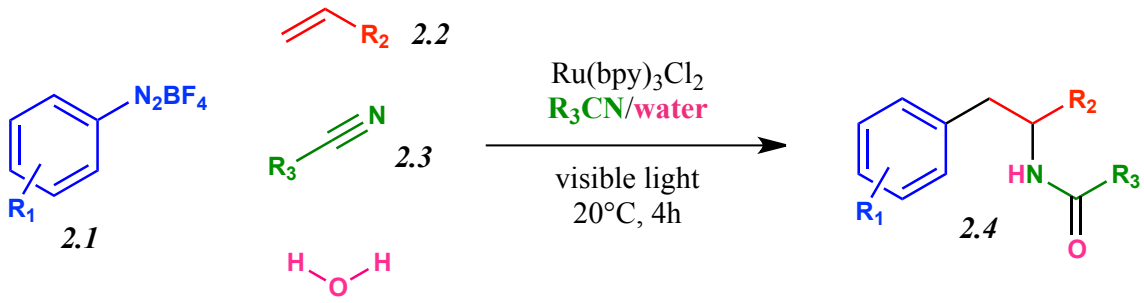

This MCR gives efficient access to different types of amides ***2.4*** under mild reaction conditions and tolerates a broad range of functional groups. Up to three different elements of diversity (since water brings no diversity input in the final product) can be introduced in the reaction product of formula ***2.4***. The mechanism of the reaction, as reported by the authors, is depicted in **Scheme 2.1.2**.

Scheme 2.1.2: Reaction mechanism

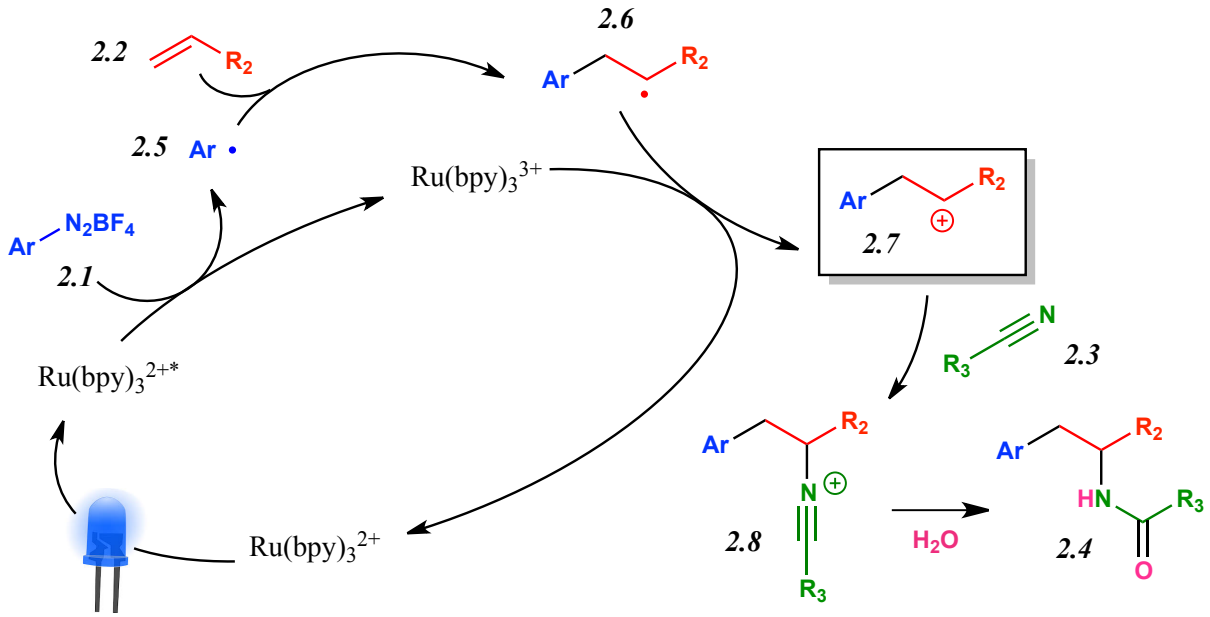

Following the visible light promoted excitation of the photoredox catalyst, an aryl radical ***2.5*** is initially formed by a SET from the excited state of $[Ru(bpy)_3]^{2+}$* to the diazonium salt ***2.1***. Addition of such aryl radical to the alkene ***2.2*** (Meerwein-type addition) yields the corresponding radical intermediate ***2.6***. The oxidation of the radical intermediate ***2.6*** to the key cationic intermediate ***2.7*** regenerates the active species of the ruthenium catalyst. Finally, the carbenium intermediate ***2.7*** is attacked by a nitrile ***2.3*** (Ritter-type addition), followed by hydrolysis, to give the amino-arylated product ***2.4***.

Aiming to develop a similar MCR, we decided to focus our attention on the cationic intermediate ***2.7*** highlighted in **Scheme 2.1.2**. In particular, we wondered weather we could establish a methodology to attack such carbocation with different nucleophiles, thus developing new MCRs (**Scheme 2.1.3**).

We reasoned that we could reproduce the well-established photoredox cycle described in **Scheme 2.1.2** to generate the target carbocation intermediate ***2.7*** in different reaction conditions, with the aim to trap the carbocation with a nucleophile. To begin with, the literature methodology was reproduced to assess whether our equipment was suitable for VLPC.

Scheme 2.1.3: Investigations towards new MCRs

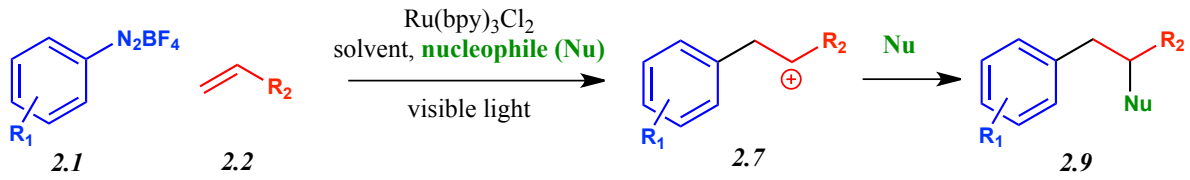

2.2 Screening of the reaction conditions and first attempts towards new multicomponent reactions

In order to start the experiments, i needed to dispose of a photoredox catalyst and a light source, along with a library of arendiazonium salts of formula ***2.1***. Looking in the direction of establishing a metal-free methodology to achieve new photoredox catalyzed MCRs, rose bengal was selected as the organocatalyst for preliminary investigations. Despite it was reported in the literature that this compound is not particularly efficient for SET reactions with arendiazonium tetrafluoroborates[2.3] it was employed for the first test reactions. As a light source, a simple white emitting compact fluroescent lamp (CFL) was employed. Following, a small library of arendiazonium tetrafluoroborates ***2.1*** was synthesized according to literature procedures[2.4].

Scheme 2.2.1: Synthesis of arendiazonium tetrafluoroborates of general formula ***2.1***

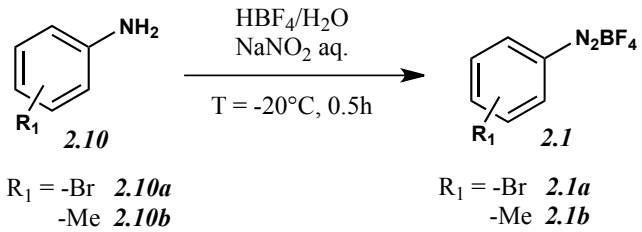

R_1 = -Br ***2.10a*** -Me ***2.10b***

R_1 = -Br ***2.1a*** -Me ***2.1b***

Arendiazonium tetrafluoroborates have been selected for use in this work. These compounds are easier to handle with respect to arendiazonium salts bearing different counteranions. In any case, it is important to handle diazonium compounds with careful attention and to store them appropriately to prevent their decomposition.

Styrene ***2.2a*** was selected as the olefinic partner for the screening of reaction conditions along with acetonitrile as both the solvent and the nitrile component of the reaction. The resulting reference reaction for the screening of the reaction conditions is depicted in **Scheme 2.2.2**.

Scheme 2.2.2: Intermolecular amino-arylation of alkenes attempt

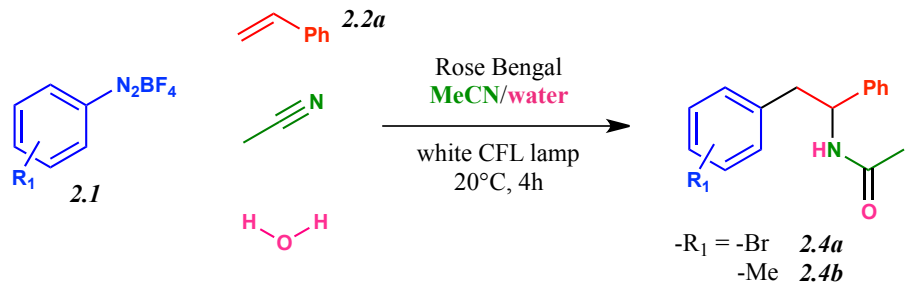

The first attempts to perform this reaction didn't afford the desired products of general formula ***2.4***. As a consequence, the photoredox catalyst was changed to $Ru(bpy)_3Cl_2$ which was used in combination with a 440 nm laser as a light source. With the new photocatalytic system, the results obtained by Konig could be reproduced with success.

Scheme 2.2.3: Intermolecular amino-arylation of alkenes: reproducibility test

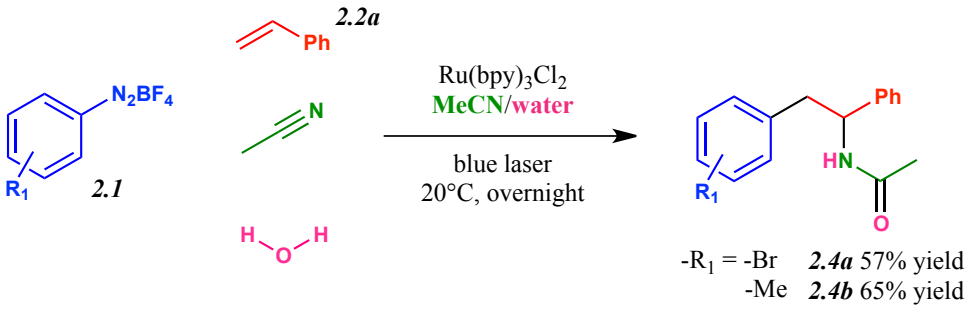

Once the reactions conditions were established, I focused my attention on the attempt to modify them to achieve a new MCR, as it was represented in **Scheme 2.1.3**. Since our research group possesses decades of experience on isocyanide based MCRs, i started my investigations trying to exploit isocyanides as nucleophiles in this transformation. The expected product of this transformation, with general formula ***2.15***, is depicted in Scheme 2.2.4. Such compound would derive by the nucleophilic attack of the isocyanide ***2.11*** on the carbocation ***2.7***, followed first by the attack of the carboxylic acid ***2.12*** on the resulting nitrilium ion ***2.13*** and second by acyl migration.

All reactions were performed with dry solvents in inert atmosphere to prevent undesired reactions to take place.

Such reaction has been attempted with various isocyanides ***2.11*** and carboxylic acids ***2.12***, screening their stochiometric use. Various solvents have also been screened for the desired transformation.

Scheme 2.2.4: Partial mechanistic depiction of new potential isocyanide based MCRs

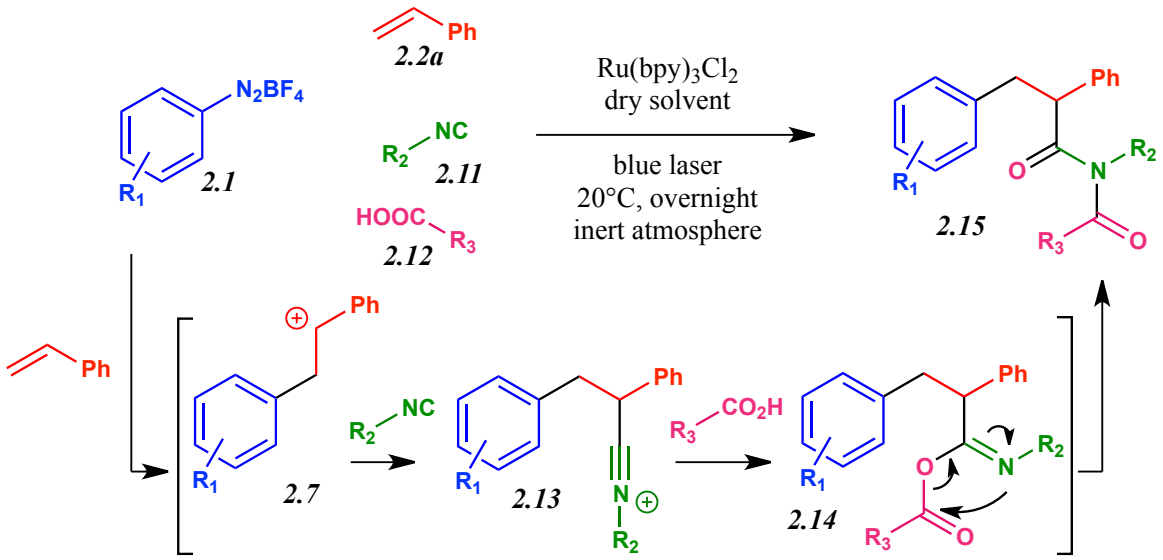

Various solvents have also been screened for the desired transformation. Unfortunately, the expected product ***2.15*** has never been identified. Remarkably, the nucleophilic attack of the carboxylic acid ***2.12*** to the key cationic intermediate ***2.7***, which was postulated as a potential side reaction to the desired transformation, leading to product ***2.16*** has also never been observed.

Scheme 2.2.5: unsuccessful attempts towards new potential isocyanide based MCRs

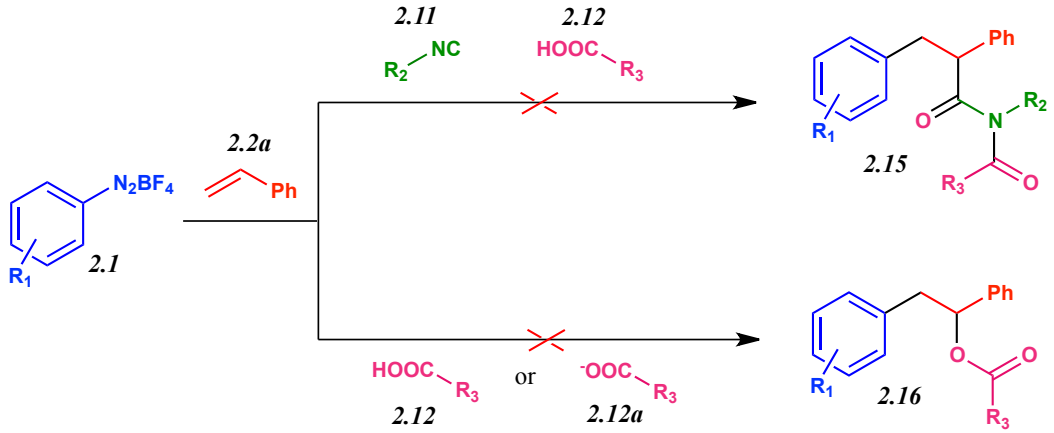

Noticeably, also when the nucleophilic power of the carboxylic acid was augmented by the utilization of a carboxylate ***2.12a*** (in the absence of isocyanide reagent) no product could be observed. Modifications of the reaction conditions such as: prolonging the irradiation time, raising the reaction temperature (up to 50°C), changing the olefinic partner (also methyl methacrylate was tested) or changing the arendiazonium tetrafluoroborate, did not lead to any improvement in the unsuccessful outcome of the reaction. As a consequence, the screening study was extended attempting to trap the cationic intermediate ***2.7*** with other nucleophiles such as alcohols and thiols.

Some nucleophiles have been left out of the screening list due to their known reactivity with diazonium salts; in similar conditions phenols and aromatic amines are known to yield azo dye compounds while aliphatic amines lead to decomposition of the substrate[2.5]. Unfortunately, the desired trapping reaction of the cationic intermediate ***2.7*** was never successful with the selected nucelophiles. On the other hand, some undesired trapping of the key intermediate by solvents or additives was curiously observed, but none of these results was considered innovative or interesting enough to further investigate its formation.

Scheme 2.2.6: unexpected reaction products

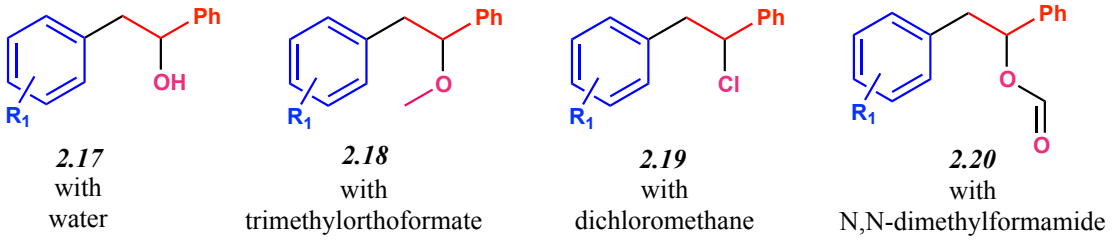

At this stage it was rationalized that the cationic intermediate moiety could be more conveniently attacked in an intramolecular fashion, with the nucleophilic group appropriately displayed by one of the two reagents.

Scheme 2.2.7: intramolecular trapping of cationic species

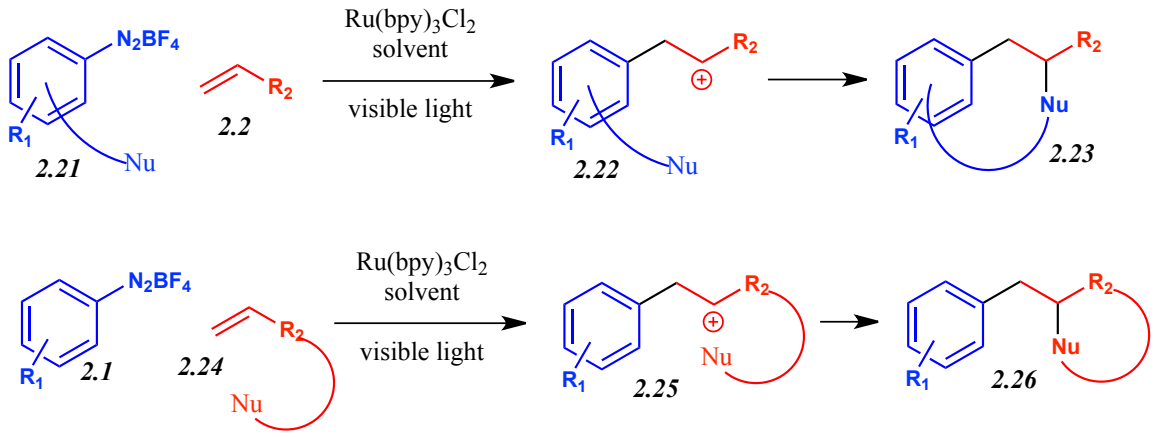

top: nucleophilic function embedded in the arendiazonium salt;
bottom: nucleophilic function embedded in the olefinic substrate

Therefore, in order to proceed with the project, it was necessary to abandon the multicomponent approach in favour of an intramolecular attack. Upon inspection of the literature data, no methodology could be found for similar transformations. An exception can be made for the one example regarding the previously mentioned synthesis of benzothiophenes starting from ortho-methylthioarendiazonium salt[2.6]. As a consequence, the aim of the doctoral work was renewed towards the development of an intramolecular cyclization involving cationic intermediates of formula ***2.22*** and ***2.25***.

2.3 Synthesis of isochromanones via intramolecular cyclization of carboxylic and esteric functions displayed by aromatic cores

To begin with, a new library of arendiazonium salts of general formula ***2.21*** bearing an additional functionality on the aromatic ring, namely an alcoholic (***2.21a***), thiolic (***2.21b***) and carboxylic (***2.21c***) function, has been prepared for the purpose of involving it in an intramolecular attack towards the synthesis of compounds ***2.27-2.29***.

Scheme 2.3.1: Intramolecular cyclization of differently substituted arendiazonium salts

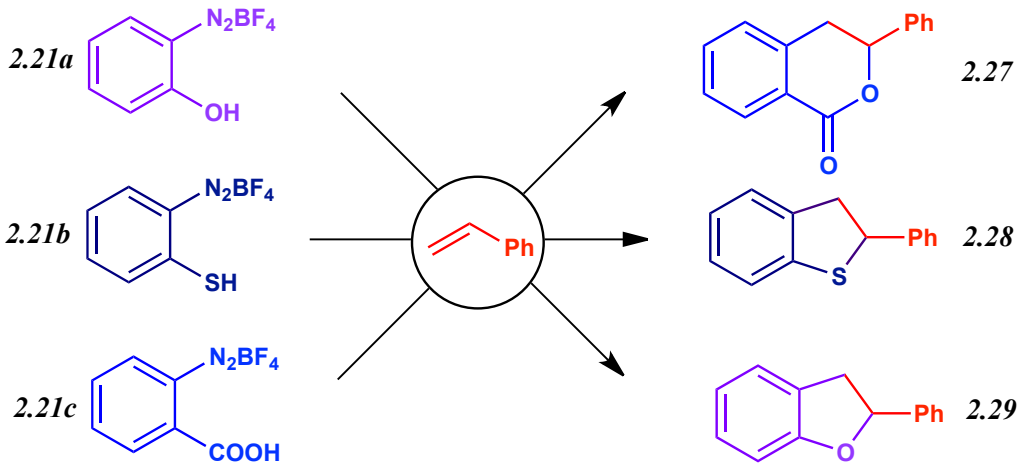

The reactions of the readily obtained arendiazonium derivatives were performed with styrene as an olefinic substrate; unfortunately both the alcoholic and the thiolic function did not show any sign of reactivity towards the expected cyclization. The reaction involving 2-carboxybenzendiazonium tetrafluoroborate ***2.21c*** furnished instead the desired 3-phenylisochroman-1-one product ***2.27***.

As a result, a new transformation leading to the isochromanone heterocyclic scaffold ***2.30a*** was disclosed.

Scheme 2.3.2: successful reaction with 2-carboxybenzendiazonium tetrafluoroborate ***2.21c***

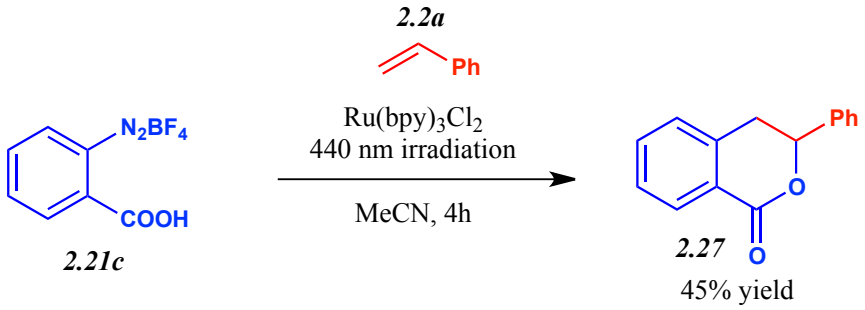

The isochromanone moiety ***2.30a***, being related with the isocoumarin structure ***2.30b***, recurrently appears both in nature[2.7] and in a large number of molecules recognised to have biological and pharmacological activities[2.8]. Among these substances phyllodulcin ***2.31*** is known for being a sweetener 400 times stronger than sugar[2.9].

Scheme 2.3.3: structure of natural and biologically active compounds possessing an isochromanone skeleton

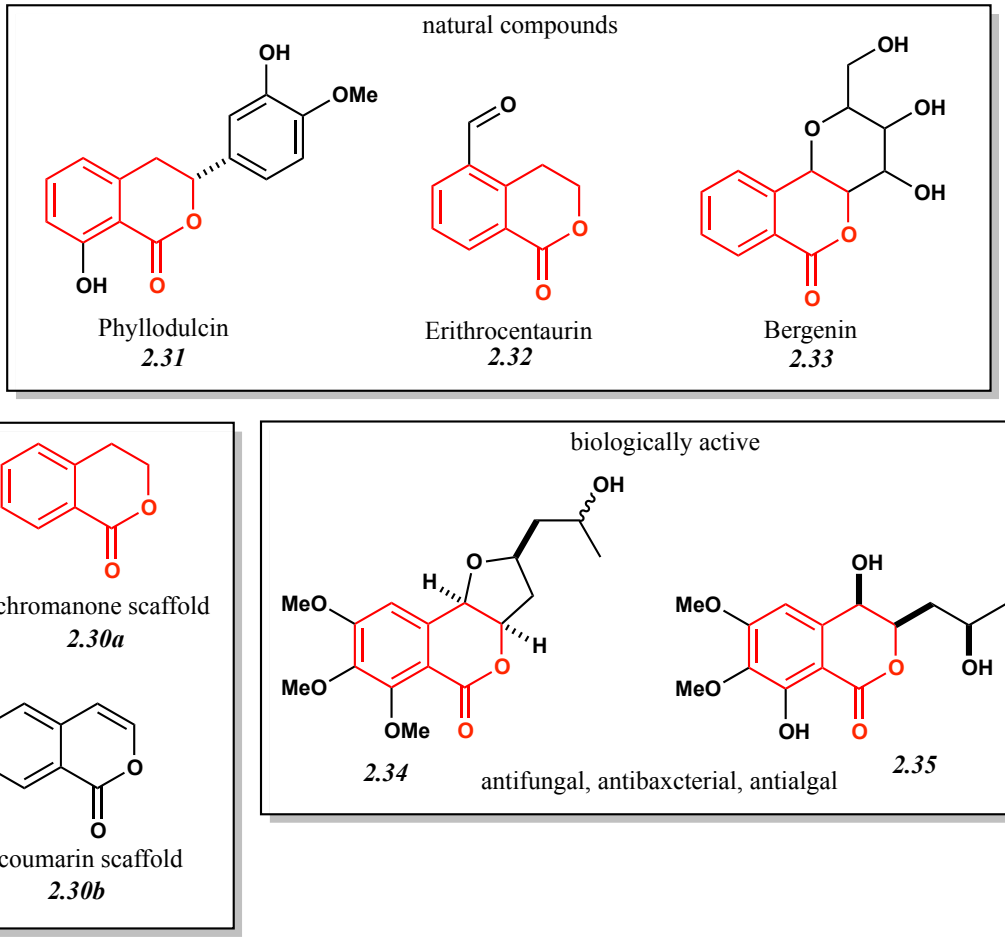

As a consequence, a quick reaction optimization was performed.

Table 2.3.1: Optimization of the reaction conditions leading to compound ***2.27***

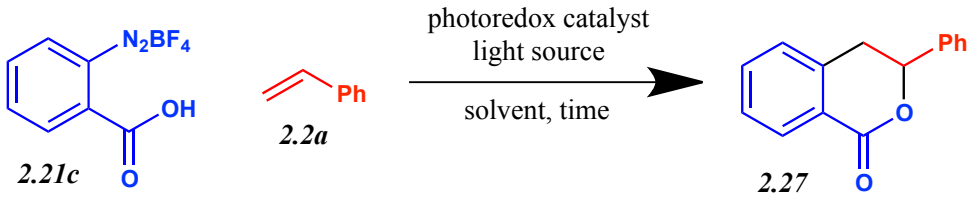

entry	***2.21c*** (eq.)	***2.2a*** (eq.)	Photocatalyst	Solvent (M)	time	Light source	***2.27*** yield
1	1	1	$Ru(bpy)_3Cl_2$	MeCN (0.25 M)	4h	440 nm laser	45%
2	1	2	$Ru(bpy)_3Cl_2$	MeCN (0.25 M)	4h	440 nm laser	53%
3	1	2	$Ru(bpy)_3Cl_2$	MeCN (0.25 M)	4h	440 nm LEDs	53%
4	1	3	$Ru(bpy)_3Cl_2$	MeCN (0.25 M)	4h	440 nm LEDs	50%
5	2	1	$Ru(bpy)_3Cl_2$	MeCN (0.25 M)	4h	440 nm LEDs	41%
6	1	2	$Ru(bpy)_3Cl_2$	MeCN (0.1 M)	4h	440 nm LEDs	51%
7	1	2	$Ru(bpy)_3Cl_2$	MeCN (0.25 M)	6h	440 nm LEDs	57%
8	1	2	$Ru(bpy)_3Cl_2$	MeCN (0.25 M)	8h	440 nm LEDs	54%
9	1	2	$Ru(bpy)_3Cl_2$	MeCN 8:2 Toluene (0.25 M)	6h	440 nm LEDs	64%
10	1	2	Rose bengal	MeCN 8:2 Toluene (0.25 M)	6h	CFL white	/

The use of an inert atmosphere did not lead to a significant improvement. No change was observed also when 440 nm LEDs were employed instead of the laser light source. Since LEDs are less energy consuming with respect to the laser, the following reactions were always performed with the former. The best reaction conditions were identified as reported by entry 9. The addition of toluene to the solvent mixture was sometimes necessary to afford a better solubilization of styrene. Having an optimized procedure in hand, a small library of arendiazonium tetrafluoroborates of general formula ***2.36*** was built first, followed by that of target compounds of structure ***2.38*** as shown in **Scheme 2.3.4**.

Scheme 2.3.4: Library of compounds ***2.38a-g***

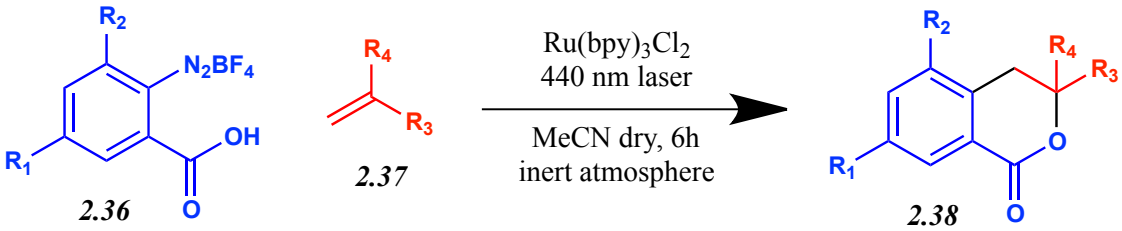

2.23	R_1 = H, R_2 = H	***2.2a***	R_3 = Ph, R_4 = H	***2.38a***	64%
2.36a	R_1 = Me, R_2 = H	***2.2a***	R_3 = Ph, R_4 = H	***2.38b***	58%
2.36b	R_1 = Cl, R_2 = H	***2.2a***	R_3 = Ph, R_4 = H	***2.38c***	71%
2.36c	R_1 = H, R_2 = Me	***2.2a***	R_3 = Ph, R_4 = H	***2.38d***	30%
2.23	R_1 = H, R_2 = H	***2.37a***	R_3 = COOMe, R_4 = Me	***2.38e***	70%
2.36a	R_1 = Me, R_2 = H	***2.37a***	R_3 = COOMe, R_4 = Me	***2.38f***	68%
2.36c	R_1 = H, R_2 = Me	***2.37a***	R_3 = COOMe, R_4 = Me	***2.38g***	21%

Remarkably, the complete solubilization of the arendiazonium tetrafluroborates of general formula ***2.36*** employed always resulted quite complicated due to the free carboxylic acid function they bear. Having in mind to adapt this synthetic procedure to flow conditions, with the aim to improve the methodology, it was decided to test the reactivity of ester ***2.39*** towards this cyclization, being the latter more soluble in the selected solvents with respect to compound ***2.21***.

Scheme 2.3.5: Reaction of 2-(ethoxycarbonyl)benzenediazonium tetrafluoroborate ***2.39*** with styrene ***2.2a***

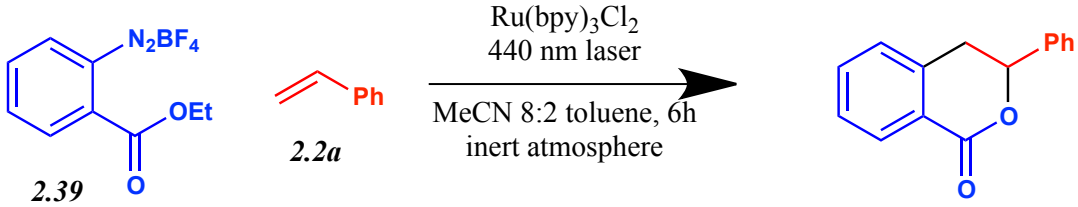

2.27 65% yield

When the reaction reported in **Scheme 2.3.5** was performed, the desired product ***2.27*** was successfully obtained in comparable yield with respect with the previously reported reaction of diazonium salt ***2.21c***. Notably, the reaction mixture immediately resulted perfectly clear and homogeneous with the diazonium salt ***2.39*** dissolving with ease in acetonitrile.

The mechanistic explanation of the cyclization step leading to isochromanone ***2.27*** starting from compound ***2.39*** will be given in **Paragraph 2.5**. As a consequence of this result, the same compounds previously reported in **Scheme 2.3.4** were prepared starting from a new library of arendiazonium tetrafluoroborates of general formula ***2.40***, bearing this time an ester functional group instead of a free carboxylic one.

Scheme 2.3.6: Library of compounds ***2.42a-m***

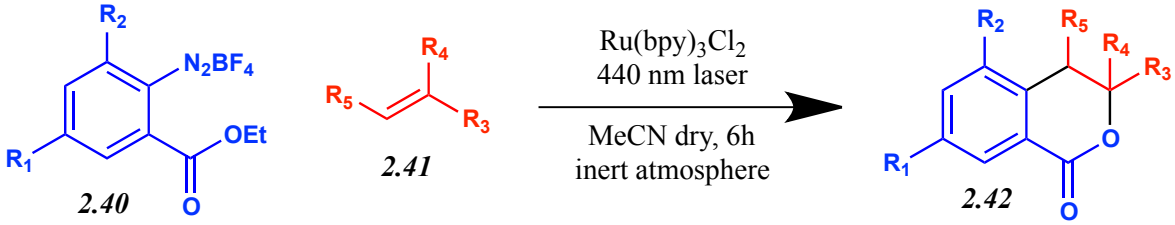

2.40a	R_1 = H, R_2 = H	***2.2a***	R_3 = Ph, R_4 ,R_5 = H	***2.42a***	65%
2.40b	R_1 = Me, R_2 = H	***2.2a***	R_3 = Ph, R_4 ,R_5 = H	***2.42b***	56%
2.40c	R_1 = Cl, R_2 = H	***2.2a***	R_3 = Ph, R_4 ,R_5 = H	***2.42c***	89%
2.40d	R_1 = H, R_2 = Me	***2.2a***	R_3 = Ph, R_4 ,R_5 = H	***2.42d***	39%
2.40a	R_1 = H, R_2 = H	***2.37a***	R_3 = COOMe, R_4, = Me, R_5 = H	***2.42e***	72%
2.40b	R_1 = Me, R_2 = H	***2.37a***	R_3 = COOMe, R_4, = Me, R_5 = H	***2.42f***	67%
2.40d	R_1 = H, R_2 = Me	***2.37a***	R_3 = COOMe, R_4, = Me, R_5 = H	***2.42g***	22%
2.40c	R_1 = Cl, R_2 = H	***2.37a***	R_3 = COOMe, R_4, = Me, R_5 = H	***2.42h***	71%
2.40e	R_1 = Br, R_2 = H	***2.37a***	R_3 = COOMe, R_4, = Me, R_5 = H	***2.42i***	53%
2.40d	R_1 = H, R_2 = Me	***2.41a***	R_3 = Ph, R_4, = H, R_5 = Ph	***2.42l***	19%
2.40e	R_1 = Br, R_2 = H	***2.2a***	R_3 = Ph, R_4 ,R_5 = H	***2.42m***	34%

Since our research group had previous experience of improving methodologies by means of the application of flow conditions[2.10] it was decided to try the same approach with this new transformation.

2.4 Application of the methodology for the synthesis of isochromanones to flow conditions

In order to determine wheather the applicaton of flow conditions to the previously described synthetic procedure could be advantageous, two different flow reactors were employed. The first one was a microflow device (Labtrix Start System, Chemtrix, SOR3223, 10 µl inner volume).

Figure 2.4.1: Microflow Labtrix Start System device

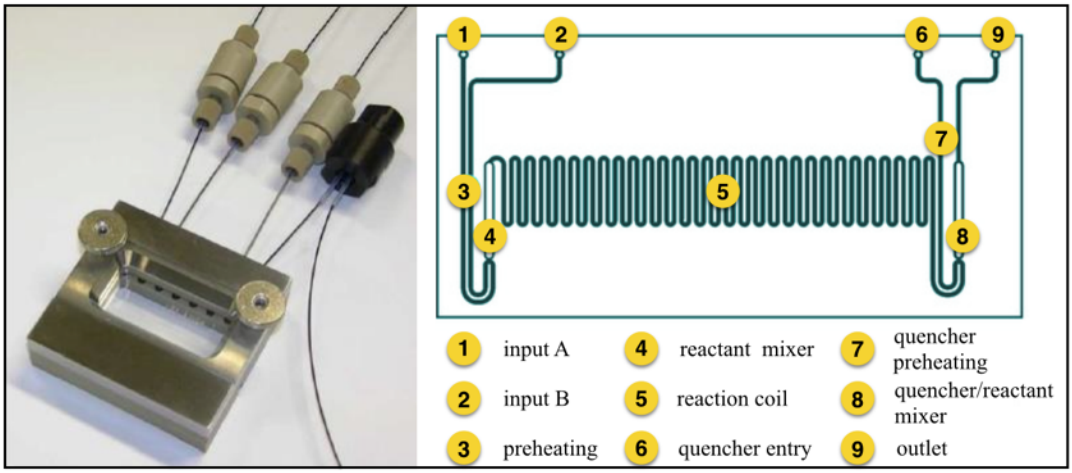

This microflow device is constituted by a carved, transparent, rigid glass chip, containing a 10 µl serpentine together with an efficient mixer. The chip fits in a metallic support, to which the inlet and outlet capillaries can be connected by means of rubber septa. The capillaries, bearing an inner diameter of 1/32”, are provided with backpressure controllers. A light source can be fixed on top of the glass reactor and a syringe pump can be employed to establish the flow of the reactant solutions.

The advantage of this reactor lays in the possibility to employ small amounts of reactant solution to test the reaction outcome. The dead-volume of solution is in the order of few microliters. In addition, this microflow device is designed to perform an highly efficient mixing of different solutions, which can be merged together by means of a T-mixer. On top of that, both glass and metal, constituting and enveloping the reactor, minimize the heating of the solution, either deriving from the light source or from an exotherimic process. Coming to the disadvantages, the small size of the reactor generally allows only small amounts of solution to be treated in the time unit. Therefore, collecting bigger amounts of solution, to be used for example for bigger scale purification steps, would require a longer time. But the main disadvantage connected with this device relies in its tendency towards clogging, which is highly enhanced by the reduced dimensions. Cleaning this device is not trivial, because the inner bends of the serpentine are hardly reached by the cleaning solution, requiring time-consuming sonication procedures.

The second reactor employed was a hand-made mesoflow device built inside the research group.

Figure 2.4.2: Hand-made mesoflow device

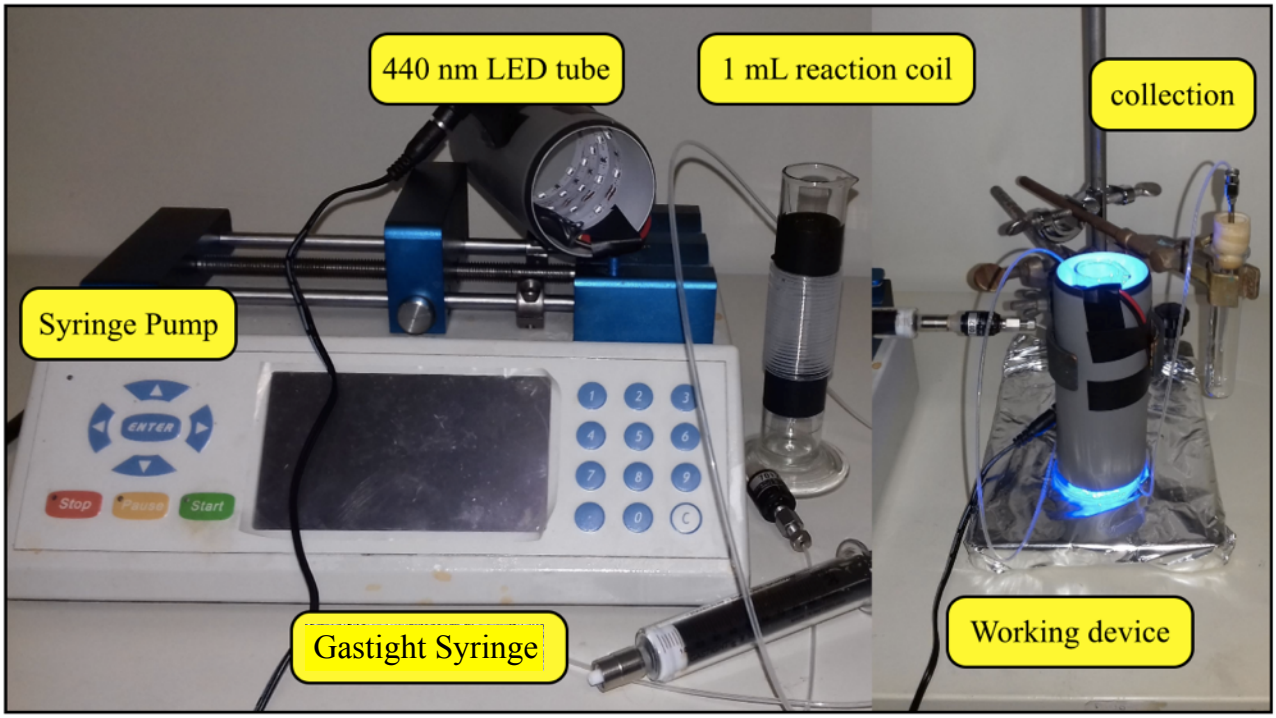

This device consists of a serpentine of FEP tubing , with inner diameter of 0.8 mm, wrapped around a 25 mL glass cylinder, used as a simple support. The irradiation is furnished by a 440 nm LED stripe wrapped inside a metal hollow cylinder of 5 cm of diameter. The irradiated tubings of the

reactor had a volume of 1 mL while the connecting tubings had a dead volume of approximately 1 mL. The advantage of this hand-made system lays in the possibility to process a considerable amount of reactant solution in the time unit.

A model reaction was selected for the screening of flow reaction conditions, aiming to improve the reaction yield. In microflow conditions, the reactant solution was supplied by two different syringes, with the arendiazonium tetrafluoroborate in the first syringe and all other reactants and catalyst in the second one. In mesoflow conditions instead, all reagents and catalyst were supplied with a single syringe. It has been checked that no side reaction nor decomposition of the reactants takes place inside the syringe even after several hours. In both cases, the syringes were kept shielded from the light to avoid the occurrence of undesired reactivity inside. The outcome of the screening is reported in **Table 2.4.1**.

Table 2.4.1: Optimization of flow reaction conditions

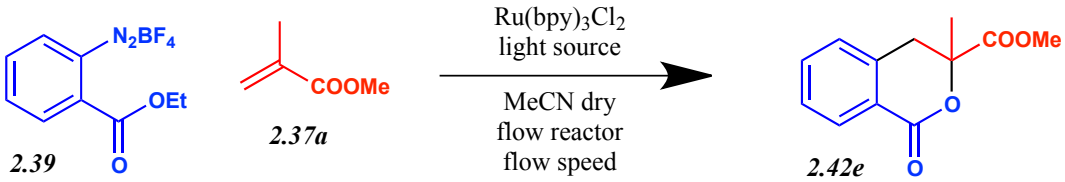

entry	residence time	reactor	reaction scale	Concentration	flow speed	light source	***2.42e*** Yield
1	6 min	micro	2 mL	0.1 M	100 ul/h	laser	15%
2	10 min	micro	2 mL	0.1 M	60 ul/h	laser	28%
3	15 min	micro	2 mL	0.1 M	40 ul/h	laser	30%
4	30 min	micro	2 mL	0.1 M	20 ul/h	laser	34%
5	30 min	micro	2 mL	0.1 M	20 ul/h	LED	34%
6	2 h	meso	10 mL	0.1 M	0.5 mL/h	LED	40%
7	3.3 h	meso	10 mL	0.1 M	0.3 mL/h	LED	53%
8	10 h	meso	10 mL	0.1 M	0.1 mL/h	LED	68%
9	10 h	meso	10 mL	0.13 M	0.1 mL/h	LED	71%
10	10 h	meso	10 mL	0.15 M	0.1 mL/h	LED	67%
11	10 h	meso	10 mL	0.05 M	0.1 mL/h	LED	50%

By looking at **Table 2.4.1** it is evident that the application of the flow conditions to the target reaction did not bring a significant improvement with respect to batch reactions. In fact, no better result is achieved with respect to batch conditions, which leaded to compound ***2.42e*** with the same rection yield achieved with the better the best flow conditions, reported by entry 9. In addition, in order to parallel the yields of the batch experiments, it was necessary to considerably slow down the

flow speed (entry 9, best conditions), reaching a retention time (10h) which was actually longer than the batch irradiation time (6-8h). The irradiation source did not affect the reaction (entry 4 VS entry 5). Also excessive dilution was counterproductive for the reaction outcome (entry 11).

The batch and flow reactions were put to comparison as shown in **Table 2.4.2**.

Table 2.4.2: Batch VS flow yields

entry	compound	batch yield	flow yield
1	***2.42e***	59%	71%
2	***2.42a***	60%	53%
3	***2.42g***	22%	29%
4	***2.42i***	53%	73%
5	***2.42l***	19%	20%

As it can be seen by the table, the yield obtained under flow conditions are comparable to those obtained under batch conditions.

2.5 Investigation of the reaction mechanism

Taking into consideration the cyclization of arendiazonium tetrafluoroborates of general formula ***2.36***, it would be reasonable to expect that the -OH group displayed by the carboxylic group would attack the cationic site of intermediate ***2.45*** with concomitant loss of a proton.

Scheme 2.5.1: reasonable reaction mechanism before disclosure of further experimental evidence

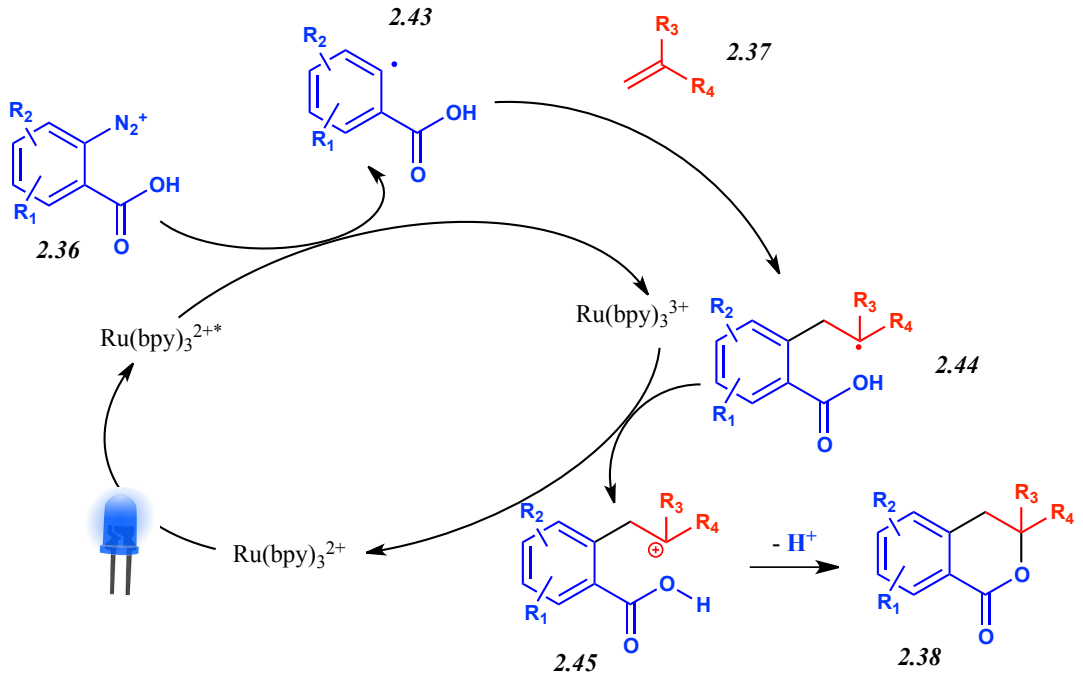

In order to validate this proposal, the arendiazonium tetrafluoroborate ***2.46***, bearing a primary amidic function on the aromatic ring, was submitted to the reaction conditions. Reasonably, it was to be expected to achieve the dihydroisoquinolinone ***2.47***, postulating an intramolecular attack of the -NH_2 group. Contrary to the expectations, the isochromanone ***2.27*** was achieved with 60% yield instead.

Scheme 2.5.2: Reaction of arendiazonium tetrafluoroborate ***2.46*** with styrene ***2.2a***

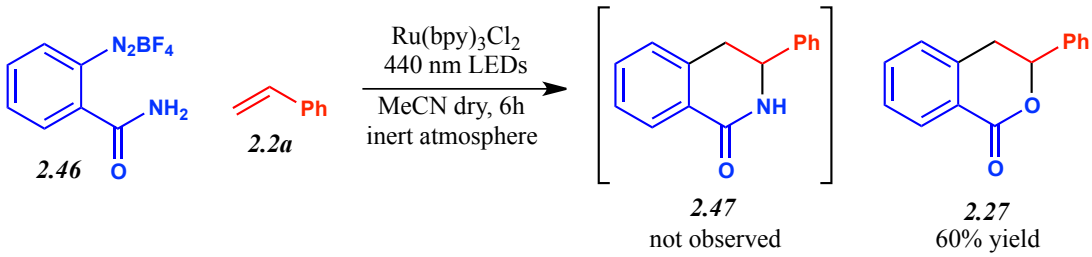

Presumably, the cyclization takes place with the carbonyl oxygen attacking the cationic site of intermediate ***2.50*** generating an imidate derivative ***2.51*** which furnishes the isochromanone ***2.27*** following hydrolysis.

Scheme 2.5.3: Plausible reaction mechanism

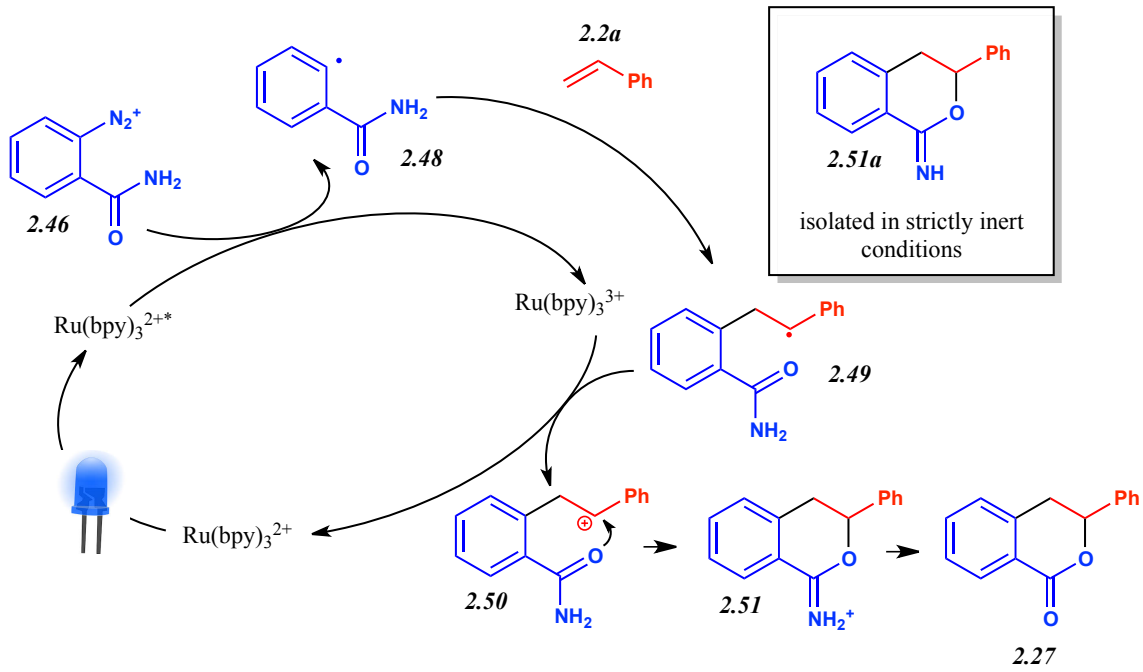

Upon a second investigation, by conducting again the reaction in strictly inert conditions followed by a quick column chromatography, the imidate ***2.51a*** was isolated, confirming that oxygen is the atom taking part in the intramolecular cyclization.

As a consequence of the observation that the carbonyl oxygen is the atom attacking the positive carbon of the cationic intermediate, it is not surprising that arendiazonium tetrafluoroborates bearing an ester function in ortho position afford the same product as those deriving from free acids.

Even more so, it was demonstrated that the steric hindrance deriving from the ester does not affect the cyclization at all.

Scheme 2.5.4: Effect of the substitution of the ester group of the arendiazonium salt

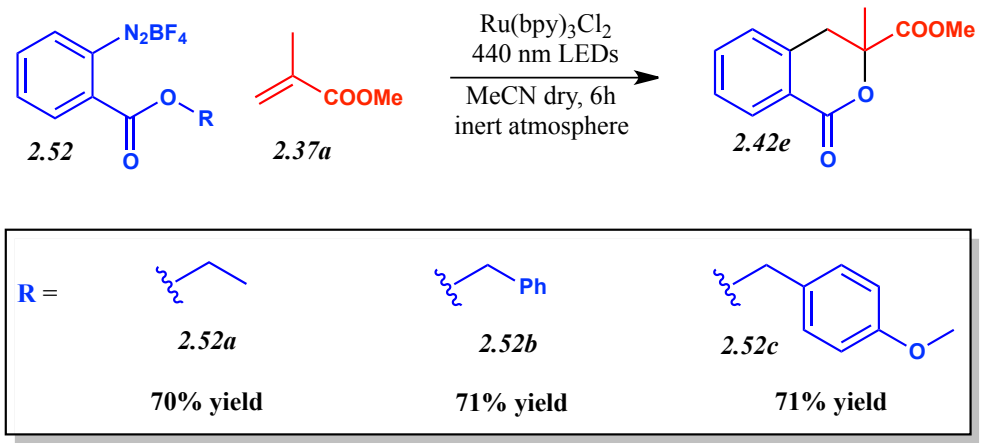

At this stage, we were intrigued by the fate of the -R group displayed by arendiazonium salts of general formula ***2.52*** since its fragment was not incorporated in the respective reaction product ***2.42e***. For example, when the ethyl ester ***2.52a*** was employed, no side product could be observed upon analysis of the reaction crudes. When benzyl and para-methoxybenzyl esters ***2.52b*** and ***2.52c*** were employed instead, stoichiometric amounts of acetamides ***2.53*** and ***2.54*** were isolated.

Scheme 2.5.5: Partial mechanistic depiction of the reactivity of arendiazonium salts ***2.52b-c***

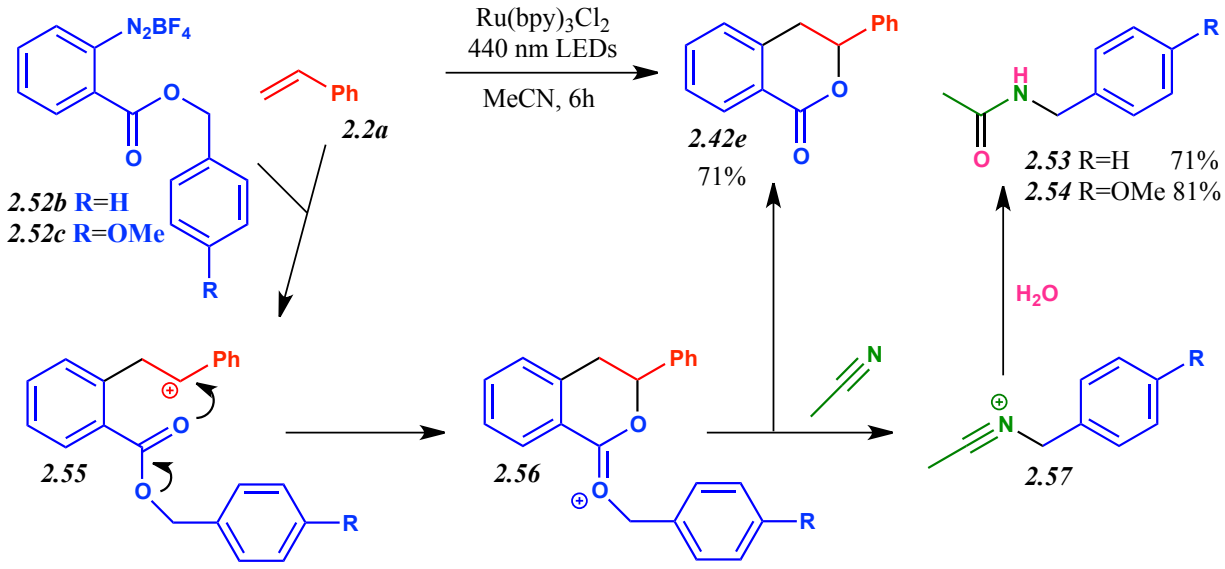

As a consequence, it could be rationalized that the fragment deriving from the ester group displayed by the arendiazonium salt is expelled as a carbocation which is eventually trapped from the solvent acetonitrile (intermediate ***2.57***), finally yielding acetamide ***2.53*** or ***2.54*** according to a Ritter-type reaction.

Remarkably, when the same arendiazonium tetrafluoroborates ***2.52b*** or ***2.52c*** were reacted in acetone as a solvent, slightly lower yields of the isochromanone ***2.42e*** were obtained (around 60% yield) and no detectable derivative of the R group could be isolated. Presumably this species could not find a straightforward reaction pathway. Upon TLC (thin layer chromatography) staining with cerium molibdate of the crude reactions, a plethora of red spots indicative of benzyl and para-methoxybenzyl carbocationic species were revealed, supporting our hypothesis.

2.6 Synthesis of isobenzofuranones and serendipitous discovery of a reaction pathway leading to benzoxazepinone derivatives

Having set up a methodology for the synthesis of isochromanones we wondered wheather we could access isobenzofuranone derivatives ***2.59*** by reacting simple arendiazonium tetrafluoroborates of general formula ***2.1*** with functionalized styrene derivatives of formula ***2.58***, bearing an ester function on the aromatic ring.

Scheme 2.6.1: Expected reactivity of arendiazonium salts ***2.1*** with functionalized olefins ***2.58***

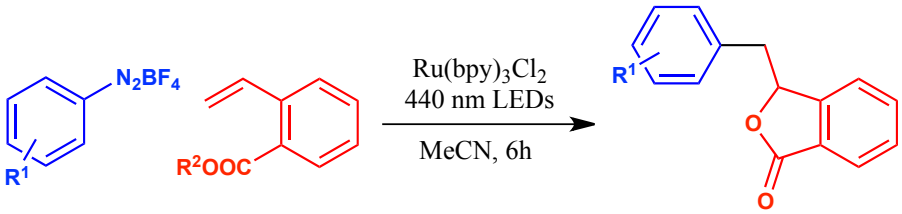

2.1 *2.58* *2.59*

In order to verify our hypothesis, 2-vinylbenzoic acid ***2.58a*** and its ester derivative product ***2.58b*** were consequently submitted to our reaction conditions together with simple arendiazonium tetrafluoroborate ***2.1c***. As a result, it was demonstrated that both the free acid ***2.58a*** and the ethyl ester ***2.58b*** furnished the same desired isobenzofuranone ***2.59a*** with moderate yields.

Scheme 2.6.2: Experimental evidence upon reaction of diazonium salts ***2.1*** with olefins ***2.58***

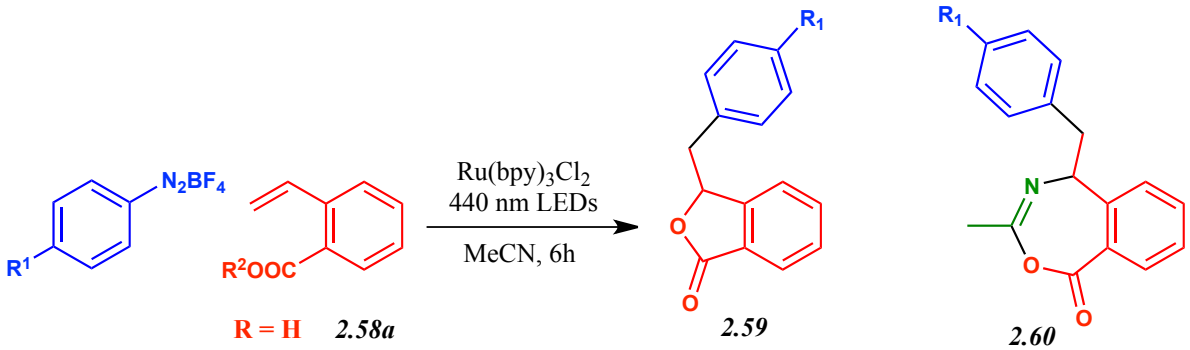

2.1c R_1 = OMe

R = H *2.58a*
R = Et *2.58b*

2.59

2.60

2.59a R_1 = OMe, R_2 = H 30%
R_1 = OMe R_2 = Et 31%

2.60a R_1 = OMe, R_2 = H 17%
R_1 = OMe R_2 = Et 17%

Unexpectedly though, together with the desired isobenzofuranone derivative ***2.59a***, a novel benzoxazepinone derivative ***2.60a*** was obtained (**Scheme 2.6.2**).

Scheme 2.6.3: Partial mechanistic depiction of the reaction of diazonium salt ***2.1c*** with olefin ***2.58b***

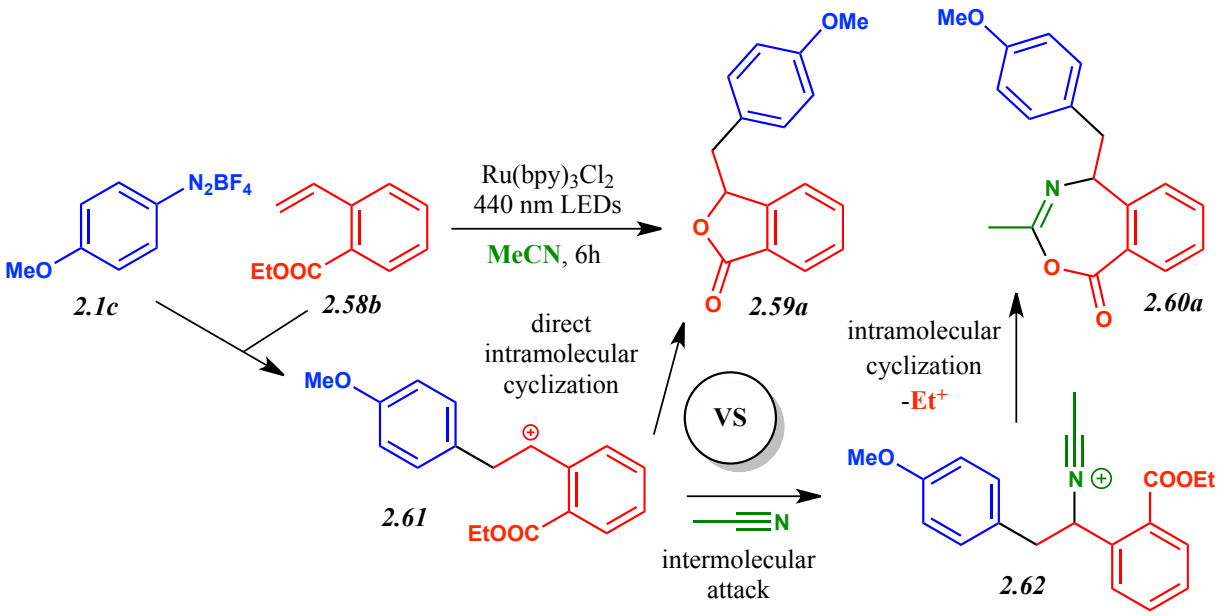

Apparently, the intermolecular attack of acetonitrile to the carbocationic intermediate ***2.61*** competes with the intramolecular cyclization of the ester group in the reaction conditions. Following the insertion of the acetonitrile moiety yielding derivative ***2.62***, the intramolecular cyclization presumably takes place on the resulting nitrilium ion, affording the benzoxazepinone ***2.60a***. Reasonably, the direct intramolecular cyclization of intermediate ***2.61*** leading to the isobenzofuranone ring is hampered by steric strain, thus allowing the attack of the solvent acetonitrile to be competitive with it.

As a result, a novel three-component reaction was serendipitously discovered. The structure of benzoxazepinone ***2.60a*** was unprecedently known in the literature. It is reasonable to think that a similar process could not take place in the reactions discussed in the previous paragraph. Presumably, when the ester function is displayed by arendiazonium salts of general formula ***2.52***, the intramolecular cyclization leading to an eight-membered ring of formula ***2.63*** would be presumably disfavoured (**Scheme 2.6.4**).

Scheme 2.6.4: Formation of compound ***2.63*** is not observed

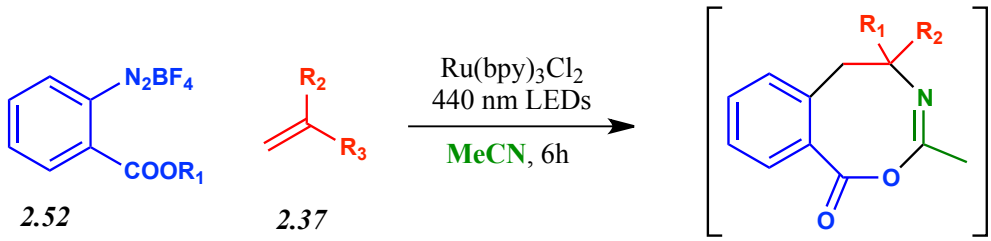

2.52 ***2.37*** ***2.63***

not observed, disfavoured cyclization

Supporting this hypothesis, the formation of compound ***2.63*** was never observed.

Remarkably, when the same reaction was performed in acetone media, the isobenzofuranone ***2.59a*** was selectively obtained with 40% yield.

Since we were interested by the structure of compound ***2.60a*** we started an investigation of the reaction conditions aiming to selectively achieve benzoxazepinones ***2.60*** over isochromanones ***2.59***.

2.7 Study of the reaction conditions aiming to the selective formation of benzoxazepinone derivatives

Following the serendipitous discovery of the MCR leading to benzoxazepinone derivatives ***2.60*** a more detailed investigation of the reaction was performed. Some preliminary attempts to employ acetonitrile as a stoichiometric reagent in a different solvent media (acetone, DMF) did not allow the formation of the desired product. Only when acetonitrile is used as a solvent, which means in very large excess, the MCR takes place. As a consequence, the use of acetonitrile as a solvent was fixed as a constant for the transformation under investigation. In addition, it could be expected that the modification of the molarity of the reaction would be uneffective towards altering the competition among the direct intramolecular cyclization and the nitrile attack, being the solvent already in large excess. On the basis of the previous experimental evidence, it was reasonable to think that the variation of the reaction temperature could reasonably affect the selectivity of the reaction. In particular, it could be expected that a lower reaction temperature would imply a slower intramolecular cyclization, thus favouring the competitive nitrile attack on the carbocation intermediate.

As a consequence, a set of reactions was performed varying the temperature; the results are reported in **Table 2.7.1**. The outcome of a different electronic substitution on the aromatic ring of the diazonium salt is also reported in the table.

Table 2.7.1: Investigation of the reaction conditions

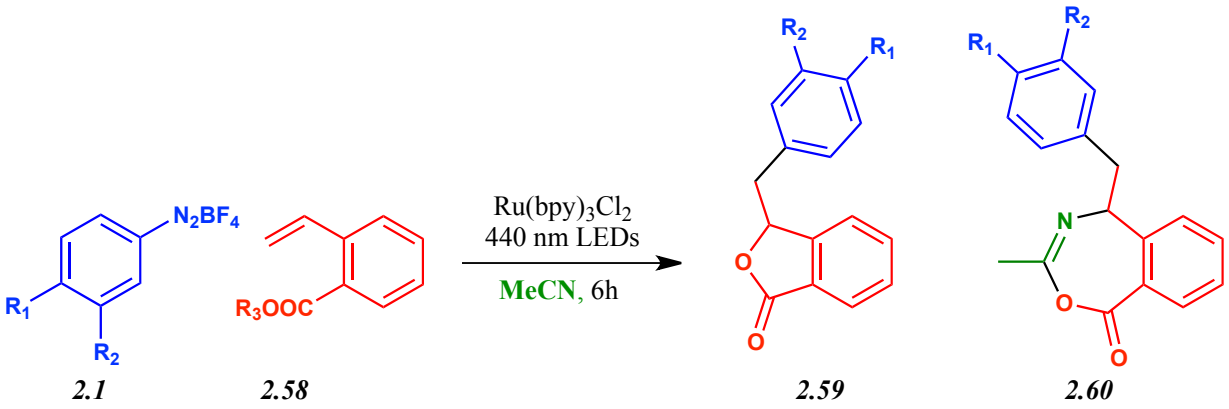

2.1 *2.58* *2.59* *2.60*

2.1c R_1 = OMe, R_2 = H
2.1b R_1 = Me, R_2 = H
2.1d R_1 = CF_3, R_2 = Cl

2.59a R_1 = OMe, R_2 = H
2.59b R_1 = Me, R_2 = H
2.59c R_1 = CF_3, R_2 = Cl

2.60a R_1 = OMe, R_2 = H
2.60b R_1 = Me, R_2 = H
2.60c R_1 = CF_3, R_2 = Cl

entry	R_1	R_2	R_3	Prod ratio ***2.59*:*2.60***	T (°C)	yield
1	OMe	H	Et	65:35	rt	48%
2	OMe	H	Et	65:35	0	50%
3	OMe	H	Et	64:36	-10	55%
4	OMe	H	Et	68:32	-15	62%
5	OMe	H	Et	65:35	-25	35%
6*	OMe	H	Et	100:0	rt	40%

entry	R_1	R_2	R_3	Prod ratio ***2.59*:*2.60***	T (°C)	yield
7	OMe	H	H	46:54	rt	41%
8	Me	H	Et	23:77	-15	43%
9*	Me	H	Et	100:0	rt	34%
10	Me	H	H	<5:95	rt	41%
11	CF_3	Cl	Et	/	rt	traces

*reactions performed in acetone as a solvent

As it can be seen in the table, the variation of the reaction temperature did not lead to significant success towards the selectivity control of the reaction; no conditions allowing the selective formation of benzoxazepinones ***2.60*** over isobenzofuranones ***2.59*** were identified. Noteworhty, the reaction yield could be sometimes improved by lowering the reaction temperature (entry 4). On the other hand, the modification of the susbtitution pattern of diazonium salts ***2.1*** seemed to affect the reactivity considerably. In fact, a much higher selectivity towards benzoxazepinone ***2.60b*** could be achieved with 4-methylbenzendiazonium tetrafluoroborate ***2.1b*** (entries 8 and 10). Moreover, when more electron deficient susbtitutents were displayed by the aromatic ring of the diazonium salt, the reaction efficiency was seriously compromised (entry 11). Sadly, the experimental investigation of the reaction conditions neither leaded to selectivity control nor to considerable yield improvement. When the reaction described in entry 1 of **Table 2.7.1** was performed in flow conditions, using the mesoflow device described in **Paragraph 2.4**, the resulting reaction outcome was totally comparable with that of the batch reaction.

When the reaction between arendiazonium tetrafluoroborate ***2.52a*** and olefin ***2.58b*** was performed, only one of the three potentially achievable products was obtained.

Scheme 2.7.2: Experimental outcome of the reaction among diazonium salt ***2.52a*** and olefin ***2.58b***

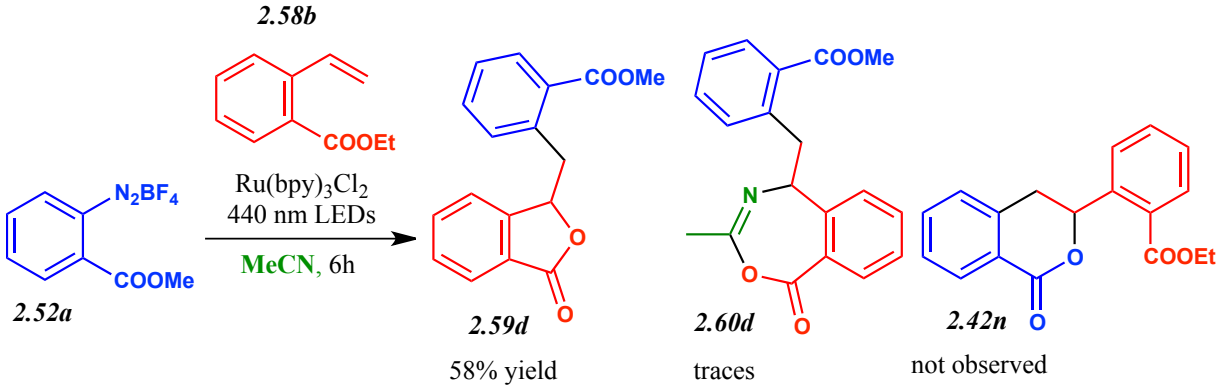

In conclusion, despite a very attractive transformation was disclosed, according to the experimental investigation which was carried on during the doctoral research, it was not possible to establish an efficient and selective methodology for the synthesis of benzoxazepinone derivatives.

2.8 A photocatalytic Meerwein approach to Isochromanones and Isochromenones

While i was working at the project described in the previous paragraph, the groups of König and Fagnoni concomitantly investigated a similar synthetic pathway and eventually disclosed their results[2.11]. As it can be seen from **Scheme 2.8.1** the two synthetic procedures are very similar under all aspects. In particular, method A proceeds faster than method B (2 hours versus 6-8 hours) in accordance with a higher loading of catalyst (2 mol% versus 0.5 mol%) and a higher excess of olefinic trap ***2.37*** (3 equivalents VS 2 equivalents). Both methods require the use of 2-carboxybenzendiazonium tetrafluoroborates ***2.36*** although relative esters (***2.36a***) can also be employed via method B, with the advantage of a better solubility. The mechanism leading to isochromanones ***2.38*** reported by König and Fagnoni parellels the one described in **Scheme 2.5.1**.

Scheme 2.8.1: Comparison among the work by König and Fagnoni and this work

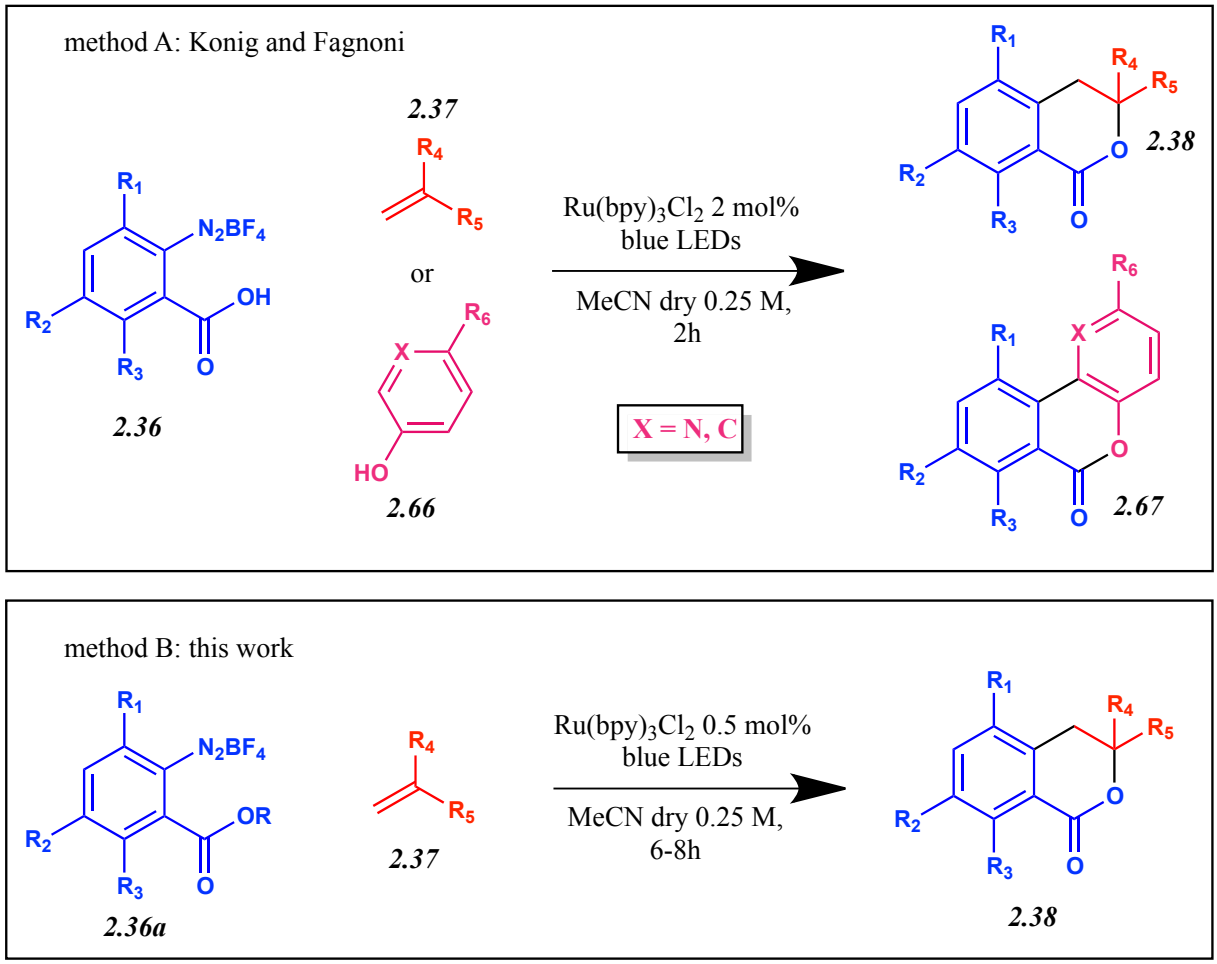

In addition, method B also envisions the employment of phenol or pyridine derivative ***2.66*** to access the isochromenone structure ***2.67***. The mechanism of this transformation, as it is proposed by the authors, is depicted in **Scheme 2.8.2**.

Scheme 2.8.2: Reaction mechanism as it is proposed by the authors

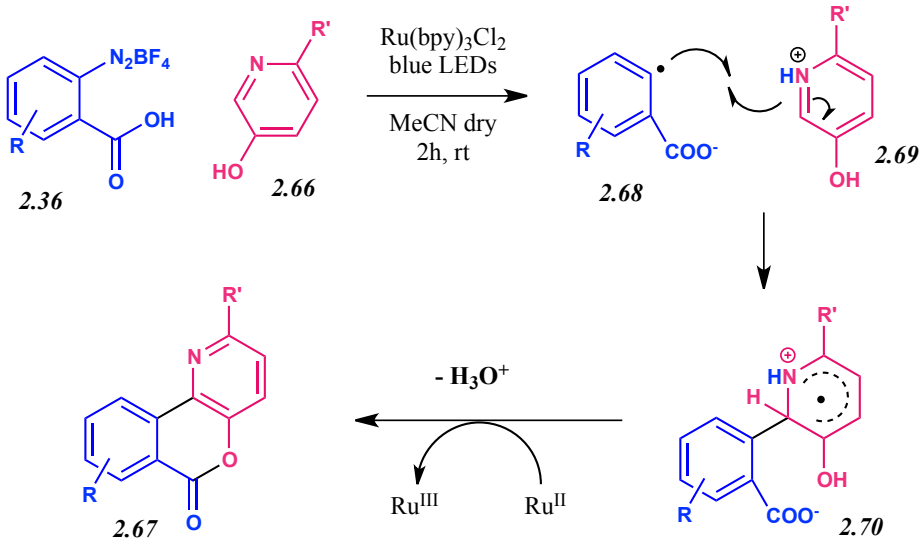

Following the reduction of the arendiazonium ion and acid-base reaction, the aryl radical ***2.68*** attacks the aromatic ring of compound ***2.69*** generating the adduct ***2.70*** which is stabilized by resonance. The oxidation of this intermediate, with concomitant expulsion of water and a proton, furnishes the isochromenone ***2.67***.

2.9 Conclusions

In conclusion, a visible light photocatalyzed synthetic methodology leading to iscohromanones, isobenzofuranones and benzoxazepinones was successfully established. A modification of this methodology, disclosed by other research groups, also allows for the formation of isochromenone products in a similar fashion.

Straightforward access to isochromanone derivatives is now available thanks to VLPC. Unfortunately, the synthetic procedure leading to isobenzofuranones and benzoxazepinones suffers from some disadantages, such as low efficiency and lack of selectivity. The work described in this chapter could be extended in different ways. For example, different substrates could be exploited for the generation of the reactive aryl radical or diverse heterocyclic scaffolds could be achieved by varying the functionalization of the starting diazonium salt. Nonetheless, it was decided to shift the research topic of my Ph.D. towards different aims, mainly due to a serendipitous discovery which will be discussed at the beginning of **Chapter 3**.

The primary target of my Ph.D. work, aimed at the development of new MCRs by means of VLPC, has not been hit. On the other hand, the experiments which were conducted in this direction allowed us to discover new profitable research pathways. As a consequence, my work has been directed towards new and different objectives. Hopefully, the experience gained by my working group in VLPC will allow future projects in this research field.

2.10 References

2.1
M. Anselmo; L. Moni; H. Ismail; D. Comoretto; R. Riva; A. Basso *Beilstein J. Org. Chem.* **2017**, *13*, 1456–1462.

2.2
D. P. Hari; T. Hering; B. König *Angew. Chem. Int. Ed.* **2014**, *53*, 725 –728.

2.3
(a) P. Schroll; D. P. Hari; B. König Chemistry Open 2012, 1, 3, 130-133.
(b) W. Guo; L. Lu; Y. Wang; Y. N. Wang; J. R. Chen; W. J. Xiao *Angew. Chem. Int. Ed.* **2015**, *54*, 7, 2265-2269.

2.4
P. Hanson; J. R. Jones; A. B. Taylor; P. H. Walton; A. W. Timms *J. Chem. Soc. Perkin Trans. 2* **2002**, 1135-1150.

2.5

M. R. Heinrich *Chem. Eur. J.* **2009**, *15*, 820-833.

2.6

D. P. Hari; T. Hering; B. König *Org. Lett.* **2012,** *14*, 5334–5337.

2.7

(a) J. Barbier; R. Jansen; H. Irschik; S. Benson; K. Gerth; B. Bohlendorf; G. Hofle; H. Reichenbach; J. Wegner; C. Zeilinger; A. Kirsching; R. Muller *Angew. Chem. Int. Ed.* **2012**, *51*, 1256–1260

(b) K. Nozawa; M. Yamada; Y. Tsuda; K. Kawai; S. Nakajima *Chem. Pharm. Bull.* **1981**, *29*, 2689–2691.

(c) N. Fusetani; T. Sugawara; S. Matsunaga; H. Hirota *J. Org. Chem.* **1991**, *56*, 4971–4974.

(d) P. Kongsaeree; S. Prabpai; N. Sriubolmas; C. Vongvein; S. Wiyakrutta *J. Nat. Prod.* **2003**, *66*, 709–711.

(e) M. Yoshikawa; E. Uchida; N. Chatani; N. Murakami; J. Yamahara *Chem. Pharm. Bull.* **1992**, *40*, 3121–3123.

(f) M. Toshikawa; E. Uchida; N. Chatani; H. Kobayashi; Y. Naitoh; Y. Okuno; H. Matsuda; J. Yamahara; N. Murakami *Chem. Pharm. Bull.* **1992**, *40*, 3352–3354.

2.8

(a) B. V. McInerney; W. C. Taylor *Stud. Nat. Prod. Chem.* **1995**, *15*, 381–422.

(b) S. Pal; V. Chatare; M. Pal *Curr. Org. Chem.* **2011**, *15*, 782–800.

(c) M. Yoshikawa; H. Matsuda; H. Shimoda; H. Shimada; E. Harada; Y. Naitoh; A. Miki; J. Yamahara; N. Murakami *Chem. Pharm. Bull.* **1996**, *44*, 1440–1447.

(d) P. Jiao, J. B. Gloer, J. Campbell, C. A. Shearer *J. Nat. Prod.* **2006**, *69*, 612–615.

2.9

Ramacciotti A.; Fiaschi R.; Napolitano E. *J. Org. Chem.* **1996**, *61*, 5371-5374.

2.10

S. Garbarino; S. Protti; A. Basso *Synthesis* **2015,** *47,* 2385–2390.

2.11

S. Crespi; S. Jäger; B. König; M. Fagnoni *Eur. J. Org. Chem.* **2017**, 2147–2153.

CHAPTER 3:
VISIBLE LIGHT PHOTOREDOX CATALYZED GENERATION AND SYNTHETIC EXPLOITATION OF THE ACETONYL RADICAL

In this chapter, a mild and convenient methodology for the generation of the acetonyl radical via VLPC and flow chemistry is discussed. During the doctoral research, it was possible to access different heterocyclic scaffolds by exploitation of the work described in the following paragraphs. A synthetic procedure for the functionalization of silyl enol ethers was also developed. Recently (2019), the work described in this chapter, conducted in collaboration with the PhotoGreen Lab, University of Pavia, Italy, has been accepted for publication on the journal ACS Catalysis.

3.1 Serendipitous discovery of a reaction pathway leading to an unexpected isobenzofuranone derivative

In **Paragraph 2.6** a visible light photoredox catalyzed methodology for the synthesis of isobenzofuranone derivatives was described. As it was previously discussed, it is possible to gain selective access to this class of compounds by using acetone as a solvent. Unfortunately, this transformation proceeds with only a moderate yield for the desired product. Aiming to enhance the reaction yield, a quick optimization study concerning the reaction concentration was performed.

Table 3.1.1: Optimization of the reaction conditions

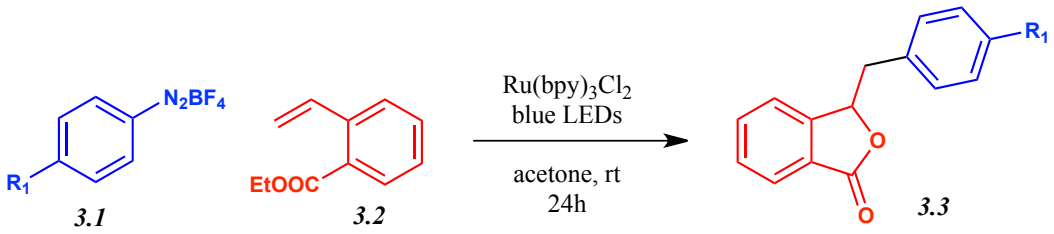

entry	R_1	concentration	***3.3*** yield
1	OMe	0.25 M	41%
2	OMe	0.5 M	22%
3	OMe	0.1 M	40%
4	OMe	0.05 M	15%
5	Me	0.25 M	34%
6	Me	0.05 M	9%

As it can be seen from the table, a quick optimization study did not lead to any improvement in the reaction yield. On the other hand, when the reactions described by entries 4 and 6 were performed, the desired compounds of general formula ***3.3*** were obtained only as secondary products. In fact, the main reaction product in these conditions was surprisingly compound ***3.4***.

Scheme 3.1.1: Unexpected reaction outcome

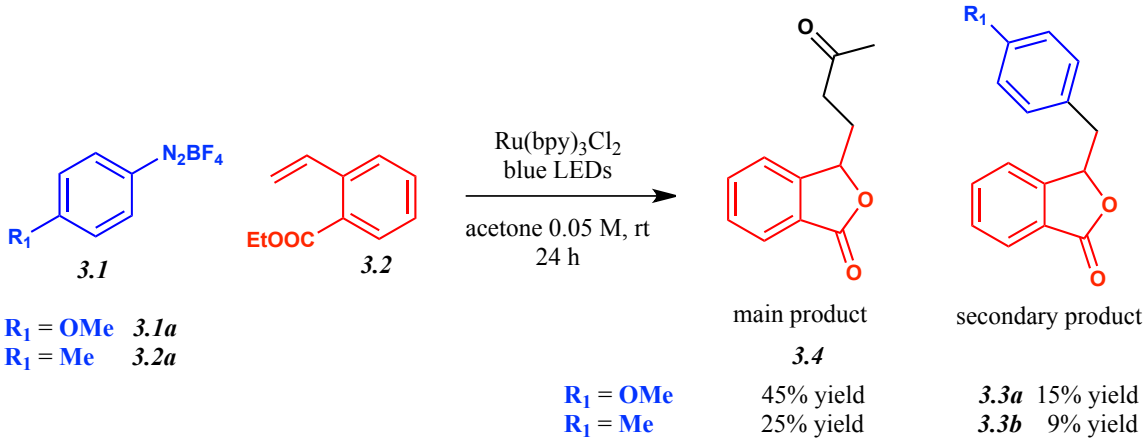

Noteworthy, compound ***3.4*** does not bear the aromatic moiety deriving from the arendiazonium tetrafluoroborate ***3.1***. On the other hand, such reaction product reveals the insertion of a molecule of acetone, which is employed as the solvent. As it can be seen in **Scheme 3.1.2**, the isobenzofuranone ***3.4*** is a known natural metabolite of the cardiovascular drug n-butylphtalide ***3.5***[3.1].

Scheme 3.1.2: Some metabolites of n-butylphtalide

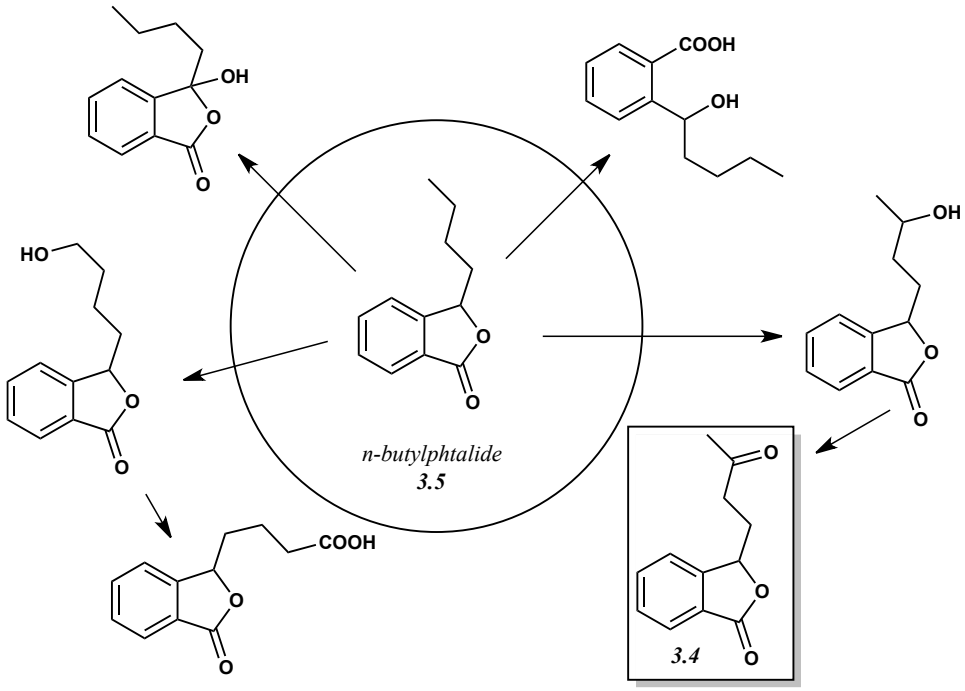

Attracted by the novel transformation leading to isobenzofuranone ***3.4*** we decided to further investigate it.

3.2 Postulated mechanism and optimization of the batch reaction leading to isobenzofuranone *3.4*

On the basis of the experimental evidence, it was postulated that, in the reaction conditions, the reactive acetonyl radical species ***3.6*** could be generated and thus intercept the ethyl-2-vinylbenzoate substrate ***3.2*** giving rise to the reaction product ***3.4***. An accurate analysis of the reaction crude was performed by GC-MS analysis to possibly gather more insight on the unknown reaction. Such analysis revealed the formation, together with the two isobenzofuranone products ***3.4*** and ***3.3***, of arene ***3.7*** deriving from the reduction of the diazonium salt ***3.1***.

Scheme 3.2.1: Experimental outcome of the reactions among diazonium salts ***3.1*** and olefin ***3.2***

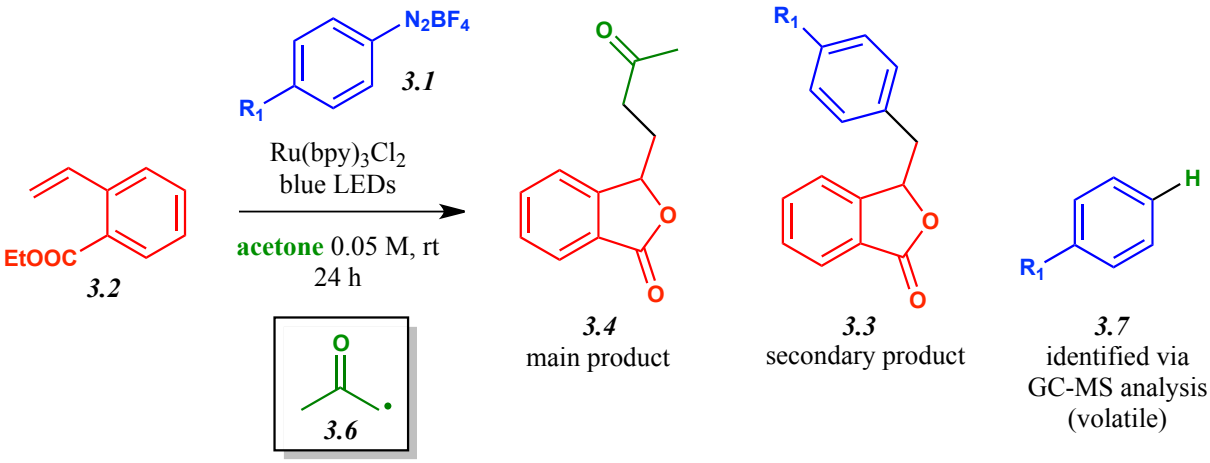

Having considered the experimental evidence, it was reasonable to believe that an hydrogen atom abstraction reaction could be responsible for the transformation. In particular it was postulated that the aryl radical ***3.8***, deriving from reduction of diazonium salt ***3.1***, could abstract an hydrogen atom from the solvent, generating the acetonyl radical ***3.6***. The postulated reaction mechanism is reported in **Scheme 3.2.2**.

It is known from the literature that aryl radicals ***3.8*** can promote HAT reactions[3.2].

Scheme 3.2.2: Postulated reaction mechanism

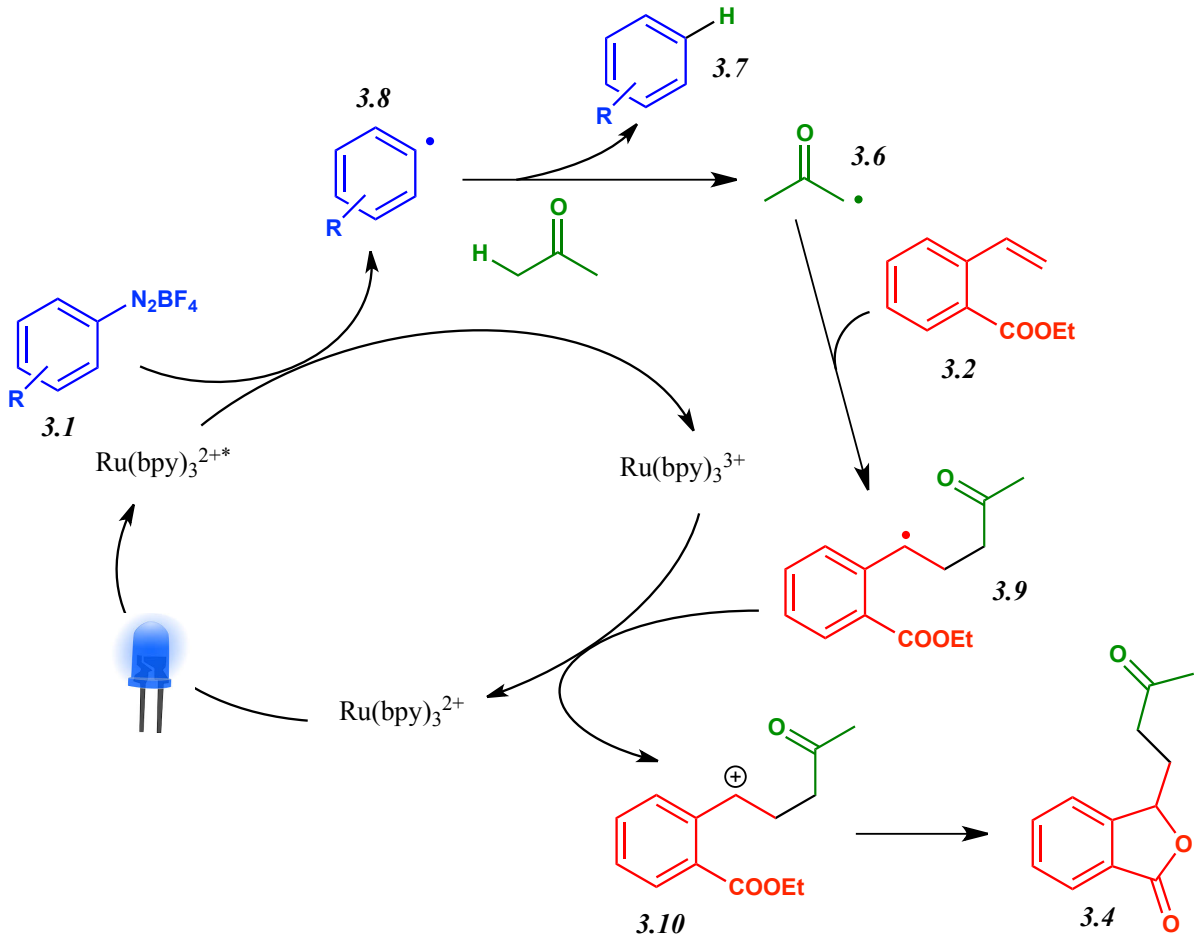

In order to synthetically exploit this transformation, it was first of all necessary to make it selective towards the desired product ***3.4***. By a quick optimization study, reported in **Table 3.2.1**, the formation of the undesired isobenzofuranone ***3.3*** was first reduced to traces (entry 2) and then completely prevented (entry 3) by applying more diluted conditions. Performing the reaction at even higher dilution (entry 4) did not bring to any improvement. At this stage, the reaction was performed in both the absence of catalyst (entry 5) and visible light irradiation (entry 6). In both cases, no product was detected in the reaction mixture, thus confirming that the process is photoredox catalyzed. In addition, it was determined that the reaction well tolerates the presence of up to 10% of water in the solvent mixture (entries 7 and 8) while on the contrary the addition of MeCN is deleterious even in small amounts (entries 9 and 10).

Table 3.2.1: Optimization of the reaction conditions

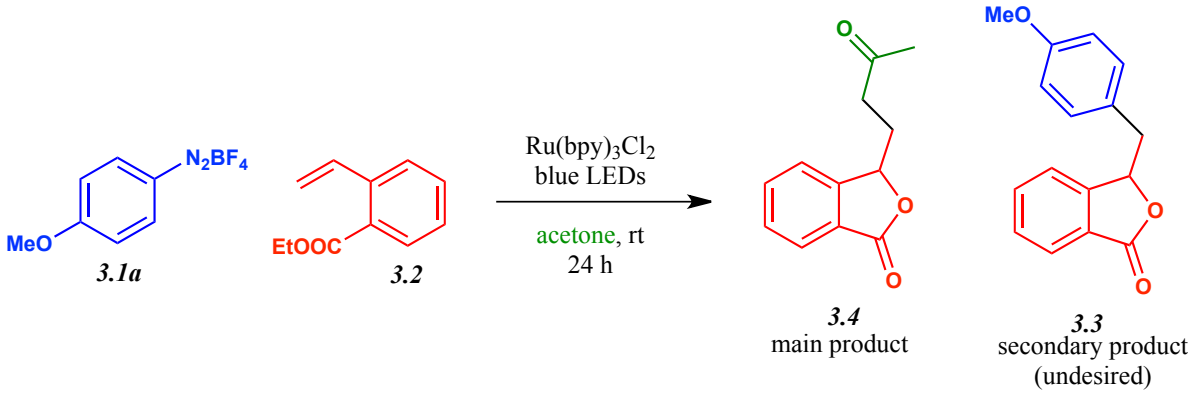

entry	C [M]	*3.4* yield	*3.3* yield	Notes
1	0.05 M	45%	15%	-
2	0.02 M	53%	traces	-
3	0.01 M	60%	/	-
4	0.005 M	59%	/	-
5	0.01 M	/	/	no catalyst

entry	C [M]	*3.4* yield	*3.3* yield	Notes
6	0.01 M	/	/	reaction in the dark
7	0.01 M	53%	/	5% water added to the solvent mixture
8	0.01 M	48%	/	10% water added to the solvent mixture
9	0.01 M	/	/	50% MeCN added to the solvent mixture
10	0.01 M	10%	/	10% MeCN added to the solvent mixture

Before proceeding with further experiments to validate the proposed reaction mechanism, some more experiments aimed towards the optimization of the reaction conditions were performed.

3.3 Application of flow conditions for the optimization of the reaction leading to isobenzofuranone *3.4*

Since the optimized batch reaction didn't exceed moderate yields, flow conditions were applied with the aim to improve the efficiency of the reaction. The screening of different flow-rates was performed by running the reaction inside the mesoflow hand-made device described in **Chapter 2** (**Figure 2.4.2**). The outcome of the screening is reported in **Table 3.3.1**.

Table 3.3.1: Applicaton and optimization of flow conditions

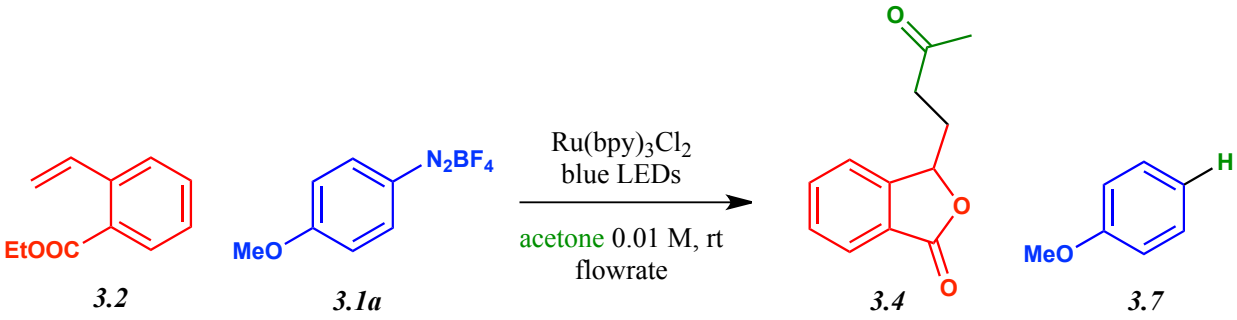

3.2 *3.1a* *3.4* *3.7*

entry	flowrate	residence time	*3.4* yield
1	1 mL/h	60 min	88% yield
2	10 mL/h	6 min	88% yield

entry	flowrate	residence time	*3.4* yield
3	20 mL/h	3 min	79% yield
4	1 mL/min (60 mL/h)	1 min	40% yield

With great delight it was observed that, in this case, the application of flow conditions greatly enhanced the reaction efficiency. In fact, by means of flow chemistry, not only it was possible to obtain the desired product ***3.4*** in higher yield (entry 1) with respect to the batch reaction (entry 3, **Table 3.2.1**), but the reaction time was considerably shortened. Indeed, it was demonstated that, by application of the flow conditions, the same moderate yield obtained by the batch reaction in 24 hours of irradiation could be obtained in just a few minutes! Possibly, this outcome has to be imputed to the high level of dilution of this peculiar transformation. Such outcome greatly differs from what it was observed for the flow reactions described in **Paragraphs 2.4** and **2.7**, which were approximately unaffected in comparison to batch transformations. Indeed, no appreciable improvement was observed by the application of flow conditions to reactions described in **Chapter 2**. The difference between the two synthetic methodologies is in terms of molarity; the concentration of the reactants solution of reactions described in **Chapter 2** (0.2 M) is bigger than one order of magnitude with respect to the new transformation discussed in this chapter (0.01 M). Possibly, this is one of the reasons for which such a different behaviour towards flow application was observed.

Having successfully optimized the reaction conditions, some experiments were performed with the aim to verify the reaction mecanism suggested in **Paragraph 3.2**.

3.4 Verification of the suggested reaction mechanism

In order to verify the mechanism proposed in **Scheme 3.2.2**, it was decided to submit an arendiazonium tetrafluoroborate bearing a bigger ester moiety to the reaction conditions. The experimental evidence to support the proposed mechanism was searched in the possible isolation of an arene derivative proving the HAT performed by the corresponding aryl radical. As a consequence, following their preparation, benzyloxycarbonyl- and *p*-methoxybenzyloxycarbonyl

benzendiazonium tetrafluoroboroates ***3.11a*** and ***3.11b*** were successfully submitted to the reaction conditions.

Scheme 3.4.1: Reaction of arendiazonium salts ***3.11a*** and ***3.11b*** with olefin ***3.13***

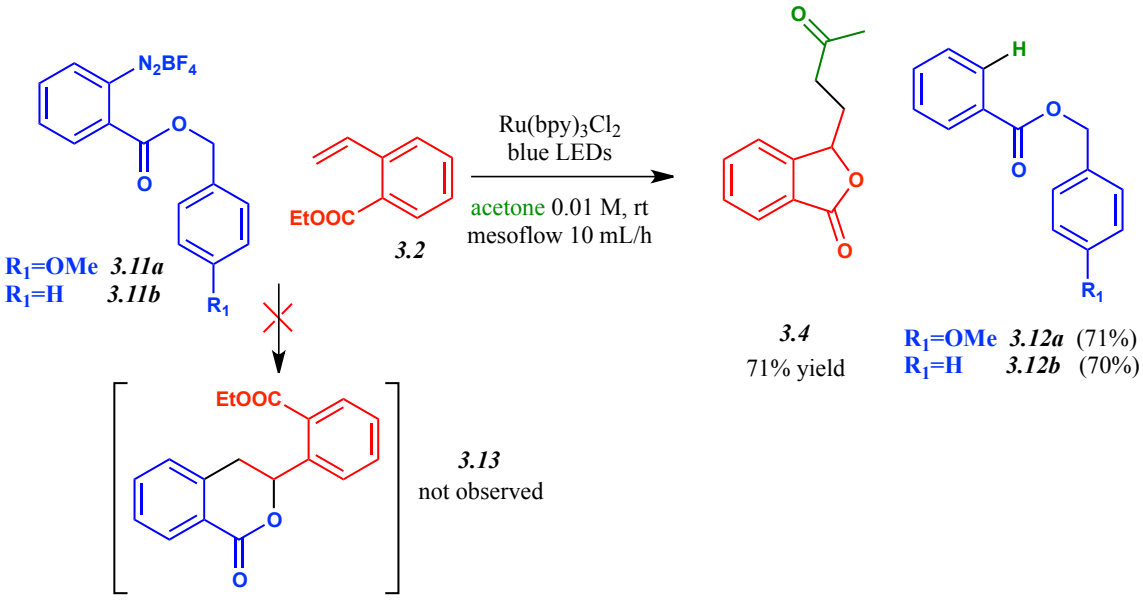

In both cases, a stoichiometric amount of the reduced arene (***3.12a*** and ***3.12b***) was obtained and isolated, supporting the proposed mechanism. Noticeably, in the reaction conditions, no isochromonanone ***3.12*** was obtained. In accordance to what was previously discussed, the transformation leading to the isochromanone ring is prevented by highly diluted solution conditions.

Subsequently, aiming to further inspect the reaction mechanism, the use of hexadeuteroacetone as the reaction solvent was investigated.

At first, the reaction of 4-methoxybenzendiazonium tetrafluoroborate ***3.1a*** with ethyl-2-vinylbenzoate ***3.2*** was performed in optimized conditions.

Scheme 3.4.2: Reaction of arendiazonium salt ***3.1a*** with olefin ***3.2*** in hexadeuteroacetone

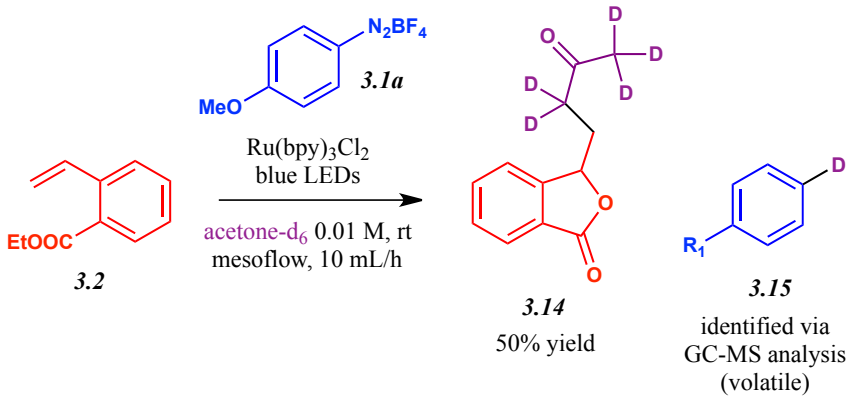

The desired pentadeuterated compound ***3.14*** was obtained with moderate yield. As it was previously discussed in **Paragraph 3.2**, the deuterated arene ***3.15*** deriving from the reduction of the diazonium salt could only be identified by GC-MS analysis, due to its volatility. Noticeably, when the same reaction described in **Scheme 3.4.2** was performed in batch overnight, no formation of compound ***3.14*** was observed. This fact suggests that deuterium abstraction might be a slower process with respect to hydrogen abstraction. With the aim to confirm this hypothesis, the same reaction was repeated with slower flow rates; the outcome of this screening is reported in **Table 3.4.1**.

Table 3.4.1: Optimization of the reaction conditions in hexadeuteroacetone

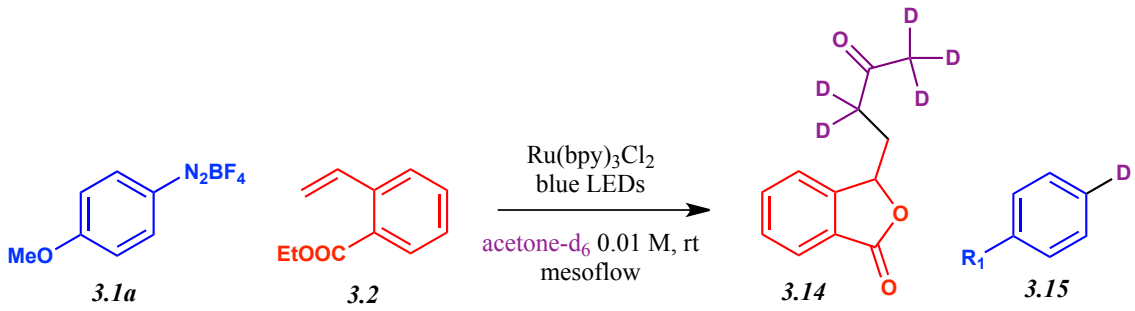

entry	flowrate	residence time	product ***3.14*** yield
1	10 mL/h	6 min	50%
2	5 mL/h	12 min	60%
3	1 mL/h	1 h	83%
4	0.5 mL/h	2 h	82%

As expected, the deuterium abstraction process is favoured by longer reaction times. In fact, by prolonging the residence time (entry 1 to 4), an increase of the reaction yield is observed.

Following, in order to further confirm the reaction mechanism, *p*-methoxybenzyloxycarbonyl benzendiazonium tetrafluoroboroate ***3.11a*** was employed as a reactant in deuterated acetone with the newly optimized conditions.

As it was also the case for the reactions prevously discussed in this paragraph, the formation of the respective deuterated arene ***3.16*** in comparable amount with the product ***3.14*** could be detected.

Scheme 3.4.3: Experimental evidence supporting the proposed reaction mechanism

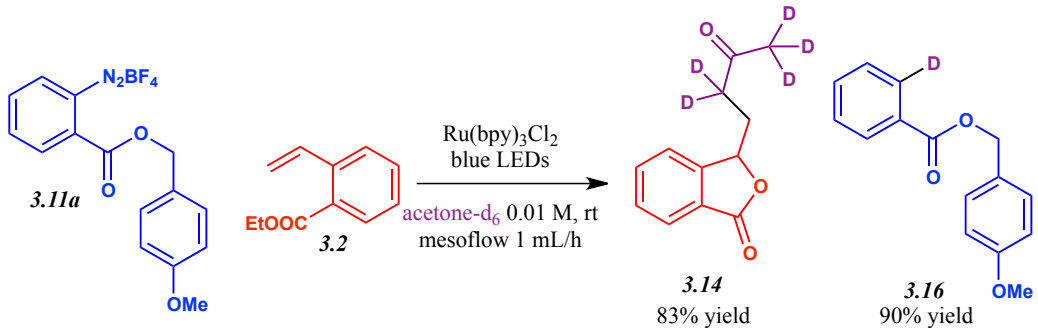

The kinetic isotopic effect (KIE) of the reaction was measured as well by running the same reaction in a 1:1 mixture of acetone and hexadeuteroacetone with a flow rate of 1 mL/h.

Scheme 3.4.4: Kinetic isotopic effect measurement

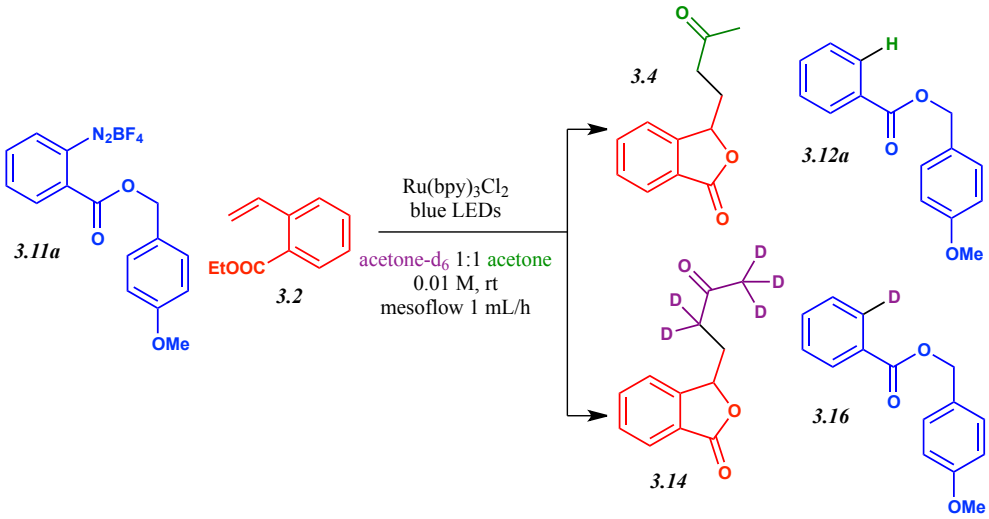

By means of GC-MS analysis, the ratio of the product mixture (***3.4***/***3.14***) was determined to be 6.5/1 in favour of the non-deuterated compound ***3.4***. Similarly, the ratio of the arene derivatives (***3.12a***/***3.16***) was determined to be 7/1, also in favour of the non-deutarated compound ***3.12a***. As a consequence, a primary KIE was pointed out for the selected process.

Having collected such evidence of the HAT reaction occurrence, the role of the arendiazonium tetrafluoroborate in this reaction was clarified. In order to generate the acetonyl radical (or its deuterated analogous), the reaction requires the use of a stoichiometric amount of diazonium salt. When the latter is employed in substoichiometric amount, it behaves as the limiting reagent, preventing full conversion of the olefinic trap, as it is shown by the screening reported in **Table 3.4.2**.

Table 3.4.2: Investigation of the stoichiometry of the reaction

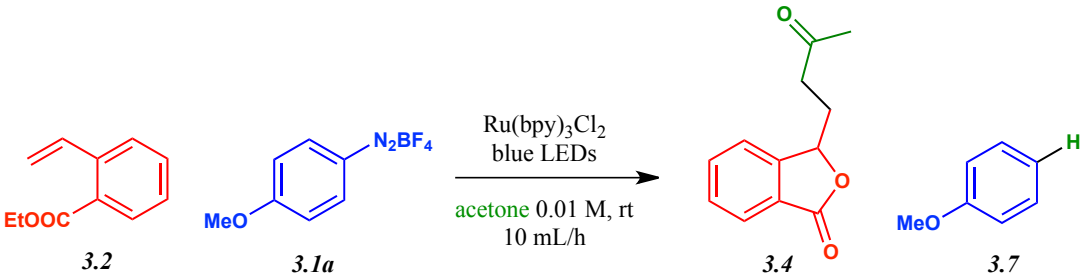

entry	*3.1a* eq.	*3.2* eq.	*3.4* yield	substrate *3.2* recovery
1	0.5	1	40%	55%
2	0.25	1	19%	74%
3	0.1	1	traces	89%

The trend showed by the table confirms that no radical chain process takes place in the reaction conditions and the product ***3.4*** formation is stoichiometric with the amount of diazonium salt used.

3.5 Effect of the electronic substitution of the diazonium salt aromatic ring on the hydrogen abstraction reaction

Following the mechanistic studies discussed above, an investigation of the dependence of the reaction outcome from the use of different diazonium salts was performed. With the aim to elucidate the electronic effect of the aromatic ring of the diazonium salt on the HAT performed by the respective aryl radical ***3.8***, only para-substituted diazonium salts were employed.

Table 3.5.1: Investigation on the effect of the electronic substitution on the aromatic ring of the arendiazonium tetrafluoroborate ***3.1***

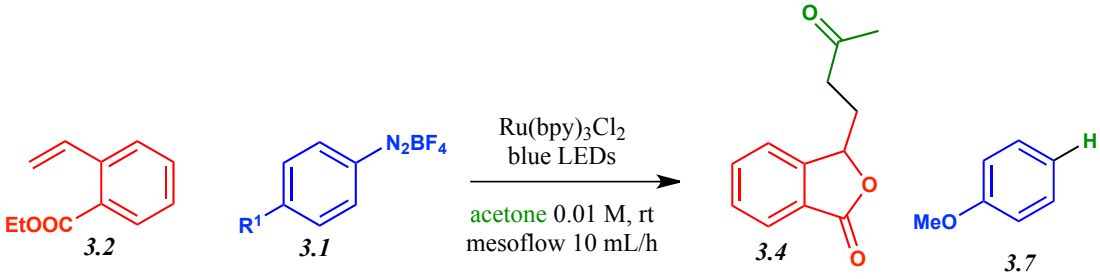

entry	R_1	product *3.4* yield	substrate *3.2* recovery
1	-OMe	88%	7%
2	-Me	68%	18%
3	-H	39%	41%

entry	R_1	product *3.4* yield	substrate *3.2* recovery
4	-Cl	47%	51%
5	-F	5%	82%

As it can be deduced by the table, the best result is achieved with the most electron donating substitutent of the aromatic ring (entry 1). Following, the second best result is given by the second best electron donating substitutent (entry 2). When the substituent is instead charachterized by a rather poorly electron donating or electron withdrawing effect, the product yield achieved is only moderate (entries 3 to 5). In particular, when the susbtituent is fluorine (entry 5) almost no product is achieved at all. This outcome could be explained with the reactivity of the respective aryl radical ***3.8***. Reasonably, an electron rich aryl radical could be more reactive towards HAT with respect to an electron poor one. In order to support this theory, a theorethical investigation by Density Functional Theory (DFT) approach was performed. The results of DFT calculations are reported in **Table 3.5.2**.

Table 3.5.2: Computational calculations on the HAT step

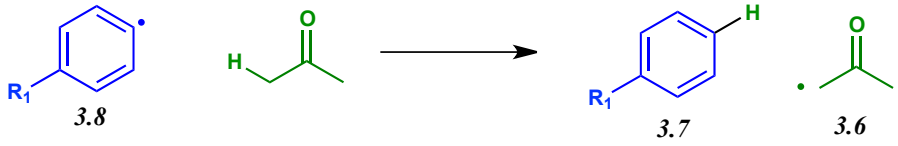

entry	R_1	$\Delta G^{\ddagger}$ (kcal/mol)	ΔG (kcal/mol)
1	OMe	10.49	-16.68
2	Me	10.55	-15.93
3	F	10.94	-16.83
4	H	11.24	-15.63

The relevant geometries have been optimized adopting the (unrestricted) ω-B97XD functional with the 6-31G(d,p) basis set in the gas phase. Careful inspection of the frequency calculations performed on the optimized geometries at the same level of theory allowed to identify the stationary points either as minima or transition states. In the latter case, it was verified as well that the only imaginary frequency described the motion along the desired reaction coordinate. Finally, solvent effects were included via single point calculation adopting the implicit SMD model and acetone as the reaction medium. As reported in **Table 3.5.2**, the efficiency of *para*-substituted aryl radicals ***3.8*** in the HAT from acetone depends on the nature of the aromatic substituent. In particular, whereas all the examined processes occur with a largely negative Gibbs free energy change (ΔG), different behavior can be identified in terms of Gibbs free energy barriers ($\Delta G^{\ddagger}$). Thus, while the *p*-methyl and the *p*-methoxy substituted aryl radicals show $\Delta G^{\ddagger}$ values around + 10.5 kcal·mol^{-1} (entries 1, 2), the unsubstituted derivative and the *p*-F one (entries 3, 4) show higher barriers, around 11.0 kcal·mol^{-1}. Noteworthily, the trend suggested by computational work supports the experimental data, illustrated in **Table 3.5.1**.

As a consequence of these results, being 4-methoxybenezendiazonium tetrafluoroborate ***3.1a*** the salt generating the most efficient aryl radical among the ones inspected, it was used as the standard reactant for all the experiments described in the following paragraphs.

3.6 Application of the reaction conditions to different solvents

Having disclosed the previously described tranformation, it was considered interesting to attempt its application to different solvents in order to possibly generate different reactive radicals and exploit their reactivity. Acetone is a peculiar ketone, charachterized by a high solubilizing power and a low boiling point; for this reasons, it is an excellent solvent. Reasonably, these qualities make it an excellent solvent for the ongoing study. Other ketones of similar molecular weight do not posses the same features; for this reason their utilization implies some difficulties. For example, Pinacolone (tert-butyl methyl ketone) is an expensive, dense and smelling liquid whose application on milliliter scale in flow conditions requires quite some precaution.

The use of different ketones and solvents has been attempted, as it is described in **Table 3.6.1**.

Table 3.6.1: Application of the reaction conditions to different solvents

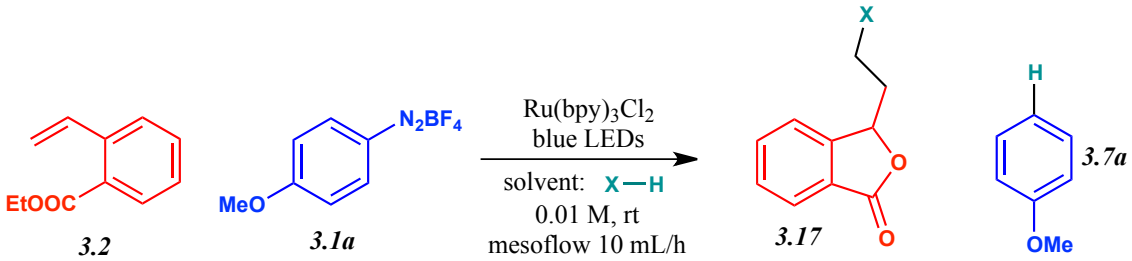

entry	solvent X-H	reaction outcome
1	AcOEt	no reaction
2	Pinacolone	no reaction
3	2-Butanone	no reaction
4	3-Chloroacetone	no reaction
5	Acetonitrile	no reaction

Unfortunately, none of the selected solvents and ketones afforded the desired reaction. In all cases but one, the substrate could be almost entirely recovered. In fact, when acetonitrile was employed as a solvent for the desired transformation, low amounts of isobenzofuranone ***3.18*** could be isolated (**Scheme 3.6.2**).

Scheme 3.6.2: Application of the reaction conditions to acetonitrile as a solvent

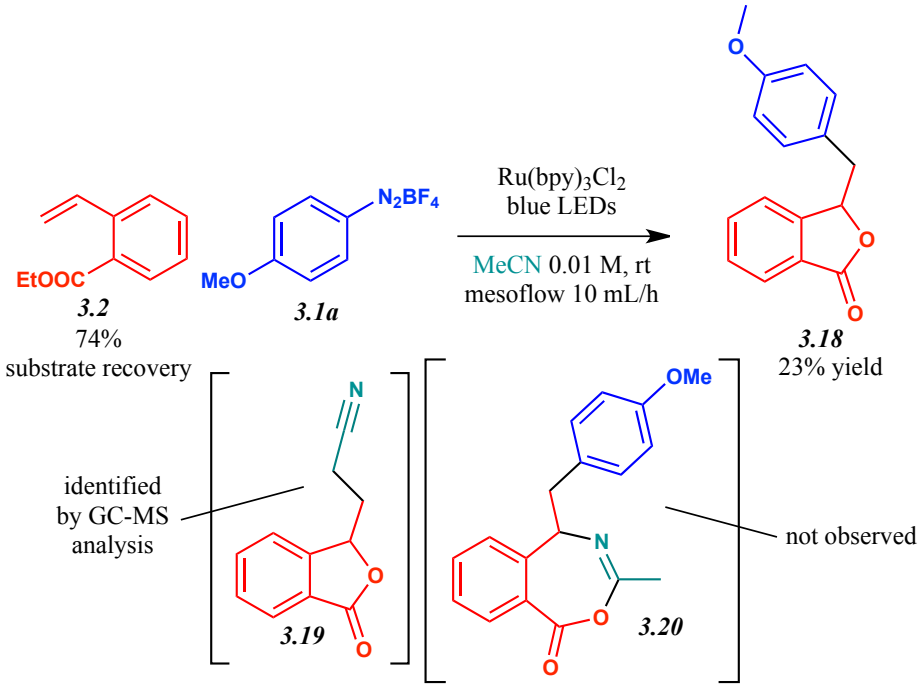

Noteworthy, no trace of benzoxazepinone ***3.20*** could be detected. Also, upon GC-MS analysis of the reaction crude, traces of the expected product ***3.19***, deriving from acetonitrile insertion, could be effectively identified.

The same set of reactions was performed at slower flow rate (1 mL/h), having comparable results in return. Apparently, the methodology under investigation could not be easily extended to other solvent systems. Nonetheless, the putative HAT reactivity of the aryl radical in acetonitrile media prompted us to further investigate it.

3.7 Investigation towards the application of the methodology towards the generation of the acetonitrile radical

Upon examination of the literature, a limited amount of procedures for the generation and synthetic application of the acetonyl radical were identified[3.3]. This is quite astonishing, considering that the acetonyl radical has recently attracted the scientific community for his surprisingly high concentration in the troposphere where it affects NO_x, HO_x and O_3 cycles[3.4]. Among these publications, it was considered of particular relevance for the ongoing study the work of Li et al on the alkylarylation of activated alkenes enabled by VLPC[3.5]. With this work, the authors established a methodology for the generation of both the acetonyl and the acetonitrile radicals starting from aryl radicals generated from arendiazonium salts. Taking into consideration their procedure for the generation of the acetonyl radical, illustrated in **Scheme 3.7.1**, many aspects of their reaction conditions aroused our attention.

Scheme 3.7.1: Generation and trapping of the acetonyl radical by Li et al

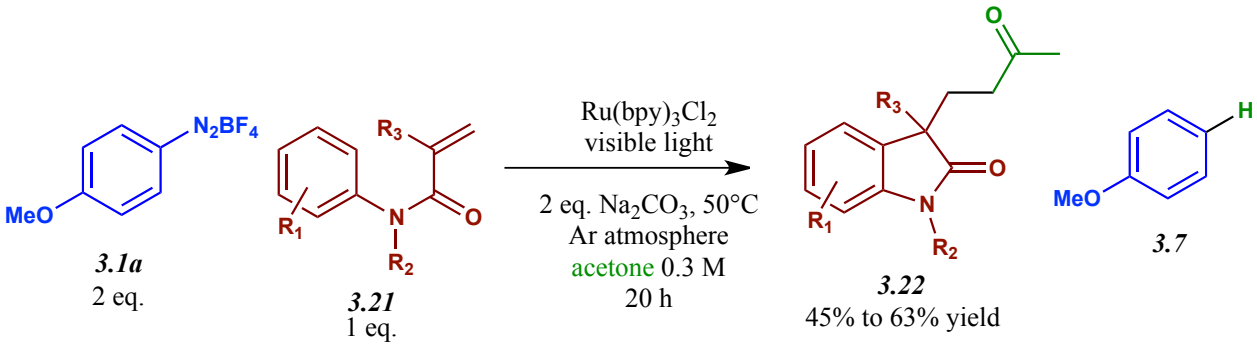

In fact, in front of the apparent similarity of their procedure with our work, the two methodologies instead differ quite considerably in terms of reaction conditions. Noteworthy, Li's procedure seems to require an highly concentrated solution of the reagents (0.3 M of the olefinic trap ***3.21***, 0.6 M of the diazonium salt ***3.1a***). In these conditions, one would expect the direct attack of the aryl radical to be reasonably favoured over the HAT leading to the acetonyl radical. As it was previously discussed in **Paragraphs 3.2** and **3.4**, the use of diluted conditions (0.01M of both the olefinic trap ***3.2*** and the diazonium salt ***3.1***) lays instead at the basis of the herein described doctoral project. In his paper, Li suggests that the use of basic conditions, along with warming, is responsible for disfavouring the competitive aryl radical attack which was previously reported in the literature[3.6].

By application of the same reaction conditions, Li was also able to efficiently generate and trap the acetonitrile radical.

Scheme 3.7.2: Generation and trapping of the acetonitrile radical by Li et al

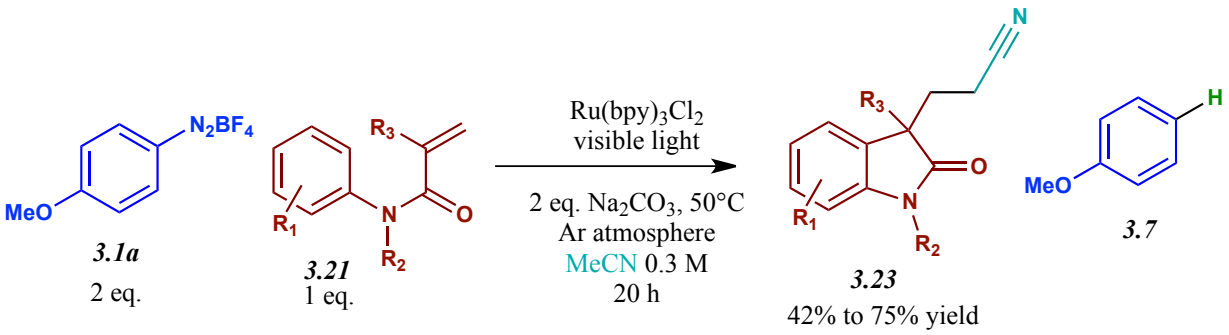

Having acquired some experience on the reactivity of aryl radicals in concentrated acetonitrile solution (see **Chapter 2**), we were quite astonished by this result. As a consequence, believing that the structure of acrylamides ***3.21*** used by Li could reasonably play a crucial role towards the transformation, it was decided to submit it to our reaction conditions. A screening of the reactivity of both acetone and acetonitrile, in concentrated and diluted conditions, was performed on the acylamide ***3.21a***.

Table 3.7.1: Screening of reaction conditions involving diazonium salt ***3.1a*** and acrylamide ***3.21a***

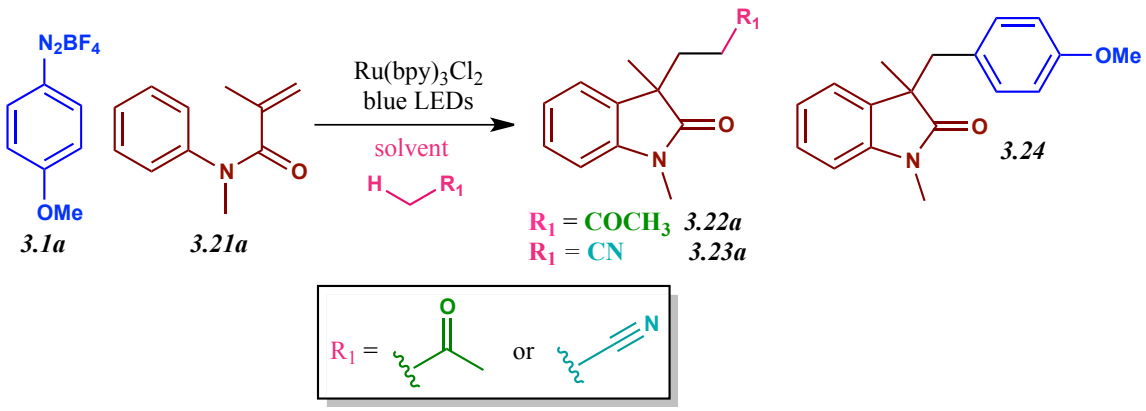

entry	solvent	concentration	conditions	product yield	product ***3.24*** yield	substrate ***3.21a*** recovery
1	acetone	0.01 M	mesoflow 10 mL/h	***3.22a*** 18%	not observed	80%
2	acetone	0.005 M	mesoflow 2 mL/h	***3.22a*** 50%	not observed	46%
3	MeCN	0.005 M	mesoflow 1 mL/h	***3.23a*** 2%	not observed	79%
4	acetone	0.2 M	batch 24h	***3.22a*** 74%	not observed	traces
5	MeCN	0.2 M	batch 24h	***3.23a*** 25%	15%	10%

When our optimized flow conditions were applied to acrylamide ***3.21a*** (entry 1), the expected product ***3.22a*** was obtained with low yield. A better result could be achieved with a slower flow speed (entry 2) but, when applied to acetonitrile, the methodology only afforded traces of the desired product ***3.23a*** (entry 3). Surprisingly, when the reaction was performed in higher concentration of acetone, the compound ***3.22a*** was achieved with high yield (entry 4). Apparently, in this case Li's reaction could be reproduced without any need of excess reagents, base and warming. This result may imply that the structure of acrylamide ***3.21a*** behaves as a particular case towards this reactivity. Less surprising was the outcome of the concentrated reaction in acetonitrile (entry 5); in this case, a mixture of products ***3.23a*** and ***3.24*** was obtained. As a consequence of the collected results, no further attempt to extend our methodology to acetonitrile nor any other tested solvent was performed.

Following, a potenital enantioselective route towards the metabolite ***3.4*** was investigated.

3.8 Enantioselective reaction attempt towards the formation of isobenzofuranone *3.4*

With the final aim to establish a potential stereoselective transformation, the esterification reaction of 2-vinylbenzoic acid ***3.2a*** with enantiomerically pure (-)-menthol was performed (**Scheme 3.8.1**).

Scheme 3.8.1: Esterification reaction leading to enantiomerically pure olefin ***3.2b***

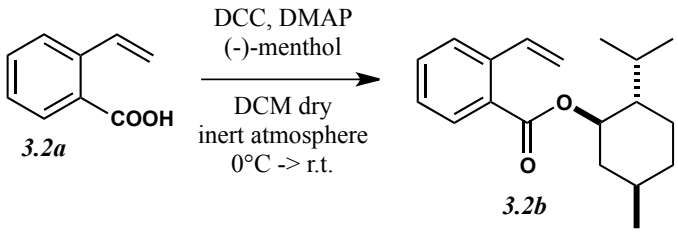

The desired starting material (1R,2S,5R)-2-isopropyl-5-methylcyclohexyl 2-vinylbenzoate ***3.2b*** was obtained by means of a Steglich Esterification[3.7].

The readily obtained olefinic trap ***3.2b*** was submitted to the optimized reaction conditions leading to isobenzofuranone ***3.4***.

Scheme 3.8.2: Potentially stereoselective reaction of diazonium salt ***3.1a*** with olefin ***3.2b***

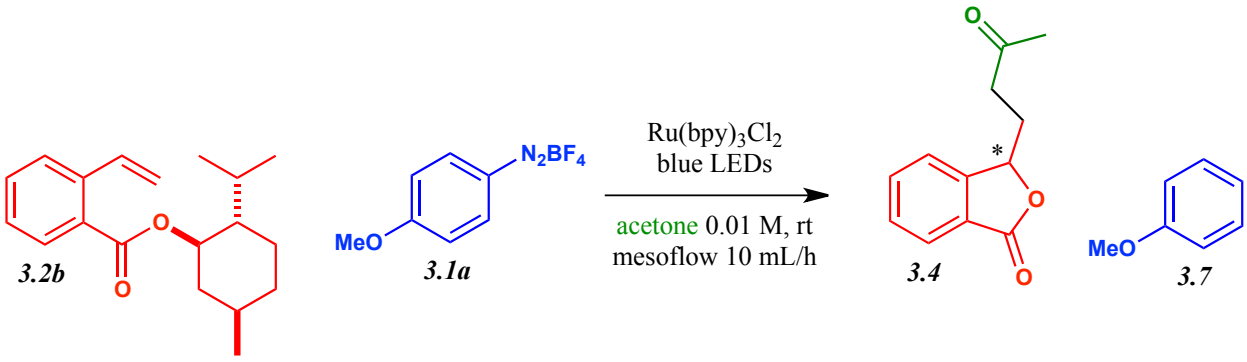

On a theoretical point view, the steric hindrance of the ester moiety displayed by compound ***3.2b*** along with the high density of chiral centers on the menthol side chain could be responsible for a potential chiral induction.

Scheme 3.8.3: Rationale behind the potential stereoinduction of the intramolecular cyclization

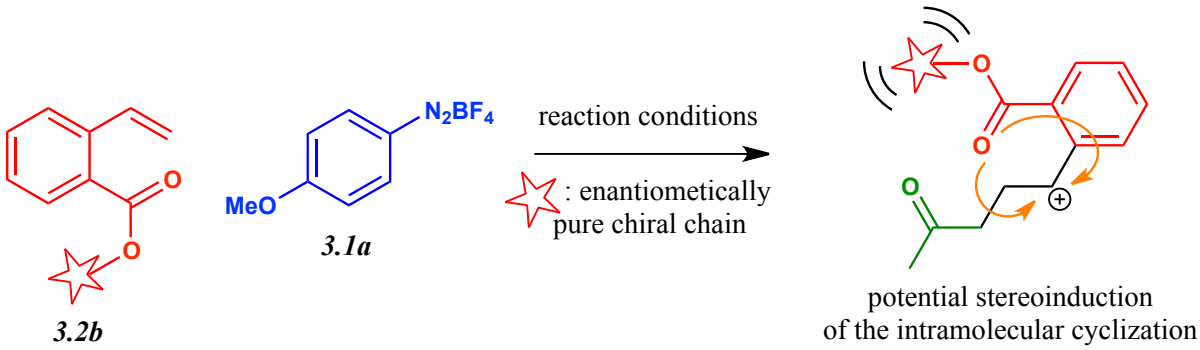

The desired product ***3.4*** was achieved with a satisfying 75% yield, indicating that the use of sterically hindered olefinic traps do not affect the reaction outcome. Noteworhty, no side-product possessing the menthol fragment could be isolated. Upon analysis of the reaction product via both optical rotation measurement and chiral HPLC (high performance liquid chromatography), it could be asserted that the isobenzofuranone ***3.4*** was obtained as a racemic mixture. As a consequence, a methodology leading to enanthiomerically enriched compounds could not be established.

3.9 Application of the acetonyl radical generation reaction towards a new synthetic methodology

Looking forward to synthetically exploit the newfound reaction, a series of experiments was performed. To begin with, the C-C coupling reaction between the acetone moiety and simple olefins was envisioned.

Scheme 3.9.1: Expected reaction outcome upon submission of olefins of general formula ***3.25*** to the reaction conditions

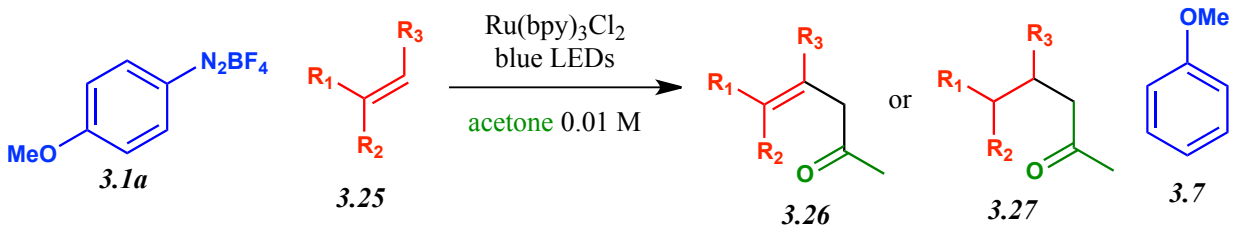

In fact, such a transformation would be a highly valuable tool for synthetic organic chemists, allowing the functionalization of double bonds in mild conditions. Noteworthy, radical alkenylation reactions occupy a relevant position in the synthetic organic chemistry panorama[3.8].

Several olefinic substrates were submitted to standard reaction conditions with a set of screening experiments illustrated in **Scheme 3.9.2**.

Unfortunately, the data collected from the set of experiments did not lead to the establihment of a new methodology towards the acetonylation of olefins. In fact, the coupling reaction between the acetonyl radical and the olefins represented in **Scheme 3.9.2** was not successful.

Scheme 3.9.2: Attempts to establish a methodology for the acetonylation of olefins ***3.25***

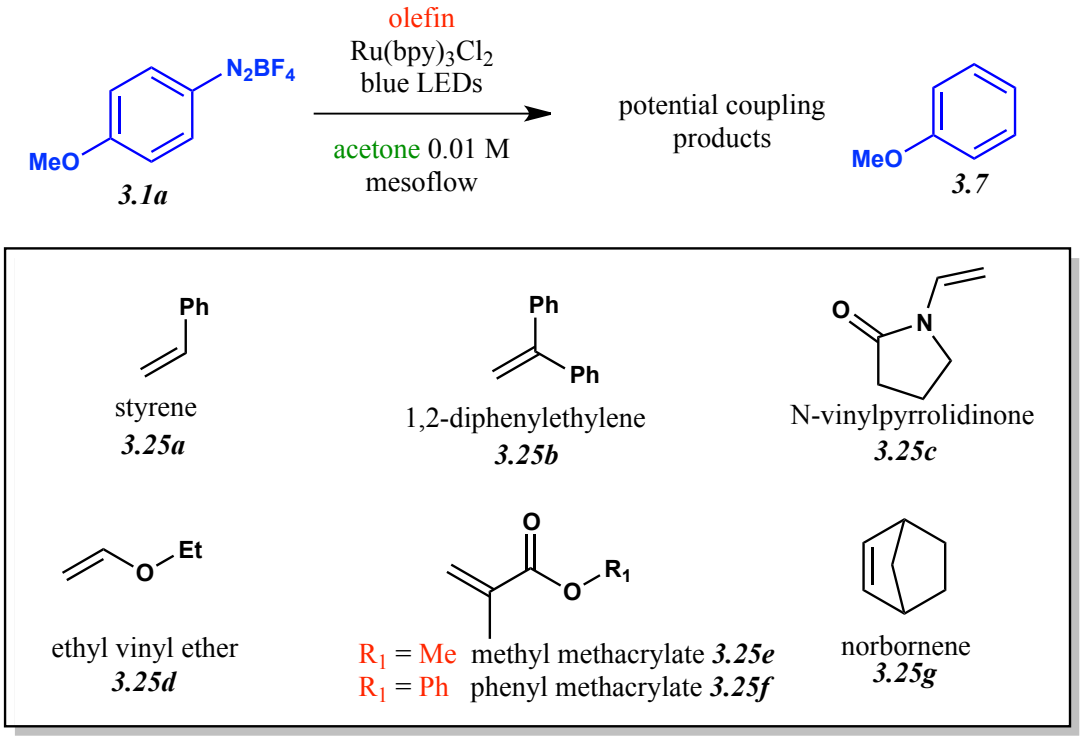

standard reaction conditions: 4-methoxyarendiazonium tetrafluoroborate ***3.1a*** 1 eq., olefin ***3.25*** 1 or 2 eq., $Ru(bpy)_3Cl_2$ 5 mol%, acetone 0.01 M, mesoflow 1 to 10 mL/h

The reason for this outcome is probably connected with the reactivity of the radical intermediate ***3.28*** and/or the cationic intermediate ***3.29*** deriving from the coupling reaction of the acetonyl radical ***3.6*** with the olefin.

Scheme 3.9.3: Presumably formed reaction intermediates

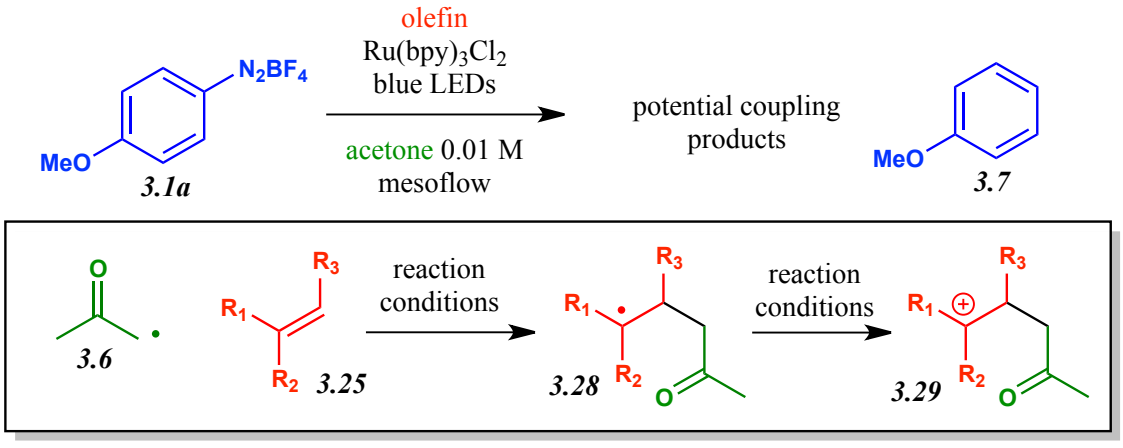

In fact, no straightforward direction is known for the evolution of such intermediates, for which an intermolecular reaction, such as water addition (leading for example to compound ***3.31***) or base promoted proton abstraction (leading for example to compound ***3.30***) could be in principle expected.

Scheme 3.9.4:Reactvity pathways of the reaction intermediates

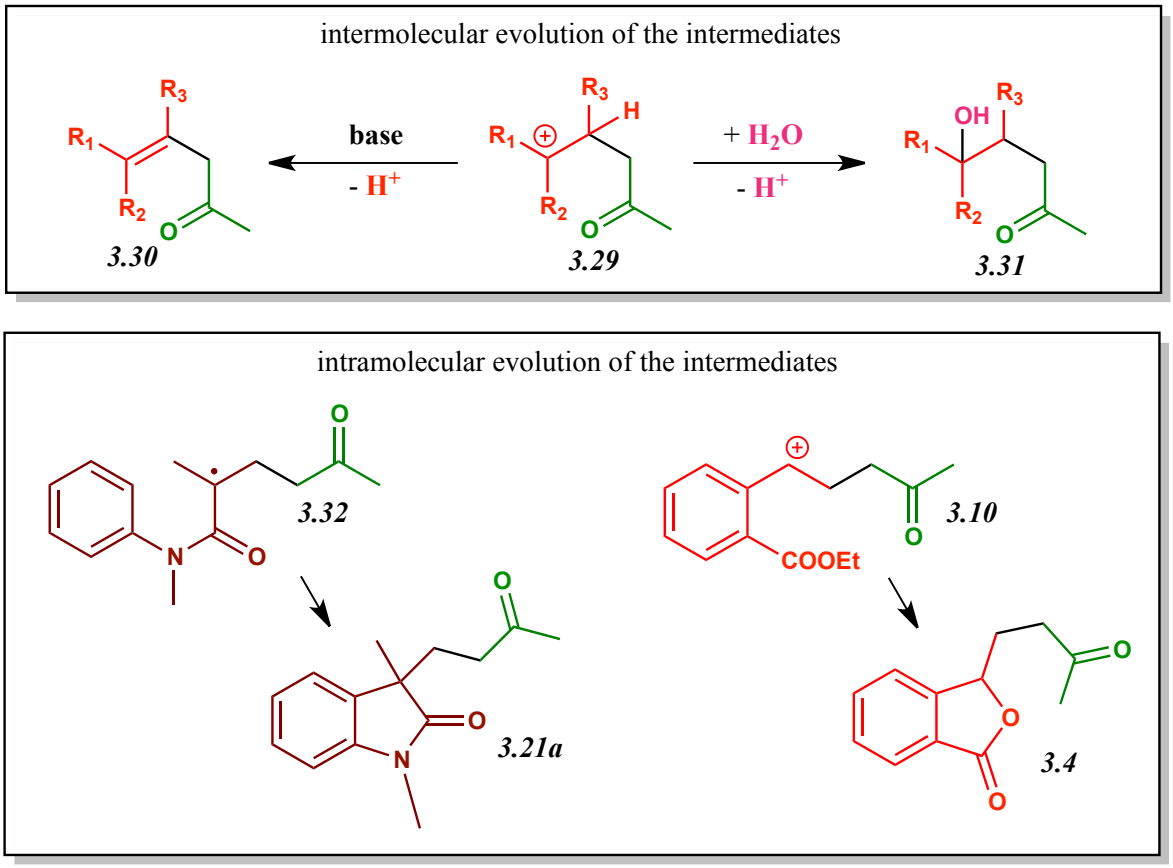

On the contrary, when the olefinic traps ***3.21*** and ***3.2*** are attacked by the acetonyl radical (as reported in **Scheme 3.2.2** and **Scheme 3.7.2**) the respective intermediates (***3.32*** and ***3.10*** respectively) evolved intramolecularly in a straightforward way.

In order to favour the reactivity of the intermediates, different additives, such as acids, bases and nucleophiles, were added to the reaction conditions; several experiments were performed. Nonetheless, no definite reaction pathway could be anyway identified. Noteworthy, the reaction of phenylmethacrylate ***3.25h*** in the optimized conditions discussed in the previous paragraphs could in principle lead to an intramolecular cyclization similar to that showed by N-methyl-N-phenylmethacrylamide ***3.21a***. Instead, no product is achieved when this olefin is employed.

Scheme 3.9.5: Different intramolecular cyclization outcomes of different substrates

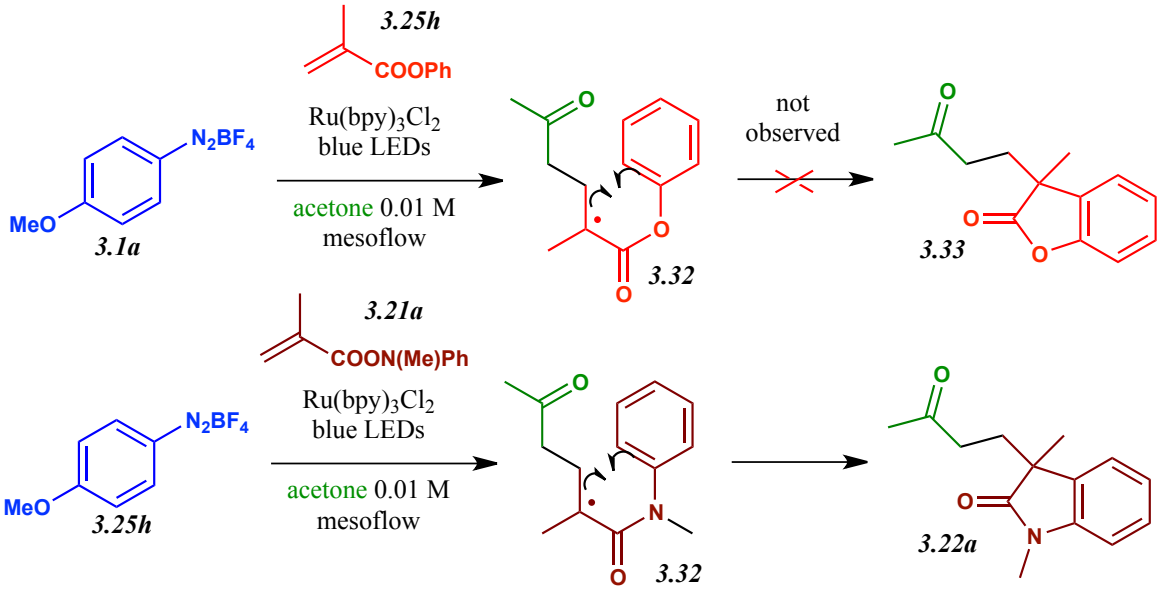

Evidently the electronic effect of nitrogen and oxygen, along with the steric hindrance of the methyl group in case of the amide ***3.21a***, makes a distinct difference among the two reaction pathways.

The reactivity of triple bonds in the reaction conditions was investigated as well, without a significant difference in terms of results when it comes to simple alkines such as ethynilbenzene. Noteworthy, when phenyl-3-phenylpropiolate ***3.35*** was submitted to the reaction conditions, the intramolecular cyclization product ***3.36*** could be achieved with low yield.

Scheme 3.9.6: Reaction of diazonium salt ***3.1a*** with alkyne ***3.35***

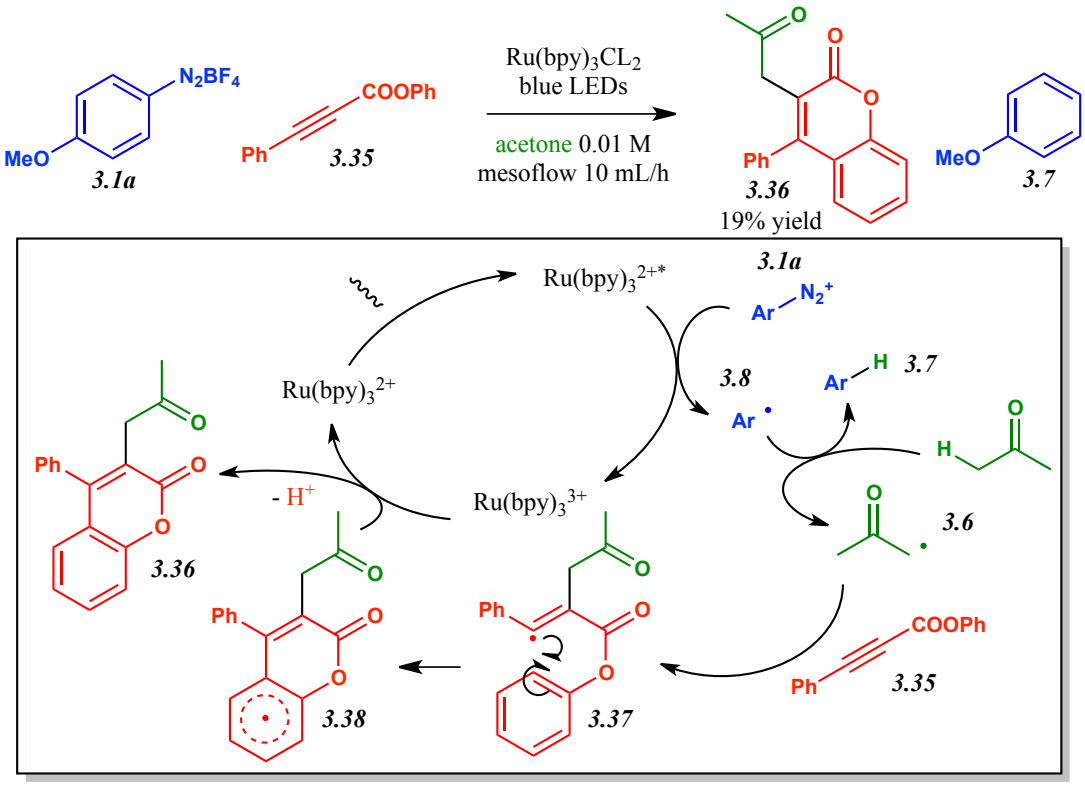

The mechanism leading to this product is illustrated in **Scheme 3.9.6** and it is consistent with literature reports[3.9].

A quick optimization of the reaction flow speed allowed to improve the yield of this reaction from low to moderate.

Table 3.9.1: Optimization of the reaction flow conditions

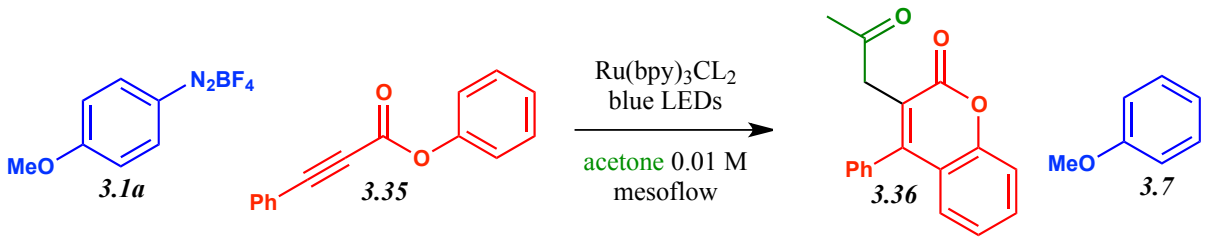

entry	flow speed	product ***3.36*** yield
1	10 mL/h	19%
2	5 mL/h	27%
3	1.5 mL/h	39%
4	0.5 mL/h	38%

With the final aim to build a small library of similar chromenone derivatives, phenyl-3-phenylpropiolate analogs ***3.35a*** and ***3.35b*** were prepared and submitted to the reaction conditions.

Scheme 3.9.7: Unsuccessful reaction of diazonium salt ***3.1a*** and alkynes ***3.35a*** and ***3.35b***

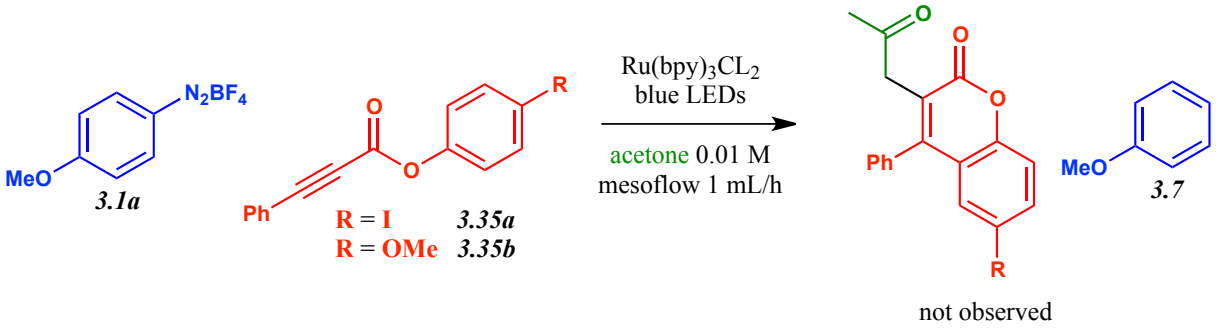

not observed

The reaction of compound ***3.35*** could not be extended since no expected product could be identified when functionalized derivatives ***3.35a*** and ***3.35b*** were employed in the reaction conditions.

Considering the outcome of the reactions with alkenes and alkines to be unsatisfactory, it was decided to investigate the reactivity of silyl enol ethers. The utilization of silyl enol ethers as radical traps is well known in the literature[3.10].

In addition, it could be envisioned that the electrophilic nature of the acetonyl radical species could promote a favourable reactivity with electron rich double bonds, like the ones presented by silyl enol ethers.

When tert-butyldimethyl((1-phenylvinyl)oxy)silane ***3.39a*** was submitted to the reaction conditions, the desired product ***3.40*** was obtained with moderate yield.

Scheme 3.9.8: Reaction of diazonium salt ***3.1a*** with silylenol ether ***3.39a***

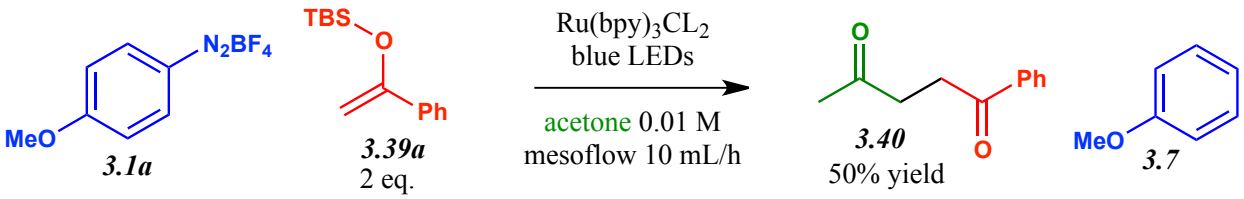

The use of excess silyl enol ether substrate ***3.39a*** was necessary to compensate for its rather unstable nature.

As a consequence, the convenient C-C coupling of two ketones was achieved via this methodology. An unpolung of acetone and acetophenone ***3.40a*** via VLPC and silyl enol ether formation enabled the achievement of a structurally attractive 1,4-dicarbonyl compound ***3.40***.

Scheme 3.9.9: Unpolung of ketones via VLPC

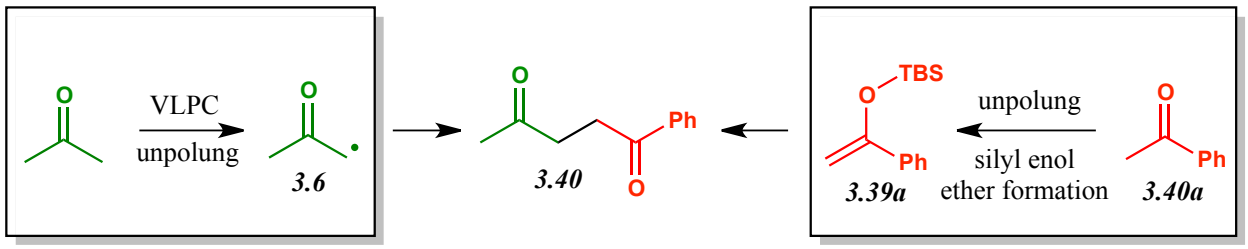

A reasonable mechanism to explain the outcome of this reaction is reported in **Scheme 3.9.10**.

Following the attack of the acetonyl radical ***3.6*** to the silyl enol ether ***3.39a*** double bond, the radical intermediate ***3.41*** is achieved. Noteworthy, the decomposition of the silyl enol ether ***3.39a*** to ketone ***3.40a*** should be hampered otherwise the reaction would be inhibited by lack of substrate.

Scheme 3.9.10: Reaction mechanism

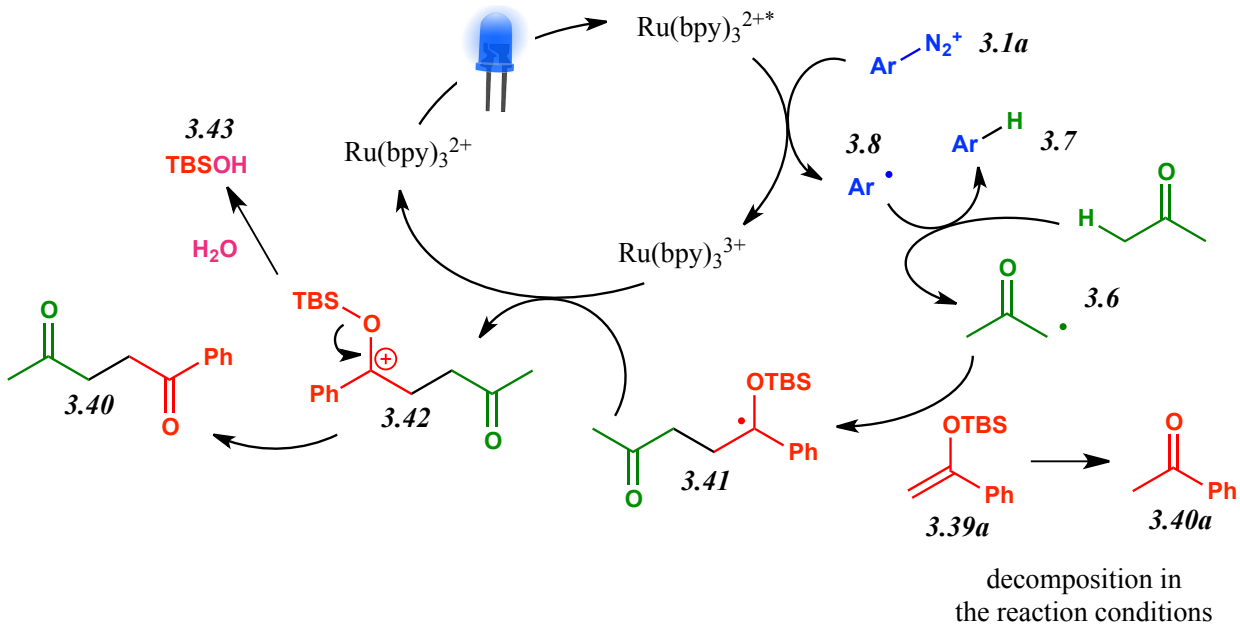

The catalytic cycle is closed by the oxidation of the radical intermediate ***3.41*** to carbocation. The key step of the transformation consists in the release of the dimethyl tert-butyl silyl cation to form the product ***3.40*** as an electronically neutral compound. In opposition to what was previously discussed in this paragraph with respect to the reactivity of olefins (**Scheme 3.9.3**), upon attack of the acetonyl radical ***3.6***, silyl enol ethers allow the formation of intermediates readily evolving to products. Reasonably, the silyl cation is captured by the water present in the reaction media to form the respective silanol ***3.43***.

Attracted by this promising transformation, further experiments were conducted with the final aim to set up a synthetic methodology. The outcome of this investigation is reported in the following paragraph.

3.10 Synthetic methodology for the formation of 1,4-dicarbonyl compouds via acetonyl radical formation followed by reaction with silyl enol ethers

To begin with, the acetonylation reaction of silyl enol ether ***3.39a*** leading to compound ***3.40***, illustrated in **Scheme 3.9.8** was used as a standard for an optimization study (**Table 3.10.1**).

Table 3.10.1: Optimization of the reaction conditions

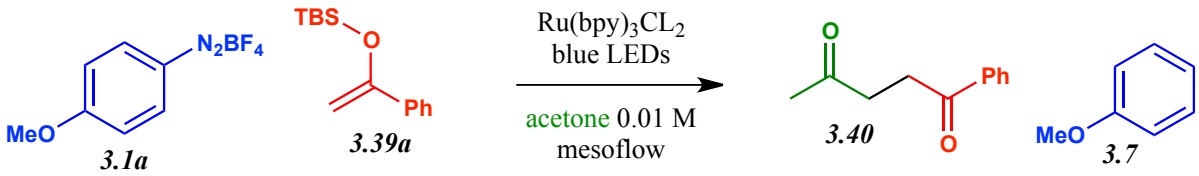

entry	silyl enol ether ***3.39*** eq.	diazonium salt ***3.1a*** eq.	flow rate	decomposition of silyl enol ether inside the syringe	product ***3.40*** yield
1	1	1	10 mL/h	yes	19%
2	1	2	10 mL/h	yes	15%
3	2	1	10 mL/h	yes	50%
4	3	1	10 mL/h	yes	50%
5	2	1	5 mL/h	yes	39%
6	2	1	20 mL/h	yes	45%
7*	2	1	10 mL/h	no	91%

reactions performed via method A: the reactants (0.25 mmol scale) and catalyst are dissolved in 25 mL of acetone and the resulting solution is withdrew with a 25 mL gasthight syringe. *method B: the reactants and catalyst are divided into 10 aliquotes (0.025 mmol scale) then each aliquote is dissolved in 2.5 mL of acetone and withdrew with a 2.5 mL gasthight syringe. Each solution is prepared and injected in the mesoflow system only when the former one is completely eluted.

When the reaction is performed with only one equivalent of silyl enol ether, the yield drops considerably (entries 1 and 2); on the other hand, the utilization of more than two equivalents does not seem to have any beneficial effect (entry 4). Contrary to the expectations, when the flow speed is decreased, the reaction yield diminishes (entry 5). This result can be explained with the deprotection of the silyl enol ether starting material ***3.39a*** inside the syringe leading to the formation of the respective ketone ***3.40a***. Despite a longer retention time reasonably favours the desired transformation in the irradiated zone, it also allows for more decomposition of the substrate in the non-irradiated ones. In order to suppress the side-reaction, the flow rate was increased; but also in this case a lower yield was achieved (entry 6). The decomposition of the silyl enol ether ***3.39a*** and its conversion to product ***3.40*** are both favoured by longer reaction times, making it difficult to optimize the reaction. The solution to this problem was found with a modification of the reaction set-up; a different method was designed (in **Scheme 3.10.1**, method A is the method previously used, while method B is the improved one).

Scheme 3.10.1: Different flow methodologies towards the acetonylation of silyl enol ethers

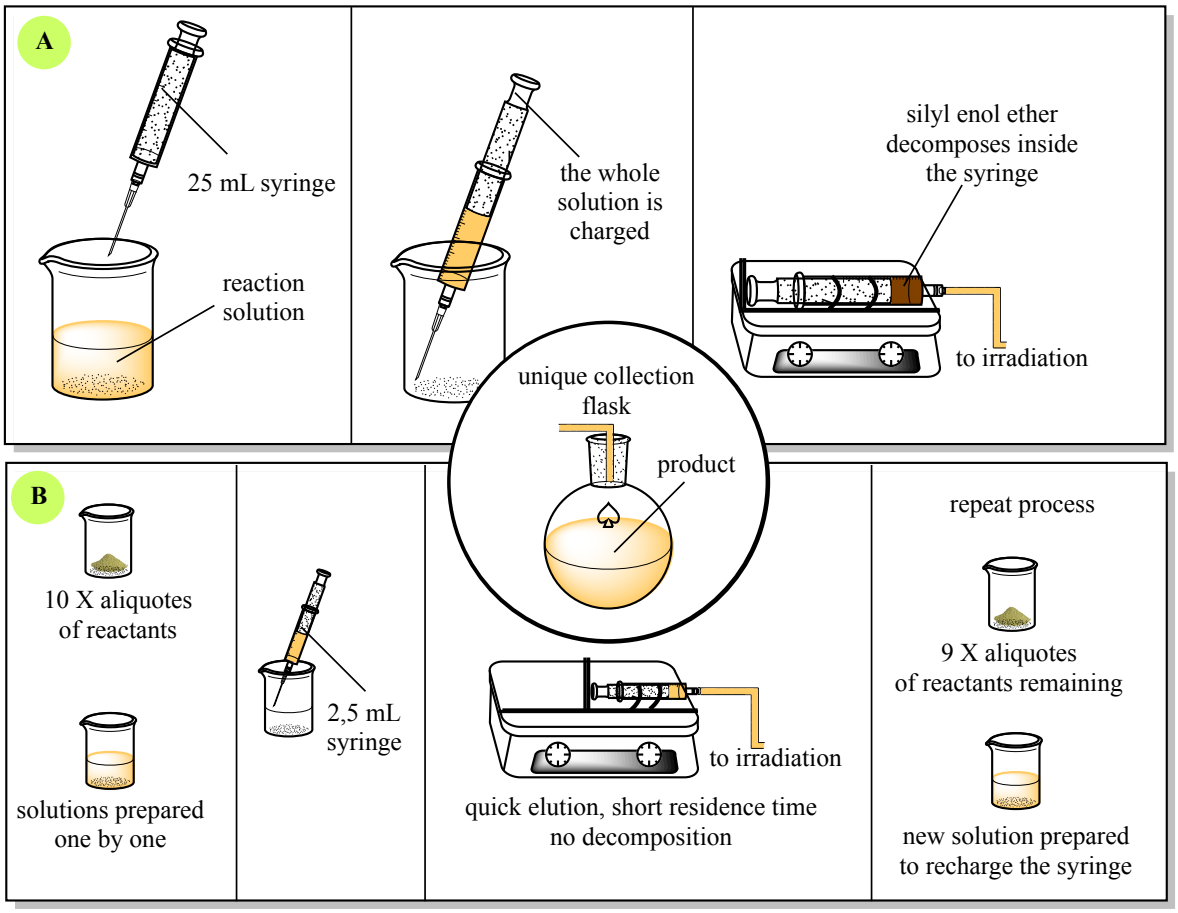

Ten aliquotes of reactants and catalyst were prepared in ten vessels. One by one, the tenfold smaller reaction solution was charged in the mesoflow system by means of a smaller syringe (2.5 mL scale instead of the standard 25 mL one). Only when the syringe was fully eluted, a new solution was quickly prepared and injected in series with the previous one. The same collection vessel was employed, getting as a final result a 25 mL reacted solution. By checking the content of the 2.5 mL syringe via TLC analysis, no silyl enol ether decomposition could be observed. As a consequence, an optimal reaction yield was achieved (Entry 7, **Table 3.10.1**).

Having both the optimized conditions and method in hand, a library of silyl enol ethers was prepared by means of literature procedures[3.11].

Scheme 3.10.2: Library of silyl enol ethers

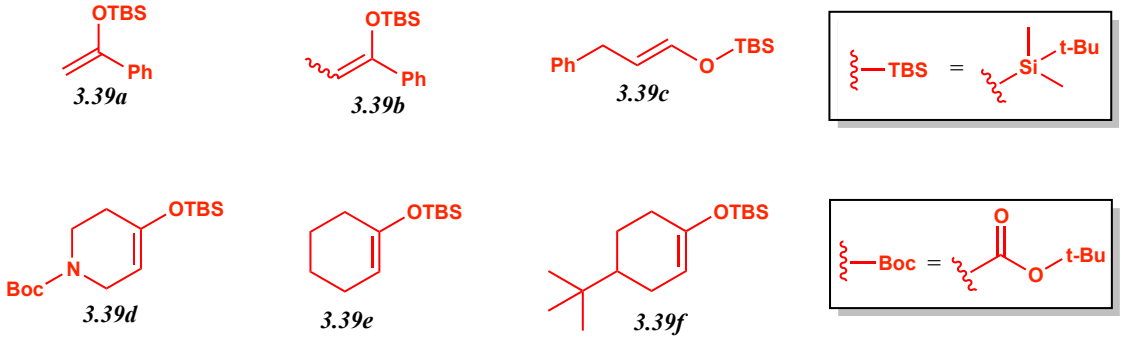

Afterwards, the readily obtained starting materials ***3.39a-3.39f*** were submitted to the optimized reaction conditions, leading to a library of 1,4-dicarbonyl compounds ***3.44-3.47*** with good to excellent yields.

Scheme 3.10.3: Acetonylation of silyl enol ethers

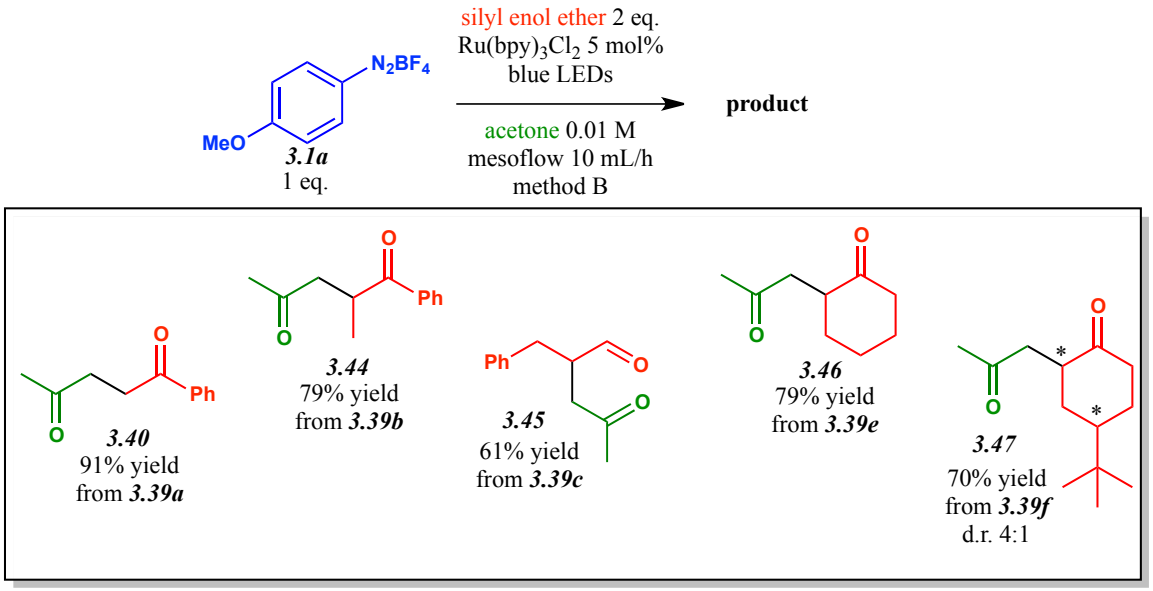

When tert-butyl((4-(tert-butyl)cyclohex-1-en-1-yl)oxy)dimethylsilane ***3.39f*** was submitted to the reaction conditions, two diasteroisomeric products were obtained with a d.r. (diastereoisomeric ratio) of 4:1 in favour of the *cis* compound ***3.47a*** (Scheme 3.10.4).

Scheme 3.10.4: Reaction of diazonium salt ***3.1a*** with silyl enol ether ***3.39f***

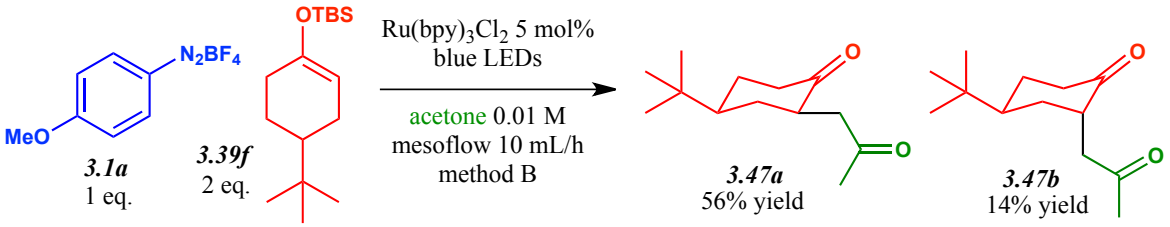

Surprisingly, when silyl enol ether ***3.39d*** was submitted to the reaction conditions, the expected product ***3.49*** was not observed in the reaction miture.

Scheme 3.10.5: Reaction of diazonium salt ***3.1a*** with silyl enol ether ***3.39d*** and unexpected product

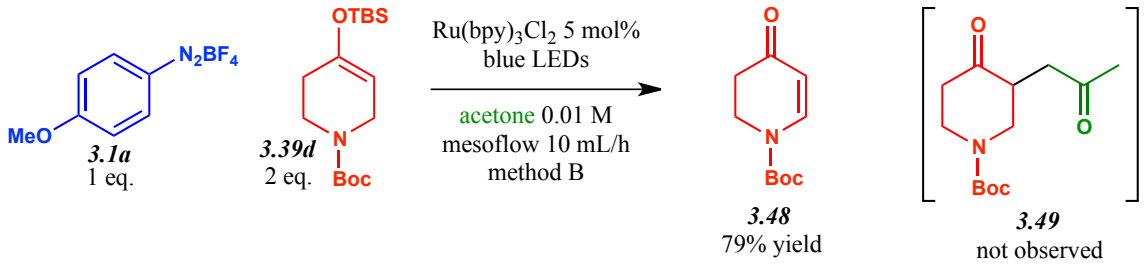

On the other hand, the unexpected compound ***3.48***, corresponding to the oxidation product of N-Boc-piperidone, was isolated with high yield. This outcome can be explained by a reasonable mechanism involving an hydrogen abstraction reaction taking place in α-position with respect to the nitrogen atom of compound ***3.39d*** rather than on the methyl of acetone.

Scheme 3.10.6: Reaction mechanism

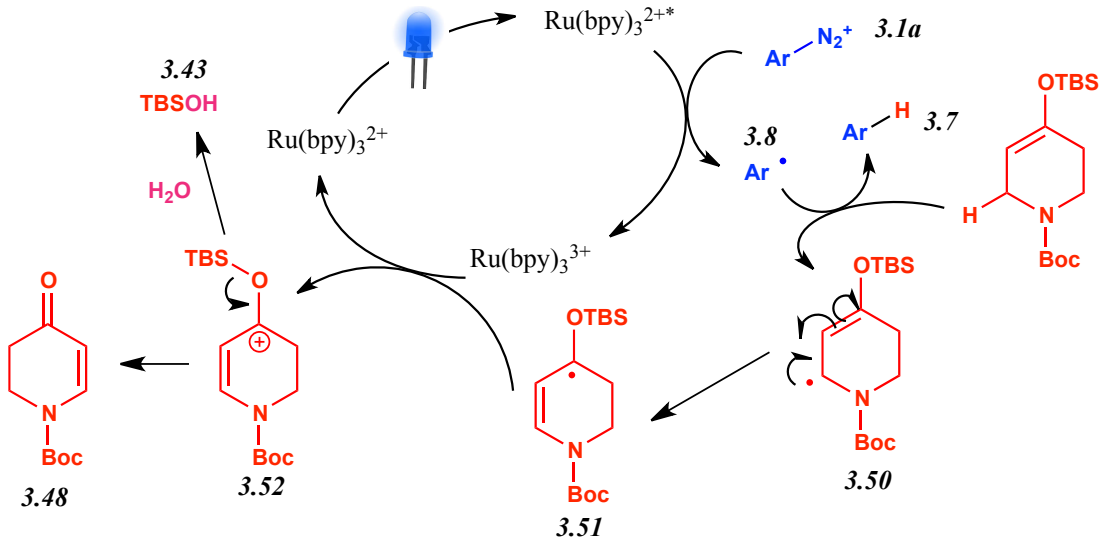

An alternative reaction mechanism to the one proposed in **Scheme 3.10.6** could involve the HAT reaction promoted by the acetonyl radical ***3.6*** rather than the by aryl radical ***3.8***. On the other hand, it is more reasonable to think that the former species ***3.6*** is never formed otherwise it would probably attack the double bond leading to the expected product ***3.49***.

By inspection of the literature it was found that the pecularíar ease of HAT in α-position to the N-Boc group is well known[3.12].

3.11 Conclusions

In conclusion, a synthetic methodology for the generation of the acetonyl radical by means of VLPC has been established. By means of this work, the construction of useful C-C bonds among the solvent acetone and olefinic substrates was disclosed. When 2-vinylbenzoic acid derivatives are employed in the described conditions, an interesting metabolite of n-butylphtalide can be achieved. Instead, interesting 1,4-dicarbonyl compounds can be accessed in mild conditions when silyl enol ethers are employed as reaction substrates.

The convenient utilization of a continuous (or semicontinuous) flow technology allowed to achieve exceptional product yields in a short reaction time.

Additional applications of this methodology will be discussed in Chapter 4.

Mechanistic investigations along with theoretical calculations allowed us to get a clear view on the chemistry described in this chapter. Nonetheless, it was not possible to extend the herein described synthetic procedure to different solvents nor to different radical traps. New reaction conditions are currently under investigation inside our laboratories in order to further extend this research project.

3.12 References

3.1
Diao X.; Deng P.; Xie C.; Li X.; Zhong D.; Zhang Y.; Chen X. *Drug Metab. Dispos.* **2013**, *41*, 430-444.

3.2
(a) Capaldo L.; Ravelli D. Eur. *J. Org. Chem.* **2017**, *15*, 2056-2071.
(b) Protti S.; Fagnoni M.; Ravelli D. *Chem. Cat. Chem.* **2015**, *7*, 1516-1523.

3.3

(a) Shiraishi Y.; Tsukamoto D.; Hirai T. *Org. Lett.* **2008**, *10*, 3117-3120.
(b) Zhu L.; Chen H.; Wang Z.; Li C. *Org. Chem. Front.* **2014**, *1*, 1299-1305.
(c) Shen X.; Cao X.; Zheng W.; Yang J.; Shi Y.; Hu J.; Wu X.; Yan G. *Chin. J. Org. Chem.* **2017**, *37*, 349-355.

3.4

(a) Espinosa-García J.; Márquez A.; Dóbé S. *Chem. Phys. Lett.* **2003**, *373*, 350-356.
(b) El-Nahas A. M.; Bozzelli J. W.; Simmie J. M.; Navarro M. V.; Black G.; Curran H. J. *J. Phys. Chem. A* **2006**, *110*, 13618-13623.
(c) Imrik K.; Farkas E.; Vasvári G.; Szilágyi I.; Sarzyński D.; Dóbé S.; Bérces T.; Márta F. *Phys. Chem. Chem. Phys.* **2004**, *6*, 3958-3968.
(d) Zügner G. L.; Szabó E.; Farkas M.; Dóbé S.; Brudnik K.; Sarzyński D.; Jodkowski J. T. *Chem. Phys. Lett.* **2013**, 568-569.

3.5

J. L. Zhang; Y. Liu; R. J. Song; G. F. Jiang, J. H. Li *Synlett.* **2014**, *25*, 1031-1035.

3.6

Fu W.; Xu F.; Fu Y.; Zhu M.; Yu J.; Xu C.; Zou D. *J. Org. Chem*. **2013**, *78*, 12202-12206.

3.7

B. Neises; W. Steglich *Angew. Chem. Int. Ed.* **1978**, *17*, 7, 522-524.

3.8

S. Tang, K. Liu, C. Liua, A. Lei *Chem. Soc. Rev.*, **2015**, *44*, 1070-1082.

3.9

L. Chen; L. Wu; W. Duan; T. Wang; L. Li; K. Zhang; J. Zhu; Z. Peng; F. Xiong *J. Org. Chem.* **2018**, *83*, 8607-8614.

3.10

(a) Esumi N.; Suzuki K.; Nishimoto Y.; Yasuda M. *Org. Lett.* **2016**, *18*, 5704-5707.
(b) Pettersson F.; Bergonzini G.; Cassani C.; Wallentin C. J. *Chem. Eur. J.* **2017**, *23*, 7444-7447.
(c) Luo J.; Jiang Q.; Chen H.; Tang Q. *RSC Adv.* **2015**, *5*, 67901-67908.
(d) Baciocchi E.; Muraglia E. *Tetrahedron Lett.* **1994**, *35*, 2763-2766.

3.11

(a) de Nanteuil F.; Waser J. *Angew. Chem. Int. Ed.* **2013**, *52*, 34, 9009-9013.

(b) Langer P.; Döring M.; Seyferth D.; Görls H. *Chem. Eur. J.* **2001**, *7*, 573-584.
(c) Sarabèr F.; Dratch S.; Bosselaar G.; Jansen B. J. M.; de Groot A. *Tetrahedron* **2006**, *62*, 8, 1717-1725.
(d) Zhang J.; Wang L.; Liu Q.; Yang Z.; Huang Y. *Chem. Comm.* **2013**, *49*, 99, 11662-11664.
(e) Iwasaki K.; Wan K. K.; Oppedisano A.; Crossley S. W. M.; Shenvi R. A. *J. Am. Chem. Soc.* **2014**, *136*, 4, 1300-1303.

3.12

T. Wakaki; K. Sakai; T. Enomoto; M. Kondo; S. Masaoka; K. Oisaki; M. Kanai *Chem. Eur. J.* **2018**, *24*, 8051-8055.

CHAPTER 4:
THE SILILATIVE KETENE THREE-COMPONENT REACTION

In this chapter, the work leading to the sililative ketene three-component reaction is described along with its main applications. I would like to underline that i only partially contributed to this work, which was mainly developed by other members of the research group, since the herein described research project was not directly assigned to me. The research work reported in this chapter was the subject of a scientific publication[4.1]. In the final paragraph of this chapter, the combination of the sililative three-component reaction (S-K3CR) with the acetonyl radical methodology, previously described in **Chapter 2**, will be discussed.

4.1 The Ketene three-component reaction

In recent years, the BOG group disclosed a novel three-component transformation involving two molecules of arylacetic acid ***4.1*** and one moelcule of isocyanide ***4.2***, at high temperature, leading to captodative olefins of structure ***4.3***[4.2].

Scheme 4.1.1: Three-component reaction between isocyanides and carboxylic acids generating captodative olefins ***4.3***

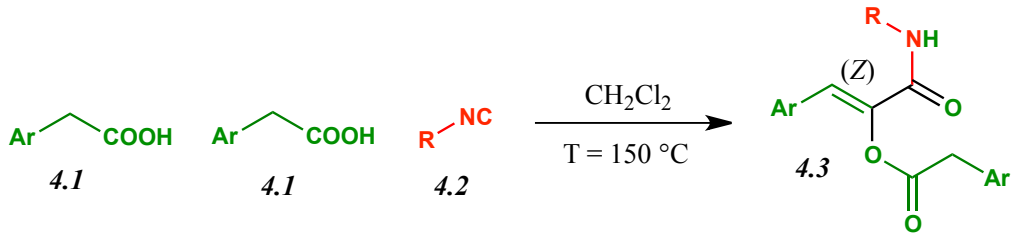

The nomenclature captodative olefins refers to alkenes with both an electron-withdrawing and an electron-donating group at the α-carbon[4.3]. These compounds have proved to be very versatile synthons for cycloadditions[4.4], Friedel–Crafts reactions[4.5], and natural product synthesis[4.6]. Noteworthy, the captodative olefins of formula ***4.3*** are obtained in a stereodefined manner, always possessing a *cis* configuration between the olefinic hydrogen and the carbonyl amide. The postulated mechanism of the reaction is reported in **Scheme 4.1.2**.

Following the formation of the adduct ***4.4*** deriving from the carboxylic acid ***4.1*** and the isocyanide ***4.2***, the intervention of a second molecule of isocyanide leads to the formation of the nitrlium ion ***4.5***. The subsequent attack of a carboxylate anion ***4.1a***, followed by acyl migration, affords the desired product ***4.3***.

Scheme 4.1.2: Reaction mechanism

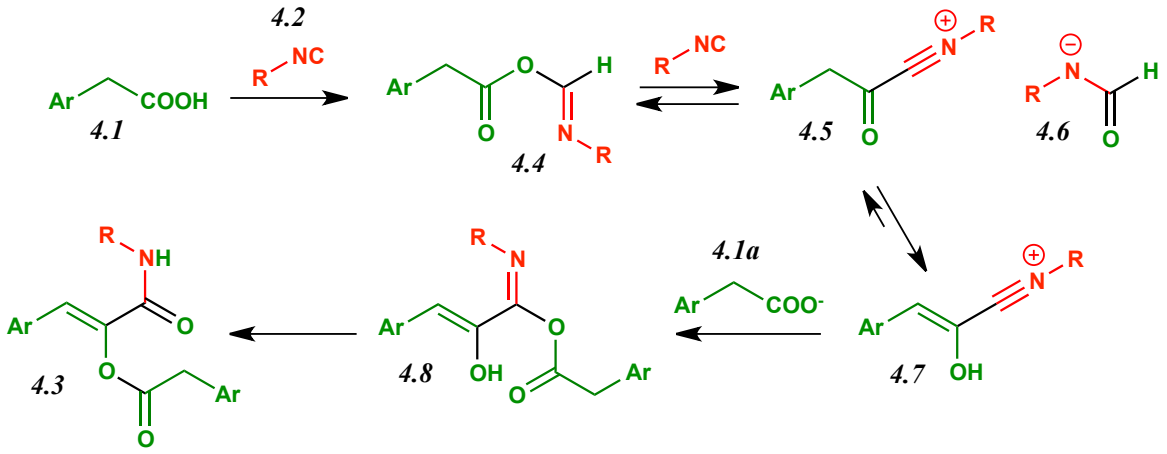

The 3-aryl-2-acyloxiacrylamides ***4.3*** achieved via this attractive transformation are able to afford interesting cyclization reactions leading to pyrrolone ***4.9*** and pyrrolidinedione ***4.8*** derivatives.

Scheme 4.1.3: Cyclization reactions of 3-aryl-2-acyloxiacrylamides ***4.3***

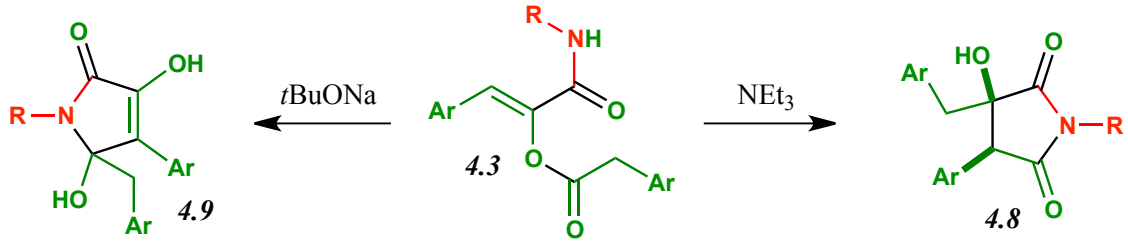

Despite the attractive features of this transformation, the limitations in terms of product diversity brought by the utilization of two identical molecules of arylacetic acid ***4.1***, standing for both the electrophilic and the nucleophilic partner, negatively affect the synthetic utility of the reaction. In fact, despite the many attempts performed, it was not possible to extend the methodology to the utilization of two different carboxylic acids.

As a consequence of the reasoning on the reaction mechanism, it was taken into consideration to substitute the electrophilic partner of the reaction with a ketene. Indeed, this idea successfully led to the discovery of the K3CR[4.7].

Scheme 4.1.4: Ketene three-component reaction

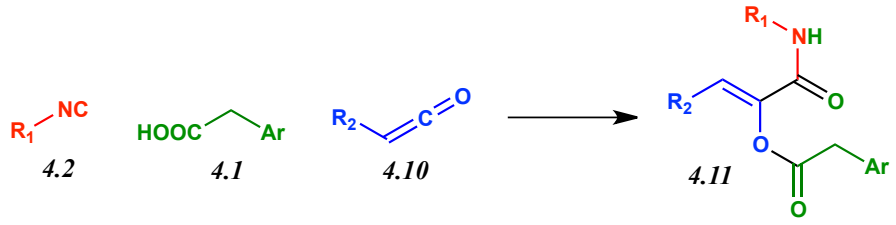

Since ketenes are unstable compounds, they necessarily need to be generated in situ; among the different available techniques for this purpose, the research group took advantage of the Wolff rearrangement of a-diazoketones[4.8]. This rearrangement can be initiated by thermolysis, metal ion catalysis or photolysis; the latter was selected to investigate a photoinduced three-component reaction.

Following optimization studies, the K3CR methodology was successfully established with the conditions illustrated in **Scheme 4.1.5**.

Scheme 4.1.5: Reaction conditions of the K3CR

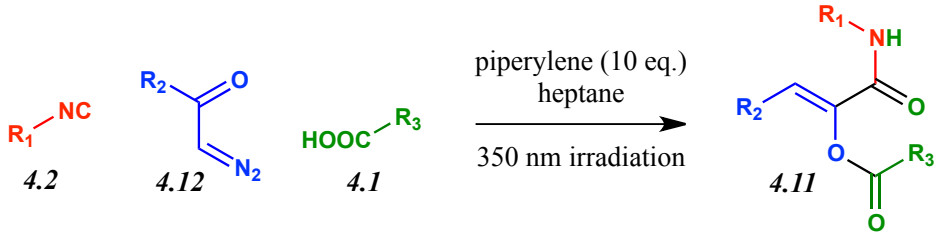

The additive trans-piperylene is employed as a quencher of triplet excited states and is necessary to suppress the UV-promoted isomerization of the reaction product ***4.11***.

The mechanism of the K3CR is reported in **Scheme 4.1.6**.

Scheme 4.1.6: Reaction mechanism

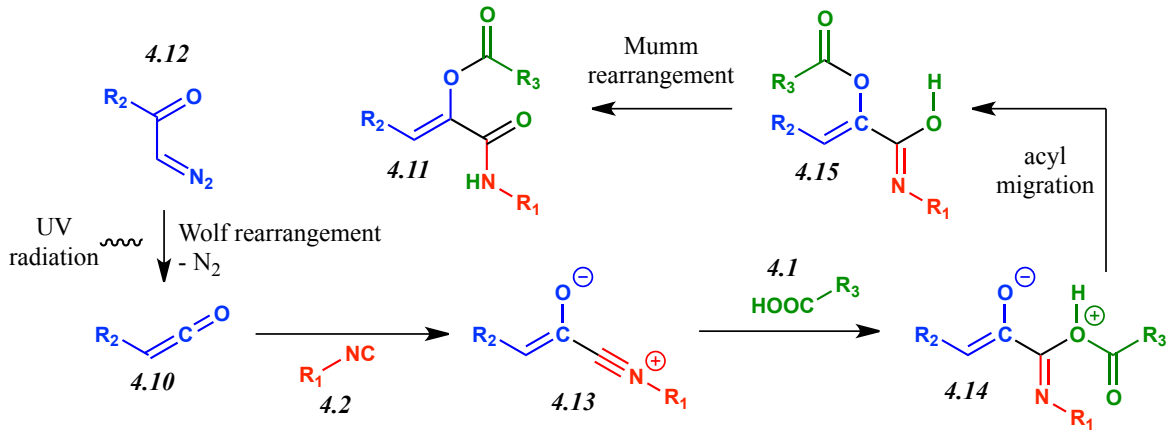

The first step consists of the photochemical formation of the ketene ***4.10*** starting from diazoketone ***4.12*** by means of a Wolf rearrangement. Secondly, the attack of the isocyanide ***4.2*** to the latter compound affords the nitrilium ion ***4.13***. Subsequently, attack of the carboxylic acid ***4.1*** followed by acyl migration leads to compound ***4.15***. The final product ***4.11*** is obtained by means of a Mumm rearrangement of intermediate ***4.15***.

A futher step in the evolution of this methodology consisted in the substitution of the acidic partner of the reaction. As it will be discussed in the following paragraph, the utilization of a silanol in place of the carboxylic acid led to the discovery of the sililative ketene three-component reaction S-K3CR.

4.2 The sililative ketene three-component reaction (S-K3CR)

The photoinduced, multicomponent reaction of α-diazoketones ***4.12***, isocyanides ***4.2*** and silanols ***4.16*** affords α-silyloxyamides ***4.17*** as synthetic equivalents of α-ketoamides ***4.18***.

Scheme 4.2.1: The sililative ketene three-component reaction

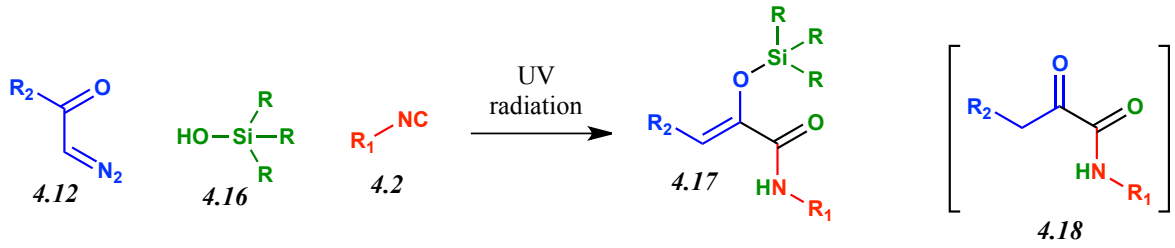

The reaction mechanism, analogous to the one reported for the K3CR (**Scheme 4.1.6**), is reported in **Scheme 4.2.2**.

Scheme 4.2.2: Reaction mechanism

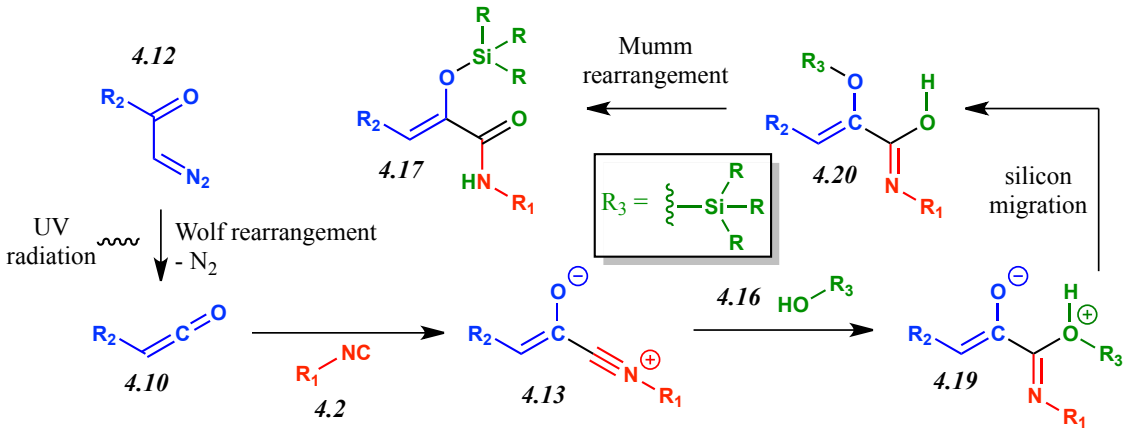

The reaction mechanism parallels the one reported in **Scheme 4.1.6** for the K3CR in the first two steps, leading to the nitrilium ion ***4.13***. At this point, the attack of silanol ***4.16*** affords intermediate ***4.19***, analagous to intermediate ***4.14***. Silicon migration, analogous to acyl migration, leads to intermediate ***4.20*** which affords the final product ***4.17*** upon Mumm rearrangement.

Silanols are appropriate analogous of carboxylic acids in this transformation, because both classes of compounds posses a nucleophilic site (OH group in both cases), an electrophilic site (silicon atom in the first case, quaternary carbon in the second case) and an acidic hydrogen atom.

Noteworhty, with this modification of the K3CR, the resulting reaction product is contemporary belonging to the class of captodative olefins and to that of silyl enol ethers. Moreover, the α-silyloxyamide structure, which can be accessed with this methodology, is generally constructed with difficulty in organic synthesis. Despite great advances in the field of silyl enol ether synthesis have been reached, the preparation of these compounds from α-ketoamides remains a challenge, especially considering secondary amides bearing an acidic hydrogen. As a consequence, it was considered interesting to investigate this reaction for the appealing features of both the transformation itself and the achieved products.

The initial investigation began by reacting benzyldiazoketone ***4.12a*** with cyclohexyl isocyanide ***4.2a*** and triphenylsilanol ***4.16a*** under UV irradiation.

Scheme 4.2.3: Initial investigations on the S-K3CR

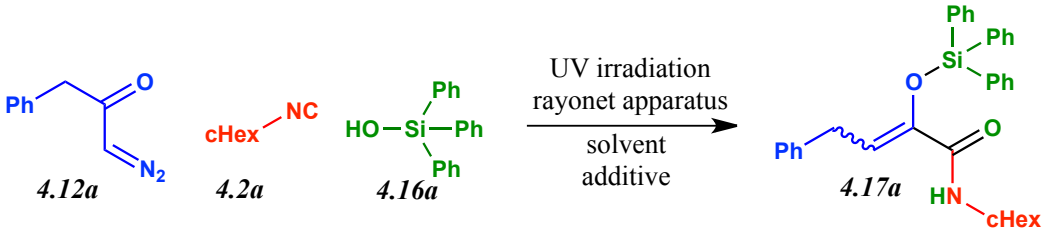

Reactions were performed inside a Rayonet apparatus, illustrated in **Figure 4.2.1**.

The choice for triphenylsilanol ***4.16a*** was dictated by the mechanism postulated for the reaction: according to the mechanism depicted in **Scheme 4.2.2**, substituents able to enhance the electrophilicity of the silicon atom should favor its migration (through a pentacoordinate intermediate).

Figure 4.2.1: Rayonet apparatus (left: whole system; right: in manteinance)

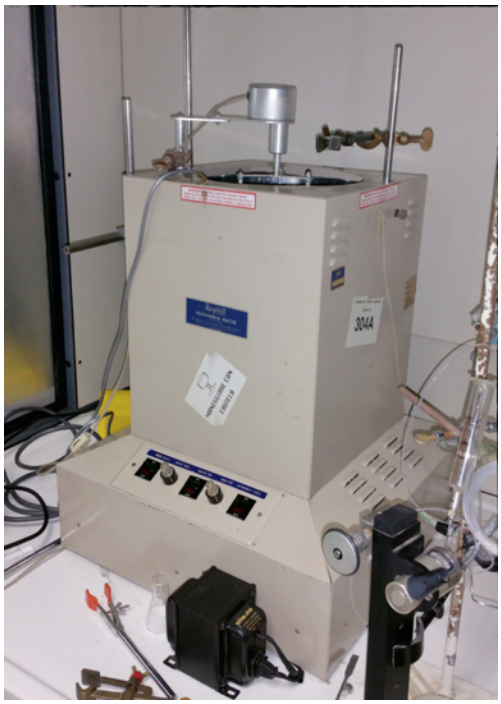

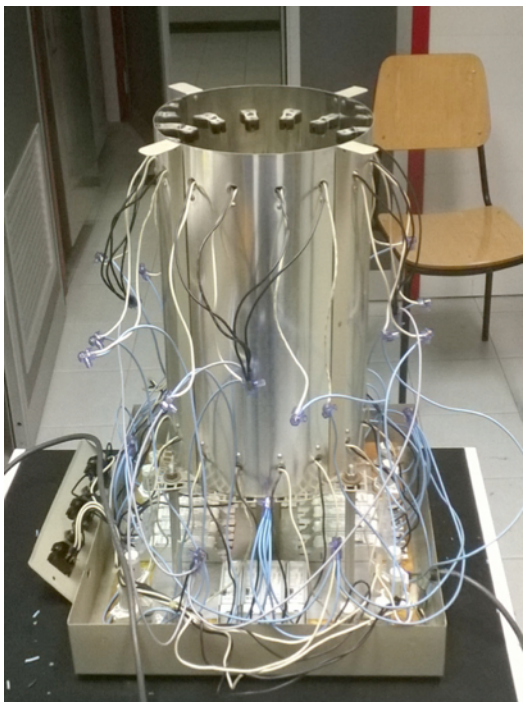

Optimization of the reaction conditions involved lamps with three different emission maxima, two different reactors, acetone or toluene as solvent, and *trans*-stilbene as an additive. The results are summarized in **Table 4.2.1**.

In accordance to what was previously discussed for trans-piperylene, the addition of trans-stilbene resulted beneficial towards the achievement of both higher yield and higher stereoselectivity. The inhibition of *Z/E* isomerization occurring during irradiation is evident by comparing entries 2 and 3, where the presence/absence of the additive strongly influences the stereochemical ratio. Toluene generally performed better than acetone as a solvent (by comparison of entry 4 with 5 or entry 8 with 10). When the quartz test tube was replaced with a reactor made of borosilicate glass, *Z* selectivity was complete (entry 11). Under the latter conditions, the reaction could be also scaled up without loss of selectivity and with improvement of the overall yield (entry 12). Although use of an excess of one of the three components could slightly improve the overall yield, all reactions were always performed with equimolar amounts of the reagents for a better process economy.

Table 4.2.1: Optimization of the reaction conditions

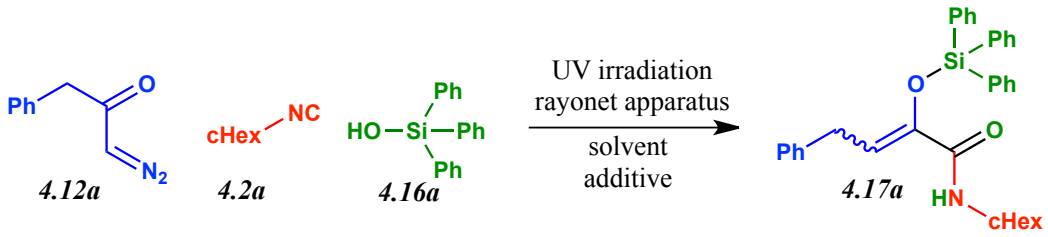

entry	irradiation	solvent	reactor	*trans*-stilbene	time	***4.17a*** yield (*Z*/*E*)
1	254	toluene	quartz	1 eq.	6	67 (83:17)
2	254	acetone	quartz	1 eq.	6	73 (80:20)
3	254	acetone	quartz	/	6	75 (53:47)
4	352	acetone	quartz	/	24	22 (88:12)
5	352	toluene	quartz	/	16	47 (96:4)
6	352	toluene	quartz	1 eq.	24	60 (97:3)
7	300	toluene	quartz	/	5	38 (96:4)
8	300	toluene	quartz	1 eq.	22	55 (96:4)
9	300	toluene	quartz	0.1 eq.	6	72 (96:4)
10	300	acetone	quartz	1 eq.	28	40 (90:10)
11	300	toluene	botrosilicate glass	0.1 eq.	9	56 (100:0)
12*	300	toluene	borosilicate glass	0.1 eq.	14	66 (100:0)

The d.r. was determined on crude reactions by NMR analysis. Reactions were perfomed on a 1:1:1 mixture of the three reagents (0.3 mmol each) in 3 mL of solvent. *reaction scaled-up to 2 mmol scale.

Having the optimized conditions in hand, the scope of the reaction was investigated. The starting materials illustrated were reacted in different combinations, as reported in **Table 4.2.2**.

Table 4.2.2: Scope of the S-K3CR and library of α-silyloxyacrylamides ***4.17a-k***

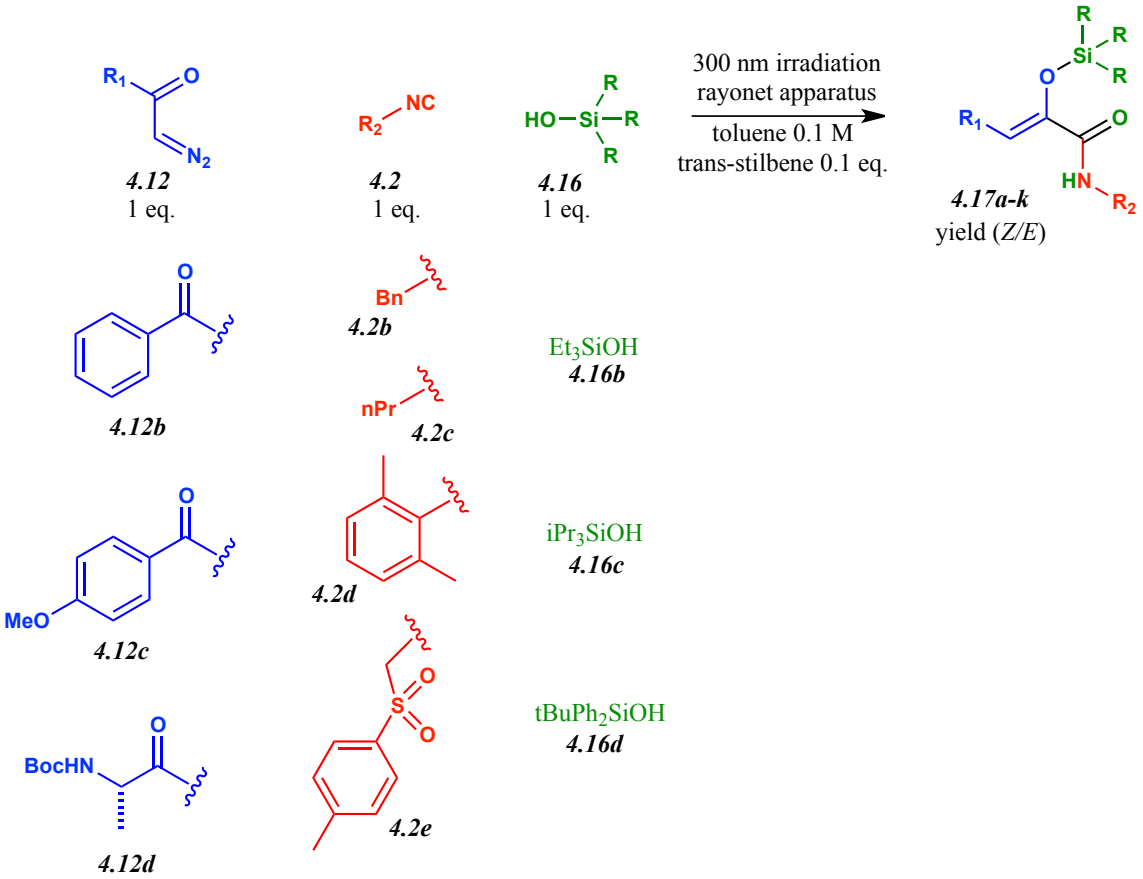

entry	diazoketone ***4.12***	isocyanide ***4.2***	silanol ***4.16***	product ***4.17***	yield (*Z*/*E*)
1	***4.12b***	***4.2a***	***4.16b***	***4.17b***	27 (98:2)
2	***4.12a***	***4.2a***	***4.16b***	***4.17c***	49 (100:0)
3	***4.12b***	***4.2a***	***4.16a***	***4.17d***	80 (98:2)
4	***4.12c***	***4.2a***	***4.16a***	***4.17e***	75 (67:33)
5	***4.12d***	***4.2b***	***4.16a***	***4.17f***	35(100:0)
6	***4.12a***	***4.2d***	***4.16a***	***4.17g***	69 (93:7)
7	***4.12a***	***4.2c***	***4.16a***	***4.17h***	68 (100:0)
8	***4.12a***	***4.2e***	***4.16a***	***4.17i***	80 (100:0)
9	***4.12a***	***4.2a***	***4.16c***	***4.17j***	30 (100:0)
10	***4.12a***	***4.2a***	***4.16d***	***4.17k***	50 (91:9)

Following, the applicability of the method was investigated by subjecting the reaction products to various reaction conditions typical of silyl enol ethers.

4.3 Reactions of α-silyloxyacrylamides *4.17*

Not surprisingly, the compounds achieved by means of the S-K3CR are typically unstable under both acidic and basic conditions; partial decomposition to the respective ketoamide ***4.18*** is in fact observed also by their purification via silica gel column chromatography. For this reason, reactions with aldehydes under Mukayama conditions failed to afford the desired products. Nevertheless, generation of the enolate in situ with addition of tetra-*n*-butyl ammonium fluoride (TBAF) was successful: Mannich reaction of compound ***4.17a*** with Eschenmoser's salt ***4.21***[4.9] gave the desired product ***4.22*** in high yield.

Scheme 4.3.1: Mannich reaction of α-silyloxyacrylamides ***4.17a*** with Eschenmoser's salt

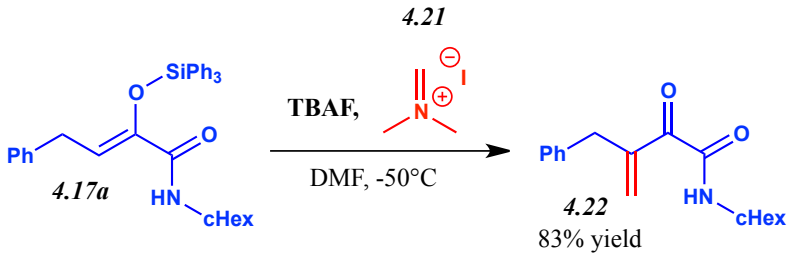

α,β-unsaturated ketoesters analogous to the achieved product have been efficiently employed in asymmetrical conjugate additions[4.10] and cycloadditions[4.11]; therefore this method offers new substrates to assemble diverse structures of interests.

Moreover, Saegusa oxidation[4.12] of compound ***4.17c*** with $Pd(OAc)_2$ resulted in the formation of α,β-unsaturated ketoamide ***4.23*** in good yield.

Scheme 4.3.2: Saegusa oxidation of α-silyloxyacrylamides ***4.17c***

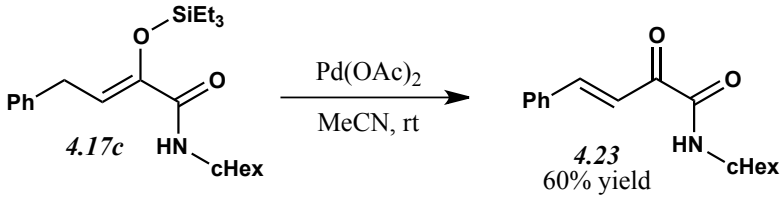

Therefore, unsaturated ketoamides ***4.22*** and ***4.23*** could be alternatively obtained by simply varying the reaction conditions.

Subsequently the conjugate addition of α-silyloxyacrylamides ***4.17*** with α,β-unsaturated ketones was investigated. When compound ***4.17a*** was reacted with butenone ***4.24***, the Michael-aldol product ***4.25*** was obtained with moderate yield as the *trans*-diastereoisomer (**Scheme 4.3.3**).

Scheme 4.3.3: Conjugate addition of α-silyloxyacrylamide ***4.17a*** with α,β-unsaturated ketone ***4.24***

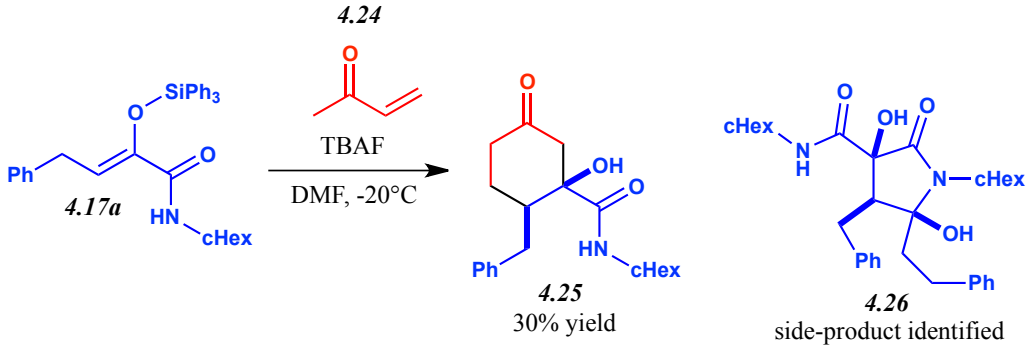

Interestingly, under the mild conditions developed, the competitive formation of side-product ***4.26*** was observed, presumably deriving from an aldol dimerization of the starting material ***4.17a*** followed by cyclization. When butenone ***4.24*** was not added to the reaction mixture, compound ***4.26*** was isolated as the sole product in high yield and complete stereoselectivity.

Scheme 4.3.4: Dimerization of α-silyloxyacrylamide ***4.17a***

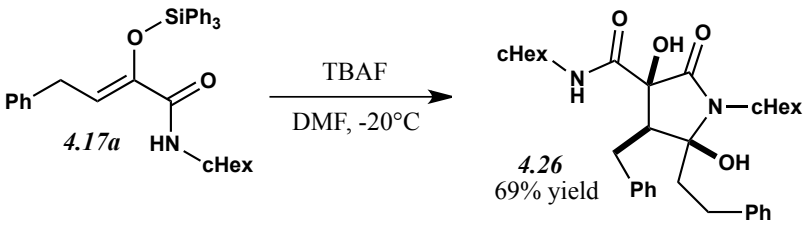

The structure of compound ***4.26*** is analogous to that of anchinopeptolides, peptide alkaloides isolated from Mediterranean sponges[4.13]. This is the first example of aldol dimerization and hemiaminal formation performed on silyl enol ethers. Moreover, the complete stereoselectivity observed opens up the route to the total synthesis of these natural products and analogues; this topic is currently (2018) under investigation inside the research group.

The decarboxylative cyclization of α-silyloxyacrylamides with α-amino acids, inspired by the work of Wu et al[4.14], was also performed with success.

Scheme 4.3.5: Decarboxylative cyclization of α-silyloxyacrylamides ***4.17*** with α-amino acids

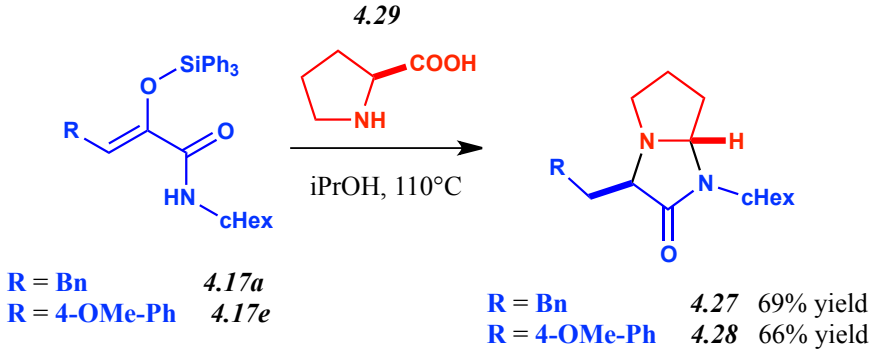

R = Bn ***4.17a***
R = 4-OMe-Ph ***4.17e***

R = Bn ***4.27*** 69% yield
R = 4-OMe-Ph ***4.28*** 66% yield

The reaction occurred with the slow, in situ, formation of the reactive α-ketoamide of formula ***4.18*** from the respective silyl enol ether. With this approach, the final compounds ***4.27*** and ***4.28*** were obtained in a completely stereoselective fashion. Apparently, the in situ cleavage of the silyl group was beneficial for the outcome of the reaction, possibly through a slow release of the reacting ketoamide.

Subsequently, α-silyloxyacrylamides ***4.17*** were employed as substrates towards cycloaddition reactions; in particular benzaldehyde ***4.17a*** was used as a starting material for a modification of the classic Paternò-Buchi reaction[4.15].

Scheme 4.3.6: Paternò-Buchi reaction of α-silyloxyacrylamide ***4.17a*** with benzaldehyde ***4.30***

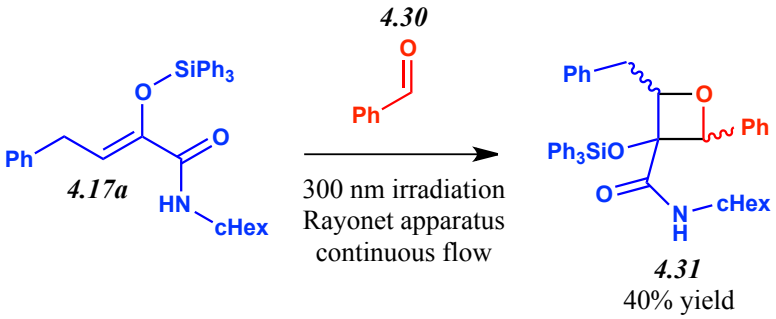

4.31
40% yield

Regioselectivity of the reaction was complete and assigned through 2D-NMR experiments; moreover, only one diastereoisomer was detected in the crude mixture. Unfortunately, NOE experiments were not conclusive to assign the correct stereochemistry, and analysis of the coupling constants in the ^{1}H NMR spectrum was fruitless.

Finally, acetonylation of α-silyloxyacrylamides ***4.17*** was successfully performed with the VLPC flow-methodology discussed in the previous chapter.

4.4 Application of the acetonyl radical methodology to α-silyloxyacrylamides *4.17* generated via S-K3CR

The versatility of the methodology discussed in **Chapter 3** was further demonstrated by extending the protocol to non-classic silyl enol ethers ***4.17a*** and ***4.17d*** like those achieved via the S-K3CR.

Scheme 4.4.1: Application of the VLPC acetonylation method to α-silyloxyacrylamides ***4.17***

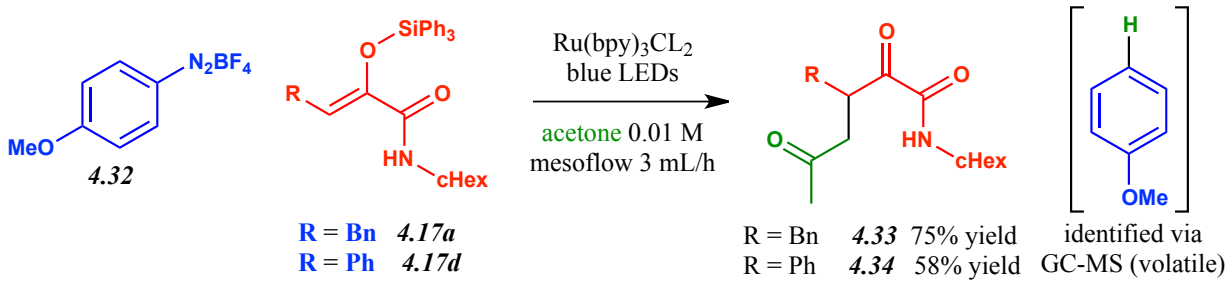

The desired products ***4.33*** and ***4.34*** were achieved in good yield. A slight modification of the optimized conditions reported in **Paragraph 3.9** was employed for this reaction: the use of only one equivalent of silyl enol ether (while normally two equivalents were employed) required a slower flow rate (3 mL/h instead of 10 mL/h) to accomplish a satisfying result in terms of yield.

The synthesis of compound ***4.33*** was also optimized in a one-pot fashion.

Scheme 4.4.2: One-pot synthesis of 4.17a and consecutive acetonylation via VLPC

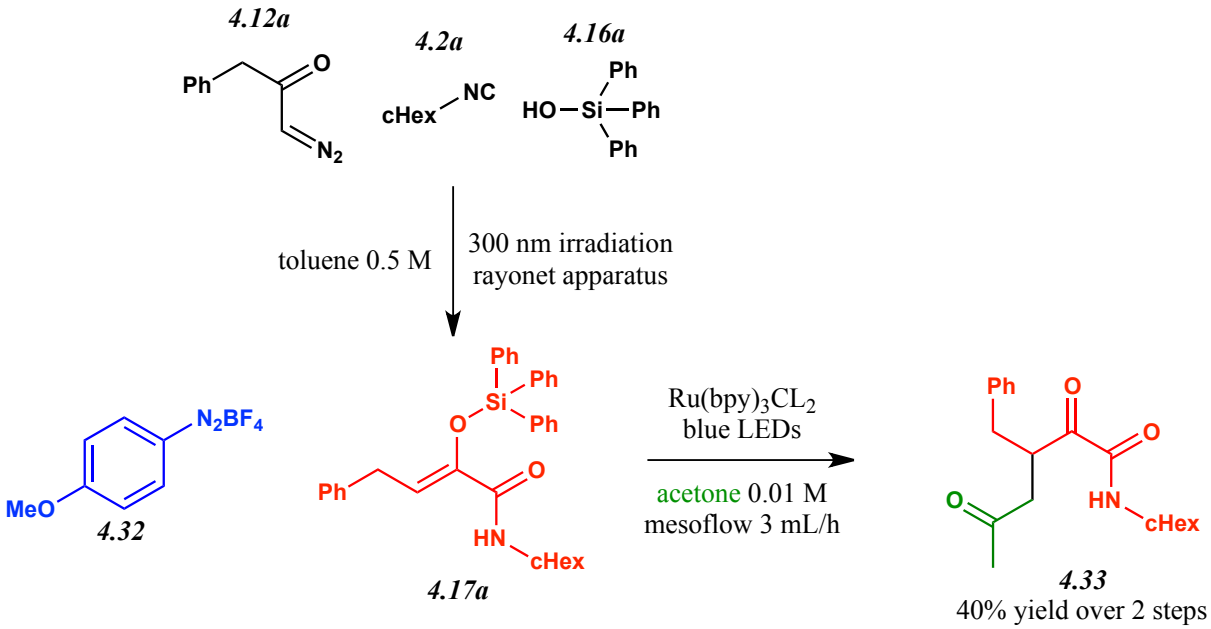

Diazoketone ***4.12a***, silanol ***4.16a*** and isocyanide ***4.2a*** were irradiated in toluene (0.5 M) in order to induce the formation of the silyl enol ether ***4.17a***, as discussed in **Paragraph 4.2**. Noteworthy, no *trans*-stilbene additive was employed as an additive into the S-K3CR, based on the assumption that both isomers should be equally reactive towards radical acetonylation. Upon consumption of the diazoketone ***4.12a***, the solution was diluted with acetone (up to 0.01 M, based on a theoretical 100% yield for comppound ***4.17a***), then the diazonium salt ***4.32*** was added along with $Ru(bpy)_3Cl_2$ as a photocatalyst to the resulting mixture, which was flown through our homemade mesoflow apparatus (see **Chapter 2** and **3**) at the flow rate of 3 mL/h.

As a result, compound ***4.33*** was successfully isolated with moderate yield, thus demonstrating that the acetonylation methodology is also compatible with crude mixtures deriving from a multicomponent process.

Since 1,4-dicarbonyl compounds are exstensively used n the field of organic synthesis[4.16], it was decided to demonstrate the synthetic utility of compound ***4.33*** by submitting it to Paal-Knorr reaction conditions[4.17].

Scheme 4.4.3: Paal-Knorr synthesis of pyrrole derivative ***4.36*** starting from compound ***4.33***

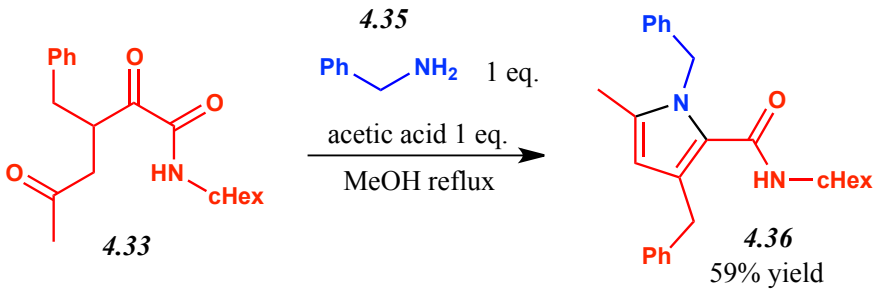

When compound ***4.33*** was reacted with benzylamine ***4.35***, in presence of acetic acid, the densely functionalized pyrrole derivative ***4.36*** was successfully achieved with good yield.

4.5 Conclusions

In conclusion, an extension of the K3CR, previously developed by our research group, was disclosed. A new multicomponent approach towards α-silyloxyacrylamide derivatives ***4.17*** was established.

The reactivity of this class of compounds was deeply investigated, revealing its successful application towards a number of interesting transformations. Among the others, the utilization of these substrates in the visible light photoredox catalyzed radical acetonylation discussed in **Chapter 3** offered an additional opportunity to demonstrate its synthetic utility.

Inside our laboratories, synthetic attempts to exploit α-silyloxyacrylamide derivatives achieved by means of this methodology towards natural product synthesis are currently under development.

4.6 References

4.1
F. Ibba; P. Capurro; S. Garbarino; M. Anselmo; L. Moni; A. Basso *Org. Lett.* **2018**, *20*, 1098-1101.

4.2
A. Basso; L. Banfi; A. Galatini; G. Guanti; F. Rastrelli; R. Riva *Org. Lett.* **2009**, *11*, 18, 4068-4071.

4.3
H. G. Viehe; Z. Janousek; R. MerØnyi; L. Stella *Acc. Chem. Res.* **1985**, *18*, 148-154.

4.4
J. Lasri, S. Mukhopadhyay, M. A. J. Charmier *J. Heterocycl. Chem.* **2008**, *45*, 1385-1389.

4.5
R. Aguilar, A. Benavides, J. Tamariz *Synth. Commun.* **2004**, *34*, 2719-2735.

4.6
R. Sanabria, R. Herrera, R. Aguilar, C. Gonzalez-Romero, H. A. JimØnez-Vàsquez, F. Delgado, B. C. G. Soderberg, J. Tamariz *Helv. Chim. Acta* **2008**, *91*, 1807-1827.

4.7
Basso A.; Banfi L.; Garbarino S.; Riva R. *Angewandte Chemie International Edition* **2013,** *52*, 2096-2099.

4.8
G. B. Gill in Comprehensive Organic Synthesis; Selectivity, Strategy and Efficiency in Modern Organic Chemistry, Vol. 3 (Eds.: B. M. Trost, I. Fleming), Pergamon, Oxford,
1991, 887-912

4.9
J. L. Roberts; P. S. Borromeo; C. D. Poulter *Tetrahedron Lett.* **1977**, *18*, 19, 1621-1623.

4.10
Gremaud L.; Alexakis A. *Angew. Chem. Int. Ed.* **2012**, *51*, 794− 797.

4.11
Ouyang B.; Yu T.; Luo R.; Lu G. *Org. Biomol. Chem.* **2014**, *12*, 4172−4176.

4.12
Y. Ito, T. Konoike, T. Saegusa *J. Am. Chem. Soc.* **1975**, *97*, 3, 649-651.

4.13
Casapullo A.; Minale L.; Zollo F.; Lavayre J. *J. Nat. Prod.* **1994**, *57*, 1227−1233.

4.14
Wu J. S.; Jiang H. J.; Yang J. G.; Jin Z. N.; Chen D. B. *Tetrahedron Lett*. **2017**, *58*, 546−551.

4.15
Vogt F.; Jödicke K.; Schröder J.; Bach T. *Synthesis* **2009**, 4268−4273.

4.16
Khaghaninejad S.; Heravi M. M. *Advances in Heterocyclic Chemistry*, **2014**, *111*, 95-146. Ed. Katritzky, A. R.; Elsevier Academic Press (San Diego, USA)

4.17
(a) Paal C. *Eur. J. Inorg. Chem.* **1885**, *18*, 1, 367–371.
(b) Paal, C. *Eur. J. Inorg. Chem.* **1885**, 18, 2, 2251–2254.
(c) Knorr, L. *Eur. J. Inorg. Chem.* **1885**, 18, 1, 299–311.

CHAPTER 5:
VISIBLE LIGHT PHOTOREDOX CATALYZED GENERATION AND SYNTHETIC APPLICATION OF ACYL RADICALS

In the time period occurring between the beginning of October 2017 and the end of March 2018 I had the pleasure to move to the working group of Professor Burkhard König in the University of Regensburg, Germany. The research group which hosted me is particularly active in the field of VLPC but it is also interested in Molecular Recognition, Sustainable Chemistry and Medicinal Chemistry.

During the internship, i was assigned to a project dedicated to the generation of acyl radicals by VLPC and their subsequent utilization in organic synthesis. This work was briefly initiated by the colleague Johanna Schwartz and i collaborated with another colleague and readily become dear friend Daniel Petzold.

5.1 State of the art at the beginning of my contribution

As anticipated in **Paragraph 1.7**, the issue concerning the generation of acyl radicals by means of VLPC started appearing in the literature some time before the beginning of our work on the topic. Existing acyl radical precursors in VLPC were at the time ketoacids and anhydrides, which required decarboxylation to generate the desired species[5.1]. In particular, the group of Xu disclosed for the first time the possibility to employ aroyl chlorides as precursors for acyl radicals by means of VLPC[5.2].

Scheme 5.1.1: Use of aroyl chlorides as aroyl radical precursors by Xu et al

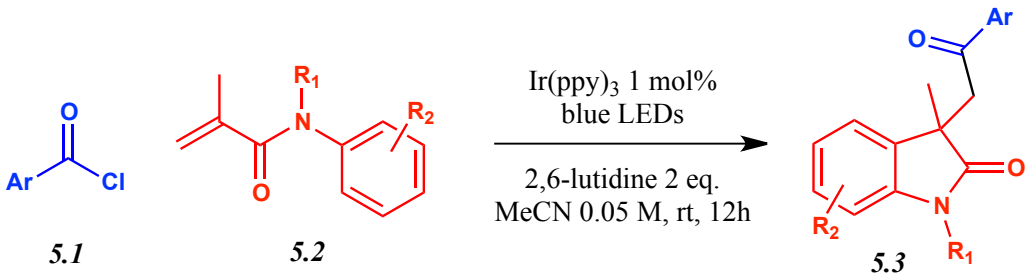

5.1 *5.2* *5.3*

Noteworthy, the same radical trap of formula ***5.2*** discussed in **Paragraph 3.7** was employed for this transformation despite the different philicity[5.3] of the attacking radical species; while acetonyl radical is electrophilic, acyl radicals are nucleophilic instead. The mechanism proposed by the authors for this transformation is reported in **Scheme 5.1.2**.

Scheme 5.1.2: Reaction mechanism as it is proposed by the authors

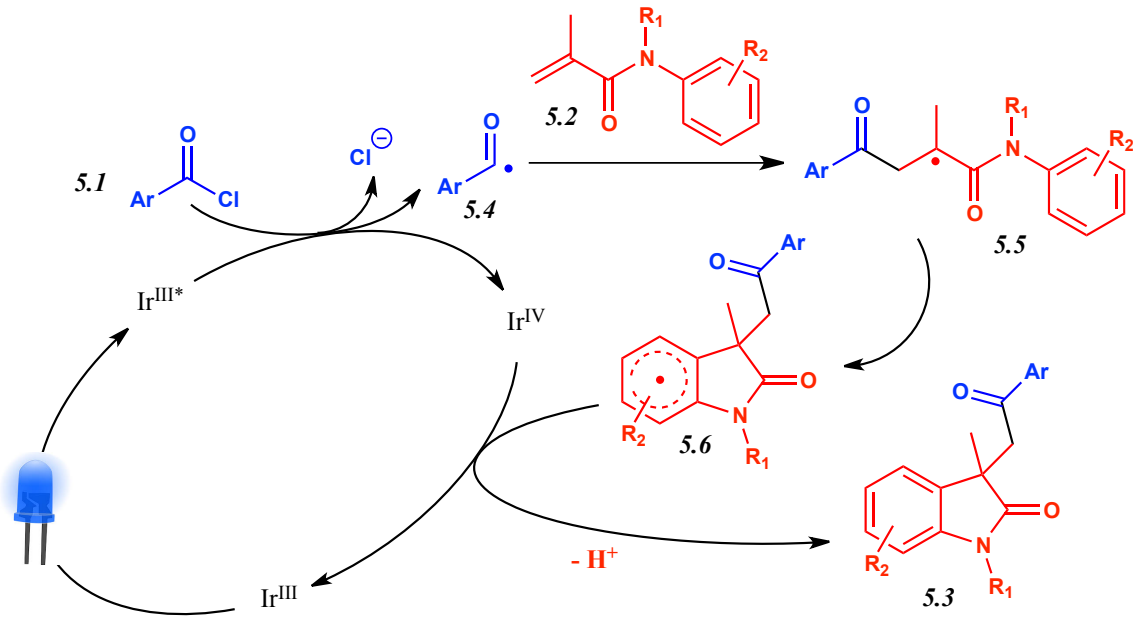

The iridium photoredox catalyst reaches the excited state upon visible light excitation and consequently acquires a sufficient potential to reduce the aroyl chloride ***5.1*** to the desired aroyl radical ***5.4*** via chloride anion elimination. This radical species subsequently attacks the olefinic trap ***5.2*** affording the intermediate ***5.5*** which is able to afford the other intermediate ***5.6*** upon cyclization. The catalytic cycle is closed via oxidation of intermediate ***5.6*** along with proton abstraction, in a similar way to what was discussed in **Paragraph 3.7**.

Inspired by this work the research group decided to investigate the possibility to establish a methodology for the acylation of simple olefins by means of VLPC.

Scheme 5.1.3: Target methodology for the acylation of simple olefins

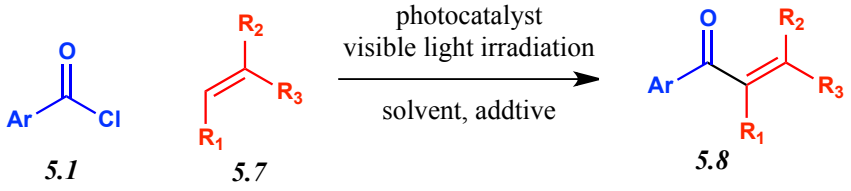

This method would in fact be highly desirable for the simple generation of α,β-unstaurated ketones ***5.8*** in mild conditions.

5.2 First experiments and optimization of the reaction conditions

Some preliminary experiments were conducted submitting the reaction conditions reported by Xu to some simple olefins and aromatic compounds. In particular the use of styrene ***5.9***, vinylacetate ***5.10***, N-methylpyrrole ***5.11*** and trimethoxybenzene ***5.12*** was tested.

Scheme 5.2.1: First experiment towards the establishment of a new methodology

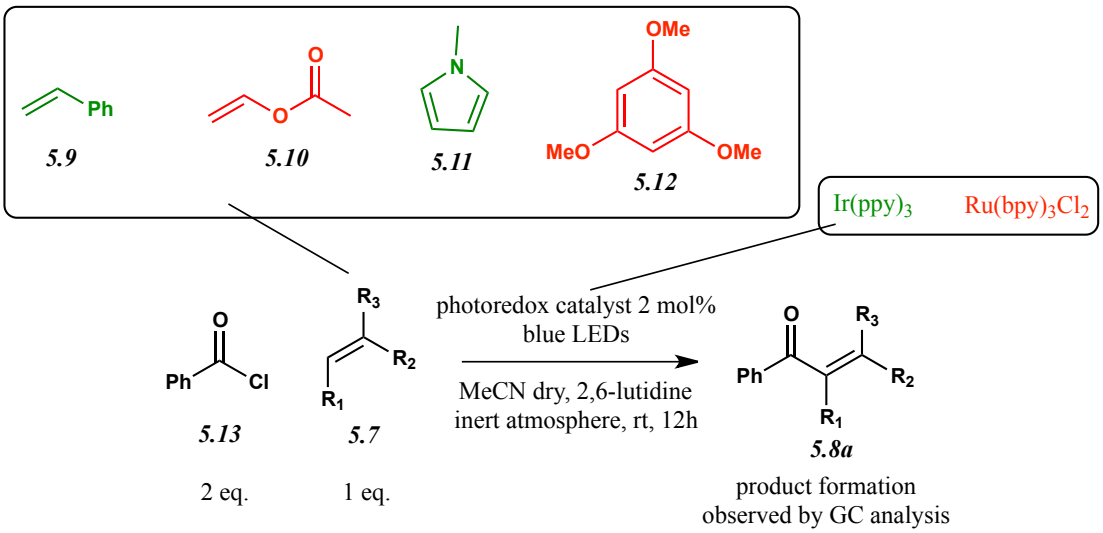

Among the tested substrates, styrene and N-methylpyrrole furnished promising results. Since $Ru(bpy)_3Cl_2$ did not seem to be effective for the desired transformation, the same photocatalyst employed by Xu, $Ir(ppy)_3$, was used. As a consequence, the reaction of benzoyl chloride ***5.13*** with styrene ***5.9*** was selected as the model transformation to carry out some preliminary investigations.

An initial optimization of the reaction conditions involved the selection of the best solvent, molarity, reaction time and reactant ratio, along with the use of additives. The reactions were monitored by GC analysis which was also used for the determination of the reaction yield using naphthalene as an internal standard. The outcome of the initial screening is reported in **Table 5.2.1**.

Table 5.2.1: Optimization of the reaction conditions

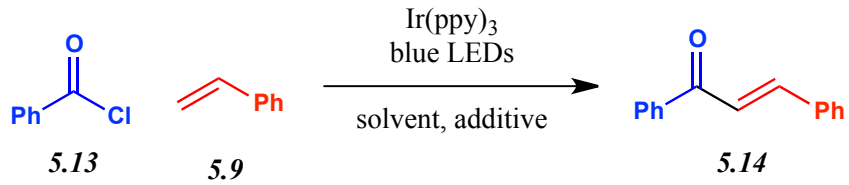

5.13 *5.9* *5.14*

entry	Benzoyl Chloride eq.	Styrene equivalents	Dry Solvent (mL)	Reaction Time	additive (eq.)	Product Yield
1	1	1	MeCN (1)	1h	lutidine (1)	24%
2	1	1	DMF (1)	1h	lutidine (1)	33%
3	1	1	DCM (1)	1h	lutidine (1)	51%
4	1	1	DMSO (1)	1h	lutidine (1)	40%
5	1	1	THF (1)	1h	lutidine (1)	traces
6	1	1	DCM (1)	2h	lutidine (1)	60%
7	1	1	DCM (1)	4h	lutidine (1)	59%
8	2	1	DCM (1)	2h	lutidine (1)	45%
9	1	2	DCM (1)	2h	lutidine (1)	69%
10	1	3	DCM (1)	2h	lutidine (1)	68%
11	1	2	DCM (2)	2h	lutidine (1)	73%
12	1	2	DCM (4)	2h	lutidine (1)	59%
13	1	2	DCM	2h	lutidine (2)	65%
14	1	2	DCM	2h	/	32%
15	1	2	DCM	2h	DIPEA (1)	42%
16	1	2	DCM	2h	DBU (1)	traces
17	1	2	DCM	2h	NEt_3 (1)	35%

reactions were performed at 0.1 mmol scale under inert atmosphere at room temperature in the presence of 0.02 eq. of $Ir(ppy)_3$.

Dichloromethane afforded the best initial result among the tested solvents (entry 3 compared to entries 1-5). Increasing the reaction time to two hours was beneficial (entry 6) while extending it further was not improving the yield (entry 7). The use of two equivalents of styrene was revealed to be the most efficient reactant ratio (entry 9 compared to 8-10). The dilutuion was investigated revealing that 0.05 M reactions were the best (entry 11 compared to entries 9 and 12). It was then found that the use of an excess of base (entry 13) was not beneficial for the transformation, while no addition of base (entry 14) implied a severe drop in product yield. Finally, 2,6-lutidine was determined to be the best base among the ones tested (entries 15-17).

Noteworthy, when the reaction was performed in non-inert conditions with common solvents (not dry) the product yield was only slightly decreased. Control experiments with no light and no catalyst confirmed that the reaction only occurred under VLPC conditions. When the same transformation was attempted on benzoic acid, rather than benzoyl chloride ***5.13***, no reaction was observed.

The proposed mechanism for the reaction herein discussed is reported in **Scheme 5.2.2**.

Scheme 5.2.2: Proposed reaction mechanism

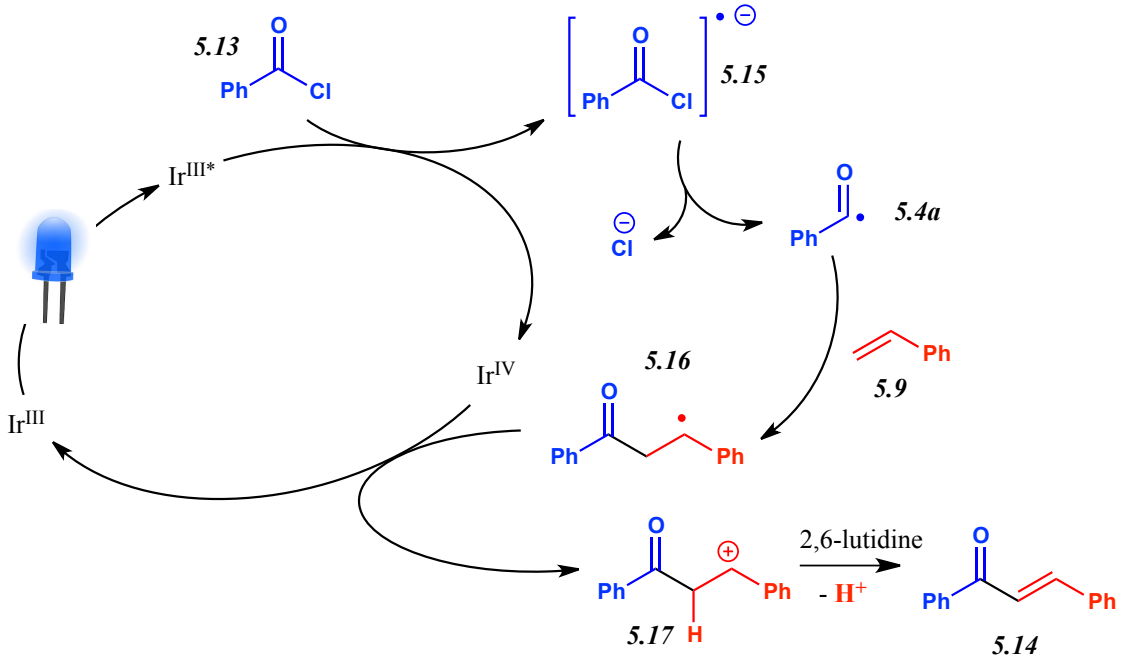

Upon interaction with the excited state photocatalyst, benzoyl chloride ***5.13*** is reduced to the radical anion ***5.15*** which, upon elimination of a chloride anion, furnishes the desired benzoyl radical ***5.4a***. Subsequently, this reactive species attacks the double bond of styrene ***5.9*** affording the radical intermediate ***5.16***. Oxidation of the intermediate ***5.16*** to the respective cation ***5.17***, followed by proton abstraction promoted by the base additive, leads to the desired product ***5.14***.

Having the optimized conditions in hand, more experiments were conducted with the final aim to build a library of α,β-unstaurated aromatic ketones of formula ***5.8***.

5.3 Reaction of Benzoyl Chloride with α-methylstyrene

When α-methylstyrene ***5.18*** was submitted to the optimized reaction conditions the unexpected product ***5.20*** was obtained (**Scheme 5.3.1**).

Scheme 5.3.1: Reaction of benzoyl chloride ***5.13*** with olefin ***5.18***

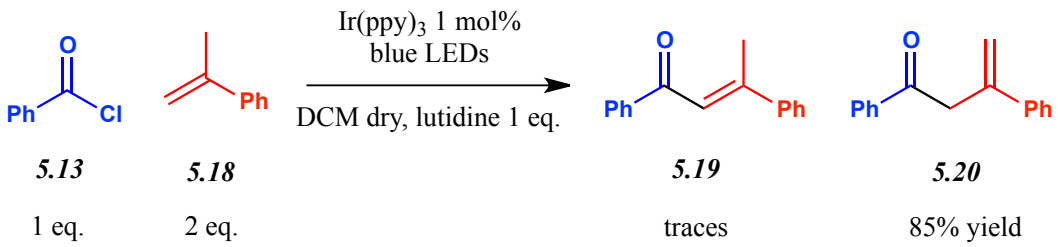

5.13	***5.18***	***5.19***	***5.20***
1 eq.	2 eq.	traces	85% yield

Apparently, the deprotonation of the cationic intermediate ***5.21*** achieved upon closure of the catlytic cycle is favoured on the less substituted postion.

Scheme 5.3.2: Rationale behind the formation of the unexpected product ***5.20***

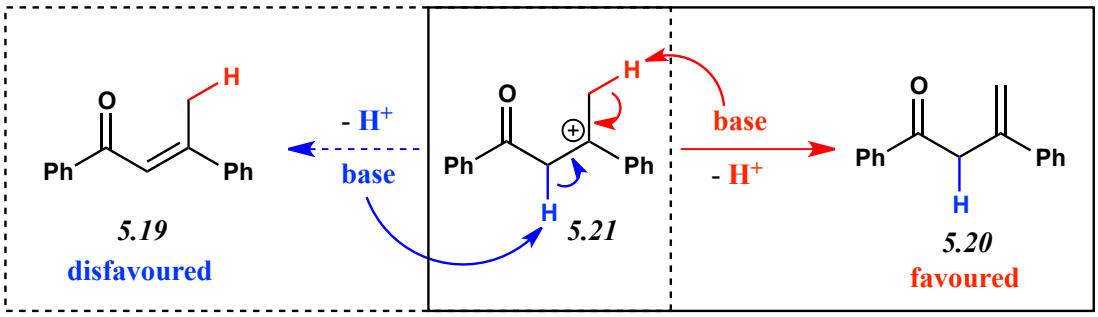

A reasonable explanation may be given as a matter of sterics; presumably the most easily accessed hydrogen (highlighted in red in **Scheme 5.3.2**) is favourably removed by the base, despite it is in principle less acidic compared to the hydrogen displayed by the carbon in α-position with respect to the ketone (highlighted in blue in **Scheme 5.3.2**). Additional experiments conducted with differently hindered bases always afforded 1,3-diphenylbut-3-en-1-one ***5.20*** as the main product. Noteworthy, when the reaction was performed in the absence of a base, the selectivity ratio was affected, leading to a slight increase of 1,3-diphenylbut-2-en-1-one ***5.19*** (62% yield, 5:1 in favour of 1,3-diphenylbut-3-en-1-one ***5.20***). Control experiments without photocatalyst and without light did not afford any product, confirming that the process is entirely relying on VLPC. The utilization of a lower loading of photocatalyst was also attempted: surprisingly, an almost quantitative yield of 1,3-diphenylbut-3-en-1-one ***5.20*** could be afforded by lowering the amount of catalyst used (**Table 5.3.1**, entry 4).

Table 5.3.1: Optimization of the catalyst loading

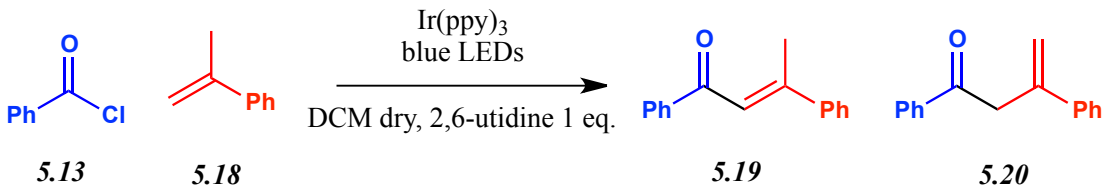

5.13 ***5.18*** ***5.19*** ***5.20***

entry	catalyst loading	1,3-diphenylbut-3-en-1-one ***5.19*** yield
1	2 mol%	85%
2	1 mol%	88%
3	0.5 mol%	91%
4	0.2 mol%	95%

Reactions performed on 0.1 mmol scale, irradiatiing the mixture for 2h under inert atmosphere in 2 mL of dry DCM using 2 eq. of a-methylstyrene and 1 eq. of lutidine.

The use of a minor loading of catalyst did not prolong the reaction time significantly. A reasonable explanation of this outcome might be connected with the issue of light permeation: possibly, a better light harvesting is achieved with a minor amount of absorbing photocatalyst dissolved inside it. For this reason, the newly optimized conditions were submitted to the reaction with styrene ***5.9*** (illustrated in **Scheme 5.2.2**) leading to a higher reaction yield (78% yield of product ***5.14***).

When the same reaction was performed adding an acid as an additive instead of a base, the reaction was inhibited, leading to the dimerization of the olefinic substrate ***5.18***.

Scheme 5.3.3: Use of trifluoroacetic acid as an additive to the reaction conditions instead of 2,6-lutidine

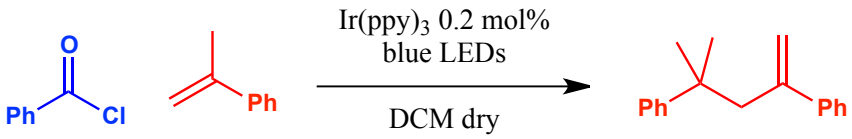

5.13 1 eq. ***5.18*** 2 eq. ***5.22*** quantitative yield

The dimerization reaction leading to olefin ***5.22*** takes places also in the absence of Benzoyl Chloride, photocatalyst and light; such reaction was in fact already described in the literature[5.4].

Following, i tried to apply the reaction conditions to both compound ***5.20***, achieved by the reaction of benzoyl chloride ***5.13*** with α-methylstyrene ***5.18***, and compound ***5.22***, achieved by the dimerization of the latter olefin (**Scheme 5.3.4**).

Scheme 5.3.4: Reactions of benzoyl chloride ***5.13*** with olefins ***5.20*** and ***5.22***

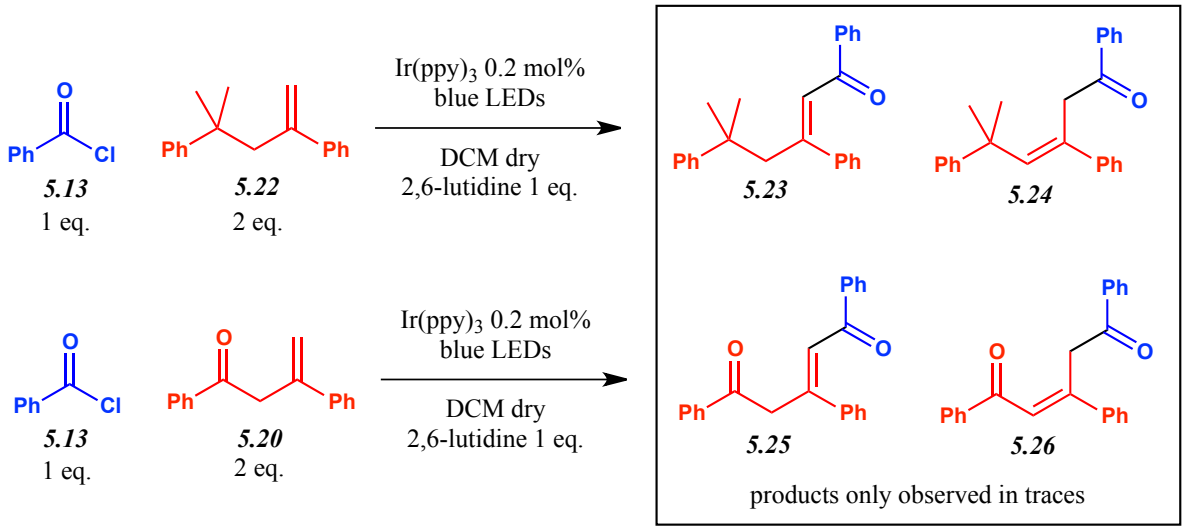

Unfortunately, the reaction of both compounds ***5.20*** and ***5.22*** led to dirty reaction crudes, from which only traces of desired products could be achieved. Possibly, the substitution pattern of both olefinic substrates leads to side reactivity and decomposition of the intermediates. For this reason, their utilization was not investigated any further.

5.4 Reactions of Benzoyl Chloride with Vinylbenzoic Acid

Based on my former experience with vinylbenzoic acid derivatives (see **Chapters 2** and **3**), i investigated the utilization of the acid ***5.27*** as a substrate for the new methodology involving acyl radicals; the reaction was performed according to the optimized conditons previously discussed.

Scheme 5.4.1: Reaction of benzoyl chloride ***5.13*** with olefin ***5.27***

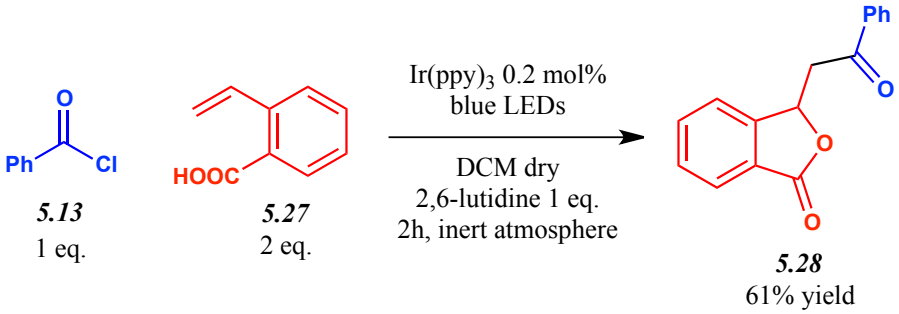

The desired isobenzofuranone ***5.28*** was achieved with good yield. Noteworthy, when the reaction illustrated in **Scheme 5.4.1** was repeated without addition of a base and with only one equivalent of vinylbenzoic acid ***5.27***, the product yield was increased to 90%. This could be reasonably explained by observing that in this case no deprotonation on the cationic intermediate skeleton is necessary to afford the final product ***5.28***. Apparently in this case the absence of a base in the reaction media is beneficial. The supposed mechanism of the reaction is analogous to that discussed in **Chapters 2** and **3**.

The **Scheme 5.4.2** summarises all the transformations leading to isobenzofuranone derivatives discussed in this thesis.

Scheme 5.4.2: Summary of all transformations leading to isobenzofuranone derivatives discussed in **Chapters 2**, **3** and **5**

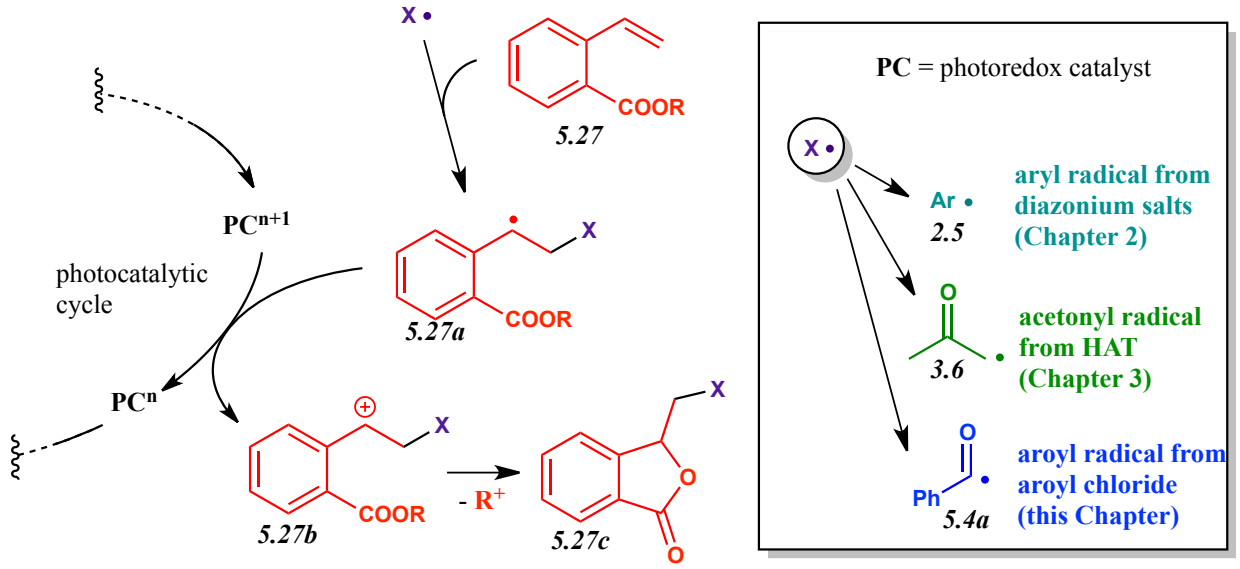

When the reaction was conducted in acetonitrile as a solvent, the expected isobenzofuranone ***5.28*** was obtained in low yield together with the relative benzoxazepinone derivative ***5.29***, also obtained in low yield.

Scheme 5.4.3: Reaction of benzoyl chloride ***5.13*** with olefin ***5.27*** in acetonitrile media

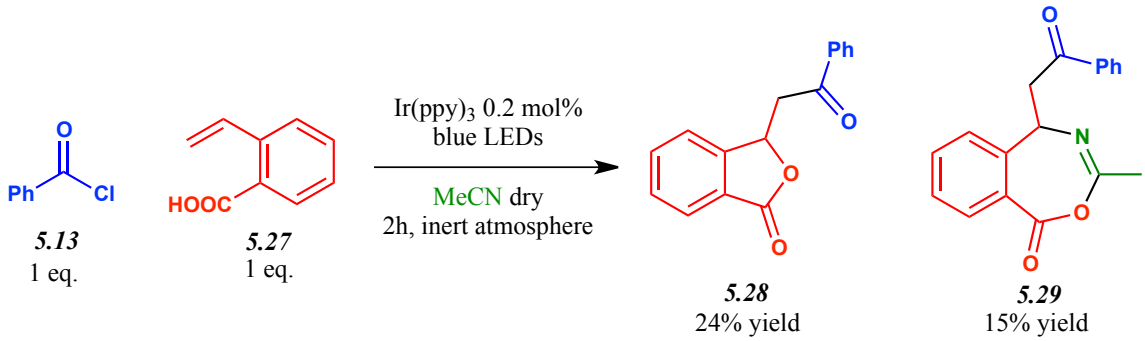

Similarly to what was discussed in **Paragraph 2.6**, the intermolecular insertion of acetonitrile in the cationic intermediate is competitive with its intramolecular cyclization.

When the reaction was performed in high dilution of acetone (0.01 M with respect to both benzoyl chloride ***5.13*** and vinylbenzoic acid ***5.27***) only a low yield (20%) of isobenzofuranone ***5.28*** was achieved. Noteworthy, no sign of HAT was observed, meaning that benzoyl radical ***5.4a*** is presumably not capable to asbract an hydrogen atom from acetone with a similar efficiency to aryl radicals (see **Chapter 3**).

5.5 Scope of the coupling reaction of benzoyl chloride with olefins

The optimized conditions described in **Paragraph 5.2** were applied to build a library of compounds starting from olefinic substrates as illustrated in **Scheme 5.5.1**.

Scheme 5.5.1: Scope of the reaction and library of compounds ***5.31a-f***

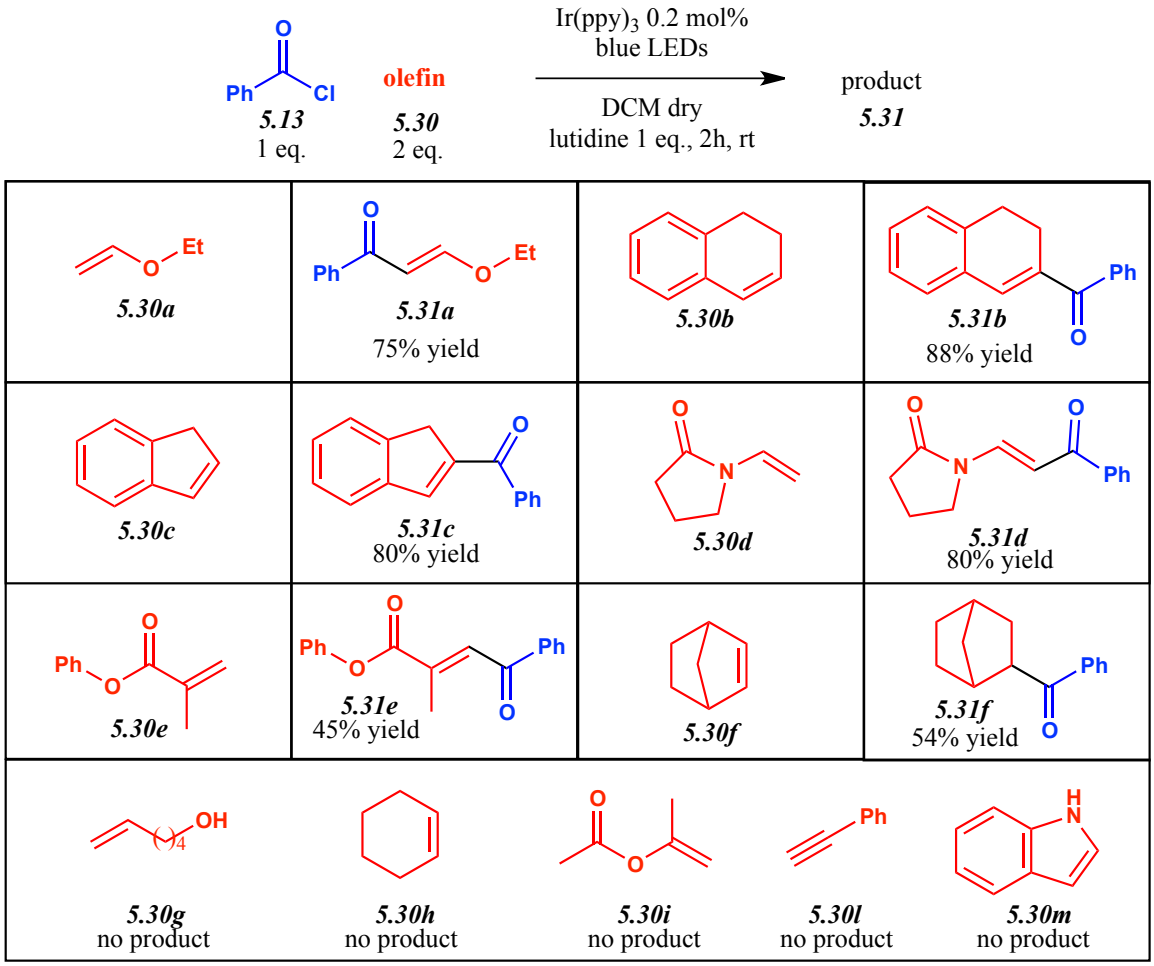

A library of 9 new compounds ***5.31*** (considering compounds ***5.31a-5.31f*** illustrated in **Scheme 5.5.1** plus compounds ***5.14***, ***5.20***, ***5.28*** previously discussed in this chapter) was achieved with moderate to excellent yield. Noteworthy, when norbornene ***5.30f*** was submitted to the reaction conditions, the completely saturated product ***5.31f*** was achieved.

Apparently, in this case a different reaction pathway was followed. The free alkylic alchol functionality was proved to be unefficient towards this methodology; direct addition of 5-hexen-1-ol ***5.30g*** to the acyl chloride was observed upon its submission to the reaction conditions (**Scheme 5.5.2**).

Scheme 5.5.2: Reaction of benzoyl chloride ***5.13*** with olefin ***5.30g***

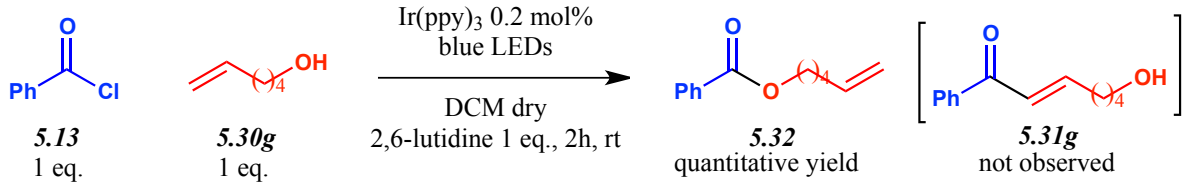

No reactivity with alkynes could be observed; a reasonable explanation lies in the high reactivity of vinyl radicals which would be generated as reaction intermediates.

5.6 One-pot methodology to access aroyl radicals starting from benzoic acid derivatives

Having demonstrated the synthetic utility of the trasformation under investigation by showing its applicability to different olefinic substrates, we decided to scope the acyl chloride starting material. Since acyl chlorides ***5.1*** are not commonly found among commercially available compounds, a methodology to conveniently access the desired reactivity starting from accessible benzoic acid derivatives ***5.33*** was highly desirable. In order to do so, the in situ-generation of benzoyl chloride ***5.13*** starting from benzoic acid ***5.33a***, followed by the addition of reactants and photocatalyst was attempted.

Scheme 5.6.1: Generation of aroyl radicals starting from benzoic acid derivatives by means of a one-pot methodology and VLPC

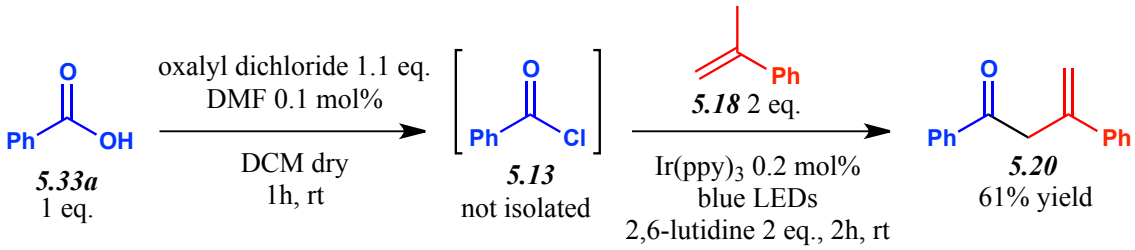

With our delight, the desired product ***5.20*** could be achieved with good yield. An additional equivalent of base was employed in order to quench the hydrochloric acid generated by the reaction of oxalyl dichloride.

Having established this new methodology, a new set of reactions was performed with the final aim to build a second library of compounds (**Scheme 5.6.2**).

Scheme 5.6.2: Scope of the reaction and library of compounds ***5.31h-p***

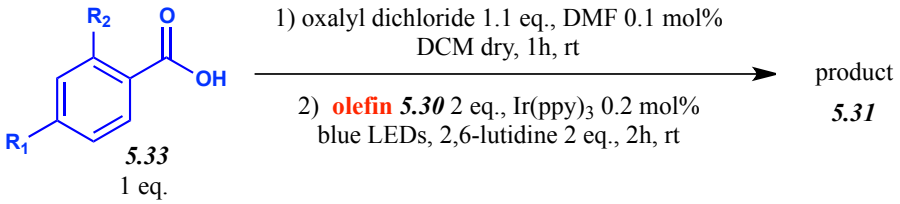

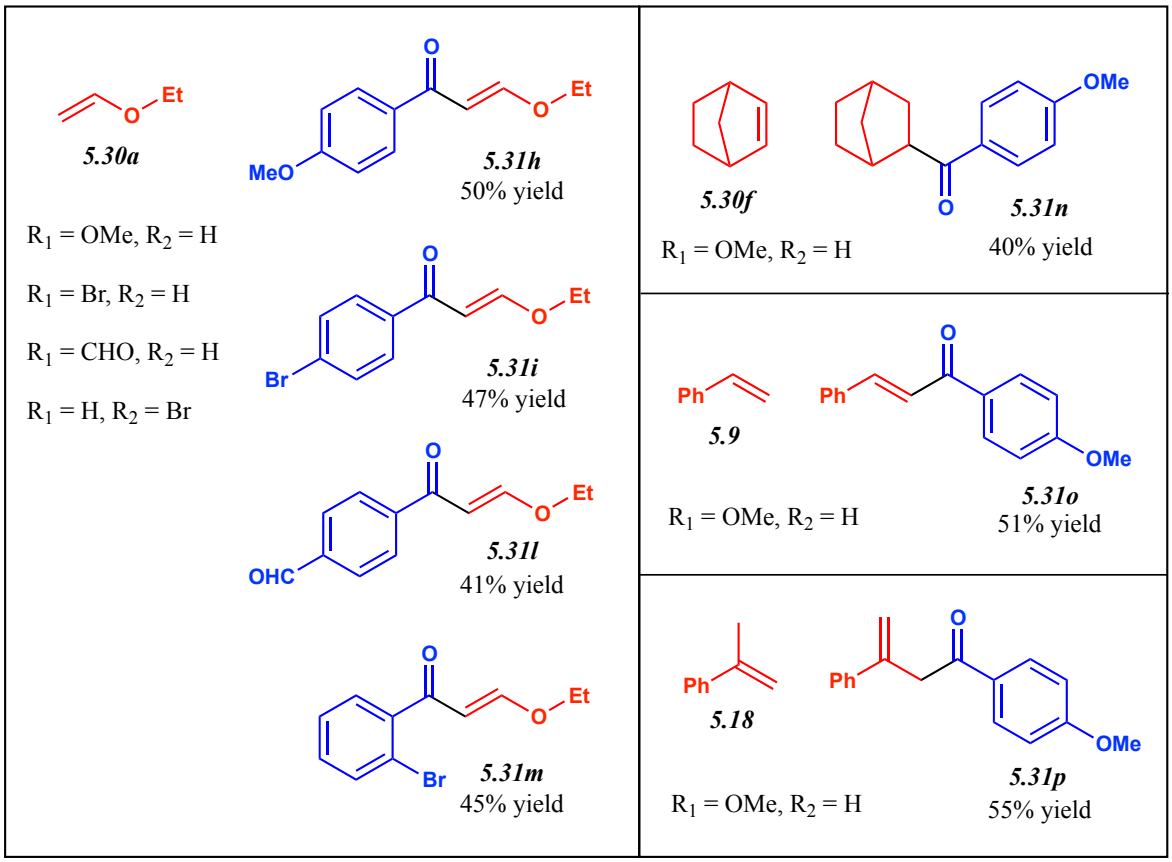

As a result, 7 new compounds (***5.31h-5.31p***) were achieved with moderate yield. Evidently, the one-pot procedure is less effective in terms of product yield compared to the methodology exploiting simple benzoyl chloride ***5.13***. This was confirmed by the reaction of *p*-anisoyl chloride with styrene, which was performed in optimized conditions, leading to 80% yield of product ***5.31o*** (compared to 51% yield achieved via one-pot methodology). On the other hand, the possibility to access the desired reactivity starting from simple and readily available benzoic acid derivatives ***5.33*** was considered of relevance.

5.7 Visible-Light-Promoted Synthesis of 1,4-Dicarbonyl Compounds via Conjugate Addition of Aroyl Chlroides

While we were working at the optimization of the one-pot procedure described in the previous paragraph, Wang et al released a publication covering the very topic of our research[5.5].

With this contribution a VLPC based methodology for the conjugate addition of aroyl radicals ***5.4*** to electron deficient olefins ***5.34*** was established.

Scheme 5.7.1: VLPC based methodology for the conjugate addition of aroyl radicals ***5.4*** to electron deficient olefins ***5.34*** by Wang et al

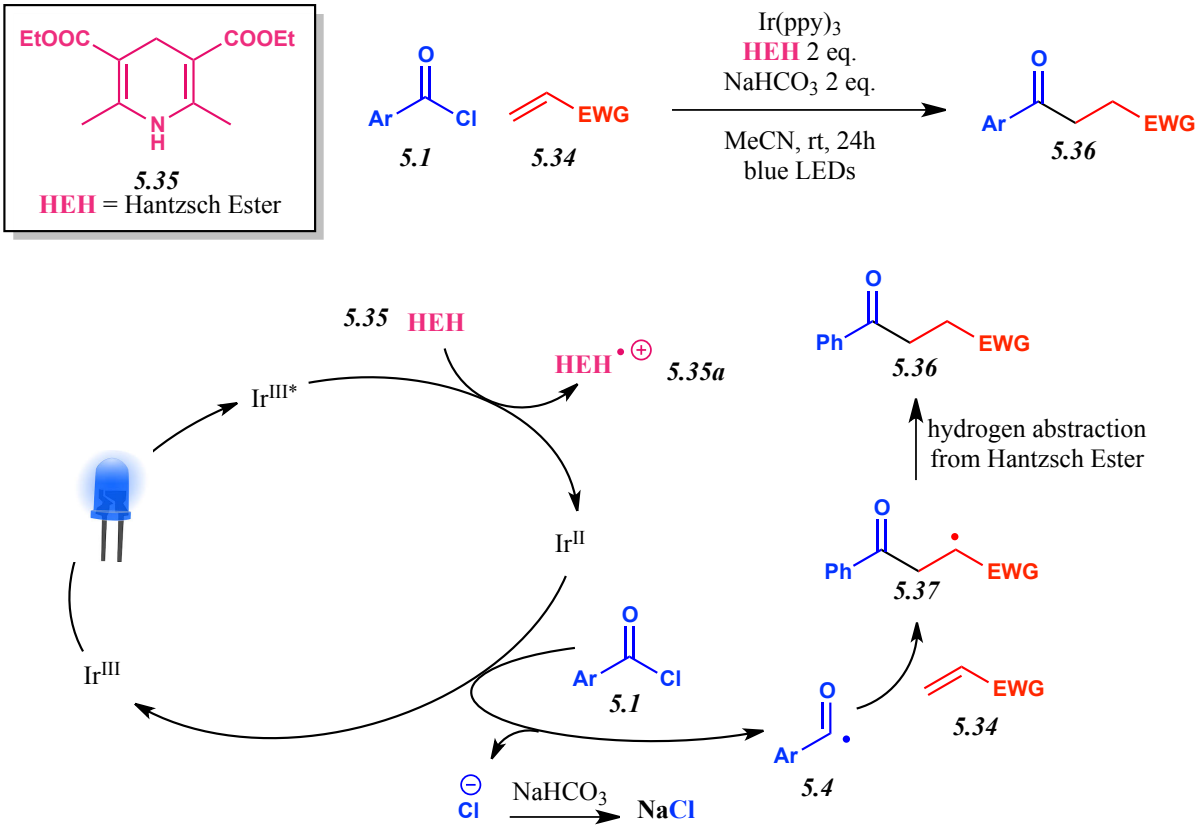

As illustrated in **Scheme 5.7.1** this synthetic methodology exploits the oxidation of Hantzsch Ester ***5.35*** to form an Iridium^{II} active photocatalytic species able to reduce aroyl chlorides ***5.1*** to aroyl radicals ***5.4*** in basic conditions. Following the coupling reaction of the aroyl radical ***5.4*** with electron deficient olefins ***5.34*** to form the radical intermediate ***5.37***, an HAT reaction takes place furnishing the saturated coupling product ***5.36***. A wide reaction scope was demonstrated, both in terms of electron deficient olefins and aroyl chlorides.

Upon analysis of this procedure, analogies and differences with our methodology can be denoted. At first, the two mechanistic pathways differ despite the photocatalytic compound used is the same. In fact, Wang takes advantage of Hantzsch Ester ***5.35*** as a reductant to generate an active photocatalytic species and also to generate the final 1,4-dicarbonyl product ***5.36*** via HAT. Secondly, while our procedure exploits a basic media to deprotonate the cationic intermediate ***5.17*** formed (see **Scheme 5.2.3**), the methodology proposed by Wang requires it mainly to neutralize the reaction solution. In addition, the procedure by Wang adopts mainly electron deficient olefins ***5.34***, while our procedure is in principle applied to all olefins. Last but not least, the two reaction products are different: while the compounds ***5.36*** achieved via the procedure by Wang are saturated

1,4-dicarbonyls, the products ***5.31*** deriving from our methodology are mainly α-unsaturated ketones.

Following this event, a second work covering the topic of the generation of aroyl radicals via VLPC starting from aroyl chlorides was disclosed[5.6].

As a consequence, it was our belief that our work would not have been considered innovative any more following the event of the publication by Wang. For this reason we decided to try to extend our methodology towards aliphatic acyl chlorides.

5.8 Investigations towards the generation of aliphatic acyl chlorides via VLPC

Upon analysis of the literature, it was found that general procedures for the generation and exploitation of aliphatic acyl radicals by means of VLPC were quite uncommon at the time of this study (2018). Worth mentioning among the existing methodologies are the oxidation of acylsilanes via Decatungstate anion photocatalysis[5.7], the visible light mediated decarboxylation of a-ketoacids[5.8] along with Nickel based dual-catalytic methods[5.9]. As a consequence, it was our belief that a procedure for the generation and exploitation of aliphatic acyl radicals starting from simple and readily available acyl chlorides would have been highly desirable and innovative; this consideration prompted us to investigate this research topic.

By reading through both the work of Xu and Wang, the Iridium photocatalyzed methodology applied to aroyl chlorides was not effective when extended to aliphatic acyl chlorides. According to the literature, the reduction potential of simple acetyl chloride ($E_{1/2}^{red}$ = −1.98 V vs SCE)[5.10] is beyond the reducing ability of the excited $Ir(ppy)_3$ photocatalyst, thus preventing its reduction to radical anion. On the other hand, the reduction potential of cyclohexancarbonyl chloride ($E_{1/2}^{red}$ = −1.48 V vs SCE)[5.11] should allow its reduction by means of the excited Iridium catalyst. Nonetheless, Xu et al report the failure of their procedure when applied to this aliphatic acyl chloride, explaining this outcome with the potential instability of the acyl radical species.

When cyclohexancarbonyl chloride ***5.38*** was submitted to the optimized reaction conditions described in **Paragraph 5.2** for aroyl chlorides in the presence of styrene ***5.9*** as a radical trap, no reactivity could be observed.

Scheme 5.8.1: Extension of the VLPC methodology to aliphatic acyl chlorides is unsuccessful

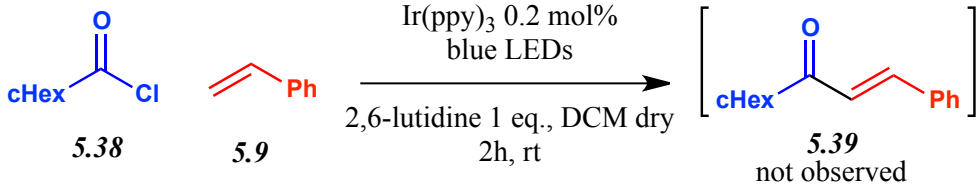

The same outcome was achieved by attempting the reaction on other starting materials such as phenylacetyl chloride and 1,2-diphenylethylene; no trace of aliphatic acyl radical formation or addition to the olefin could be observed.

In order to pursue our aim, we decided to adopt the following strategy: the incorporation of a redox active moiety (an electroauxiliary group) in the acyl radical precursor could drive the desired redox step with positive effects. In other words, we started investigating the in-situ transformation of the aliphatic acyl chloride ***5.40*** in a new reactive species ***5.41*** by means of an activating agent (AA), aiming to involve the latter in the visible light mediated photocatalytic generation of the aliphatic acyl radical.

Scheme 5.8.2: Strategy towards the generation of aliphatic acyl radicals by means of VLPC: use of activating agents (AA)

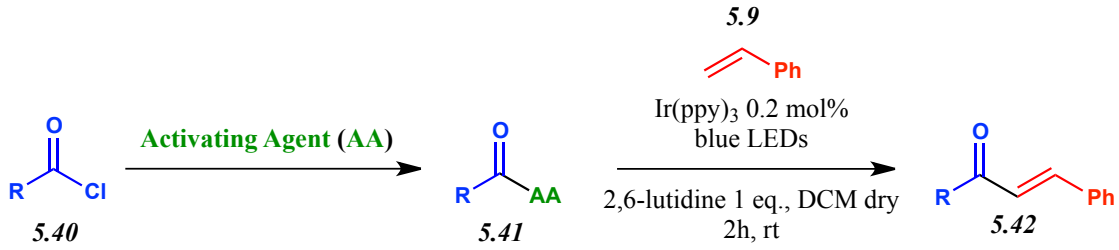

This approach is not new to the field of VLPC[5.12].

Taking into account the chemical reactivity of acyl chlorides, the most straightforward way to transform them is undoubtedly by means of a Nucleophilic Acyl Substitution (S_NAc). In fact, many readily available nucleophilic compounds are able to quickly attack acyl chlorides in mild conditions, affording potentially easily reducible derivatives. We planned to adopt two different approaches towards this strategy. The first approach regarded the in-situ transformation of the acyl chloride ***5.40*** in a stoichiometric amount of reactive species ***5.41*** which could be reduced to the desired acyl radical (**Scheme 5.8.3**, method *a*).

Scheme 5.8.3: Two startegies for the use of activating agents

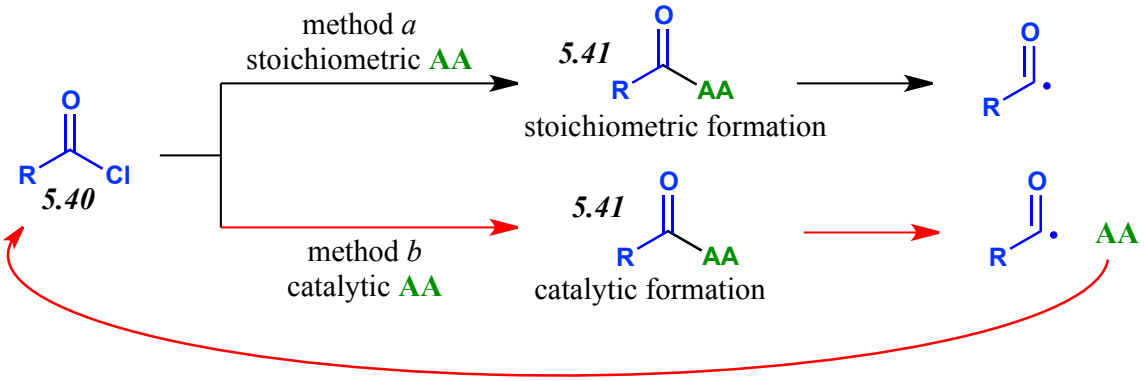

The second approach instead regarded the use of a catlytic amount of nucleophilic activating agent. In this way we expected the formation of a catalytic amount of activated species ***5.41***, which upon formation of the acyl radical would eliminate the nucleophilic activating agent, restoring its ability to activate a new molecule of acyl chloride ***5.40*** (**Scheme 5.8.3**, method *b*). The development of a method possessing the features of method *b* would be desirable because it would allow a lower waste of material, reasonably leading to cleaner reaction crudes and more effective transformations.

Based on this reasoning, three different classes of nucleophilic activating agents were investigated, based respectively on the reactivity of oxygen, nitrogen or sulfur atoms.

5.9 Investigations towards the generation of aliphatic acyl radicals by addition of oxygen, nitrogen and sulfur based nucleophilic activating agents

To begin with, a screening of simple and available nucleophiles was performed. In order to quickly search for a promising result, a set of reactions was prepared for each activating agent to be taken into consideration. Different combinations of aliphatic acyl chlorides ***5.40*** and olefins were employed; for each combination, both stoichiometric and catalytic amounts of potential activating agent were tested for reactivity. The typical screening investigation of an activating agent was performed as illustrated in **Scheme 5.9.1**.

Scheme 5.9.1: Method used for the screening of reaction conditions

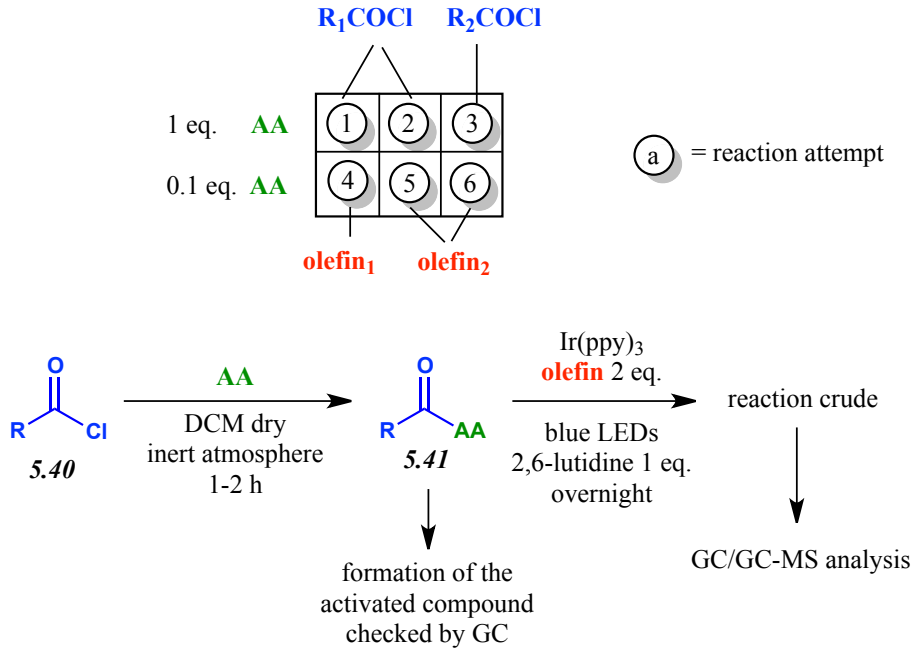

The desired aliphatic acyl chloride ***5.40*** was treated with the nucleophilic activated agent and then submitted to the photocatlytic reaction conditions in a one-pot fashion. For all reactions performed, the formation of the activated compound was checked by GC. The analysis of the reaction crude after irradiation overnight was also performed by GC; in case a decrease of the starting material or the formation of a new peak was observed, showing a potential sign of desired reactivity, further analysis were performed by NMR and GC-MS.

Referring to **Scheme 5.9.1** for the one-pot reaction methodology, an overview of the tested aliphatic acyl chlorides ***5.40***, nucleophilic activating agents and olefins is given in **Scheme 5.9.2**.

Scheme 5.9.2: Aroyl chlorides, activating agents and olefins scoped towards desired reactivity

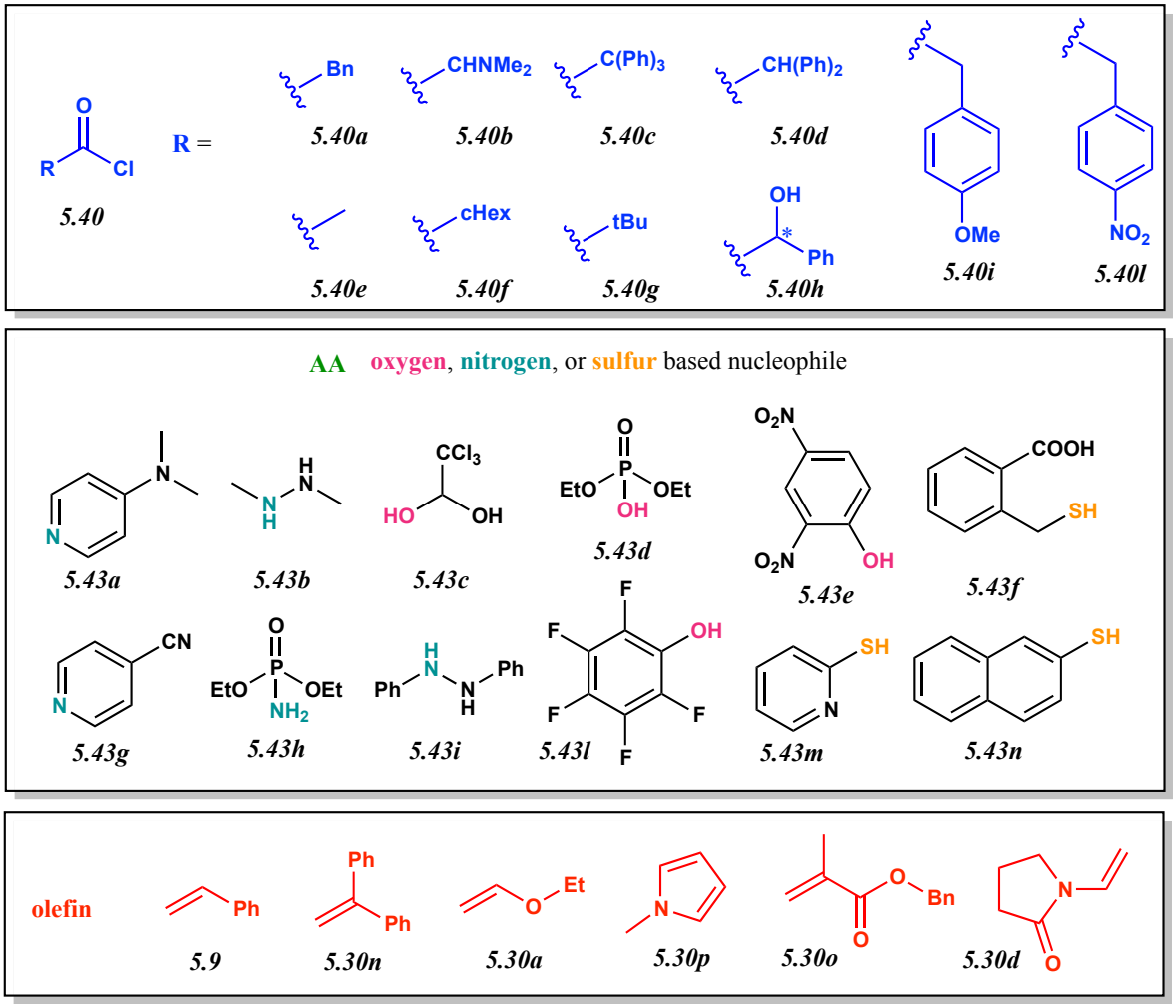

Unfortunately, no promising results were achieved with oxygen and nitrogen based nucleophiles. On the other hand, some desired reactivity was observed adopting 2-(mercaptomethyl)benzoic acid ***5.43f*** as a reagent. Noteworthy, when this reactant was tretated in the reaction conditions previously illustrated, no product ***5.39*** could be observed.

Scheme 5.9.3: Unsuccessful reaction using 2-(mercaptomethyl)benzoic acid ***5.43f*** as an AA

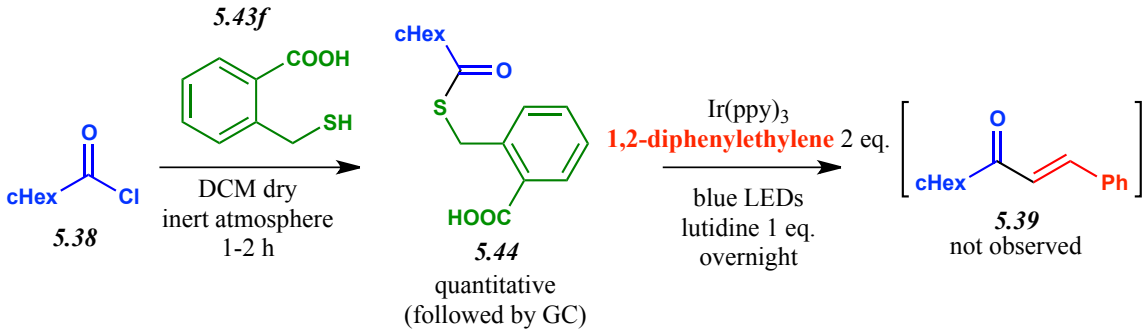

In another experiment, an additional step was performed in one-pot fashion, that is the treatment of the thioester ***5.44*** formed in situ with oxalyl chloride.

Scheme 5.9.4: Successful reaction using 2-(mercaptomethyl)benzoic acid ***5.43f*** as an AA

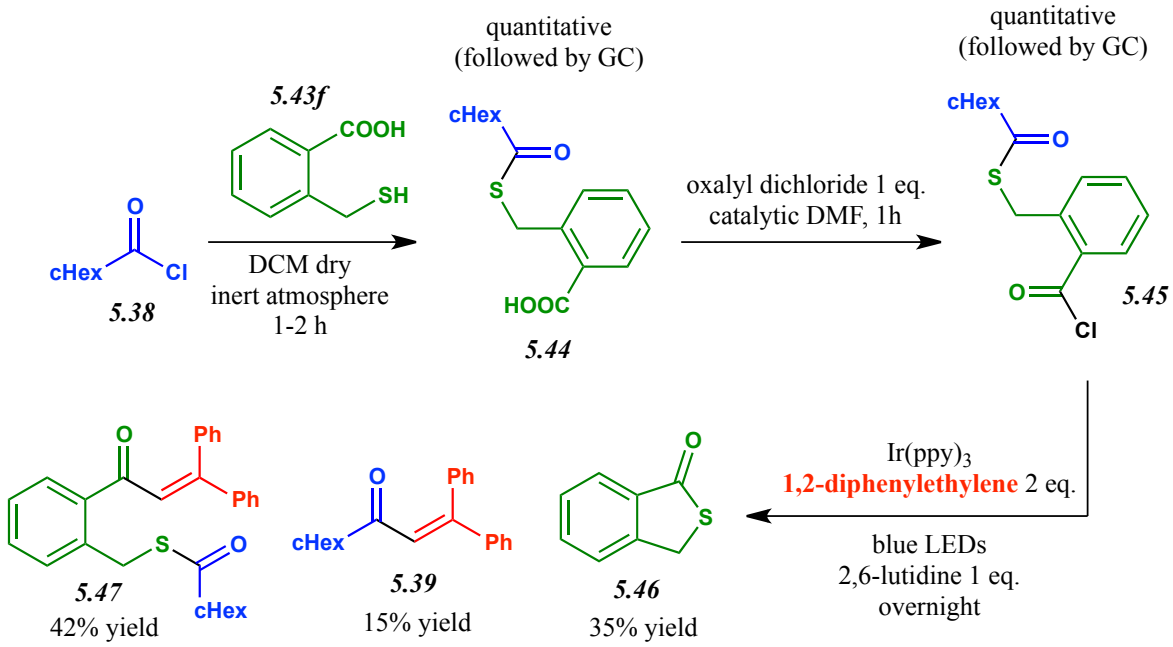

The experiment illustrated above furnished the desired α,β-unsaturated ketone ***5.39*** in low yield together with the two other products ***5.46*** and ***5.47***. A reasonable explanation of this outcome is given in **Scheme 5.9.5**.

Scheme 5.9.5: Rationale behind the utilization of 2-(mercaptomethyl)benzoic acid ***5.43f*** as an AA

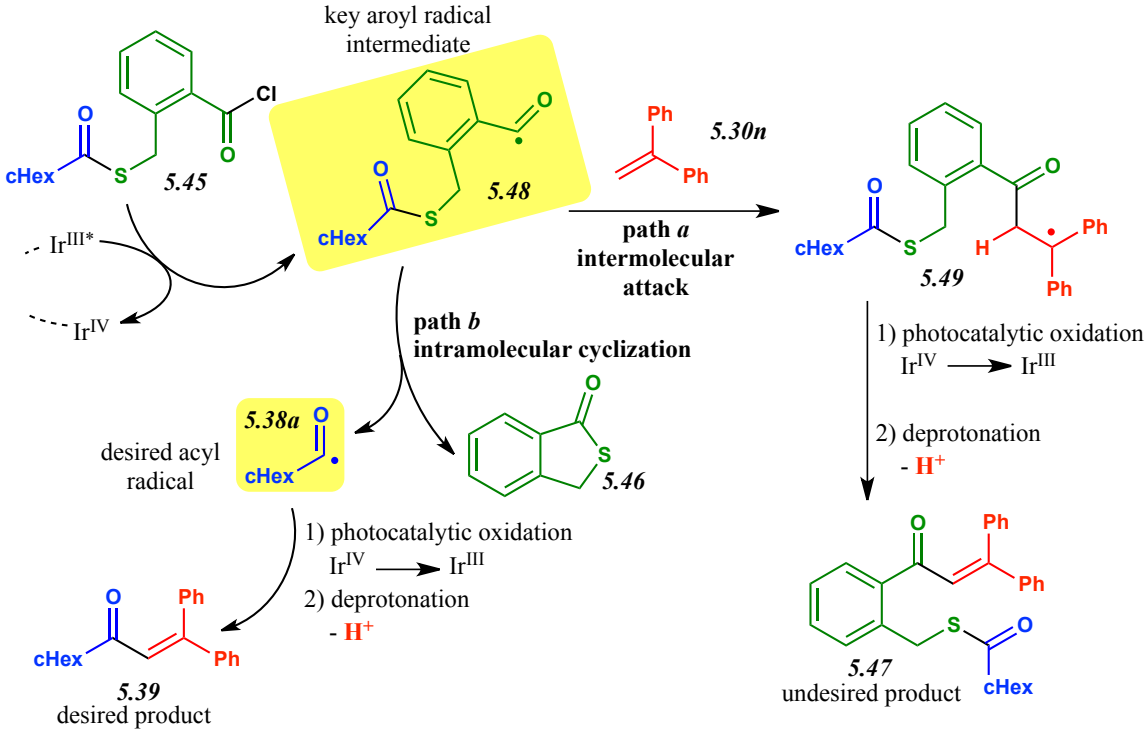

In fact, this reaction exploits the reactivity of aroyl chlorides previously described in this chapter. Following the formation of the key aroyl radical intermediate ***5.48*** from in-situ generated aroyl chloride ***5.45***, two possible reaction pathways may take place. Path *a* leads to the direct attack of the key aroyl radical ***5.48*** to the olefinic substrate ***5.30n***, leading to the formation of undesired product ***5.47***. Noteworthy, no intramolecular cyclization takes place in this case, presumably because the resulting product would be a seven membered heterocycle. On the other hand, path *b* leads to the intramolecular cyclization of the key aroyl radical intermediate ***5.48*** which affords benzo[c]thiophen-1(3H)-one ***5.46*** along with the desired aliphatic acyl radical ***5.38a***. At this point, such acyl radical species is able to attack the olefinic substrate ***5.30n*** in order to furnish the desired product ***5.39***.

The intramolecular radical cyclization taking place via path *b* (**Scheme 5.9.5**) is a typical cyclization reaction occurring with sulfur containing compounds; similar examples can be found in the literature[5.13]. The key factor allowing this kind of radical intramolecular cyclization lies in the remarkable dimensions of the sulfur atom.

Despite an interesting reaction was discovered which allowed to afford the desired aliphatic acyl radical species ***5.38a***, the competition among the two reaction pathways illustrated in **Scheme 5.9.5** discouraged us to further investigate it. In fact, this kind of approach would result too complex when working to set-up an useful synthetic methodology.

5.10 Photoredox and Photechemical reactivity of Organic Xanthates towards aliphatic acyl radical generation

When potassium ethyl xanthogenate ***5.50*** was employed both in stoichiometric and catalytic amount as an activating agent, the desired reactivity was observed.

Scheme 5.10.1: Promising result furnished by the use of potassium ethyl xantogenate as an AA

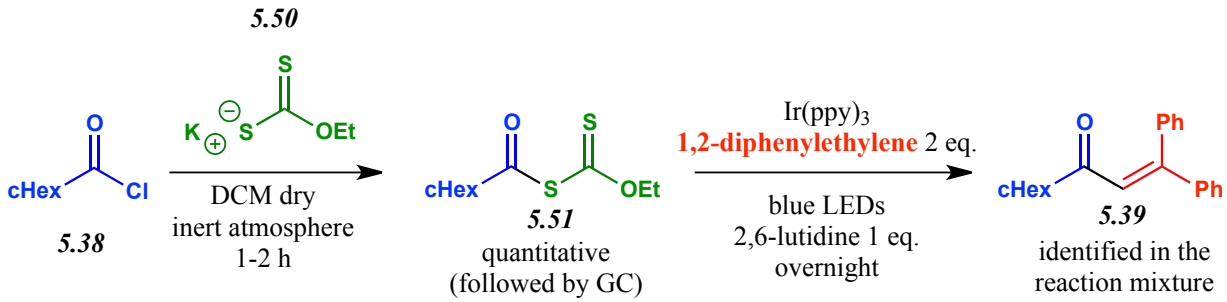

On a first analysis of this result, it was thought that potassium ethyl xanthogenate ***5.50*** could successfully fill the role of activating agent, by generating an organic xanthate ***5.51*** which could easily be reduced by the excited state photocatalyst. As a consequence, an investigation of the reaction conditions was performed; use of potassium xanthogenate ***5.50*** was tested from catalytic to excess amount. Direct use of preformed organic xanthate ***5.51*** was also submitted to the reaction conditions. The results of this investigation are reported in **Table 5.10.1**.

Table 5.10.1: Optimization of the reaction conditions

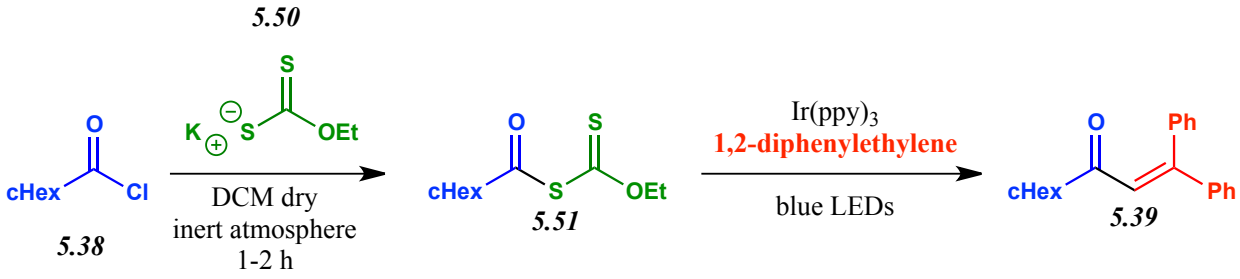

entry	cyclohexancarbonyl chloride (eq.)	potassium ethyl xantogenate (eq.)	preformed organic xantate ***5.51*** (eq.)	1,2-diphenylethylene (eq.)	base (eq.)	product ***5.39*** yield
1	1	1	/	2	lutidine (1)	10%
2	1	0.1	/	2	lutidine (1)	traces
3	1	1	/	2	DIPEA (1)	25%
4	1	0.1	/	2	DIPEA (1)	18%
5	/	/	1	2	DIPEA (1)	26%
6	2	2	/	1	DIPEA (1)	51%
7	/	/	2	1	DIPEA (1)	55%
8	/	/	4	1	DIPEA (1)	51%
9	/	/	2	1	DIPEA (2)	45%
10	/	/	2	1	/	no product

Reactions performed on 0.1 mmol scale, under blue LEDs irradiation, with 0.2 mol% $Ir(ppy)_3$ in dry DCM at rt for 24h. Reaction yields were calculated by GC analysis of the crudes.

Preliminary reactions performed with 2,6-lutidine (entries 1 and 2) led to worse results with respect to those performed with DIPEA (entries 3 and 4). Noteworthy, a catalytic behaviour of potassium xanthogenate was demonstrated (entry 4): 0.018 mmol of product ***5.39*** were achieved starting from 0.01 mmol of potassium xanthogenate. Better results were achieved by using an excess of acyl chloride ***5.38*** with respect to the oelfinic trap ***5.30n*** (entry 6). In addition, direct use of preformed organic xanthate ***5.51*** furnished no sensible difference in terms of product ***5.39*** yield with respect to its formation in situ (entry 3 VS entry 1 and entry 7 VS entry 5).

The use of a further excess of acyl chloride ***5.38*** (entry 8) did not improve the reaction yield. In a similar way, also the use of excess base proved uneffective (entry 9). Remarkably, when no base was employed, no product was observed; on the other hand, the unexpected product ***5.52*** was isolated in low yield.

Scheme 5.10.2: Formation of the unexpected product ***5.52*** in absence of basic media

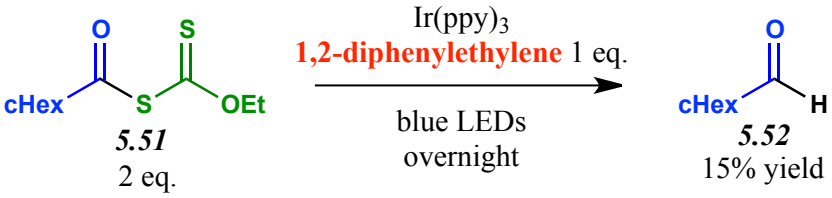

A reasonable explanation of this outcome may be given with the hypothesis that the acyl radical ***5.38a*** performs hydrogen abstraction from the solvent leading to the respective aldehyde ***5.52***. Further investigations on this reaction pathways will be discussed in **Paragraph 5.11**.

In order to gain further insight on the reaction under investigation, some control experiments were performed.

Table 5.10.2: Control experiments of the reaction leading to product ***5.39***

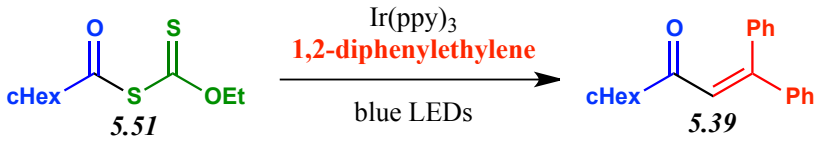

entry	$Ir(ppy)_3$ mol%	irradiation	product ***5.39*** yield
1	0.2 mol%	455 nm	55%
2	0.2 mol%	no irradiation	/
3	/	455 nm	55%
4	/	400 nm	/
5	/	530 nm	/

Reactions performed on 0.1 mmol scale, with 2 eq. of preformed organic xanthate ***5.51***, 1 eq. of 1,2-diphenylethylene, 1 eq. of DIPEA in DCM at rt for 24h. Reaction yields were calculated by GC analysis of the crudes.

When the reaction was performed in the dark, no product was observed (entry 2). On the other hand, when no photoredox catalyst was added to the reaction mixture, the product ***5.51*** was equally achieved (entry 3 VS entry 1). As a result, it must be deduced that the process is purely photochemical and not photocatalytic. In addition, it was demonstrated that the organic xanthate absorbs in the blue region of the visible spectra, because the reaction is uneffective when irradiation is performed at different wavelenghts (entries 4 and 5).

Upon inspection of the literature, confirmation of the purely photochemical reactivity of organic xanthates was found[5.14]. As a consequence it was rationalized that an homolytic cleavage of the C-S bond of the organic xantate ***5.51*** was responsible for the formation of the desired acyl radical ***5.38a***.

Scheme 5.10.3: Homolytic cleavage of the C-S bond of compound ***5.51*** is responsible for the formation of the acyl radical ***5.38a***

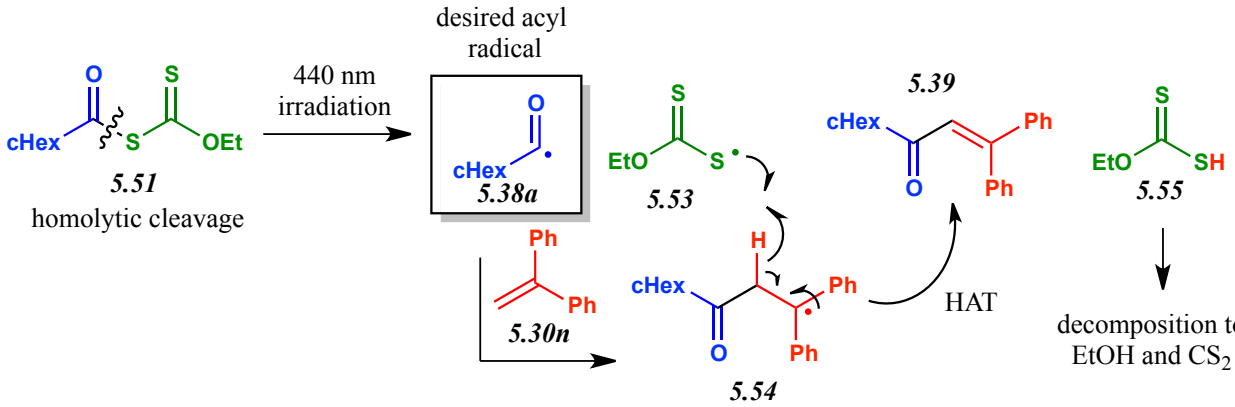

Reasonably, the homolytic cleavage of the C-S bond of the organic xanthate ***5.51*** leads to the formation of radical species ***5.38a*** and ***5.53***. Then, following the radical coupling leading to radical intermediate ***5.54***, the product ***5.39*** along with xanthic acid ***5.55*** are achieved by means of hydrogen transfer from intermediate ***5.54*** to the radical ***5.53***.

The high number of radical species generated by the proposed mechanism of the reaction is reasonably responsible for the dirty and difficult to purify reaction crudes achieved via this methodology.

Looking forward to establish a photochemical methodology for the generation and exploitation of aliphatic acyl radicals, more experiments were conducted. It was found that, upon portionwise addition of an excess of organic xanthate ***5.51*** to the reaction mixture, almost quantitative formation of the desired product ***5.39*** was achieved.

Scheme 5.10.4: Optimized reaction conditions and photochemical method

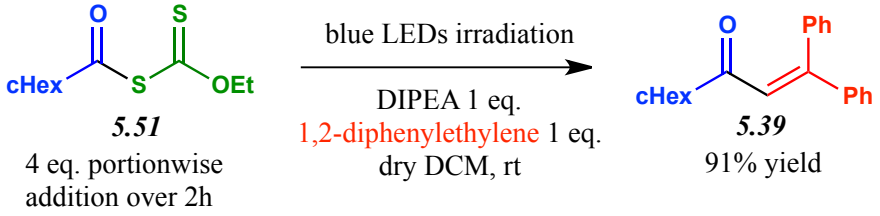

Reasonably, by slow addition of the organic xanthate ***5.51***, the generation of the acyl radical ***5.38a*** and concomitant trapping of the olefin is more efficient. Unfortunately, when the procedure was applied to different olefins such as ethyl vinyl ether, styrene and various acrylates, no respective product could be identified. Presumably, only 1,2-diphenylethylene ***5.30n***, being an excellent radical scavenger, is able to undergo the transformation illustrated in **Scheme 5.10.3**.

A similar problem was verified when another procedure was set-up using catalytic potassium xanthogenate ***5.50***. In fact, by developing what was previously observed in entry 4, **Table 5.10.1**, a dual-catalytic procedure was investigated.

Scheme 5.10.5: Dual-catalytic reaction of cyclohexancarbonyl chloride ***5.38*** with olefin ***5.30n***

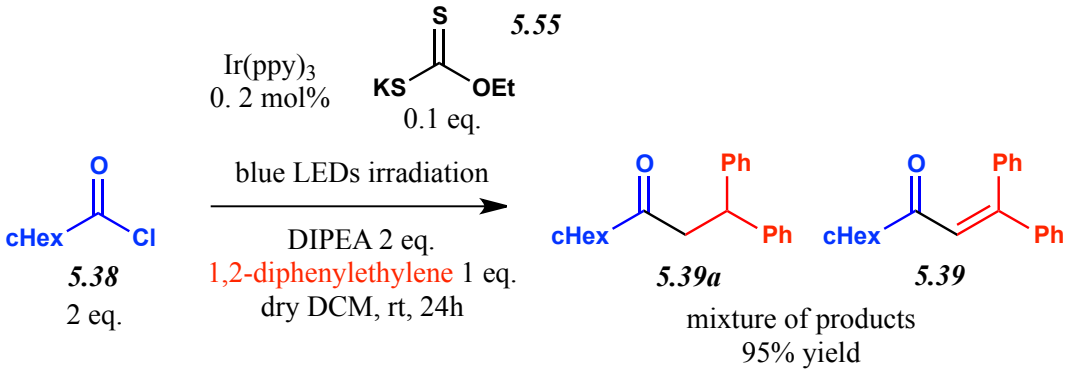

Noteworthy, only slight modifications of the conditions reported by entry 4 in **Table 5.10.1** led to full conversion of the olefinic trap ***5.30n***. A reasonable mechanistic explanation of this outcome is given in **Scheme 5.10.6**.

Scheme 5.10.6: Plausible reaction mechanism

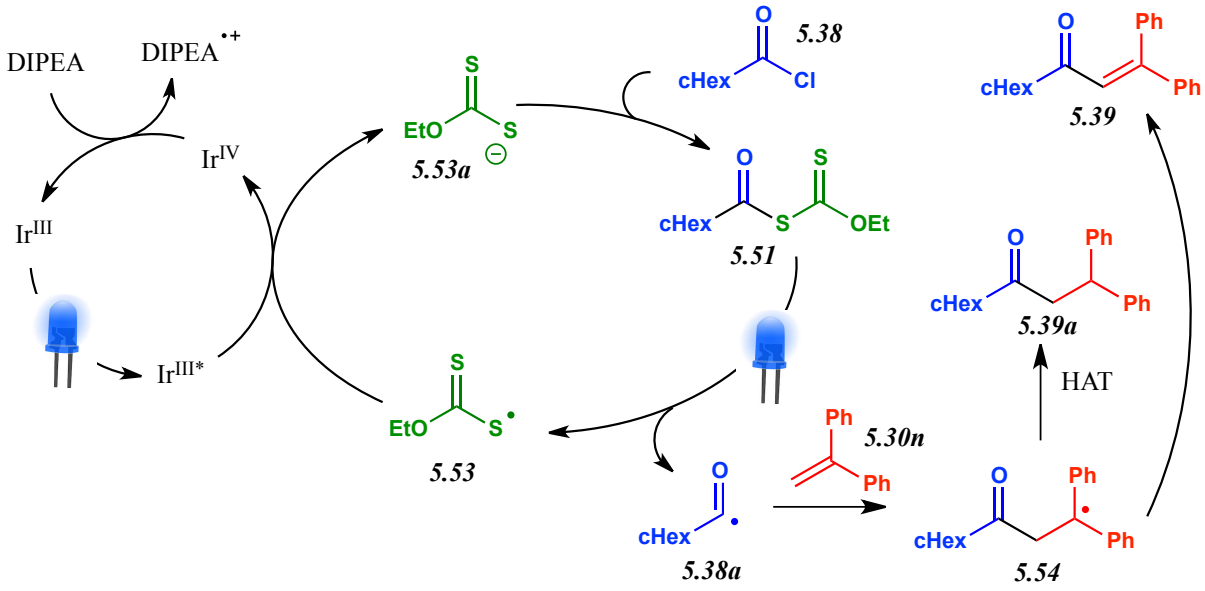

The organic xanthate ***5.51*** undergoes photochemical homolytic cleavage affording acyl radical ***5.38a*** and ethyl xanthogenate radical ***5.53***. The latter is reduced to the respective xanthogenate anion ***5.53a*** by the action of the excited state iridum photocatalyst. The iridum catalytic cycle is closed by means of DIPEA as a sacrificial electron donor, which reduces back the oxidized form of the photocatalyst. The xanthogenate anion ***5.53a*** is then able to attack the acyl chloride ***5.38*** via a nucleophilic acyl substitution furnishing a new molecule of organic xanthate ***5.51***. The obtained acyl radical ***5.38a*** is then able to attack the olefinic trap ***5.30n***. Noteworthy, potassium xanthogenate ***5.50*** or preformed xanthate ***5.51*** are equally successfully employed in catalytic amounts, thus supporting the proposed mechanism.

An alternative reaction mechanism can also be rationalized, in order to explain the formation of product ***5.39***.

Scheme 5.10.7: Alternative reaction mechanism

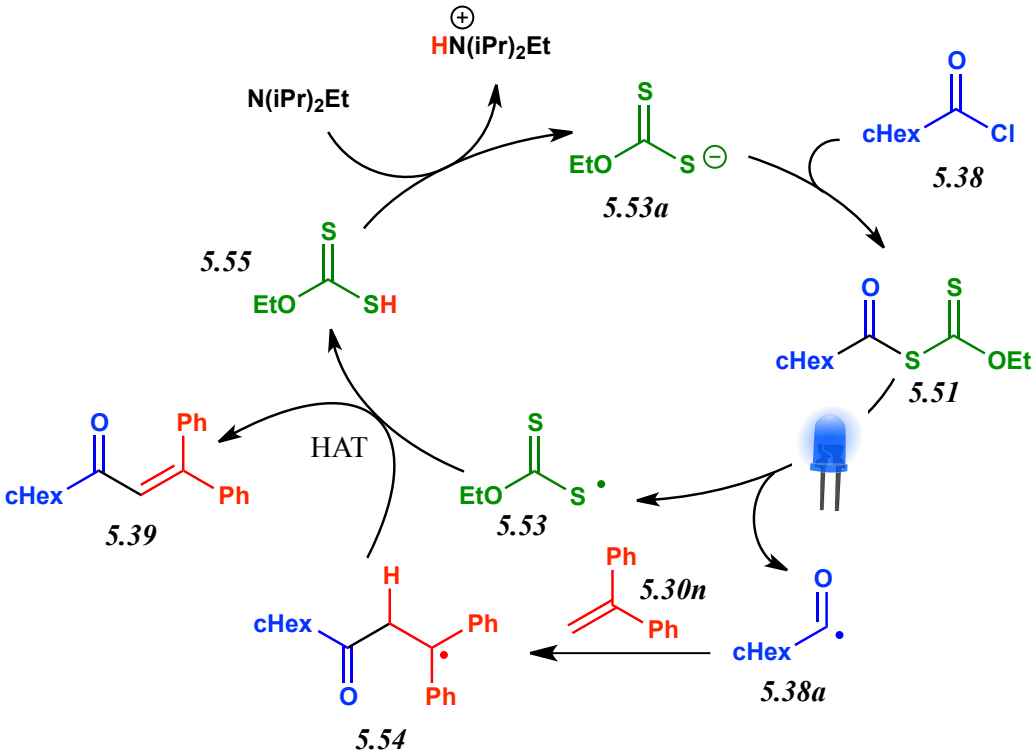

In this case, the xantogenate radical ***5.53*** supposedly abstracts and hydrogen from the radical intermediate ***5.54*** affording the desired product ***5.39*** along with xantic acid ***5.55***. The deprotonation of xantic acid by means of DIPEA reconstitutes the xantogenate anion ***5.53a*** which is able to restart the catalytic cycle by attacking a new acyl chloride ***5.38*** molecule. Presumably both mechanisms take place in the reaction conditions even though the second one does not explain why the reaction yield is definitely better in the presence of the Iridium catalyst. In addition, the known instability of xantic acid ***5.55*** makes the second mechanism proposed less reasonable.

With this method, cleaner reaction crudes with respect to the photochemical strategy previously discussed are achieved. As anticipated, also in this case the methodology failed when extended to different olefins. As a consequence, the results described in this paragraph remain at the moment unpublished.

5.11 Investigations towards the reduction of aliphatic carboxylic acids to the respective aldehydes

Aldehydes are versatile compounds in organic synthesis; despite their intrinsic benefits, there are relatively few methods for their preparation[5.14]. In particular, only a few methods to access the aldehyde function starting from the respective carboxylic acid are known[5.15]. For this reason it was considered interesting to investigate the possibility to establish a methodology for the reduction of carboxylic acids by means of the reactivity discussed in **Paragraph 5.10** (see **Scheme 5.10.2**).

In fact, following the discovery of the purely photochemical charachter of the reaction of organic xantate ***5.51***, discussed in **Paragaraph 5.10**, the reduction of cyclohexancarbonylchloride ***5.38*** to the respective aldehyde ***5.52*** was achieved in low yield.

Scheme 5.11.1: Photochemical reduction reaction of cyclohexancarbonylchloride ***5.38*** to the respective aldehyde ***5.52***

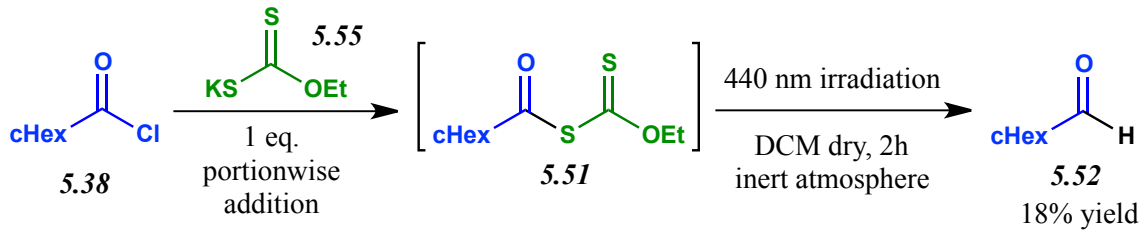

A higher reaction yield in the desired aldehyde ***5.52*** was achieved by directly submitting to the blue LEDs irradiation the preformed organic xantate ***5.51*** (25% yield) via portionwise addition. Reasonably, the reaction occurrs via an hydrogen atom abstraction reaction performed by the acyl radical ***5.38a***.

With all probabilities, the hydrogen atom source would be the reaction solvent. With the aim to enhance the efficiency of the reaction, Hantzsch ester ***5.35*** was added to the reaction mixture as a stoichiometric hydrogen donor (**Scheme 5.11.2**).

Scheme 5.11.2: Addition of Hantzsch ester to the reaction conditions

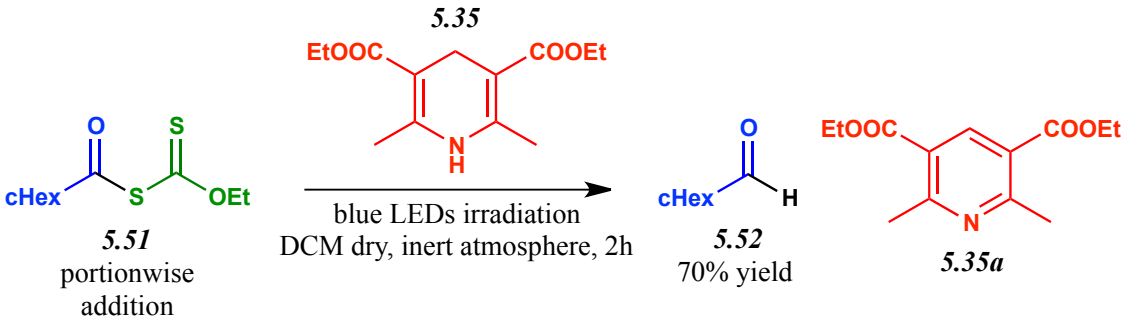

The addition of Hantzsch ester as an hydrogen source proved to be effective towards the desired reactivity. The product of the oxidation of the Hantzsch ester (compound ***5.35a***) was detected in the reaction mixture.

Following this result, an investigation of the reaction conditions was performed. Different solvents were tested (water, benzene, MeCN, $CHCl_3$) but the best results were achieved using dichloromethane as a solvent. The use of a different hydrogen donating compound, cyclohexadiene, was tested with worse results (20% yield). When no inert atmosphere was employed, a reaction yield drop was observed (from 70% to 40%). Confirming what was discussed in **Paragraph 5.10**, no reaction was observed when the irradiation wavelenght was modified to 400 nm or 530 nm. Finally, when $Ir(ppy)_3$ was added to the reaction mixture, no yield improvement was observed. In addition, when DIPEA was added in combination with the iridium photocatalyst, no product was detected, confirming what was previously observed.

The procedure proved to be effective also when Dodecylcarbonyl chloride was submitted to the reaction conditions (53% yield) instead of cyclohexancarbonyl chloride. Also in this case, the direct use of the respective preformed organic xantate furnished better results in terms of reaction yield (60% yield).

Unfortunately, when the direct one-pot procedure starting from cyclohexancarboxylic acid was attempted, no satisfying result was obtained, since the desired aldehyde could only be isolated in low yield.

Scheme 5.11.3: One-pot photochemical reduction of carboxylic acids

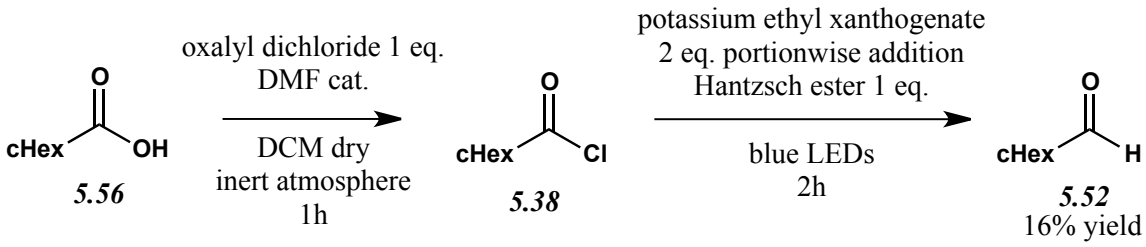

The one-pot methodology suffers from some limitations. First, the acidic media generated by the use of oxalyldichloride cannot be neutralized since the desired reactivity is apparently not compatible with the addition of a base. Secondly, the different steps involved in the procedure do not allow the reaction to remain totally inert. Last but not least, the in-situ formation of the reactive organic xantate ***5.51*** is less efficient with its direct addition, compromising the final product yield.

5.12 Conclusions

In conclusion, my internship spent in the research group of Professor König was the occasion to acquire a great deal of experience not only in the field of VLPC but generally in the panorama of Organic Chemistry. I had the opportunity to learn from experts in the field and to establish new connections which will be hopefull fruitful in the future for the two research groups.

The work inherent with the generation of aroyl radicals starting from aroyl chlorides could not be the subject of a scientific publication due to lack of innovation; unfortunately for us, the topic was disclosed by a different research group while we were still working at it.

The work inherent with the generation of acyl radicals starting from aliphatic acyl chlorides could not be finished for reasons of time; both me and my colleague Daniel have reached the end of our doctoral program while the project was in due course. This work furnished many interesting insights which will hopefully lead to a continuation in the near future. In fact, by inspection of a very recent (2018) review on the topic[5.16], the mild generation of aliphatic acyl radical starting from the respective acyl chlorides is still not fully disclosed.

5.13 References

5.1

(a) J. Liu; Q. Liu; H. Yi; C. Qin; R. P. Bai; X. T. Qi; Y. Lan; A. W. Lei *Angew. Chem., Int. Ed.*, **2014**, 53, 502-506.
(b) H. Tan; H. J. Li; W. Q. Ji; L. Wang *Angew. Chem., Int. Ed.*, **2015**, *54*, 8374-8377.
(c) G. Z. Wang; R. Shang; W. M. Cheng; Y. Fu *Org. Lett.*, **2015**, 17, 4830-4833.
(d) G. Bergonzini; C. Cassani; C.J. Wallentin *Angew. Chem. Int. Ed.*, **2015**, *54*, 14066-14069.
(e) G. Bergonzini; C. Cassani; H. Lorimer-Olsson; J. Hörberg; C.-J. Wallentin *Chem.-Eur. J.*, **2016**, *22*, 3292-3295.
(f) Q. Q. Zhou; W. Guo; W. Ding; X. Wu; X. Chen; L. Q. Lu; W.-J. Xiao *Angew. Chem. Int. Ed.*, **2015**, *54*, 11196-11199.
(g) L. Chu; J. M. Lipshultz; D. W. C. MacMillan *Angew. Chem. Int. Ed.*, **2015**, *54*, 7929-7933.
(h) W. M. Cheng; R. Shang; H. Z. Yu; Y. Fu *Chem. Eur. J.,* **2015**, *21*, 13191-13195
(i) H. Huang; G. Zhang; Y. Chen *Angew. Chem. Int. Ed.*, **2015**, *54*, 7872-7876.

5.2

(a) C. G. Li; G. Q. Xu; P. F. Xu *Org. Lett.,* **2017**, *19*, 3, 512–515.

(b) S. M. Xu; J. Q. Chen; D. Liu; Y. Bao; Y. M. Lianga; P. F. Xu *Org. Chem. Front.*, **2017**, *4*, 1331-1335.

5.3

P. K. Chattaraj; B. Maiti; U. Sarkar *J. Phys. Chem. A*, **2003**, *107*, *25*, 4973–4975.

5.4

C. Peppe; E. S. Lang; F. M. de Andrade; L. B. de Castro *Synlett* **2004**, 10, 1723-1726.

5.5

C. M. Wang; D. Song; P. J. Xia; H. Y. Xiang; H. Yang *Chem. Asian J.* **2018**, *13*, *3*, 271-274.

5.6

Y. Liu; Q. Wang; C. Zhou; B. Xiong; P. Zhang; C. Yang; K. Tang *J Org Chem*. **2018,** *83*, 4, 2210-2218.

5.7

L. Capaldo; R. Riccardi; D. Ravelli; M. Fagnoni *ACS Catal.* **2018**, *8*, 1, 304-309.

5.8

(a) J. Liu; Q. Liu; H. Yi; C. Qin; R. P. Bai; X. T. Qi; Y. Lan; A. W. Lei *Angew. Chem., Int. Ed.*, **2014**, 53, 502-506

(b) W. M. Cheng; R. Shang; H. Z. Yu; Y. Fu *Chem. Eur. J.* **2015**, *21*, 13191-13195.

5.9

(a) C. L. Joe, A. G. Doyle *Angew. Chem. Int. Ed.* **2016**, 55, 4040-4043.

(b) L. Chu; J. Lipshultz; D. MacMillan W. *Angew. Chem. Int. Ed.* **2015**, *54*, 7929–7933.

(c) X. Zhang; D. W. MacMillan J. Am. Chem. Soc. **2017**, *139*, 11353-11356.

5.10

D. Occhialini; K. Daasbjerg; H. Lund *Acta. Chem. Scand.*, **1993**, *47*, 1100-1111.

5.11

G. A. Urove; D. G. Peters *J. Electrochem. Soc.*, **1993**, *140*, 928-932.

5.12

(a) Yoshida J.; Kataok, K.; Horcajada R.; Nagaki A. *Chem*. *Rev*. **2008**, *108*, 2265−2299.

(b) Tyson E. L.; Farney E. P.; Yoon T. P. *Org*. *Lett*. **2012**, *14*, 1110−1113.

5.13

(a) Beckwith A. L. J.; Duggan S. A. M. *J. Chem. Soc. Perkin Trans. 2* **1994**, 1509-1518.

(b) Crich D.; Hao X. *J. Org. Chem.* **1997**, *62*, 5982-5988.

5.14

Larock R. C. Comprehensive Organic Transformation; VCH Publisher: New York, 1989; 585

5.15

(a) M. Falorni; G. Giacomelli; A. Porcheddu; M. Taddei *J. Org. Chem.* **1999**, *64*, 24, 8962-8964.

(b) Babler J. H.; Invergo B. J. *Tetrahedron Lett.* **1981**, *22*, 11-13.

(c) Four P.; Guibe F. *J. Org. Chem.* **1981**, *46*, 4439-4445.

(d) Fleet G. W. J.; Harding P. J. C.*Tetrahedron Lett.* **1979**, *20*, 975-978.

(e) Burgstahler A. W.; Weigel L.O.; Shaefer C. G. *Synthesis*, **1976**, *11*, 767-768.

(f) Citron J. D. *J. Org. Chem.* **1969**, *34*, 1977-1979.

5.16

Banerjee A.; Lei Z.; Ngai M.Y. *Synthesis* article in press, DOI:10.1055/s-0037-1610329

CHAPTER 6:
EXPERIMENTAL SECTION

6.1 General experimental methods

a) related to the experimental work at Università degli Studi di Genova, Genova, Italy Department of Chemistry and Industrial Chemistry (DCCI), BOG group

NMR spectra were taken in $CDCl_3$ or in d_6-DMSO at 300 MHz (^1H) and 75 MHz (^{13}C), using, as internal standard, TMS (^1H NMR in $CDCl_3$; 0.000 ppm) or the central peak of DMSO (^1H NMR in d_6-DMSO; 2.506 ppm) or the central peak of $CDCl_3$ (^{13}C in $CDCl_3$; 77.02 ppm), or the central peak of DMSO (^{13}C in d_6-DMSO; 39.43 ppm). Chemical shifts are reported in ppm (δ scale), coupling constants are reported in Hertz. Peak assignments were also made with the aid of gCOSY and gHSQC experiments.

TLC analyses were carried out on silica gel plates (thickness = 0.25 mm), viewed at UV (254 nm) and developed with Hanessian stain (dipping into a solution of $(NH_4)_4MoO_4 \cdot 4H_2O$ (21 g) and $Ce(SO_4)_2 \cdot 4H_2O$ (1 g) in H_2SO_4 (31 mL) and H_2O (469 mL) and warming), or with ninhydrin (ninhydrin (900 mg) in nBuOH (300 mL) and AcOH (9 mL)), followed by warming. R_f values were measured after an elution of 7–9 cm.

GC–MS analyses were carried out on a Hewlett Packard 5890 Series II, using a HP-1 column, coupled with a HP-5971A spectrometer (electron impact). Analysis conditions are as follows: flow (He) 0.9 mL/min; initial temperature 100 °C; initial time 2 min; gradient temperature 20 °C/min; final temperature 280 °C; final time 5 min.

HPLC–MS analyses were carried out on a Hewlett Packard 1100, using a Gemini C6-Phenyl (150x3mm) column, coupled with a Microsaic 4000 MiD Mass Spectrometer (electrospray). Analysis conditions are as follows: flow 0.34 mL/min; temperature 26 °C; solvent A: water + 0.1% formic acid; solvent B: acetonitrile + 0.1% formic acid; gradient: from 10% B to 100% B in 20 min.

Column chromatography was performed with the "flash" methodology using 220–400 mesh silica.

Solvents employed as eluents and for all other routinary operations, as well as anhydrous solvents and all reagents used were purchased from commercial suppliers and employed without any further purification.

Visible light photoinduced reactions were performed with blue LEDs (LED stripe GBC SMD 3528 INDOOR BLU 12Vcc) or LASER (CNI diode laser MDL-442, 40 mW power driven by power supply unit model PSU-III-LED. The output of laser is coupled to an optical fiber).

UV-Photoinduced reactions were performed by means of a Southern New England Ultraviolet Company Rayonet® apparatus equipped with 16 Iles Optical lamps (300 nm).

b) related to the experimental work at University of Regensburg, Regensburg, Germany Faculty of Chemistry and Pharmacy, AK König research group

Commercial reagents and starting materials were purchased from Aldrich, Fluka, VWR or Acros and used without further purification. Solvents were used as p. a. grade or dried and distilled prior to use as described in common methods if required by the experimental procedure[6.1].

Visible light irradiation was performed using LED lamps OSRAM Oslon SSL 80 LD H9GP-3T3U-35 (royal-blue, λ = 455 ± 15 nm, 700 mA, P = 1.12 W), Philips LUXEON Rebel LXML-TRo1-0225 (blue, λ = 455 ± 15 nm, 700 mA, P = 3.0 W).

The plain-bottomed glass vials which were employed for all photochemical reactions inside the LEDs setups were the following: 20mm Rollrandflasche, Klarglas, 5ml, 38.5mm (H) x 22.0mm (AD), WICOM. The vials were provided with a stirring bar and the solid reagents and catalysts then sealed with disposable caps. The vials fit precisely in the LEDs setup which is thermostated at 25°C. The glass vials were irradiated by the bottom side.

All reactions were monitored by thin-layer chromatography (TLC) on alumina plates coated with silica gel (Merck silica gel plates 60 F_{254}, 0.2 mm) and visualized by UV light excitation (λ = 254 nm), or by naked eye.

Flash column chromatography was carried out on a Biotage Isolera One automated flash purification system with UV/VIS detector using Sigma Aldrich MN silica gel 60 M (particle size 40-63 μm).

Nuclear magnetic resonance spectra were recorded on a Bruker Avance 300 (^{1}H: 300.1 MHz, ^{13}C: 75.5 MHz, T = 300 K) spectrometer equipped with a robotic sampler. Data for ^{1}H-NMR are reported as follows: chemical shift, multiplicity, integration, and coupling constant. Chemical shifts are reported in δ [ppm] relative to tetramethylsilane (TMS) as the external standard. Characterization of the signals: s=singlet, d=doublet, t=triplet, q=quartet, quint=quintet, dd=doublet of doublets, dt=doublet of triplets, tt=triplet of triplets, m = multiplet, bs = broad singlet. The relative number of protons is determined by integration. Coupling constants J are given in Hertz [Hz]. Data for ^{13}C-NMR are reported in terms of chemical shift. Error of reported values: chemical shift 0.01 ppm for ^{1}H-NMR, 0.1 ppm for ^{13}C-NMR, coupling constant 0.1 Hz. The solvent used is reported for each spectrum.

6.2 Photocatalyzed synthesis of isochromanones and isobenzofuranones under batch and flow conditions: synthesis and spectral charachterization of compounds

*General procedure for the synthesis of benzendiazonium tetrafluoroborates of general formula **2.1***

Benzenediazonium salts were prepared from the corresponding anilines according to literature procedures[6.2].
An aniline of general formula ***2.10*** (3 mmol, 1 eq.) was added to 5 ml of a cold (-20 °C) aqueous HBF_4 (25% w/w) solution. Following, a cold (-20 °C) solution of Sodium Nitrite (3.3 mmol, 1.1 equiv.) in 1 mL of water was slowly added. After 0.5 h the resulting precipitate was filtered and crystallized by acetone/diethyl ether.
The spectroscopic data of benzendiazonium tetrafluoroborates achieved are in accordance with the literature.

*Synthesis of isochromanones of general formula **2.38** under batch conditions*

A solution of the appropriate benzendiazonium tetrafluoroborate of general formula ***2.1*** (1 mmol, 1 eq.) and $Ru(bpy)_3Cl_2$ (0.005 eq.) in MeCN (4 mL, 0.25 M with respect to the diazonium salt) was added with alkene of general formula ***2.37*** (2 mmol, 2 eq. in a glass vial (d= 1.2 cm). The vial was exposed to the light generated by 440 nm LED bulbs for 6–8 hours. The solution was transferred into a round-bottomed flask, evaporated, and the crude was subsequently purified by column chromatography (PE/EA mixtures) to afford the final products as white solids/foams.

*Synthesis of isochromanones of general formula **2.38** under flow conditions*

Reactions in flow conditions were performed by means of a handmade mesoflow reactor consisting of a FEP tubing (internal d = 0.8 mm) wrapped up a glass cylinder (d = 2.5 cm) for a length corresponding exactly of 1 mL. The tube was equipped at one end with a connection for a gastight syringe (10 mL), fitting in a syringe pump. The wrapped cylinder was fitted inside a plastic cylinder (d = 4.5 cm) covered inside with LED bulbs (440 nm, model of the stripe).

A solution of benzendiazonium tetrafluoroborate of general formula ***2.1*** (1 eq.) and $Ru(bpy)_3Cl_2$ (0.005 eq.) in MeCN (0.13 M with respect to the diazonium salt) was added with alkene of general formula ***2.37*** (2 eq.). The resulting clear solution was collected inside a 10 mL gastight syringe and pumped inside the flow reactor by means of a syringe pump at 0.1 mL/h. A fixed volume of the reacted solution was collected in a shielded round-bottomed flask, evaporated, and purified by column chromatography (PE/EA mixtures) to afford the final products as white solids/foams.

*Synthesis of isobenzofuranones of general formula **2.59** and benzoxazepinones of general formula **2.60** under batch conditions*

A solution of benzendiazonium tetrafluoroborate of general formula ***2.1*** (1 mmol, 1 eq.) and $Ru(bpy)_3Cl_2$ (0.005 eq.) in MeCN (4 mL, 0.25 M with respect to the diazonium salt) was added with alkene of general formula 2.37 (1.2 mmol, 1.2 eq.) in a glass vial (d = 1.2 cm). The vial was exposed to the light generated by 440 nm LED bulbs for 6–8 hours. The solution was transferred into a round-bottomed flask, evaporated, and the crude was subsequently purified by column chromatography (PE/EA mixtures) to afford the final products as white solids/foams.

*Synthesis of isobenzofuranones of general formula **2.59** and benzoxazepinones of general formula **2.60** under flow conditions*

The same conditions applied for the synthesis of of general formula ***2.38*** were applied.

Analytical data

Methyl 7-chloro-3-methyl-1-oxoisochroman-3-carboxylate (***2.42h***)

White solid, m.p.= 82.9-84.2°C
R_f = 0.22 (PE:EA=4:1)
^{1}H NMR ($CDCl_3$, 300 MHz) δ: 8.01 (d, J = 2.2, 1H Ar), 7.46 (dd, J = 8.2, 2.2, 1H Ar), 7.16 (d, J = 8.2, 1H Ar), 3.60 (s, 3H), 3.35 (d, J = 16.5, 1H), 3.16 (d, J = 16.5, 1H), 1.73 (s, 3H).
^{13}C NMR ($CDCl_3$, 75 MHz) δ: 171.94, 163.12, 134.59, 134.14, 134.09, 129.87, 129.10, 126.09, 82.12, 53.24, 36.53, 24.96.
HPLC-MS: 13.0 min, 257 (255) $[M+H]^+$.
GC-MS: 7.2 min, 256 (2, M, ^{37}Cl), 254 (6, M, ^{35}Cl), 197 (30, ^{37}Cl), 195 (30, ^{35}Cl), 169 (12, ^{37}Cl), 167 (40, ^{35}Cl), 124 (11), 89 (25), 63 (13), 43 (73).

7-Chloro-3-phenylisochroman-1-one (***2.42c***)

White solid, m.p.= 139.2-141.5°C
R_f = 0.44 (PE:EA=4:1)
^{1}H NMR ($CDCl_3$, 300 MHz) δ: 8.12 (d, J = 2.1, 1H), 7.53 (dd, J = 8.1, 2.1, 1H), 7.49 – 7.35 (m, 5H), 7.24 (d, J = 8.3, 1H), 5.53 (dd, X part of ABX system, J = 12.3, 3.1, 1H), 3.30 (dd, A part of ABX system, J = 16.5, 12.3, 1H), 3.13 (dd, B part of ABX system, J = 16.5, 3.1, 1H).
^{13}C NMR ($CDCl_3$, 75 MHz) δ: 164.23, 138.24, 137.28, 134.07, 134.02, 130.31, 128.99, 128.94, 128.88, 126.72, 126.21, 80,12, 35.09.
HPLC-MS: 13.5 min, 261 (259) $[M+H]^+$.

GC-MS: 9.2 min, 260 (2, M, ^{37}Cl), 258 (5, M, ^{35}Cl), 154 (29, ^{37}Cl), 152 (100,^{35}Cl), 126 (9, ^{37}Cl), 124 (29, ^{35}Cl), 89 (23).

Methyl 3-methyl-1-oxoisochroman-3-carboxylate (***2.42e***)

White solid, m.p.= 99.5-101.3°C
R_f = 0.29 (PE:EA=4:1)

^1H NMR ($CDCl_3$, 300 MHz) δ: 8.04 (d, J = 7.6, 1H Ar), 7.50 (td, J = 7.6, 1.2, 1H Ar), 7.35 (t, J = 7.6, 1H Ar), 7.19 (d, J = 7.6, 1H Ar), 3.58 (s, 3H), 3.38 (d, J = 16.4, 1H), 3.20 (d, J = 16.4, 1H), 1.73 (s, 3H).
^{13}C NMR ($CDCl_3$, 75 MHz) δ: 172.28, 164.31, 136.33, 134.13, 130.16, 128.20, 127.57, 124.57, 82.02, 53.12, 37.07, 25.09.
HPLC-MS: 11.7 min, 221 $[M+H]^+$.
GC-MS: 6.5 min, 220 (2, M), 162 (11), 161 (100), 133 (64), 105 (14), 91 (11), 90 (24), 89 (22), 63 (11), 43 (45).

3-Phenylisochroman-1-one (***2.42a***)

White solid, m.p.= 83.8-85-7°C
R_f = 0.55 (PE:EA=4:1)

^1H NMR ($CDCl_3$, 300 MHz) δ: 8.16 (d, J = 7.8, 1H Ar), 7.57 (td, J = 7.5, 1.0, 1H Ar), 7.49-7.35 (m, 6 H Ar), 7.29 (d, J = 7.6, 1H Ar), 5.56 (dd, X part of ABX system, J = 11.9, 4.6, 1 H), 3.35 (dd, A part of ABX system, J = 15.8, 11.9, 1 H), 3.13 (dd, B part of ABX system, J = 15.8, 4.6, 1H).
^{13}C NMR ($CDCl_3$, 75 MHz) δ: 165.46, 139.05, 138.66, 134.05, 130.55, 128.81, 128.78, 128.01, 127.48, 126.24, 125.24, 80.09, 35.74.
HPLC-MS: 12.8 min, 225 $[M+H]^+$.
GC-MS: 8.4 min, 224 (9, M), 178 (6), 119 (18), 118 (100), 90 (68), 89 (26), 77 (13), 63 (10), 51 (12).

Methyl 3,5-dimethyl-1-oxoisochroman-3-carboxylate (***2.42g***)

White solid, m.p.= 69.8-72.4°C
R_f = 0.30 (PE:EA=4:1)

^1H NMR ($CDCl_3$, 300 MHz) δ: 7.95 (d, J = 7.7, 1H Ar), 7.38 (d, J = 7.7, 1H Ar), 7.27 (t, J = 7.7, 1H Ar), 3.61 (s, 3H), 3.47 (d, J = 16.6, 1H), 2.99 (d, J = 16.6, 1H), 2.31 (s, 3H), 1.77 (s, 3H).
^{13}C NMR ($CDCl_3$, 75 MHz) δ: 172.63, 164.75, 135.50, 135.49, 135.11, 128.08, 127.60, 124.62, 81.56, 53.20, 34.23, 25.37, 19.00. HPLC-MS (ESI+): 13.6 min, 235 $[M+H]^+$.
GC-MS: 6.8 min, 234 (4, M), 175 (100), 147 (39), 105 (10), 104 (11), 103 (12) 78 (11), 77 (13), 43 (28).

5-Methyl-3-phenylisochroman-1-one (***2.42d***)

White solid, m.p.= 137.1-139.4 °C
R_f = 0.60 (PE:EA=4:1)

^{1}H NMR ($CDCl_3$, 300 MHz) δ: 8.03 (dd, J = 7.7, 0.6, 1H Ar), 7.52-7.26 (m, 7H Ar), 5.52 (dd, J = 9.8, 5.6, 1H), 3.14 (m, 2H), 2.33 (s, 3H).
^{13}C NMR ($CDCl_3$, 75 MHz) δ: 165.87, 138.95, 137.66, 135.42, 135.25, 128.83, 128.80, 128.41, 127.40, 126.31, 125.22, 79.53, 33.00, 19.04.
HPLC-MS: 14.4 min, 239 $[M+H]^+$.
GC-MS: 9.0 min, 238 (2, M), 132 (100), 104 (33), 103 (13), 78 (15), 77 (16).

Methyl 3,7-dimethyl-1-oxoisochroman-3-carboxylate (***2.42f***)

Foam
R_f = 0.19 (PE:EA=5:1)

^{1}H NMR ($CDCl_3$, 300 MHz) δ: 7.86 (s, 1H Ar), 7.30 (dd, J = 7.7, 1.4, 1H Ar), 7.08 (d, J = 7.7, 1H Ar), 3.58 (s, 3H), 3.33 (d, J = 16.3, 1H), 3.15 (d, J = 16.3, 1H), 2.34 (s, 3H), 1.72 (s, 3H).
^{13}C NMR ($CDCl_3$, 75 MHz) δ: 172.40, 164.58, 138.08, 134.96, 133.35, 130.39, 127.44, 124.33, 82.09, 53.08, 36.76, 25.07, 21.08. HPLC-MS: 12.2 min, 235 $[M+H]^+$.
GC-MS: 6.9 min, 234 (7, M), 175 (100), 147 (51), 104 (15), 103 (12), 78 (11), 77 (13) 43 (28).

7-Methyl-3-phenylisochroman-1-one (***2.42b***)

White solid, m.p.= 129.5-131.4°C
R_f = 0.35 (PE:EA=6:1)

^{1}H NMR ($CDCl_3$, 300 MHz) δ: 7.97 (s, 1H Ar), 7.50-7.36 (m, 6H Ar), 7.18 (d, J = 7.7, 1H Ar), 5.53 (dd, X part of ABX system, J = 12.2, 2.8, 1H), 3.29 (dd, A part of ABX system, J = 18.0, 12.2, 1H), 3.10 (dd, B part of ABX system, J = 18.0, 2.8, 1H), 2.41 (s, 3H).
^{13}C NMR ($CDCl_3$, 75 MHz) δ: 165.72, 138.81, 137.90, 136.12, 134.92, 130.78, 128.78, 128.72, 127.36, 126.25, 125.01, 80.20, 35.39, 21.18.
HPLC-MS: 13.4 min, 239 $[M+H]^+$.
GC-MS: 8.9 min, 238 (28, m), 178 (19), 132 (100), 104 (100), 78 (23), 77 (34).

Methyl 7-bromo-3-methyl-1-oxoisochroman-3-carboxylate (***2.42i***)

White solid, m.p.= 87.0-88.9°C R_f = 0.34 (PE:EA=4:1)

^{1}H NMR ($CDCl_3$, 300 MHz) δ: 8.20 (d, J = 2.1, 1H Ar), 7.63 (dd, J = 8.1, 2.1, 1H Ar), 7.10 (d, J = 8.1, 1H Ar), 3.62 (s, 3H), 3.35 (d, J = 16.7, 1H), 3.15 (d, J = 16.7, 1H), 1.75 (s, 3H).
^{13}C NMR ($CDCl_3$, 75 MHz) δ: 172.02, 163.05, 137.04, 135.08, 132.98, 129.31, 126.34, 121.95, 82.12, 53.35, 36.67, 25.08.

HPLC-MS: 15.3 min, 301 (299) $[M+H]^+$.
GC-MS: 7.8 min, 300 (9, M, ^{81}Br), 298 (9, M, ^{79}Br), 241 (88), 239 (90), 213 (31), 211 (33), 170 (11), 168 (11), 132 (24), 89 (43), 43 (100).

7-Bromo-3-phenylisochroman-1-one (***2.42m***)

White solid, m.p.= 141.5-143.3°C
R_f = 0.16 (PE:EA=10:1)

^1H NMR ($CDCl_3$, 300 MHz) δ: 8.28 (d, J = 2.0, 1H Ar), 7.68 (dd, J = 8.2, 2.2, 1H Ar), 7.48-7.37 (m, 5H Ar), 7.18 (d, J = 8.2, 1H Ar), 5.55 (dd, X part of ABX system, J = 12.3, 2.7, 1H), 3.28 (dd, A part of ABX system, J = 16.5, 12.3, 1H), 3.12 (dd, B part of ABX system, J = 16.5, 2.7, 1H).
^{13}C NMR ($CDCl_3$, 75 MHz) δ: 164.11, 138.20, 137.76, 136.95, 133.28, 129.21, 128.95, 128.88, 126.94, 126.20, 121.67, 80.06, 35.16.
HPLC-MS: 16.2 min, 305 (303) $[M+H]^+$.
GC-MS: 9.7 min, 304 (7, M, ^{81}Br), 302 (7, M, ^{79}Br), 198 (94, ^{81}Br), 196 (100, ^{79}Br), 170 (26, ^{81}Br), 168 (27, ^{79}Br), 89 (41), 77 (14), 63 (18).

trans 3,4-Diphenylisochroman-1-one (***2.42l***)

White solid, m.p.= 135.1-137.2°C
R_f = 0.43 (PE:EA=6:1)

^1H NMR ($CDCl_3$, 300 MHz) δ: 8.24 (dd, J = 7.4, 1.7, 1H Ar), 7.50 (td, J = 7.4, 1.7, 1H Ar), 7.47-7.41(m, 1H Ar), 7.27-7.14 (m, 8H Ar), 7.03-7.00 (m, 2H Ar), 6.92 (d, J = 7.4,1H Ar), 5.64 (d, J = 10.0, 1H), 4.51 (d, J = 10.0, 1H).
^{13}C NMR ($CDCl_3$, 75 MHz) δ: 165.06, 142.67, 137.93, 137.42, 134.20, 130.44, 129.71, 128.94, 128.58, 128.30, 128.15, 127.98, 127.80, 127.20, 125.17, 85.40, 51.11.
HPLC-MS: 18.1 min, 301 $[M+H]^+$.
Decomposes during GC-MS analysis

3-(4-Methoxybenzyl)isobenzofuran-1(3H)-one)(***2.59a***)

Foam
R_f = 0.40 (PE:EA=4:1)

^1H NMR ($CDCl_3$, 300 MHz) δ: 7.84 (d, J = 7.5, 1H Ar), 7.60 (td, J = 7.5, 1.1, 1H Ar), 7.48 (t, J = 7.5, 1H Ar), 7.17 (dd, J = 7.5 Hz, 0.8, 1H Ar), 7.13-7.09 (m, 2H Ar), 6.84-6.79 (m, 2H Ar), 5.65 (t, X part of ABX system, J = 6.3, 1H), 3.78 (s, 3H), 3.23 (dd, A part of ABX system, J = 14.1, 6.3, 1H), 3.10 (dd, B part of ABX system, J = 14.1, 6.3, 1H)
^{13}C NMR ($CDCl_3$, 75 MHz) δ: 170.41, 158.81, 149.28, 133.78, 130.87, 129.24, 126.97, 126.42, 125.78, 122.4, 114.03, 81.50, 55.34, 40.03.

HPLC-MS: 13.0 min, 239 $[M+H]^+$.
GC-MS: 9.1 min, 254 (22, M), 133 (19), 121 (100), 78 (12) 77 (25).

3-(4-Methylbenzyl)isobenzofuran-1(3H)-one (***2.59b***)

White solid, m.p.= 87.7-89.4°C
R_f = 0.47 (PE:EA=4:1)

^{1}H NMR ($CDCl_3$, 300 MHz) δ: 7.85 (d, J = 7.6, 1H Ar), 7.60 (td, J = 7.6, 1.2, 1H Ar), 7.49 (t, 7.6, 1H Ar), 7.16 (dd, J = 7.6, 0.8, 1H Ar), 7.10 (s, 4H Ar), 5.67 (t, X part of ABX system, J = 6.4, 1H), 3.26 (dd, A part of ABX system, J = 14.1 ,6.5, 1H), 3.10 (dd, B part of ABX system, J = 14.1, 6.5, 1H), 2.32 (s, 3H).
^{13}C NMR ($CDCl_3$, 75 MHz) δ: 170.47, 149.35, 136.91, 133.80, 131.97, 129.72, 129.38, 129.28, 126.42, 125.82, 122.48, 81.51, 40.58, 21.23.
HPLC-MS: 14.5 min, 239 $[M+H]^+$.
GC-MS: 8.4 min, 238 (5, M), 133 (34), 106 (12), 105 (100), 77 (15).

Methyl 2-((3-oxo-1,3-dihydroisobenzofuran-1-yl)methyl)benzoate (***2.59c***)

White solid, m.p.= 107.8-109.5°C
R_f = 0.36 (PE:EA=4:1)

^{1}H NMR ($CDCl_3$, 300 MHz) δ: 8.03 (dd, J = 8.1, 1.4, 1H Ar), 7.96-7.84 (m, 1H Ar), 7.66 (td, J = 7.5, 1.1, 1H Ar), 7.59-7.44 (m, 3H Ar), 7.40-7.34 (m, 2H Ar), 5.77 (dd, X part of ABX system, J = 9.0, 3.5, 1H), 3.95 (dd A part of ABX system, J = 13.7, 3.5, 1H), 3.94 (s, 3H), 3.12 (dd B part of ABX system, J = 13.7, 9.0, 1H).
^{13}C NMR ($CDCl_3$, 75 MHz) δ: 170.62, 167.86, 149.99, 138.77, 134.03, 133.06, 132.64, 131.30, 129.31, 129.16, 127.52, 126.23, 125.73, 122.67, 82.12, 52.28, 40.65.
HPLC-MS: 13.4 min, 283 $[M+H]^+$.
GC-MS: 9.5 min, 282 (1, M), 250 (6), 149 (11), 133 (100), 105 (13), 77 (21), 51 (11).

3-Methyl-5-(4-methoxybenzyl)benzo[e][1,3]oxazepin-1(5H)-one (***2.60a***)

Foam
R_f = 0.45 (PE:EA=4:1)

^{1}H NMR ($CDCl_3$, 300 MHz) δ: 7.77 (d, J = 7.6, 1H Ar), 7.59 (td, J = 7.6, 1.1, 1H Ar), 7.45 (t, J = 7.6, 1H Ar), 7.19 (dd, J = 7.6, 0.6, 1H Ar), 6.75-6.72 (m, 2H Ar), 6.69-6.66 (m, 2H Ar), 5.42 (dd, X part of ABX system, J = 7.4, 3.1, 1H), 3.74 (s, 3H), 3.47 (dd, A part of ABX system, J = 12.8, 7.4, 1H), 3.19 (dd, B part of ABX system, J = 12.8, 3.1, 1H), 2.66 (s, 3H).
^{13}C NMR ($CDCl_3$, 75 MHz) δ: 171.47, 167.94, 158.64, 145.55, 133.83, 130.81, 130.76, 128.82, 127.17, 125.16, 123.53, 113.73, 60.13, 55.27, 37.65, 25.73.

HPLC-MS: 10.3 min, 296 $[M+H]^+$.
GC-MS: 9.6 min, 295 (3, M), 132 (17), 121 (100), 77 (13), 43 (13).

3-Methyl-5-(4-methylbenzyl)benzo[e][1,3]oxazepin-1(5H)-one (***2.60b***)

White solid, m.p.= 109.1-110.7°C
R_f = 0.52 (PE:EA=4:1)
^{1}H NMR ($CDCl_3$, 300 MHz) δ: 7.77 (d, J = 7.6, 1H Ar), 7.59 (td, J = 7.6, 1.1 Hz, 1H Ar), 7.45 (t, J = 7.6, 1H Ar), 7.18 (d, J = 7.6, 1H Ar), 6.95 (d, J = 8.0, 2H Ar), 6.72 (d, J = 8.0, 2H Ar), 5.44 (d, X part of ABX system, J = 7.6, 2.9, 1H), 3.50 (dd, A part of ABX system, J = 12.8, 7.6, 1H), 3.18 (dd, B part of ABX system, J = 12.8, 2.9, 1H), 2.66 (s, 3H), 2.26 (s, 3H).
^{13}C NMR ($CDCl_3$, 75 MHz) δ: 171.46, 167.95, 145.57, 136.62, 133.80, 132.09, 130.79, 129.65, 129.03, 128.80, 125.12, 123.56, 60.06, 38.11, 25.74, 21.19.
HPLC-MS: 11.8 min, 280 $[M+H]^+$.
GC-MS: 8.9 min, 279 (9, M), 132 (100), 105 (48), 77 (13), 43 (14).

6.3 Generation and exploitation of the acetonyl radical: synthesis and spectral charachterization of compounds

*General Procedure for the synthesis of Silyl Enol Ethersof general formula **3.39***

A solution of the starting ketone (2 mmol, 1 eq.), triethylamine (2 mmol, 1 eq.), dimethyl-tert-butylsilyl chloride (2.5 mmol, 1.25 eq.) in dry hexane (2.5 mL) was prepared under inert atmosphere and magnetic stirring. To this mixture, a solution of sodium iodide (3.1 mmol, 1.55 eq.) in dry MeCN (3 mL) was slowly added by means of a dropping funnel in a time range of 15 minutes. After 12 hours, the white precipitate was decanted and the crude was extracted with hexane-MeCN. The hexane phase was washed with brine, dried over sodium sulfate, evaporated under reduced pressure and quickly filtered on silica (PE with 1% triethylamine). The obtained silyl enol ethers of general formula ***3.39*** were employed as substrates for batch and flow reactions without further purification.

General Procedure for batch reactions (Visible Light Photoredox Catalyzed Radical Acetonylation reaction)

A solution of arenediazonium tetrafluoroborate of general formula ***3.1*** (0.25 mmol, 0.01 M), $Ru(bpy)_3Cl_2$ (1 mol%) and radical trap (0.25 mmol, 1 eq. in case of alkenes and alkines or 0.5 mmol, 2 eq. in case of silyl enol ethers of general formula ***3.39***) in 25 mL of acetone was prepared under magnetic stirring and inert atmosphere inside a closed vial. Visible light irradiation was performed by means of 440 nm blue LED lamps. The reaction was typically run overnight, then the crude was evaporated under reduced pressure and purified by flash column chromatography (PE/EA

mixture) affording the pure products. Reactions employing acetone-d6 were performed on a 0.01 mmol scale (1 mL of acetone).

General Procedure for flow reactions (Visible Light Photoredox Catalyzed Radical Acetonylation reaction)

A solution of arenediazonium tetrafluoroborate of general formula ***3.1*** (0.25 mmol, 0.01 M), $Ru(bpy)_3Cl_2$ (1 mol%) and radical trap (0.25 mmol, 1 eq. or 0.5 mmol, 2 eq. in case of silyl of general formula ***3.39***) in 25 ml of acetone was prepared under magnetic stirring and inert atmosphere inside a closed vial. The solution was then charged in a Hamilton gastight syringe (25 mL) and flown through our house-made mesoflow apparatus equipped with 440 nm blue LEDs via a syringe pump (1 to 10 mL·h–1). The solution was collected inside a flask, evaporated under reduced pressure and purified by flash column chromatography (PE/EA mixture) to afford the pure products. Reactions employing acetone-d_6 were performed on a 0.05 mmol scale (5 mL of solvent).

Analytical data

*3-(3-oxobutyl)isobenzofuran-1(3H)-one **3.4***

Colorless oil
^{1}H NMR ($CDCl_3$, 300 MHz) δ: 7.90 (d, J = 7.6 Hz, 1H), 7.69 (t, J = 7.5 Hz, 1H), 7.54 (t, J = 7.5 Hz, 1H), 7.48 (d, J = 7.6 Hz, 1H), 5.52 (dd, J = 2.7 Hz, 8.6, 1H), 2.81-2.69 (m, 1H), 2.60-2.42 (m, 2H), 2.15 (s, 3H), 1.90-1.80 (m, 1H).
^{13}C NMR ($CDCl_3$, 75 MHz) δ: 207.4, 170.3, 149.5, 134.2, 129.3, 125.9, 125.7, 121.9, 80.1, 38.3, 30.1, 28.4.

*3-(3-oxo-2,2,4,4,4-pentadeuterobutyl)isobenzofuran-1(3H)-one **3.14***

Colorless oil
^{1}H NMR ($CDCl_3$, 300 MHz) δ: 7.90 (dt, J = 1.0, 7.6 Hz, 1H), 7.69 (td, J = 1.0, 7.5 Hz, 1H), 7.54 (tt, J = 0.8, 7.5 Hz, 1H), 7.47 (ddd, J = 0.8, 1.7, 7.6 Hz, 1H), 5.52 (dd, J = 3.2, 8.8 Hz, 1H), 2.47 (dd, J = 3.2, 14.6 Hz, 1H), 1.85 (dd, J = 8.8, 14.6 Hz, 1H).
^{13}C NMR ($CDCl_3$, 75 MHz) δ: 207.6, 170.3, 149.5, 134.2, 129.3, 125.9, 125.8, 121.9, 80.1, 38.1(broad), 29.7(broad), 28.3.
HRMS (ESI^+): calculated for $C_{12}H_8D_5O_3^+$ = 210.1173; found = 210.1185.
GC-MS: 6.67 min, 209 (10, M), 163 (11), 147 (100), 133 (77), 105 (30), 77 (39), 76 (12), 63 (10), 46 (30), 40 (22).

*4-Methoxybenzyl benzoate **3.12a***

Colorless oil
^{1}H NMR ($CDCl_3$, 300 MHz) δ: 8.08-8.04 (m, 2H), 7.58-7.51 (m, 1H), 7.46-7.37 (m, 4H), 6.94-6.89 (m, 2H), 5.30 (s, 2H), 3.81 (s, 3H).
^{13}C NMR ($CDCl_3$, 75 MHz) δ: 166.5, 159.6, 132.9, 130.3, 130.0, 129.6, 128.3, 128.2, 114.0, 66.5, 55.3.

4-(Methoxy)benzyl 2-deuterobenzoate ***3.16***

Colorless oil
^{1}H NMR ($CDCl_3$, 300 MHz) δ: 8.07-8.03 (m, 1H), 7.58-7.52 (m, 1H), 7.45-7.38 (m, 4H), 6.93-6.89 (m, 2H), 5.30 (s, 2H), 3.82 (s, 3H).
^{13}C NMR ($CDCl_3$, 75 MHz) δ: 166.5, 159.6, 132.9, 130.2, 130.0, 129.6, 128.3, 128.2, 114.0, 66.5, 55.3.
HRMS (ESI^+): calculated for $C_{15}H_{14}DO_3^+$ = 244.1078; found = 244.1090.
GC-MS: 9.47 min, 243 (100, M), 134 (15), 122 (100), 105 (79), 104 (78), 89 (32), 76 (65), 50 (19).

1,3-dimethyl-3-(3-oxobutyl)indolin-2-one ***3.22a***

Pale yellow oil
^{1}H NMR ($CDCl_3$, 300 MHz) δ: 7.29 (t, J = 7.6 Hz, 1H), 7.16 (d, J = 7.3 Hz, 1H), 7.07 (t, J = 7.4 Hz, 1H), 6.87 (d, J = 7.7 Hz, 1H), 3.23 (s, 3H), 2.28-2.05 (m, 3H), 1.98 (s, 3H), 1.93 (dd, J = 10.3, 5.4 Hz, 1H), 1.38 (s, 3H)
^{13}C NMR ($CDCl_3$, 75 MHz) δ: 207.62, 180.1, 143.1, 133.2, 128.0, 122.7, 122.6, 108.0, 47.3, 38.5, 31.7, 29.8, 26.1, 23.6.

3-(2-oxopropyl)-4-phenyl-2H-chromen-2-one ***3.36***

Yellow oil
^{1}H NMR ($CDCl_3$, 300 MHz) δ: 7.54-7.48 (m, 4H), 7.38 (d, J = 8.1 Hz, 1H), 7.28-7.24 (m, 2H), 7.18-7.14 (m, 1H), 7.03 (d, J = 7.4 Hz, 1H), 3.50 (s, 2H), 2.18 (s, 3H).
^{13}C NMR ($CDCl_3$, 75 MHz) δ: 204.7, 161.6, 153.0, 152.9, 134.2, 131.2, 129.0, 128.9, 128.1, 127.4, 124.2, 121.0, 120.4, 116.7, 43.1, 30.2

1-Phenylpentane-1,4-dione ***3.40***

Colorless oil
^{1}H NMR ($CDCl_3$, 300 MHz) δ: 8.00-7.96 (m, 2H), 7.58-7.52 (m, 1H), 7.49-7.43 (m, 2H), 3.28 (t, J = 6.3 Hz, 2 H), 2.88 (t, 6.3 Hz, 2H), 2.25 (s, 3H).
^{13}C NMR ($CDCl_3$, 75 MHz) δ: 207.3, 198.5, 136.6, 133.1, 128.6, 128.0, 37.0, 32.4, 30.1

2-Methyl-1-phenylpentane-1,4-dione ***3.44***

colorless oil
^{1}H NMR ($CDCl_3$, 300 MHz) δ: 7.98 (dd, J = 5.2, 3.3 Hz, 2H), 7.61-7.52 (m, 1H), 7.51-7.42 (m, 2H), 3.97 (dqd, J = 14.4, 7.2, 5.1 Hz, 1H), 3.17 (dd, J = 18.0, 8.5 Hz, 1H), 2.55 (dd, J = 18.0, 5.0 Hz, 1H), 2.18 (s, 3H), 1.19 (d, J = 7.2 Hz, 3H);
^{13}C NMR ($CDCl_3$, 75 MHz) δ: δ 207.2, 203.4, 136.1, 133.1, 128.8, 128.6, 47.0, 36.3, 30.2, 17.9

2-Benzyl-4-oxopentanal ***3.45***

Colorless oil
^{1}H NMR ($CDCl_3$, 300 MHz) δ: 9.80 (s, 1H), 7.34-7.29 (m, 3H), 7.17-7.15 (m, 2H), 3.25-3.16 (m, 1H), 3.08 (dd, *J* = 13.8, 6.4 Hz, 1H), 2.83 (dd, *J* = 18.0, 8.0 Hz, 1H), 2.70 (dd, *J* = 13.8, 8.0 Hz, 1H), 2.44 (dd, *J* = 18.1, 5.0 Hz, 1H), 2.13 (s, 3H).
^{13}C NMR ($CDCl_3$, 75 MHz) δ: 206.4, 202.7, 137.9, 129.0, 128.7, 126.7, 48.3, 41.7, 34.5, 30.0

Acetylcyclohexanone ***3.46***

Colorless oil
^{1}H NMR ($CDCl_3$, 300 MHz) δ: 3.00-2.88 (m, 2H), 2.40-2.31 (m, 2H), 2.18 (s, 3H), 2.18-2.02 (m, 3H), 1.89-1.61 (m, 3H), 1.42-1.29 (m, 1H).
^{13}C NMR ($CDCl_3$, 75 MHz) δ: 211.5, 207.3, 46.4, 43.2, 41.8, 34.0, 30.4, 27.8, 25.3.

(2R,4S*)-4-tert-Butyl-2-(2-oxopropyl)cyclohexane-1-one* **3.47**

Colorless oil
^{1}H NMR ($CDCl_3$, 300 MHz) δ: 9.80 (s, 1H), 7.34-7.29 (m, 3H), 7.17-7.15 (m, 2H), 3.25-3.16 (m, 1H), 3.08 (dd, *J* = 13.8, 6.4 Hz, 1H), 2.83 (dd, *J* = 18.0, 8.0 Hz, 1H), 2.70 (dd, *J* = 13.8, 8.0 Hz, 1H), 2.44 (dd, *J* = 18.1, 5.0 Hz, 1H), 2.13 (s, 3H).
^{13}C NMR ($CDCl_3$, 75 MHz) δ: 206.4, 202.7, 137.9, 129.0, 128.7, 126.7, 48.3, 41.7, 34.5, 30.0

(2R,4R*)-4-tert-Butyl-2-(2-oxopropyl)cyclohexane-1-one* ***3.47b***

Colorless oil
^{1}H NMR ($CDCl_3$, 300 MHz) δ: 3.00-2.93 (m, 2H), 2.41-2.36 (m, 2H), 2.20 (s, 3H), 2.18-2.02 (m, 4H), 1.65 (tt, *J* = 12.2, 3.0 Hz, 1H), 1.49-1.38 (m, 1H), 0.90 (s, 9H).
^{13}C NMR ($CDCl_3$, 75 MHz) δ: 211.9, 207.4, 46.9, 45.6, 43.3, 41.1, 35.0, 32.4, 30.5, 28.6, 27.6.

tert-butyl 4-oxo-3,4-dihydropyridine-1(2H)-carboxylate ***3.48***

Colorless oil
^{1}H NMR ($CDCl_3$, 300 MHz) δ: 7.80 (brs, 1H), 5.28 (d, J = 7.9 Hz, 1H), 3.96 (t, J = 7.4 Hz, 2H), 2.53 (t, J = 7.4 Hz, 2H), 1.48 (s, 9H) 1.53 (s, 9H).
^{13}C NMR ($CDCl_3$, 75 MHz) δ: 193.6, 144.0, 106.72, 83.5, 42.3, 41.2, 35.7, 28.0

6.4 The sililative ketene three-component reaction (S-K3CR): synthesis and spectral charachterization of compounds

Synthesis of diazoketones of general formula ***4.12***

A solution of diazomethane (14.3 mmol, 1.1 eq., 0.22 M, 65 mL) was added to a suspension of CaO (18.2 mmol, 1.4 eq.) in Et_2O (80 mL) in a 250 mL flask. The flask was chilled to 0°C in ice bath and then a solution of the acyl chloride (13 mmol, 1 eq.) in Et_2O (40 mL) was slowly added through a dripping funnel. The reaction was left proceeding overnight and checked by TLC. The solution was filtered under vacuum over Celite, the solvent evaporated and the crude purified by flash chromatography (PE/EA mixture).

Synthesis of silanols ***4.16-4.16d***

An aqueous solution of ammonia (10%v/v, 40 mL)was added to a solution of silyl chloride (24 mmol, 1 eq.) in THF (20 mL). The reaction proceeded overnight; the crude was extracted with DCM, washed with HCl 1N and brine and eventually dried over anhydrous sodium sulfate. Evaporation of the solvent afforded the pure product except for triphenylsilanol which was further purified by crystallization from a boiling PE/Et20 9:1 mixture.

Synthesis of α-silyloxyacrylamides of general formula ***4.17***

The respective diazoketone of general formula ***4.12*** (0.3 mmol, 1 eq.), the respective additive (0.03-0.3 mmol, 0.1-1 eq.) and the respective silanol (0.3 mmol, 1 eq.) were added to a glass or quartz vial under argon atmosphere. After addition of the solvent (acetone or toluene, 3 mL) and complete dissolution, the respective isocyanide (0.3 mmol, 1 eq.) was added and the vial was sealed with a rubber septum. The vial was exposed to the light generated by the Rayonet apparatus equipped with proper lamps for 6-28 hours. After a TLC check (PE/EA mixture, UV/Hanessian stain) for the complete consumption of the starting diazoketone, the solvent was evaporated and the crude analyzed by NMR for the E:Z ratio determination. The crude was eventually purified by flash chromatography (with silica or Florisil).

*Mannich reaction of α-silyloxyacrylamide **4.17a** with Eschenmoser's Salt*

A solution of α-silyloxy acrylamide ***4.17a*** (0.10 mmol, 1 eq.) and Eschenmoser's Salt (0.12 mmol, 1.2 eq.) in dry DCM (2 mL) in a 10 mL flask under argon was chilled at -78°C in an acetone/$CO_{2(s)}$ bath. A solution of TBAF 1M in Et_2O (0.12 mL, 1.2 eq.) was added to the flask dropwise; after 15 minutes the reaction was quenched with saturated NH_4Cl (5 mL), then extracted with DCM, dried over anhydrous sodium sulfate. The crude was further purified by flash chromatography (PE/EA mixture). Compound ***4.22*** was achieved with 83% yield.

*Saegusa oxidation of α-silyloxy acrylamide **4.17c***

An excess of $Pd(OAc)_2$ (0.18 mmol, 1.4 eq.) was added to a solution of silyloxy acrylamide ***4.17c*** (0.13 mmol, 1 eq.) in MeCN (5 mL) under argon atmosphere. The reaction went to completion overnight and was checked via TLC (PE/EA mixture); the solvent was evaporated and the crude purified by means of a flash chromatography (PE/EA mixture). Compound ***4.23*** was achieved with 60% yield.

*Michael-Aldol addition of butanone to α-silyloxyacrylamide **4.17a***

A solution of α-silyloxy acrylamide ***4.17a*** (0.07 mmol, 1 eq.) and butenone (0.35 mmol, 5 eq.) in dry THF (2 mL) in a 10 mL flask under argon was chilled at -20°C. A solution of TBAF 1M in THF (0.09 mmol, 1.2 eq.) was slowly added; after 30 minutes the reaction was quenched with $NaHCO_3$(aq)(5 mL), then extracted with DCM, dried over anhydrous sodium sulfate. The crude was further purified by flash chromatography (PE/EA mixture). Compound ***4.25*** was achieved with 30% yield.

*Dimerization of α-silyloxyacrylamide **4.17a***

Same procedure as before, without addition of butenone. Compound ***4.26*** was achieved with 69% yield.

*Decarboxylative cyclization of α-silyloxyacrylamide **4.17a**/**4.17e** with L-Proline*

The α-silyloxyacrylamide **4.17a** or **4.17e** (0.14 mmol, 1 eq.) and L-Proline (0.17 mmol, 1.2 eq) were added to a high-pressure vial and dissolved in 2-propanol (2 mL). The vial was sealed and the reaction carried out overnight at 110°C. After a TLC check (PE/EA mixture) the solvent was removed by evaporation and the crude purified via flash chromatography (PE/EA mixture) affording the product (***4.27***, 69% yield; ***4.38***, 66% yield) as an oil.

*Paternò-Buchi [2+2] cycloaddition of α-silyloxyacrylamide **4.17a** with benzaldehyde under flow conditions*

The reaction was performed in a flow system consisting of a handmade coil of FEP tubing (internal d= 0.8 mm) wrapped up a glass cylinder (d= 2.5 cm) for a length corresponding
to the volume of 2 mL placed inside the Rayonet apparatus. An external loading loop of 3 mL volume was connected to a gastight syringe (10 mL), fitting in a syringe pump. A solution of the α-silyloxy acrylamide ***4.17a*** (0.12 mmol, 1 eq.) and benzaldehyde (0.12 mmol, 1 eq.) in MeCN (3 mL) was loaded in the 3 mL loop and injected via syringe pump at 0.5 mL/h, with the gastight syringe being loaded with MeCN. The eluted solution was collected in a vial, the solvent removed by evaporation and the crude purified via flashchromatography (PE/EA mixture). Compound ***4.31*** was achieved with 40% yield.

*Visible light photoredox catalyzed radical acetonylation of α-silyloxyacrylamides **4.17a** and **4.17d** under flow conditions*

A solution of arenediazonium tetrafluoroborate ***4.32*** (0.25 mmol, 0.01 M), $Ru(bpy)_3Cl_2$ (1 mol%) and α-silyloxyacrylamide (***4.17a*** or ***4.17d***; 0.25 mmol) in 25 ml of acetone was prepared under magnetic stirring and inert atmosphere inside a closed vial. The solution was then charged in a Hamilton gastight syringe (25 mL) and flown through our house-made mesoflow apparatus equipped with 440 nm blue LEDs via a syringe pump (3 mL·h–1). The solution was collected inside a flask, evaporated under reduced pressure and purified by flash column chromatography (PE/EA mixture) to afford the pure products. Compound ***4.33*** was achieved with 75% yield while compound ***4.34*** was achieved with 59% yield.

Synthesis of α-silyloxyacrylamide **4.17a** *followed by one-pot visible light photoredox catalyzed radical acetonylation under flow conditions*

In a glass vial, Benzyldiazoketone ***4.12a*** (0.5 mmol, 1 eq.) and Triphenylsilanol ***4.16a*** (0.5 mmol, 1 eq.) were dissolved under magnetic stirring and inert atmosphere in dry Toluene (2.5 mL). Cyclohexylisocyanide ***4.2a*** (0.5 mmol, 1 eq.) was added to the solution and the sealed vial was then irradiated by means of a Rayonet apparatus equipped with 300 nm UV lamps. The crude solution was then diluted to 50 ml with Acetone before addition of 4-methoxybenzenediazonium tetrafluoroborate ***4.32*** (0.5 mmol, 1 eq.) and $Ru(bpy)_3Cl_2$ (1 mol%). The solution was then charged into a Hamilton 50 mL gastight syringe and flown through our house-made mesoflow apparatus equipped with 440 nm blue LEDs via a syringe pump (3 mL/h). The solution was collected inside a flask, evaporated under reduced pressure and then purified by flash column chromatography (PE/EA) to afford the pure product ***4.33*** as a colorless oil with 40% yield.

*Paal-Knorr synthesis of 1,3-dibenzyl-N-cyclohexyl-5-methyl-1H-pyrrole-2-carboxamide **4.36***

α-silyloxyacrylamide **4.17a** (0.1 mmol, 1 eq.), *N*-benzylamine ***4.35*** (0.1 mmol, 1 eq.) and Acetic Acid (0.1 mmol, 1 eq.) were dissolved in methanol (1.5 mL) under magnetic stirring and inert atmosphere. The mixture was refluxed overnight. The crude was evaporated under reduced pressure and purified by flash column chromatography (PE/EA) to afford the pure product ***4.36*** as a white solid with 59% overall yield.

Analytical data

Analytical data for diazoketones *of general formula **4.12*** are in accordance with the literature[6.3].

Analytical data for silanols ***4.16-4.16d*** are in accordance with the literature[6.4].

*(Z)-N-cyclohexyl-4-phenyl-2-((triphenylsilyl)oxy)but-2-enamide **4.17a***

White solid, m.p. = 99.1-102.3 °C
R_f = 0.30 (PE: Et_2O = 7:3)
^{1}H NMR ($CDCl_3$, 300 MHz) δ: 7.67 [dd, J= 8.0, 1.5 Hz, 6H], 7.54 – 7.38 [m, 9H] 7.19 – 7.07 [m, 3H], 6.82 [dd, J= 7.6, 1.8 Hz, 2H], 6.17 [t, J=7.6 Hz, 1H], 6.16 [d, J=7.6 Hz, 1H], 3.62 – 3.59 [m, 1H], 3.15 [d, J= 7.5 Hz, 2H], 1.61 – 1.49 [m, 5H], 1.30 – 1.12 [m, 2H], 1.04 – 0.84 [m, 1H], 0.63 – 0.36 [m, 2H].
^{13}C NMR ($CDCl_3$, 75 MHz) δ: 162.83, 143.16, 139.47, 135.60, 132.74, 130.86, 128.46 (x2), 128.39, 126.10, 117.90, 47.98, 32.60, 32.34, 25.56, 24.89.
HRMS (ESI+): calculated for $C_{34}H_{36}NO_2Si$ = 518.2510; found = 518.2521.

*(Z)-N-cyclohexyl-3-phenyl-2-((triethylsilyl)oxy)acrylamide **4.17b***

Yellow oil
R_f = 0.67 (PE: EA = 8:2)
^{1}H NMR ($CDCl_3$, 300 MHz) δ: 7.42 – 7.16 [m, 5H], 6.23 [s, 1H], 6.12 [d br, J = 8.1 Hz, 1H], 3.84 – 3.68 [m, 1H], 1.90-1.80 [m, 2H], 1.70 – 1.52 [m, 3H], 1.41 – 0.96 [m, 14H], 0.84 – 0.75 [m, 6H].
^{13}C NMR ($CDCl_3$, 75 MHz) δ: 163.22, 144.34, 134.70, 129.32, 128.01, 127.11, 117.17, 47.83, 32.92, 25.62, 24.86, 6.85, 5.11. HRMS (ESI+): calculated for $C_{21}H_{34}NO_2Si$ = 360.2353; found = 360.2371.

(Z)-N-cyclohexyl-4-phenyl-2-((triethylsilyl)oxy)but-2-enamide ***4.17c***

Yellow oil

R_f = 0.67 (PE:EA = 4:1)

^{1}H NMR ($CDCl_3$, 300 MHz) δ: 7.33 – 7.15 [m, 5H], 6.23 [d br, J = 8.2 Hz, 1H], 6.17 [t, J = 7.6 Hz, 1H], 3.93 – 3.71 [m, 1H], 3.47 [d, J = 7.5 Hz, 2H], 2.02 – 1.90 [m, 2H], 1.79 – 1.58 [m, 3H], 1.49 – 1.30 [m, 2H], 1.22 – 1.10 [m, 3H], 1.07 – 0.98 [m, 9H], 0.76 [qd, J = 7.8, 1.1 Hz, 6H].

^{13}C NMR ($CDCl_3$, 75 MHz) δ: 163.73, 143.84, 139.76, 128.59, 128.52, 126.29, 116.32, 48.23, 33.30, 32.06, 25.65, 25.03, 6.91, 5.41.

HRMS (ESI+): calculated for $C_{22}H_{36}NO_2Si$ = 374.2499; found = 374.2496.

(Z)-N-cyclohexyl-3-phenyl-2-((triphenylsilyl)oxy)acrylamide ***4.17d***

White foam

R_f = 0.35 (PE:Et_2O = 7:3)

^{1}H NMR ($CDCl_3$, 300 MHz) δ: 7.57 – 7.54 [m, 6H], 7.46 – 7.40 [m, 2H], 7.36 – 7.28 [m, 9H], 7.07 – 6.97 [m, 3H], 6.84 [s, 1H], 6.16 [d br, J = 8.2 Hz, 1H], 3.66 – 3.52 [m, 1H], 1.65 – 1.47 [m, 5H], 1.22 – 0.85 [m, 3H], 0.64 – 0.47 [m, 2H].

^{13}C NMR: δ 163.67, 143.18, 135.64, 134.03, 132.72, 130.55, 129.67, 128.15, 128.04, 127.44, 116.77, 48.37, 32.52, 25.55, 24.97.

HRMS (ESI+): calculated for $C_{33}H_{34}NO_2Si$ = 504.2348; found = 504.2367.

(Z)-N-cyclohexyl-3-(4-methoxyphenyl)-2-((triphenylsilyl)oxy)acrylamide **4.17e**

White foam

R_f = 0.41 (PE: EA = 4:1)

^{1}H NMR ($CDCl_3$, 300 MHz) δ: 7.64 – 7.26 [m, 17H], 6.80 [s, 1H], 6.52 [d, J = 8.8 Hz, 2H], 6.13 [d, J = 8.3 Hz, 1H], 3.72 [s, 3H], 3.67 – 3.49 [m, 1H], 1.66 – 1.44 [m, 5H], 1.31 – 1.09 [m, 2H], 1.01 – 0.84 [m, 1H], 0.64 – 0.48 [m, 2H].

^{13}C NMR ($CDCl_3$, 75 MHz) δ: 163.88, 158.96, 141.94, 135.66, 132.87, 131.15, 130.54, 128.15, 126.64, 116.53, 113.48, 55.30, 48.31, 32.55, 25.56, 24.96.

HRMS (ESI+): calculated for $C_{34}H_{36}NO_3Si$ = 534.2459; found = 534.2467.

(S,Z)-tert-butyl (5-(benzylamino)-5-oxo-4-((triphenylsilyl)oxy)pent-3-en-2-yl)carbamate ***4.17f***

Colorless oil
R_f = 0.24 (PE: EA= 4:1)
$[\alpha]_D$ = +20.6 (c 1.0, $CHCl_3$)
^{1}H NMR ($CDCl_3$, 300 MHz) δ: 7.60 [d, J = 8.1 Hz, 6H], 7.49 – 7.41 [m, 3H], 7.39 – 7.32 [m, 6H], 7.28 – 7.15 [m, 3H], 6.96 – 6.87 [m, 2H], 6.52 [s, 1H], 5.86 (d, J = 9.7 Hz, 1H), 4.35 – 3.99 [m, 4H], 1.39 [s, 9H], 0.68 [d, J = 6.4 Hz, 3H].
^{13}C NMR ($CDCl_3$, 75 MHz) δ: 163.78, 154.68, 142.53, 137.70, 135.61, 132.27, 130.89, 128.66, 128.39, 128.05, 127.46, 120.18, 79.25, 43.66, 43.26, 28.53, 20.66.
HRMS (ESI+): calculated for $C_{33}H_{39}N_2O_4Si$ = 579.2674; found = 579.2671.

(Z)-N-(2,6-dimethylphenyl)-4-phenyl-2-((triphenylsilyl)oxy)but-2-enamide ***4.17g***

Pale yellow solid, m.p. = 46.6-48.4°C
R_f = 0.60 (PE: Et_2O = 9:1)
^{1}H NMR ($CDCl_3$, 300 MHz) δ: 7.76 – 7.68 [m, 6H], 7.66 – 7.59 [m, 2H], 7.50 – 7.32 [m, 9H], 7.22 – 7.10 [m, 3H], 7.09 – 6.92 [m, 2H], 6.90 – 6.80 [m, 2H], 6.31 [t, J = 7.5 Hz, 1H], 3.21 [d, J = 7.5 Hz, 2H], 1.92 [s, 6H].
^{13}C NMR ($CDCl_3$, 75 MHz) δ: 162.10, 142.75, 139.26, 135.66, 135.56, 135.47, 135.29, 133.50, 132.82, 130.95, 128.49, 128.14, 127.12, 126.22, 118.71, 32.64, 18.36.
HRMS (ESI+): calculated for $C_{36}H_{34}NO_2Si$ = 540.2353; found = 540.2336.

(Z)-N-butyl-4-phenyl-2-((triphenylsilyl)oxy)but-2-enamide ***4.17h***

White solid, m.p. = 64.3-66.7 °C
R_f = 0.56 (PE: Et_2O = 8:2)
^{1}H NMR ($CDCl_3$, 300 MHz) δ: 7.70 – 7.61 [m, 6H], 7.54 – 7.35 [m, 9H], 7.20 – 7.08 [m, 3H], 6.82 [dd, J = 6.0, 2.2 Hz, 2H], 6.27 – 6.14 [m, 2H], 3.15 [d, J = 7.5 Hz, 2H], 3.06 – 2.95 [m, 2H], 1.14 – 0.98 [m, 4H], 0.84 – 0.70 [m, 3H].
^{13}C NMR ($CDCl_3$, 75 MHz) δ: 163.90, 142.99, 139.42, 135.56, 132.74, 130.89, 128.44, 128.40, 128.06, 126.11, 117.93, 39.17, 32.32, 31.17, 20.06, 13.85.
HRMS (ESI+): calculated for $C_{32}H_{34}NO_2Si$ = 492.2353; found = 492.2356.

(Z)-4-phenyl-N-(tosylmethyl)-2-((triphenylsilyl)oxy)but-2-enamide ***4.17i***

Pale-Yellow oil
R_f = 0.34 (PE: EA = 8:2)
^{1}H NMR ($CDCl_3$, 300 MHz) δ: 7.70 – 7.12 [m, 22H], 6.90 [t, J = 6.9 Hz, 1H],6.83 – 6.75 [m, 2H], 5.98 [t, J = 7.6 Hz, 1H], 4.37 [d, J = 6.9 Hz, 2H], 3.08 [d, J = 7.6 Hz, 2H], 2.38 [s, 3H].
^{13}C NMR ($CDCl_3$, 75 MHz) δ: 163.24, 145.31, 141.53, 138.85, 135.50, 135.29, 132.29, 131.04, 129.96, 128.89, 128.54, 128.48, 128.03, 126.31, 119.99, 60.34, 32.35, 21.86.
HRMS (ESI+): calculated for $C_{36}H_{34}NO_4SSi$ = 604.1972; found = 604.1971.

(Z)-N-cyclohexyl-4-phenyl-2-((triisopropylsilyl)oxy)but-2-enamide ***4.17j***

Yellow oil
R_f = 0.61 (PE: EA = 8:2)
^{1}H NMR ($CDCl_3$, 300 MHz) δ: 7.35 – 7.11 [m, 5H], 6.21 [d br, J = 8.3 Hz, 1H], 6.03 [t, J = 7.5 Hz, 1H], 3.88 – 3.69 [m, 1H], 3.49 [d, J = 7.5 Hz, 2H], 1.96 – 1.64 [m, 4H], 1.50 – 1.20 [m, 9H], 1.15 [d, J = 6.8 Hz, 18H].
^{13}C NMR ($CDCl_3$, 75 MHz) δ: 164.06, 144.55, 139.93, 128.61, 128.57, 126.29, 115.14, 48.37, 33.32, 32.11, 25.67, 25.09, 18.13, 13.82.
HRMS (ESI+): calculated for $C_{25}H_{42}NO_2Si$ = 416.2979; found = 416.2970.

(Z)-2-((tert-butildiphenylsilyl)oxy)-N-cyclohexyl-4-phenylbut-2-enamide ***4.17k***

White foam
R_f = 0.55 (PE: Et_2O= 7:3)
^{1}H NMR ($CDCl_3$, 300 MHz) δ: 7.35 – 7.11 [m, 5H], 6.23 – 6.10 [m, 2H], 3.90 – 3.72 [m, 1H], 3.46 [d, J=7.6 Hz, 2H], 2.03 –1.89 [m, 2H], 1.79 –1.58 [m, 3H], 1.47 –1.30 [m, 2H], 1.27 –1.06 [m, 3H], 1.03 [s, 9H], 0.19 [s, 6H].
^{13}C NMR ($CDCl_3$, 75 MHz) δ: 163.87, 143.48, 139.78, 128.60, 128.55, 126.30, 116.97, 48.27, 33.33, 32.22, 25.94, 25.64, 25.03, 18.42, -3.90.
HRMS (ESI+): calculated for $C_{22}H_{36}NO_2Si$ = 374.2510; found = 374.2516.

3-benzyl-N-cyclohexyl-2-oxobut-3-enamide ***4.22***

White foam
R_f = 0.64 (PE: EA = 4:1)
^{1}H NMR ($CDCl_3$, 300 MHz) δ: 7.37 – 7.14 [m, 5H], 7.02 [s, 1H], 6.71 [s br, 1H], 6.01 [s, 1H], 3.90 – 3.69 [m, 1H], 3.65 [s, 2H], 1.99 – 1.83 [m, 2H], 1.83 – 1.52 [m, 2H], 1.49 – 1.07 [m, 6H].
^{13}C NMR ($CDCl_3$, 75 MHz) δ: 189.16, 160.60, 143.95, 138.46, 134.35, 129.29, 128.63, 126.57, 48.50, 37.81, 32.81, 25.54, 24.85.

HRMS (ESI+): calculated for $C_{17}H_{22}NO_2$ = 272.1645; found = 272.1661.

N-cyclohexyl-2-oxo-4-phenylbut-3-enamide ***4.23***

Yellow solid, m.p. = 92.5-94.1°C
R_f = 0.59 (PE:EA = 4:1)
^{1}H NMR ($CDCl_3$, 300 MHz) δ: 7.94 [d, J = 16.1 Hz, 1H], 7.79 [d, J = 16.2 Hz, 1H], 7.73 – 7.61 [m, 2H], 7.43 [m, 3H], 7.07 [d br, J = 8.5 Hz, 1H], 3.91 – 3.72 [m, 1H], 2.03 – 1.89 [m, 2H], 1.83 – 1.58 [m, 3H], 1.50 – 1.11 [m, 5H].
^{13}C NMR ($CDCl_3$, 75 MHz) δ: 186.02, 160.44, 147.94, 134.56, 131.55, 129.29, 129.15, 118.81, 48.57, 32.86, 25.55, 24.87.

(1R,2R)-2-benzyl-N-cyclohexyl-1-hydroxy-5-oxocyclohexanecarboxamide ***4.25***

R_f = 0.09 (PE:EA = 4:1)
^{1}H NMR ($CDCl_3$, 300 MHz) δ: 7.32 – 7.12 [m, 5H], 6.86 [d, J = 8.5 Hz, 1H], 3.92 – 3.71 [m, 1H], 3.17 [d, J = 14.7 Hz, 1H], 2.82 [s, 1H], 2.77 [dd, J = 13.2, 2.9 Hz, 1H], 2.62 [tt, J = 11.8, 3.8 Hz, 1H], 2.44 – 2.23 [m, 4H], 2.03 – 1.55 [m, 7H], 1.50 – 1.09 [m, 5H].
^{13}C NMR ($CDCl_3$, 75 MHz) δ: 211.07, 172.17, 139.91, 129.36, 128.59, 126.42, 81.48, 51.30, 48.44, 43.64, 40.94, 35.83, 33.37, 33.06, 26.24, 25.61, 24.96, 24.91.
HRMS (ESI+): calculated for $C_{20}H_{28}NO_3$ = 330.2064; found = 330.2061.

(3RS,4RS,5RS)-4-benzyl-N,1-dicyclohexyl-3,5-dihydroxy-2-oxo-5-phenethylpyrrolidine-3-carboxamide ***4.26***

R_f = 0.14 (PE:EA = 4:1)
^{1}H NMR ($CDCl_3$, 300 MHz) δ: 7.34 – 7.06 [m, 8H], 6.89 – 6.80 [m, 2H], 6.68 [d, J = 8.1 Hz, 1H], 4.09 [s, 1H], 3.87 [s, 1H], 3.70 – 3.51 [m, 1H], 3.08 – 2.87 [m, 3H], 2.79 – 2.66 [m, 1H], 2.36 [td, J = 12.6, 4.4 Hz, 1H], 2.22 [td, J = 12.3, 5.4 Hz, 1H], 2.13 – 1.85 [m, 4H], 1.82 – 1.50 [m, 10H], 1.47 – 1.01 [m, 8H].
^{13}C NMR ($CDCl_3$, 75 MHz) δ: 175.65, 167.02, 141.49, 138.95,129.65, 128.54, 128.41, 128.36, 126.54, 125.89, 92.92, 78.41, 55.61, 48.71, 47.96, 36.21, 32.86, 32.69, 30.85, 30.14, 30.03, 28.94, 26.48, 26.29, 25.62, 25.46, 24.84, 24.81.
HRMS (ESI+): calculated for $C_{32}H_{43}N_2O_4$ = 519.3217; found = 519.3232.

*(3R,7aS)-3-benzyl-1-cyclohexyltetrahydro-1H-pyrrolo[1,2-a]imidazol-2(3H)-one **4.27***

Brown oil

R_f = 0.13 (PE: EA = 4:1)

^{1}H NMR ($CDCl_3$, 300 MHz) δ: 7.35 – 7.07 [m, 5H], 4.79 [td, J = 5.8, 1.9 Hz, 1H], 3.76 [tt, J = 12.0, 3.7 Hz, 1H], 3.32 – 3.15 [m, 2H], 2.86 – 2.53 [m, 3H], 2.19 – 2.00 [m, 2H], 1.98 – 1.05 [m, 14H].

^{13}C NMR ($CDCl_3$, 75 MHz) δ: 173.55, 141.98, 128.68, 128.41, 125.88, 78.00, 67.71, 56.01, 52.30, 35.35, 33.85, 32.13, 31.83, 30.42, 25.95, 25.92, 25.61, 24.89.

HRMS (ESI+): calculated for $C_{20}H_{29}N_2O$ = 313.2274; found = 313.2283.

*(3R,7aS)-1-cyclohexyl-3-(4-methoxyphenyl)tetrahydro-1H-pyrrolo[1,2-a]imidazol-2(3H)-one **4.28***

Yellow oil

R_f = 0.10 (PE: EtOAc = 4:1)

^{1}H NMR ($CDCl_3$, 300 MHz) δ: 7.19 [d, J = 8.7 Hz, 2H], 6.79 [d, J = 8.7 Hz, 2H], 4.45 [td, J = 5.9, 2.0 Hz, 1H], 3.77 [s, 3H], 3.72 – 3.54 [m, 1H], 3.42 [ddd, J = 7.6, 3.7, 2.0 Hz, 1H], 3.07 – 2.87 [m, 2H], 2.72 [dd, J = 13.5, 7.6 Hz, 1H], 2.38 [ddd, J = 9.7, 8.8, 6.1 Hz, 1H], 2.10 – 1.91 [m, 1H], 1.89 – 1.49 [m, 7H], 1.47 – 0.98 [m, 6H].

^{13}C NMR ($CDCl_3$, 75 MHz) δ: 172.94, 158.24, 130.91, 130.83, 113.57, 77.94, 70.07, 55.68, 55.37, 52.20, 38.63, 33.72, 31.81, 30.16, 25.93, 25.89, 25.60, 24.76.

HRMS (ESI+): calculated for $C_{20}H_{29}N_2O_2$ = 329.2224; found = 329.2213.

*2-benzyl-N-cyclohexyl-4-phenyl-3-((triphenylsilyl)oxy)oxetane-3-carboxamide **4.31***

R_f = 0.58 (PE: EA = 4:1)

^{1}H NMR ($CDCl_3$, 300 MHz) δ: 7.51 – 7.06 [m, 25H], 5.93 [s, 1H], 5.84 [d br, J = 8.0 Hz, 1H], 5.46 [dd, J = 9.4, 4.7 Hz, 1H], 3.71 – 3.51 [m, 1H], 3.16 [dd, J = 14.2, 9.5 Hz, 1H], 2.60 [dd, J = 14.2, 4.7 Hz, 1H], 1.67 – 1.44 [m, 4H], 1.32 – 1.08 [m, 4H], 0.99 – 0.77 [m, 2H], 0.50 – 0.25 [m, 1H].

^{13}C NMR ($CDCl_3$, 75 MHz) δ: 170.21, 137.08, 137.03, 135.61, 135.42, 134.32, 130.37, 129.29, 128.60, 128.47, 128.18, 127.22, 126.52, 87.10, 85.20, 83.28, 48.57, 38.10, 32.31, 32.05, 25.40, 24.94.

HRMS (ESI+): calculated for $C_{41}H_{42}NO_3Si$ = 624.2928; found = 624.2928.

*3-benzyl-N-cyclohexyl-2,5-dioxohexanamide **4.33***

Colorless oil

^{1}H NMR ($CDCl_3$, 300 MHz) δ: 7.32-7.27 (m, 2H), 7.24-7.19 (m, 3H), 6.78 (d, J = 9.8 Hz, 1H), 4.08 (tt, J = 9.5, 4.4 Hz, 1H), 3.77-3.70 (m, 1H), 3.12 (dd, J = 13.4, 4.8 Hz, 1H), 2.94 (dd, J = 18.5, 10.2

Hz, 1H), 2.63 (dd, J = 18.5, 4.1 Hz, 1H), 2.49 (dd, J = 13.5, 9.4 Hz, 1H), 2.06 (s, 3H), 2.00-1.87 (m, 2H), 1.78-1.60 (m, 3H), 1.42-1.31 (m, 4H), 1.22-1.18 (m, 1H).
^{13}C NMR ($CDCl_3$, 75 MHz) δ: 206.6, 200.2, 158.8, 138.3, 129.1, 128.6, 126.7, 48.5, 44.8, 41.8, 36.6, 32.7, 32.6, 29.4, 25.4, 24.7.
HRMS (ESI+): calculated for $C_{19}H_{26}NO_3^+$ = 316.1907; found = 316.1920

N-cyclohexyl-2,5-dioxo-3-phenylhexanamide ***4.34***

Colorless oil
^{1}H NMR ($CDCl_3$, 300 MHz) δ: 7.30-729 (m, 4H), 7.25-7.22 (m, 1H), 6.73 (d, J = 7.8 Hz, 1H), 5.18 (dd, J = 11.0, 4.0 Hz, 1H), 3.73-3.61 (m, 1H), 3.48 (dd, J = 18.3, 11.0 Hz, 1H), 2.90 (dd, J = 18.3, 3.9 Hz, 1H), 2.15 (s, 3H), 1.99-1.92 (m, 1H), 1.80-1.61 (m, 3H), 1.42-1.09 (m, 6H).
^{13}C NMR ($CDCl_3$, 75 MHz) δ: 206.0, 196.9, 158.4, 135.8, 128.9, 128.7, 127.6, 48.5, 47.6, 45.4, 32.6, 29.4, 25.4, 24.7.
HRMS (ESI+): calculated for $C_{18}H_{24}NO_3^+$ = 302.1751; found = 302.1764

1,3-dibenzyl-N-cyclohexyl-5-methyl-1H-pyrrole-2-carboxamide ***4.36***

White solid, m.p. = 179.5-180.8°C
^{1}H NMR ($CDCl_3$, 300 MHz) δ: 7.34-7.16 (m, 8H), 6.99-6.96 (m, 2H), 5.81 (s, 1H), 5.46 (s, 2H), 5.33 (d, J = 7.8 Hz, 1H), 4.00 (s, 2H), 3.80-3.67 (m, 1H), 2.13 (s, 3H), 1.73-1.68 (m, 2H), 1.50-1.45 (m, 3H), 1.30-1.16 (m, 2H), 1.08-0.99 (m, 1H), 0.87-0.74 (m, 2H).
^{13}C NMR ($CDCl_3$, 75 MHz) δ: 161.5, 141.1, 139.0, 133.1, 128.7, 128.4, 128.2, 126.7, 126.3, 126.1, 124.4, 123.1, 110.1, 48.0, 47.8, 33.3, 32.9, 25.5, 24.6, 12.3.
HRMS (ESI+): calculated for $C_{26}H_{31}N_2O^+$ = 387.2431; found = 387.244

6.5 Visible Light Photoredox Catalyzed generation and synthetic application of acyl radicals: synthesis and spectral characterization of compounds

General optimized procedure for reactions among benzoyl chloride and olefins ***5.30*** (also ***5.9***, ***5.18*** and ***5.27***)

A solution of the photoredox catalyst ($Ir(ppy)_3Cl_2$, 0.005mol%), benzoyl chloride ***5.13*** (0.1 mmol, 1 eq.), the radical trap of general formula ***5.30*** (or ***5.9***, ***5.18***, ***5.27***, 0.2 mmol, 2 eq.) and 2,6-lutidine (0.1 mmol, 1 eq.) in dry DCM (1 mL, 0.1M) was prepared under a nitrogen inert atmosphere inside a sealed glass vial. The reaction solution was irradiated (440 nm) at room temperature for one hour. The reaction course was monitred by TLC and GC analysis. A dryload was prepared evaporating the reaction crudes following addition of silica. Flash column chromatography affording the pure products was performed by means of an Isolera robotic machine.

One-pot methodology for the acylation of olefins ***o****f* general formula ***5.30*** (also ***5.9***, ***5.18*** and ***5.27***) *starting from benzoic acid derivatives of general formula* ***5.33***

A solution of the benzoic acid derivative of general formula ***5.33*** (0.1 mmol, 1 eq.) in dry DCM (1 mL, 0.1 M) was prepared under a nitrogen inert atmosphere. Oxalyl dichloride (0.11 mmol, 1.1 eq.) and a catalytic amount of DMF (1 mol%) were added to the solution. After 30 minutes the complete formation of the respective aroyl chloride was checked by TLC and GC analysis. The photoredox catalyst ($Ir(ppy)_3Cl_2$, 0.005mol%), the radical trap of general formula ***5.30*** (or ***5.9***, ***5.18***, ***5.27***, 0.2 mmol, 2 eq.) and 2,6-lutidine (0.2 mmol, 2 eq.) were added. The reaction solution was irradiated (440 nm) at room temperature for one hour. The reaction course was monitored by TLC and GC analysis. A dryload was prepared evaporating the reaction crudes following addition of silica. Flash column chromatography affording the pure products was performed by means of an Isolera robotic machine.

Photochemical reaction of cyclohexanecarboxylic (O-ethyl carbonothioic) thioanhydride ***5.51*** *with 1,2-diphenylethylene* ***5.30n***

To a solution of 1,2-diphenylethylene ***5.30*** (0.1 mmol, 1 eq.) and DIPEA (0.1 mmol, 1 eq.) in dry DCM (1 mL, 0.1M) was added the organic xanthate ***5.51*** (0.1 mmol, 1 eq.). The reaction was kept stirring under irradiation (440 nm) at room temperature for 30 minutes then another portion of organic xanthate ***5.51*** (0.1 mmol, 1 eq.) was added. The process was repeated other two times (2x 0.1 mmol, 1 eq. of ***5.51*** every 30 minutes) then a dryload was prepared evaporating the reaction crude following addition of silica. Flash column chromatography was performed by means of an Isolera robotic machine. Compound ***5.39*** was achieved with 91% yield.

Dual-catalytic reaction of cyclohexancarbonyl chloride ***5.38*** *with 1,2-diphenylethylene* ***5.30n*** *under visible light irradiation*

A solution of the photoredox catalyst ($Ir(ppy)_3Cl_2$, 0.005mol%), potassium ethyl xanthogenate (0.1 mmol, 0.1 eq.), cyclohexancarbonyl chloride ***5.38*** (0.1 mmol, 1 eq.), 1,2-diphenylethylene ***5.30n*** and DIPEA (0.2 mmol, 2 eq.) in dry DCM (1 mL, 0.1M) was prepared under a nitrogen inert atmosphere inside a sealed glass vial. The reaction solution was irradiated (440 nm) at room temperature overnight. The reaction course was monitored by TLC and GC analysis. A dryload was prepared evaporating the reaction crude following addition of silica. Flash column chromatography was performed by means of an Isolera robotic machine. Compounds ***5.39*** and ***5.39a*** were achieved in a mixture with 95% yield.

*Photochemical reduction reaction of Cyclohexancarbonyl chloride **5.38***

A solution of cyclohexancarbonyl chloride ***5.38*** (0.1 mmol, 1 eq.) and Hantzsch ester ***5.35*** (0.1 mmol, 1 eq.) was prepared in dry DCM (0.1 M). Potassium ethyl xanthogenate ***5.55*** was added in four portions (0.1 mmol, 1 eq. in total; 0.25 mmol each portion) over a time range of two hours. The reaction course was monitored by TLC and GC analysis. A dryload was prepared evaporating the reaction crude following addition of silica. Flash column chromatography was performed by means of an Isolera robotic machine. Aldehyde ***5.52*** was achieved with 70% yield.

*Photochemical reduction reaction of Cyclohexanecarboxylic acid **5.56***

A solution of cyclohexanecarboxylic acid ***5.56*** (0.1 mmol, 1 eq.) was prepared in dry DCM (1 mL, 0.1 M). Oxalyl dichloride (0.11 mmol, 1.1 eq.) and a catalytic amount of DMF (1 mol%) were added to the solution. After 30 minutes the complete formation of the cyclohexancarbonyl chloide was checked by TLC and GC analysis. Hantzsch ester ***5.35*** (0.1 mmol, 1 eq.) was added then potassium ethyl xanthogenate ***5.55*** was added in four portions (0.1 mmol, 1 eq. in total; 0.25 mmol each portion) over a time range of two hours. The reaction course was monitored by TLC and GC analysis. A dryload was prepared evaporating the reaction crude following addition of silica. Flash column chromatography was performed by means of an Isolera robotic machine. Aldehyde ***5.52*** was achieved with 16% yield.

Analytical data

(E)-1,3-Diphenylpropenone (***5.14***)

Yellow oil
^{1}H NMR ($CDCl_3$, 300 MHz) δ: 7.40-7.42 (m, 3H), 7.50-7.56 (m, 4H), 7.63-7.65 (m, 2H), 7.81 (d, 1H, *J* = 15.6 Hz), 8.01-8.03 (m, 2H);
^{13}C NMR ($CDCl_3$, 75 MHz) δ: 122.1, 128.5, 128.6, 128.7, 129.0, 130.6, 132.8, 134.9, 138.3, 144.9, 190.6.

(E)-1,3-diphenylbut-2-en-1-one (***5.19***):

Yellow oil
^{1}H NMR ($CDCl_3$, 300 MHz) δ: 7.98-8.00 (m, 2H), 7.52-7.58 (m, 3H),7.38-7.48 (m, 5H), 7.16 (d, J = 1.2 Hz, 1H), 2.59 (d, J = 1.2 Hz, 3H);
^{13}C NMR ($CDCl_3$, 75 MHz) δ: 191.9, 155.1, 142.8, 139.4, 132.6, 129.2, 128.6, 128.6, 128.3, 126.5, 122.1, 18.9

1,3-diphenylbut-3-en-1-one (***5.20***)

colorless oil
^{1}H NMR ($CDCl_3$, 300 MHz) δ: 7.96 (dd, J = 8.4, 1.4 Hz, 2H), 7.59 – 7.47 (m, 1H), 7.47 – 7.33 (m, 4H), 7.36 – 7.15 (m, 3H), 5.59 (s, 1H), 5.16 (s, 1H), 4.14 (s, 2H).
^{13}C NMR ($CDCl_3$, 75 MHz) δ: 197.7, 141.9, 140.3, 136.6, 133.3, 128.7, 128.5, 127.8, 125.9, 116.6, 45.3

3-phenacylphthalide (***5.28***)

White solid, m.p.=143–144 °C.
^{1}H NMR ($CDCl_3$, 300 MHz) δ: 7.97 (d, J=7.9 Hz, 2H), 7.93 (d, J=7.6 Hz, 1H), 7.67 (t, J=7.5 Hz, 1H), 7.62 (t, J=7.4 Hz, 1H), 7.59−7.54 (m, 2H), 7.50 (t, J=7.7 Hz, 2H), 6.19 (t, J=6.5 Hz, 1H), 3.79 (dd, J=17.6, 5.7 Hz, 1H), 3.40 (dd, J=17.6, 7.4 Hz, 1H).
^{13}C NMR ($CDCl_3$, 75 MHz) δ: 196.1, 170.2, 149.8, 136.2, 134.3, 133.9, 129.5, 128.9, 128.2, 125.9, 125.8, 122.9, 77.2, 43.7

(E)-3-ethoxy-1-phenylprop-2-en-1-one ***5.31a***

Colorless oil
^{1}H NMR ($CDCl_3$, 300 MHz) δ: 7.86-7.92 (m,2H), 7.76 (d,1H), 7.40-7.56 (m,3H), 6.35 (d,1H), 4.06 (q,2), 1.40 (t,3H)[6.5].

(1H-inden-2-yl)(phenyl)methanone ***5.31c***

White solid, m.p. 70-71 °C
^{1}H NMR ($CDCl_3$, 300 MHz) δ: 3.88 (s, 2H), 7.32-7.39 (m, 2H), 7.46- 7.59 (m, 6H), 7.81- 7.85 (m, 2H);
^{13}C NMR ($CDCl_3$, 75 MHz) δ: 38.5, 123.9, 124.5, 127.0, 128.1, 128.3 (2C), 128.8 (2C), 131.8, 138.9, 143.0, 143.6, 145.0, 145.1, 192.9

bicyclo[2.2.1]heptan-2-yl(phenyl)methanone ***5.31f***

^{1}H NMR ($CDCl_3$, 300 MHz) δ: 7.99-7.95 (m, 2H), 7.56-7.51 (m, 1H), 7.48-7.42 (m, 2H), 3.22 (dd, J = 8.8, 5.7 Hz, 1H), 2.53-2.51 (br m, 1H), 2.36-2.34 (br m, 1H), 2.06-1.98 (m, 1H), 1.68-1.54 (m, 2H), 1.52-1.25 (m, 4H), 1.15 (d, J = 7.7 Hz, 1H).
^{13}C NMR ($CDCl_3$, 75 MHz) δ: 201.3, 136.6, 132.6, 128.5, 128.4, 49.5, 41.0, 36.3, 36.2, 33.7, 29.7, 29.0.

E)-1-(4-Methoxyphenyl)-3-phenylprop-2-en-1-one ***5.31o***

Colorless oil
^{1}H NMR ($CDCl_3$, 300 MHz) δ: 8.07 (d, 2H, J = 8.0 Hz), 7.83 (d, 1H, J = 16.0 Hz), 7.67 (dd, 2H, J = 8.0 Hz), 7.57 (d, 1H, J = 16.0 Hz), 7.45− 7.43 (m, 2H), 7.82 (d, 2H, J = 8.0 Hz), 3.92 (s, 3H).
^{13}C NMR ($CDCl_3$, 75 MHz) δ: 188.8, 163.5, 144.0, 135.1, 131.1, 130.8, 130.3, 128.9, 128.4, 121.9, 113.9, 55.5

1-(4-methoxyphenyl)-3-phenylbut-3-en-1-one ***5.31p***

Colorless oil
^{1}H NMR ($CDCl_3$, 300 MHz) δ: 7.98 (d, *J* = 8.7 Hz, 2H), 7.44 (d, *J* = 7.9 Hz, 2H), 7.38-7.25 (m, 3H), 6.94 (d, *J* = 8.7 Hz, 2H), 5.61 (s, 1H), 5.19 (s, 1H), 4.13 (s, 2H), 3.88 (s, 3H).
^{13}C NMR ($CDCl_3$, 75 MHz) δ: 196.2, 163.5, 142.1, 140.4, 130.7, 129.7, 128.4, 127.7, 125.8, 116.2, 113.7, 55.4, 45.0

1-cyclohexyl-3,3-diphenylprop-2-en-1-one ***5.39***

Foam
^{1}H NMR ($CDCl_3$, 300 MHz) δ: 7.38-7.28 (m, 7H), 7.19-7.16 (m, 2H), 6.62 (s, 1H), 2.24 (tt, J =11.2 Hz, 3.2 Hz, 1H), 1.82-1.70 (m, 4H), 1.61-1.59 (m, 1H), 1.36-1.25 (m, 2H), 1.17-1.08 (m, 3H)
^{13}C NMR ($CDCl_3$, 75 MHz) δ: 205.04, 153.64, 141.40, 139.30, 129.53, 129.37, 128.54, 128.48,128.25, 128.23, 125.58, 50.94, 28.85, 25.96, 25.88

6.6 References

6.1
K. Schwetlick, Organikum, Wiley-VCH, Weinheim, **2009**

6.2
Schuster G. B. *J. Am. Chem. Soc*. **1995**, *117*, 5206-5211.

6.3
(a) Shu W. M.; Ma J. R.; Zheng K. L.; Sun H. Y.; Wang M.; Yang Y.; Wu A. X. *Tetrahedron* **2014**, *70*, 9321-9329.
(b) Martin L. J.; Marzinzik A. L.; Ley S. V.; Baxendale I. R. *Org. Lett.* **2011**, *13*, 320-323.
(c) Sudrik S. G.; Chavan S. P.; Chandrakumar K. R. S.; Pal S.; Date S. K.; Chavan S. P.; Sonawane H. R. *J. Org. Chem.* **2002**, *67*, 1574-1579.
(d) Garbarino S.; Banfi L.; Riva R.; Basso A. *J. Org. Chem.* **2014**, *79*, 3615-3622.

6.4
(a) Sawama Y.; Masuda M.; Yasukawa N.; Nakatani R.; Nishimura S.; Shibata K.; Yamada T.; Monguchi Y.; Suzuka H.; Takagi Y.; Sajiki H. *J. Org. Chem.* **2016**, *81*, 4190-4195.
(b) Kyasa S.; Meier R. N.; Pardini R. A.; Truttmann T. K.; Kuwata K. T.; Dussault P. H. *J. Org. Chem.* **2015**, *80*, 12100-12114.

6.5
Andersson, C. M.; Hallberg, A. *J. Org. Chem.* **1988**, *53*, 18, 4257-4263.

List of abbreviations

UV: ultraviolet
ISC: inter system crossing
PET: photoinduced electron transfer
VLPC: visible light photoredox catalysis
LED: light emitting diode
MLCT: metal to ligand charge transfer
MCR: multicomponent reaction
HAT: hydrogen atom transfer
SET: single electron transfer
DOS: diversity oriented synthesis
TOS: target oriented synthesis
MDGR: multi diveristy generating reactions
$(MC)^2R$: multicomponent multicatalytic reactions
PCET: proton coupled electron transfer
ROS: reactive oxygen species
OLED: organic light emitting diode
BDE: bond dissociation energy
API: active pharmaceutical ingredients
R&D: research and development
CGMP: current good manifacturing practice
PTFE: Politetrafluoroethylene
FEP: Fluorinated Ethylene Propylene
PMMA: Polimethylmethacrylate
UV-VIS: ultraviolet-visible
eq.: equivalent
mmol: millimole
MeCN: acetonitrile
PE: petroluem ether
EA: ethyl acetate
d: diameter
THF: tetrahydrofurane
DCM: dichloromethane
TBAF: tetra-n-butylammonium fluoride
AA: activating agent

RINGRAZIAMENTI-THANK YOU NOTES

Ringraziamenti (Italiano)

Vorrei ringraziare con tutto il cuore i miei genitori per essere stati sempre fantastici nei miei confronti. Ho ricevuto da loro tutto e più di tutto quello che avrei potuto desiderare per condurre una vita da studente nel migliore dei modi. Grazie a loro ho sempre potuto godere di gioia e serenità negli anni della mia formazione universitaria. Grazie infinite, vi voglio bene.

Grazie a tutta la mia grande famiglia per avermi sempre incoraggiato e supportato. Ringrazio di cuore mio Nonno, i miei zii ed i miei cugini, insieme a tutti gli altri componenti della famiglia. Non posso citare tutti quanti altrimenti scriverei un altra tesi per nominarvi tutti, non per questo non siete nel mio cuore.

Vorrei fare però un ringraziamento speciale a zia Mara per la generosità che mi ha sempre dimostrato.

Vorrei ringraziare Lisa per tutto quello che mi ha insegnato in questi anni. Lei e Chiara, che ci tengo a ringraziare, sono i due esempi che ho cercato e sempre cercherò di seguire per dare il meglio nel mio lavoro.

Ringrazio il Professor Banfi per essere stato il motivo originale della mia passione per la Chimica Organica e per tollerarmi nonostante la mia fede calcistica lontana dal suo credo.

Ringrazio la Professoressa Riva per tutte le opportunità e la fiducia che mi ha sempre concesso.

Vorrei ringraziare tutto lo staff in servizio al DCCI, docenti e non, per la magnifica esperienza che mi hanno fatto vivere in questi anni.

Ringrazio Paoletto per esser stato un prezioso amico su cui contare.

Vorrei ringraziare Fratellino per essere sempre lo stesso amico di quando giocavamo insieme all'asilo e Giammy per essere al mio fianco da quando giocavamo con la paletta. Ragazzi davvero non è poco.

Vorrei ringraziare la compagnia degli amici del Fanta, che mi hanno distratto il più possibile dal fare il mio dovere durante gli anni del dottorato.

Ringrazio anche la compagnia degli amici dello smazzo, che mi ha distratto ancora di più. Essendo la compagnia del Fanta anche parte della compagnia dello smazzo, essi sono doppiamente colpevoli.

Un grazie particolare a Parigi, Diego ed Orfeo perchè gli smongoli ed i nani non si dimenticano.

Ringrazio tutti gli amici di Levanto per le magnifiche estati trascorse in compagnia.

Ci tengo a ringraziare Francesca per il bellissimo tempo passato assieme.

Un grazie particolare allo Speseo, perchè a lui voglio bene più di tutti.

Vorrei ringraziare tutti gli amici dell'università: i compagni di corso, i conoscenti ed i ragazzi un pochino più giovani. La vostra compagnia è stata preziosa.

Vorrei ringraziare la Marta, che mi ha regalato mesi di laboratorio indimenticabili ed una vacanza che mi ha cambiato la vita. Nonostante tu sia sparita io (noi) ti vogliamo troppo bene.

Un grazie gigante alla Ella, che è stata il mio punto di riferimento durante gli anni del dottorato anche se per il 90% del tempo passato insieme in laboratorio mi ha odiato.

Su Pietro ho poco da dire. Una brutta persona.

Vorrei ringraziare Deianira e Gabriele per il lavoro che abbiamo svolto insieme; per me è stato un vero piacere lavorare e passare del tempo insieme a voi.

Il grazie in assoluto più grande di tutti lo devo ad Andrea, che per me è stato in questi anni un punto di riferimento da tutti i punti di vista, un esempio eccezionale come chimico e come persona. Ho vissuto sotto la sua supervisione tre anni davvero stimolanti che mi hanno fatto crescere tantissimo. Porterò nel mio bagaglio personale tantissimo di quanto mi ha trasmesso in tre anni passati seduto nella sedia affianco alla sua.

Anche su Elena ho poco da dire. Un'altra brutta persona, non a caso amica di Pietro. Grazie per avermi cambiato la vita e per esserne diventata il centro assoluto.

Thank you notes (English)

I would really like to thank Burkhard for the opportunity he gave me for working in his research group. I learnt a lot from my wonderful experience in Regensburg.

A big thank you to Daniel for the wonderful time we spent together and for being at the same time a great colleague and an even greater friend.
I would like to thank the whole research group of AK Konig for being kind and friendly with me in the time i spent with them.

I cannot avoid thanking Tobias for being such a dear and passionate friend even though we have been this far away all this time. Our friendship was born when you were a PhD student and now it is me who is getting a doctorate degree. But our friendship never stopped growing. I love you biatch.

I don't want to forget to mention my friend Jesco. Even though we lost contact, you have been a reference for me during my whole PhD as well as it has been Tobias; i miss the time when we were a great trio. '*Don't guess, do analytics'*; my motto, your words.

I would like to thank my dear Hossny for having been a super pleasant colleague and for being a dear friend.